National Library of Canada
Bibliothèque nationale du Canada

Canadian Theses Service
Service des thèses canadiennes

Ottawa, Canada
K1A 0N4

## NOTICE

The quality of this microform is heavily dependent upon the quality of the original thesis submitted for microfilming. Every effort has been made to ensure the highest quality of reproduction possible.

If pages are missing, contact the university which granted the degree.

Some pages may have indistinct print especially if the original pages were typed with a poor typewriter ribbon or if the university sent us an inferior photocopy.

Previously copyrighted materials (journal articles, published tests, etc.) are not filmed.

Reproduction in full or in part of this microform is governed by the Canadian Copyright Act, R.S.C. 1970, c. C-30.

## AVIS

La qualité de cette microforme dépend grandement de la qualité de la thèse soumise au microfilmage. Nous avons tout fait pour assurer une qualité supérieure de reproduction.

S'il manque des pages, veuillez communiquer avec l'université qui a conféré le grade.

La qualité d'impression de certaines pages peut laisser à désirer, surtout si les pages originales ont été dactylographiées à l'aide d'un ruban usé ou si l'université nous a fait parvenir une photocopie de qualité inférieure.

Les documents qui font déjà l'objet d'un droit d'auteur (articles de revue, tests publiés, etc.) ne sont pas microfilmés.

La reproduction, même partielle, de cette microforme est soumise à la Loi canadienne sur le droit d'auteur, SRC 1970, c. C-30.

NL-339 (r. 88/04)

Canada

THE UNIVERSITY OF ALBERTA

# NEAR-INFRARED DIFFUSE REFLECTANCE ANALYSIS OF OIL SAND

By

(C) Robert C. Shaw

A THESIS

SUBMITTED TO THE FACULTY OF GRADUATE STUDIES AND RESEARCH IN PARTIAL FULFILMENT OF THE REQUIREMENTS FOR THE DEGREE OF MASTER OF SCIENCE.

DEPARTMENT OF CHEMISTRY

EDMONTON, ALBERTA

SPRING, 1988

Permission has been granted to the National Library of Canada to microfilm this thesis and to lend or sell copies of the film.

The author (copyright owner) has reserved other publication rights, and neither the thesis nor extensive extracts from it may be printed or otherwise reproduced without his/her written permission.

L'autorisation a été accordée à la Bibliothèque nationale du Canada de microfilmer cette thèse et de prêter ou de vendre des exemplaires du film.

L'auteur (titulaire du droit d'auteur) se réserve les autres droits de publication; ni la thèse ni de longs extraits de celle-ci ne doivent être imprimés ou autrement reproduits sans son autorisation écrite.

ISBN 0-315-42802-3

**THE UNIVERSITY OF ALBERTA**

**RELEASE FORM**

| | |
|---|---|
| NAME OF AUTHOR: | Robert C. Shaw |
| TITLE OF THESIS: | Near-Infrared Diffuse Reflectance Analysis of Oil Sand |
| DEGREE: | Master of Science |
| YEAR THIS DEGREE GRANTED: | 1988 |

Permission is hereby granted to THE UNIVERSITY OF ALBERTA LIBRARY to reproduce single copies of this thesis and to lend or sell such copies for private, scholarly, or scientific research purposes only.

The author reserves other publication rights, and neither the thesis nor extensive extracts from it may be printed or otherwise reproduced without the author's written permission.

Robert C Shaw

(Student's Signature)

3919 – 51 Street
EDMONTON, Alberta

(Student's Permanent Address)

Date: April 27, 1988

THE UNIVERSITY OF ALBERTA

FACULTY OF GRADUATE STUDIES AND RESEARCH

The undersigned certify that they have read, and recommend to the Faculty of Graduate Studies and Research for acceptance, a thesis entitled:

**NEAR-INFRARED DIFFUSE REFLECTANCE ANALYSIS OF OIL SAND**

submitted by Robert C. Shaw in partial fulfilment of the requirements for the degree of Master of Science.

Byron Kratochvil
(Supervisor)

Gary Horlick

Loren Hepler

R. J. Dickinson

Date: 27 April 1988

**To my Wife, Patti**

## ABSTRACT

The application of near–infrared diffuse reflectance analysis for the determination of bitumen content in samples of Athabasca oil sand is described. Quantitative analysis is performed using calibrations based on the linear correlation between spectral features at a number of selected wavelengths and compositional data for a series of known samples. Preliminary investigations indicated that a measure for bitumen saturation can be related to the relative peak height of absorbance bands associated with the hydrocarbon and clay mineral constituents of the sample. Subtle differences in the curvature of the baseline and intensity of absorbance spectra among samples of similar composition provide indices for classifying oil sand samples with respect to geological origin.

Encouraging results prompted a more extensive study to be undertaken using a dedicated near–infrared diffuse reflectance spectrophotometer. Determinations for the anhydrous bitumen content of oil sand samples contained within a length of core were pursued. Spectra were obtained at 1 cm sampling intervals using an LTI Quantum 1200 NIR Analyzer. The section of core selected for this detailed inspection contains material typical of a vertical transect through the Athabasca deposit.

A variety of samples were collected from this core and analyzed using a micro–Soxhlet extraction procedure. Results provided the reference assay data for correlating spectral response. The training set included representative samples of oil sand, indurated clay, coal, and interbedded regions. A model based on the first derivative of absorbance spectra was found to provide an excellent relationship between spectral features and sample composition over the wide range of oil sand grades encountered. This model was used to predict the bitumen content of samples along the entire length of the test core section, thus providing a high resolution profile of grade variability as a function of depth.

Patterns in the structure of the resulting contour were interpreted from a geostatistical perspective employing the concept of fractal dimension. Based on the experimental semi–variogram describing the correlation among samples at increasingly larger separation distances, it was found that the structure of the grade profile can be characterized as having a fractal dimension greater than that of a randomly distributed variate. This implies that the material is extremely heterogeneous and can be considered a segregated mixture at the scale of observation used to generate the spatial series. Up to a point, the degree of segregation was found to diminish as sample size increased, or alternatively, as the resolution used for sampling decreased. Variations in oil sand composition as a function of location under these conditions appear to become more consistent with that expected for a random phenomenon. Beyond this scale of observation however, a transition zone may exist at

which segregation trends again become dominant.

Findings indicate that there are several scales of variability among regionalized estimates for the bitumen content of an oil sand deposit depending on the resolution used for measurement. This is significant and has implication with regard to the development of sampling protocols for materials that can be described in terms of a spatial series of attributes. Sampling theories that address the contribution of segregation variance to the overall level of sampling uncertainty must take into account the distinct scales of variability which may be present in the quantity of material under consideration.

## ACKNOWLEDGEMENTS

The author is extremely grateful to the management of the Syncrude Canada Ltd. Research Department for their contribution in providing the facilities, time, and financial support required for the completion of this project. Special acknowledgement is given to Dr. J. Clark, Dr. R. Schutte, Mr. D. Kershaw, and Ms. M. Veljkovic for their encouragement over the course of this research endeavor.

Appreciation is also extended to Dr. B. Kratochvil for providing the invaluable direction and supervision of this study. The author is further indebted to Mr. P. Dougan for his helpful discussions and advice related to near–infrared instrumental analysis, Dr. P. Crickmore for his insights regarding the applied mathematics of fractal dimension, and Mr. J. Hoyle for his assistance in setting up equipment in the Spectral Services Laboratory of the University of Alberta Chemistry Department. Special thanks is also given to the staff of the University of Alberta Chemistry Department Machine Shop for the design and construction of the core sampling table.

The author wishes to express his gratitude to Dr. D. Denney for his help and suggestions in formatting the text for this document.

## TABLE OF CONTENTS


| | Page |
|---|---|
| ABSTRACT | v |
| ACKNOWLEDGEMENTS | vii |
| LIST OF TABLES | xi |
| LIST OF FIGURES | xii |
| 1. INTRODUCTION | 1 |
| 2. PRELIMINARY EVALUATION OF NIR–DR TECHNIQUES FOR OIL SAND ANALYSIS | 11 |
| 2.1 Studies With a Nicolet 7199 FT–IR Spectrophotometer | 13 |
| 2.2 Studies With a Cary 17 UV–VIS–NIR Spectrophotometer | 31 |
| 3. NIR–DR MEASUREMENTS FOR THE GRADE OF OIL SAND CONTAINED WITHIN A CORE | 37 |
| 3.1 Description of the Equipment | 37 |
| 3.2 Test Section of Core | 39 |
| 3.3 Instrumental Conditions | 44 |
| 3.3.1 Sample Window | 44 |
| 3.3.2 Selection of Background Reference Material | 50 |
| 3.3.3 Sample Elevation | 51 |
| 3.3.4 Number of Scans | 63 |
| 3.3.5 Reproducibility of Sample Spectra | 68 |
| 3.3.6 Wavelength Calibration | 81 |

3.4 Micro–Soxhlet Extraction Procedure for Reference Assay Determination . . . . . 86

3.5 Training Set and Data Modelling . . . . . 93

**4. FRACTAL DIMENSION OF RUGGED CURVES** **116**

4.1 General Concepts . . . . . 116

4.2 Measurement of Fractal Dimension . . . . . 118

4.3 Fractal Dimension of Serial Data . . . . . 122

4.3.1 Fractional Gaussian Noise . . . . . 123

4.3.2 Relationship to the Semi–Variogram . . . . . 126

4.4 Application to the Geostatistical Analysis of an Oil Sand Deposit . . . . . 131

**5. FRACTAL ANALYSIS OF EXPERIMENTAL NIR–DR DATA** **134**

5.1 Variability in a Spatial Series of Oil Sand Grades at High Sampling Resolution . . . . . 134

5.2 Effect of Sample Size on the Structure of Vertical Grade Contours . . . . . 142

5.3 Implications With Respect to Sampling Theory for Segregated Bulk Materials . . . . . 155

**6. CONCLUSIONS AND SUGGESTIONS FOR FUTURE WORK** **165**

**REFERENCES** **167**

**APPENDICES** 171

A Training Set Models Relating Near–Infrared Diffuse Reflectance Spectra and Bitumen Content for Samples of Oil Sand . . . . . 171

B Point Grade Estimates for the Bitumen Content of Core Based on Samples of Varying Increment Size . . . . . 235

C Experimental Semi–Variograms and Autocorrelation Functions for Core Samples of Varying Increment Size . . . . . 243

## LIST OF TABLES


| | | Page |
|---|---|---|
| I. | Compositional data for samples obtained from core hole 22–38–60–0–0–0 as reported to the Energy Resources Conservation Board, Province of Alberta. | 8 |
| II. | Positions and assignments for NIR absorbance bands in the component spectra of oil sands. | 17 |
| III. | Assay data and replicate absorbance measurements obtained for a variety of oil sand samples. | 25 |
| IV. | Regression statistics for a linear model relating spectral features and sample bitumen content for an estuarine oil sand | 30 |
| V. | Absorbance measurements obtained from the optical template as a function of location along the sampling table. | 47 |
| VI. | Absorbance readings obtained from the spectra of an oil sand sample upon varying the number of scans used for signal averaging. | 67 |
| VII. | Absorbance measurements and associated uncertainty values obtained from the mean spectrum of various core samples. | 78 |
| VIII. | Adopted wavelengths of minimum reflectance for NBS SRM 1920 (Near–Infrared Reflectance Wavelength Standard) at various selected spectral bandwidths. | 85 |
| IX. | Preliminary estimates for the precision of bitumen and solids analyses performed on samples of lean, medium, and rich grade oil sand using the micro–Soxhlet extraction procedure. | 91 |
| X. | Data obtained for evaluating the effect of systematic errors in the analysis of oil sand samples by micro–Soxhlet extraction. | 92 |
| XI. | Precision of replicate micro–Soxhlet extraction analyses for samples of lean, medium, and rich grade oil sand. | 94 |
| XII. | Description and analytical data for training set samples. | 96 |
| XIII. | Statistical summary of the best fit models developed from the training set for relating the bitumen content of core samples and their diffuse reflectance spectra. | 112 |

## LIST OF FIGURES


| | | Page |
|---|---|---|
| 1. | Various pathways for diffuse reflectance from scattering particles. . . | 2 |
| 2. | Geographical location of the Syncrude Canada Ltd. leases. . . . . | 7 |
| 3. | Variability in the bitumen content of samples from core hole 22–38–60–0–0–0 as a function of depth within the deposit. . . . . | 9 |
| 4. | NIR diffuse reflectance attachment for Nicolet 7199 FT–IR spectrophotometer. . . . . | 14 |
| 5. | NIR diffuse reflectance spectra for bitumen and water dispersed in KBr powder. . . . . | 15 |
| 6. | NIR diffuse reflectance spectra for various clay minerals and quartz. | 16 |
| 7. | Comparison of NIR diffuse reflectance spectra for fresh and aged samples of oil sand. . . . . | 19 |
| 8. | Comparison of NIR diffuse reflectance spectra for oil sands of varying bitumen content. . . . . | 21 |
| 9. | Comparison of NIR diffuse reflectance spectra for oil sands of marine and estuarine origin. . . . . | 22 |
| 10. | Effect of surface preparation procedure on the diffuse reflectance spectra of an oil sand sample. . . . . | 23 |
| 11. | Correlation between mean relative absorbance at 1725 nm and anhydrous bitumen content for oil sand samples of marine and estuarine origin. . . . . | 26 |
| 12. | Correlation between mean relative absorbance at 2285 nm and anhydrous bitumen content for oil sand samples of marine and estuarine origin. . . . . | 27 |
| 13. | Correlation between mean relative absorbance at 2200 nm and –5.5 micron solids content for oil sand samples of marine and estuarine origin. . . . . | 28 |
| 14. | Correlation between measured bitumen assays for an estuarine oil sand sample and those predicted from a linear model based on absorbance readings at 1725, 2200, and 2285 nm. . . . . | 29 |

15. Optical diagram of an integrating sphere used for diffuse reflectance measurements. . . . . 32

16. NIR diffuse reflectance spectra obtained for a lean grade oil sand sample using a Cary 17 UV–VIS–NIR spectrophotometer and integrating sphere. . . . . 33

17. NIR diffuse reflectance spectra obtained for an average grade oil sand sample using a Cary 17 UV–VIS–NIR spectrophotometer and integrating sphere. . . . . 34

18. NIR diffuse reflectance spectra obtained for a rich grade oil sand sample using a Cary 17 UV–VIS–NIR spectrophotometer and integrating sphere. . . . . 35

19. Optical arrangement within the LTI Quantum 1200 NIR Analyzer. . 38

20. Schematic illustration of sampling table constructed for core analysis. 40

21. General arrangement of LTI Quantum 1200 NIR Analyzer, sampling table, and peripheral equipment. . . . . 41

22. Photographs of the test core section over the depth interval 83.8 – 86.1 metres. . . . . 42

23. Photographs of the test core section over the depth interval 86.1 – 88.4 metres. . . . . 43

24. Optical template used to evaluate the alignment and dimensions of the sample window for diffuse reflectance measurements. . . . . 45

25. Diffuse reflectance spectra of the light and dark regions of the optical template. . . . . 46

26. Plot of absorbance readings obtained from the optical template as a function of location along the sampling table. . . . . 48

27. Plot of absorbance readings as a function of optical template location indicating the measurements used to establish the geometry of the sample window. . . . . 49

28. Diffuse reflectance spectra of silica sand and KBr powder. . . . . 52

29. Diffuse reflectance spectra of various ceramic materials. . . . . 53

30. Diffuse reflectance spectra of carbon black and various paper test cards. 54

31. Diffuse reflectance spectra of oil sand and clay. . . . . 55

32. Diffuse reflectance spectra of oil sand and clay. . . . . 56

33. Diffuse reflectance spectra of oil sand and silica sand. . . . . 57

34. Diffuse reflectance spectra for carbon black determined at various sample elevations. . . . . 59

35. Diffuse reflectance spectra for an oil sand sample determined at various sample elevations. . . . . 61

36. Effect of instrumental gain on spectral features. . . . . 62

37. Diffuse reflectance spectra (Kubelka–Munk transform) for an oil sand sample determined at various surface elevations. . . . . 64

38. Normalized diffuse reflectance spectra for an oil sand sample determined at various sample elevations. . . . . 65

39. Relationship between spectral noise and number of scans. . . . . 66

40. Relationship between spectral noise and number of scans used for signal averaging. . . . . 69

41. Diffuse reflectance spectra of an oil sand sample illustrating the reduction in noise as a function of increasing the number of scans used for signal averaging. . . . . 70

42. Diffuse reflectance spectra of an oil sand sample illustrating the reduction in noise as a function of increasing the number of scans used for signal averaging. . . . . 71

43. Diffuse reflectance spectra of an oil sand sample obtained over the expanded wavelength region 2060–2100 nm illustrating the reduction in noise as a function of increasing the number of scans used for signal averaging. . . . . 72

44. Diffuse reflectance spectra of an oil sand sample obtained over the expanded wavelength region 2060–2100 nm illustrating the reduction in noise as a function of increasing the number of scans used for signal averaging. . . . . 73

45. Reproducibility of diffuse reflectance spectra for an oil sand sample. 74

46. Reproducibility of diffuse reflectance spectra for a sample of clay. . . 75

47. Reproducibility of diffuse reflectance spectra for an interbedded sample of oil sand and clay. . . . . 76

48. Reproducibility of diffuse reflectance spectra for carbon black. . . . . 80

49. Reproducibility of diffuse reflectance spectra for a sample of interbedded oil sand and clay illustrating the effect of instrumental drift. . . 82

50. Reproducibility of diffuse reflectance spectra for carbon black illustrating the effect of instrumental drift. . . . . 83

51. Diffuse reflectance spectrum of NBS SRM 1920 (Near–Infrared Reflectance Wavelength Standard). . . . . 84

52. Diffuse reflectance spectrum of NBS SRM 1920 (Near–Infrared Reflectance Wavelength Standard) obtained with the LTI Quantum 1200 NIR Analyzer. . . . . 87

53. Micro–Soxhlet extraction assembly used for the analysis of bitumen and solids content of oil sand. . . . . 88

54. Micro–Soxhlet extraction equipment used for the analysis of oil sand samples. . . . . 89

55. Representative diffuse reflectance spectra for samples of oil sand in the training set. . . . . 97

56. Representative diffuse reflectance spectra for samples of clay and interbedded oil sand and clay in the training set. . . . . 98

57. Representative diffuse reflectance spectra for samples of coal and interbedded oil sand and coal in the training set. . . . . 99

58. Representative diffuse reflectance spectra (first derivative of $Log(1/R)$ data for samples of oil sand in the training set. . . . . 100

59. Representative diffuse reflectance spectra (first derivative of $Log(1/R)$ data for samples of clay and interbedded oil sand and clay in the training set. . . . . 101

60. Representative diffuse reflectance spectra (first derivative of $Log(1/R)$ data for samples of coal and interbedded oil sand and coal in the training set. . . . . 102

61. Representative diffuse reflectance spectra (second derivative of $Log(1/R)$ data for samples of oil sand in the training set. . . . . 103

62. Representative diffuse reflectance spectra (second derivative of $Log(1/R)$ data for samples of clay and interbedded oil sand and clay in the training set. . . . . 104

63. Representative diffuse reflectance spectra (second derivative of $Log(1/R)$ data for samples of coal and interbedded oil sand and coal in the training set. . . . . 105

64. Structural model of an oil sand contained within the Athabasca deposit. . . . . 106

65. Correlation coefficient and its associated standard error for the relationship between compositional data and spectral features ($Log(1/R)$ data) as a function of wavelength for samples in the training set. . . 108

66. Correlation coefficient and its associated standard error for the relationship between compositional data and spectral features (first derivative of $Log(1/R)$ data) as a function of wavelength for samples in the training set. . . . . 109

67. Correlation coefficient and its associated standard error for the relationship between compositional data and spectral features (second derivative of $Log(1/R)$ data) as a function of wavelength for samples in the training set. . . . . 110

68. Comparison of predicted *versus* measured bitumen content for core samples in the training set using the best fit model based on $Log(1/R)$ spectral data. . . . . 113

69. Comparison of predicted *versus* measured bitumen content for core samples in the training set using the best fit model based on the first derivative of $Log(1/R)$ spectral data. . . . . 114

70. Comparison of predicted *versus* measured bitumen content for core samples in the training set using the best fit model based on the second derivative of $Log(1/R)$ spectral data. . . . . 115

71. Koch's Triadic Island, a fractal object that confines a finite area within an infinite boundary. . . . . 117

72. Examples of fractal objects that exhibit self–similarity over many scales. . . . . 119

73. Application of the structured walk technique to evaluate the fractal dimension of a rugged profile. . . . . 121

74. Rugged curves of differing fractal dimension generated under equivalent scales of resolution. . . . . 125

75. A typical semi–variogram possessing a sill, $C$, and nugget variance, $C_0$. . . . . 128

76. Theoretical semi–variograms. . . . . 129

77. Experimental semi–variogram for oil sand grades obtained at 60 cm spacings in the vertical direction. . . . . 132

78. Variability in bitumen content as a function of depth for the test core section. . . . . 135

79. Autocorrelation function for point grade estimates obtained at 1 cm sample spacings. . . . . 136

80. Experimental semi–variogram for point grade estimates obtained at 1 cm sample spacings. . . . . 137

81. Spherical model of the experimental semi–variogram for point grade estimates obtained at 1 cm sample spacings. . . . . 139

82. Evaluation of fractal dimension from the experimental semi–variogram for point grade estimates obtained at 1 cm sample spacings. . . . . 141

83. Grade profile and autocorrelation function for point grade estimates obtained at 2 cm sample spacings. . . . . 144

84. Experimental semi–variograms for point grade estimates obtained at 2 cm sample spacings. . . . . 145

85. Grade profile and autocorrelation function for point grade estimates obtained at 5 cm sample spacings. . . . . 146

86. Experimental semi–variograms for point grade estimates obtained at 5 cm sample spacings. . . . . 147

87. Grade profile and autocorrelation function for point grade estimates obtained at 10 cm sample spacings. . . . . 148

88. Experimental semi–variograms for point grade estimates obtained at 10 cm sample spacings. . . . . 149

89. Grade profile and autocorrelation function for point grade estimates obtained at 20 cm sample spacings. . . . . 150

90. Experimental semi–variograms for point grade estimates obtained at 20 cm sample spacings. . . . . 151

91. Relationship between fractal dimension and sample size for regularized core assay data. . . . . 152

92. Variability in bitumen content as a function of depth for core hole 22–38–60–0–0–0. . . . . 154

93. Autocorrelation function and experimental semi–variogram for core hole 22–38–60–0–0–0. . . . . 156

94. Experimental semi–variograms for core hole 22–38–60–0–0–0. . . . . 157

95. Relationship between fractal dimension and sample size for regularized core assay data indicating possible transition zone between scales of sample heterogeneity. . . . . 158

96. Relationship between fractal dimension and Visman sampling constants for segregated materials. . . . . 163

# 1. INTRODUCTION

Near–infrared diffuse reflectance (NIR–DR) analysis has become an accepted method for the quantitative measurement of organic species, mineral constituents, and moisture in a variety of solid substrates (1,2). The analysis is rapid, non–destructive in nature, and in many instances requires little or no sample preparation. A major reason for the success of the technique is that advances made in instrumentation and software permit simultaneous multi–component determinations to be performed on a single sample. Comprehensive reviews of the technology, along with surveys of the various applications, are presented by McDonald (3) and Stark *et.al.* (4).

In NIR diffuse reflectance analysis, radiation from an incandescent source is directed onto the sample where it penetrates the surface of the material for a short distance and scatters as it encounters randomly oriented particle boundaries. Radiation that is ultimately reflected back from the sample is collected over a wide range of angles and passed to a detector. As illustrated in Figure 1, the intensity of the reflected light will be diminished in relation to that of the incident radiation. This will depend on the effective thickness of the path within the sample, a function of the penetration depth and number of scattering events which can occur. Some of the incident light may also be absorbed upon exciting the vibrational modes of molecules present in the sample matrix.

The traditional approach to the analysis of diffuse reflectance spectra is based on the theory of Kubelka and Munk (5). The theory takes into account that radiation is both absorbed by the species of interest and scattered by non–absorbing particles contained within a sample. The Kubelka–Munk equation may be written as:

$$f(R) = \frac{(1-R)^2}{2R} = \frac{k}{s}$$

where $R$ is the diffuse reflectance at a given wavelength (obtained by taking the ratio of the sample spectrum and a reference spectrum), $k$ is the molar absorption

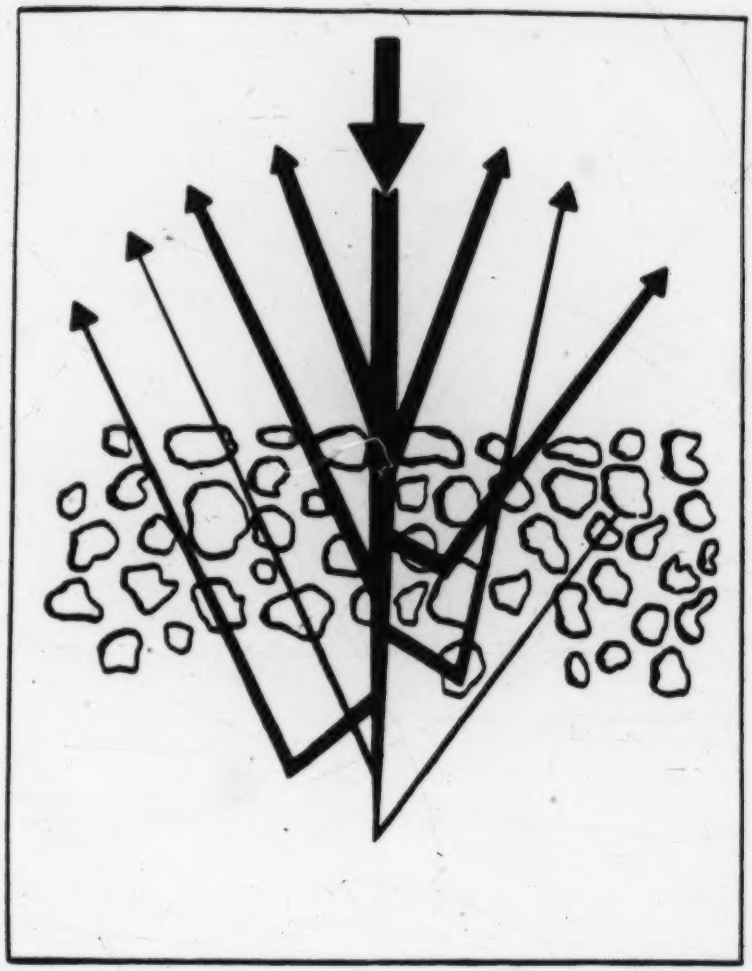

**Figure 1.** Various pathways for diffuse reflectance from scattering particles. Adapted from Wetzel (1).

coefficient, and $s$ is a scattering coefficient. The Kubelka–Munk theory predicts a linear relationship between the molar absorption coefficient and the peak value of $f(R)$ for each absorbance band, provided that the scattering coefficient remains constant.

For relatively dilute samples, the molar absorption coefficient can be related to the concentration of the absorbing species through the expression:

$$k = 2.303\epsilon c$$

where $\epsilon$ is the molar absorptivity and $c$ is the molar concentration (6). Therefore:

$$f(R) = \frac{(1-R)^2}{2R} = \frac{c}{k'} \quad \text{where} \quad k' = \frac{s}{2.303\epsilon}$$

Thus, the diffuse reflectance spectrum, $f(R)$, of a sample dispersed in finely powdered KBr, for example, might be expected to be similar to the absorbance spectrum of the sample prepared and analyzed as a KBr disc (7).

Rather than using the Kubelka–Munk theory, most practitioners in the field of near–infrared diffuse reflectance analysis relate the intensity of reflected radiation at a particular wavelength to the concentration of an absorbing species using the Beer–Lambert Law. By simple analogy to transmittance spectroscopy, the log of the inverse of the reflectance provides a measure of absorbance, $A$, which can be directly related to concentration:

$$Log\frac{1}{R} = A \propto c$$

The Wright and Wright oil sand monitor (8) used to estimate the bitumen content of ores fed to an oil sand extraction plant is based on these principles. Although the approach is not exact since it ignores the influence of scattering effects, it is commonly and successfully used and we will find it convenient to transform reflectance spectra by the function $Log(1/R)$.

The wavelength region of interest for NIR–DR work typically spans the range 1000–2500 nm. Absorptions at these wavelengths are relatively weak since they comprise overtones or combinations of fundamental bands from the mid–infrared. As a consequence, instrumentation requirements are more stringent than those for most other routine spectroscopic measurements. High signal to noise ratios must be assured by giving special consideration to factors such as source stability, optical design, sample registration, and detector sensitivity. Unfortunately, structural information that can be deduced from spectra obtained in the mid–infrared region is often obscured in the near–infrared due to the multiplicity and overlap of higher frequency overtone bands. Further, specular reflection (glare from the sample surface) and the effects of particle size, sample packing, and surface irregularities can have a substantial impact on both the overall intensity of reflected radiation and the contrast between baseline and absorbance peaks.

To alleviate these apparent shortcomings, quantitative analysis is performed using a calibration curve developed by correlating detector response at a number of selected wavelengths to known compositions for a series of standard samples. This series of standards is commonly referred to as the training set. It is essential that the mean particle diameter, particle size distribution, and other factors governing reflectance be consistently reproduced from sample to sample. The use of multivariate regression techniques and sophisticated algorithms that correct for baseline anomolies, extract and reconstruct component spectra from complex mixtures, and optimize the number of wavelength readings required for a robust and unbiased estimate for the concentration of each constituent in the sample serve to enhance the versatility of the method (9–15).

Near–infrared diffuse reflectance analysis has potential for providing a quick and comprehensive characterization of oil sand samples. The method would seem especially suited for the analysis of core. The slabbed face of a core could present an ideal surface for diffuse reflectance measurements, relinquishing the need to physically remove samples from the core barrel, subsample, and homogenize the material prior to analytical inspection.

The intent of the current research endeavor is to examine the compositional variability of an oil sand deposit in vertical cross-section based on measurements obtained from core using near infrared diffuse reflectance analysis. The specific objectives of this work are to:

- Establish the applicability of NIR-DR analysis for quantitative, non-destructive determination of bitumen in oil sand samples.
- Examine, at high spatial resolution, the variability of oil sand grade as a function of depth within a core.
- Determine whether heterogeneity of the deposit can be modelled in terms of fractal dimension and to augment current sampling theory in accordance.

Sampling equations developed to establish the size and number of sample increments required so as not to exceed a predetermined level of uncertainty when sampling bulk quantities of segregated materials are generally not designed to cope with materials that must be sampled in a systematic fashion, that is, where sample increments are collected as a function of time or location. Further, they do not address the concept of scalar self-similarity. Trends in sample data obtained as a time or spatial series may show some periodic behaviour that may or may not persist depending on the frequency at which the material was sampled and the size of the increments selected to characterize the bulk. Sampling protocols that consider the contribution of both random and segregation variance components to the overall sampling error are specific to the quantity and attributes of the bulk material under investigation. It is believed that a more unified theory can be developed, based on the use of fractal dimension, which considers the intrinsic variability in a property of the material over all scales of observation.

An assessment of the reliability of point grade estimates obtained from core hole data in describing the composition of large blocks of ore will provide a focus for more efficient reserve evaluation procedures. Further, measures of the magnitude

and persistence of variability in the bitumen content of feed to an extraction plant will yield insight as to the viability of proposed process control strategies.

The core examined over the course of this study is from the Athabasca oil sand deposit in a region of the Syncrude Canada Ltd. mine area known as Lease 22 (Core ID 22–38–60–0–0). The approximate location of the site (16,17) is indicated in Figure 2. The core was originally drilled and analyzed in 1985 . Assay data obtained on sample increments sized to represent the various geological strata are summarized in Table I. This data was provided to the Energy Resources Conservation Board, Province of Alberta, in compliance with Syncrude's licensing agreement. The core was processed and analyzed according to the procedures outlined in (18).

The slabbed and V–notched section made available for more detailed analysis has been stored under ambient conditions for a considerable time. Exposure to the atmosphere has resulted in complete dehydration of the material. This is not, however, considered a disadvantage. The condition is actually favorable in that we need not contend with changes in the position of the baseline or other features of the NIR absorbance spectra due to the presence of a strong free water peak.

Geological inspection indicates that the core transects oil sands from a variety of depositional environments. As illustrated in Figure 3, grades within the ore zone range from 1% to 15% by weight bitumen on an anhydrous basis. There is a pattern to the down–hole variation in grade which appears to be of a cyclic nature. The data reveals that, if one were to take a series of samples at regularly spaced intervals in the vertical direction, the oil sand at any given depth in the reserve will most likely be followed by an ore of comparable or lower grade. There are discontinuities in this trend however as evidenced by the dramatic shift towards high bitumen content material. The original pattern showing an inverse correlation between grade and depth is then repeated.

The thrust of this research effort is to see if this structure in the grade profile exists at a much higher spatial resolution. If so, it may be possible to characterize the reserve in terms of bitumen content and variability by examining only a small

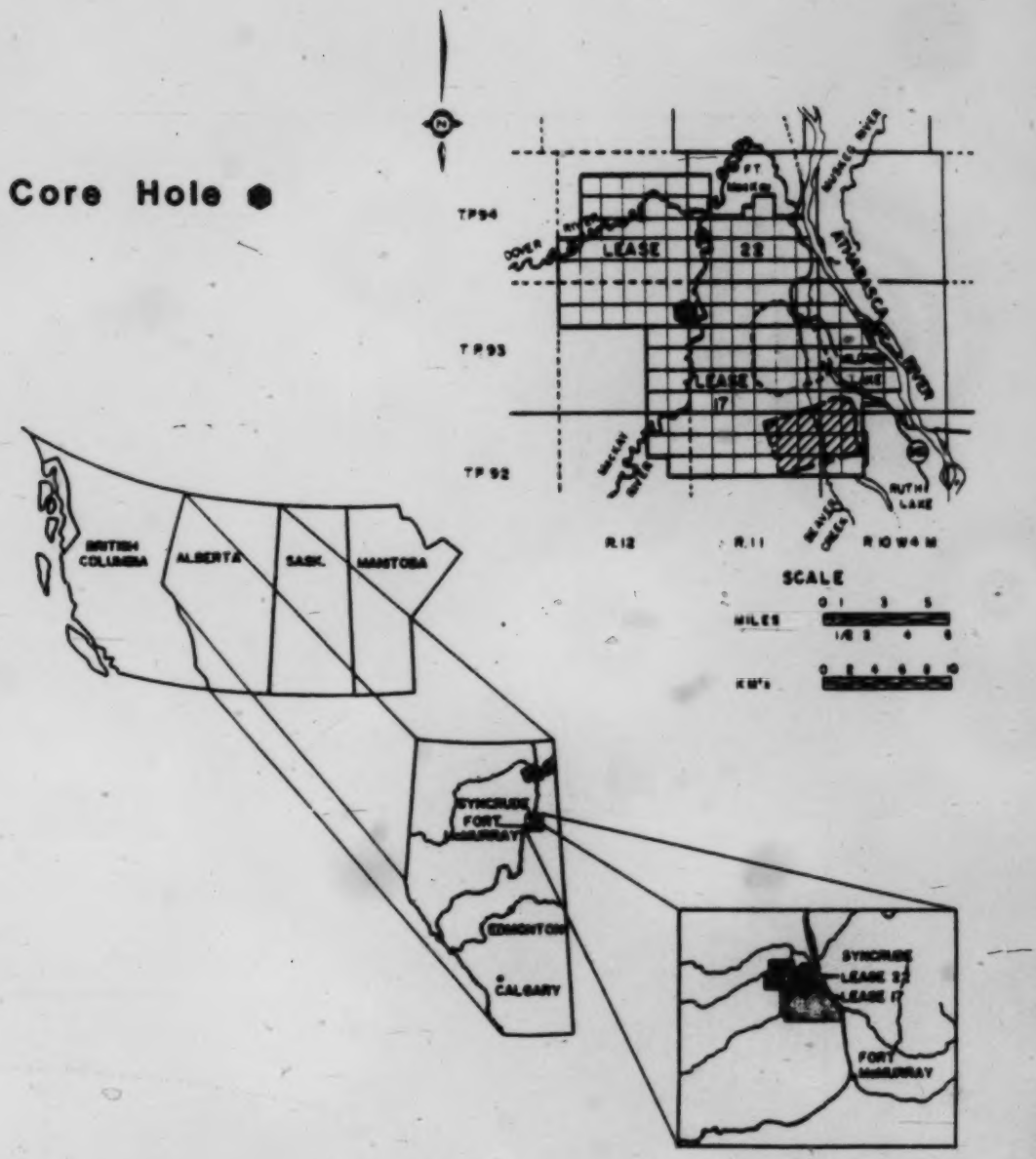


**Figure 2.** Geographical location of the Syncrude Canada Ltd. leases. Inset at upper right shows approximate location of core hole 22–38–60–0–0–0. Adapted from O'Donnell *et.al.* (16) and May *et.al.* (17).

**Table I.** Compositional data for samples obtained from core hole 22-38-60-0-0-0 as reported to the Energy Resources Conservation Board, Province of Alberta.

| DEPTH INTERVAL (metres) | BITUMEN (wt %) | WATER (wt %) | SOLIDS (wt %) | ANHYDROUS BITUMEN (wt %) |
|---|---|---|---|---|
| 0.3 - 49.8 | OVERBURDEN | | | |
| 49.8 - 51.1 | 1.0 | 12.6 | 86.4 | 1.1 |
| 51.1 - 52.4 | 3.5 | 15.4 | 81.1 | 4.1 |
| 52.4 - 53.0 | Missing Core | | | |
| 53.0 - 54.1 | 6.0 | 11.3 | 82.7 | 6.8 |
| 54.1 - 55.6 | 12.8 | 3.9 | 83.3 | 13.3 |
| 55.6 - 58.2 | 7.5 | 9.5 | 83.0 | 8.3 |
| 58.2 - 61.0 | 5.7 | 11.2 | 83.1 | 6.4 |
| 61.0 - 62.8 | 1.5 | 15.8 | 82.7 | 1.8 |
| 62.8 - 65.2 | 2.7 | 15.3 | 82.0 | 3.2 |
| 65.2 - 67.7 | 13.2 | 2.8 | 84.0 | 13.6 |
| 67.7 - 70.0 | 10.4 | 7.8 | 81.8 | 11.3 |
| 70.0 - 72.9 | 9.9 | 7.4 | 82.7 | 10.7 |
| 72.9 - 76.2 | 11.0 | 8.3 | 80.7 | 12.0 |
| 76.2 - 77.7 | 10.4 | 9.6 | 80.0 | 11.5 |
| 77.7 - 78.0 | 2.5 | 3.4 | 94.1 | 2.6 |
| 78.0 - 79.9 | 12.7 | 5.3 | 82.0 | 13.4 |
| 79.9 - 81.4 | 14.2 | 4.0 | 81.8 | 14.8 |
| 81.4 - 82.9 | 11.2 | 6.2 | 82.6 | 11.9 |
| 82.9 - 85.0 | 11.3 | 6.9 | 81.8 | 12.1 |
| 85.0 - 86.4 | 11.8 | 8.0 | 80.2 | 12.8 |
| 86.4 - 87.2 | 5.8 | 10.3 | 83.9 | 6.5 |
| 87.2 - 88.8 | 10.4 | 6.7 | 82.9 | 11.1 |
| 88.8 - 90.4 | 1.7 | 12.3 | 86.0 | 1.9 |
| 90.4 - 90.7 | 4.1 | 12.7 | 83.2 | 4.7 |
| 90.7 - 93.3 | 14.1 | 4.0 | 81.9 | 14.7 |
| 93.3 - 96.3 | 14.4 | 3.2 | 82.4 | 14.9 |
| 96.3 - 99.4 | 13.8 | 3.1 | 83.1 | 14.2 |
| 99.4 - 101.0 | 3.7 | 8.5 | 87.8 | 4.0 |
| 101.0 - 103.9 | 14.9 | 1.2 | 83.9 | 15.1 |
| 103.9 - 107.0 | 13.5 | 2.6 | 83.9 | 13.9 |
| 107.0 - 108.5 | 10.8 | 3.9 | 85.3 | 11.2 |
| 108.5 - 109.3 | Missing Core | | | |
| 109.3 - 109.6 | 3.5 | 7.3 | 89.2 | 3.8 |
| 109.6 - 114.0 | Missing Core | | | |
| 114.0 - 119.2 | LIMESTONE | | | |

$$Anhydrous\ \%Bitumen = \frac{(100)(\%Bitumen)}{100 - \%Water - \%Solids}$$

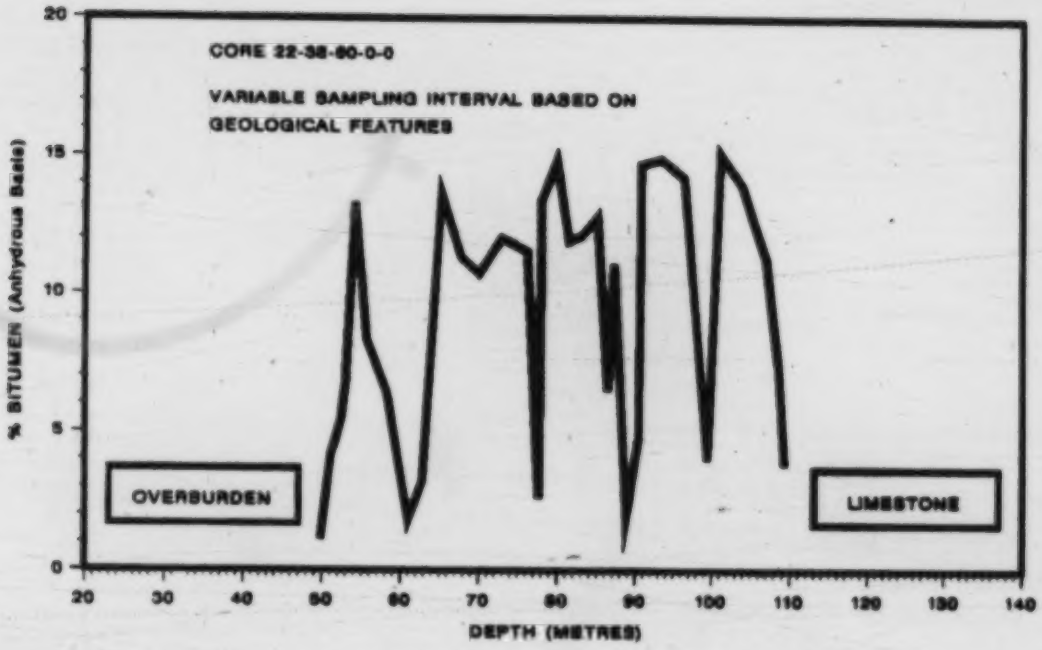


**Figure 3.** Variability in the bitumen content of samples from core hole 22-38-60-0-0-0 as a function of depth within the deposit.

portion of the core. Results will permit one to establish a more efficient sampling protocol for evaluating oil sand grades.

## 2. PRELIMINARY EVALUATION OF NIR-DR TECHNIQUES FOR OIL SAND ANALYSIS

Near-infrared diffuse reflectance analysis is predicated on the fact that the chemical composition of a substance can be determined in relation to the amount of light absorbed at various discrete wavelengths. When radiation strikes a sample of opaque material, some of the energy is absorbed and some is reflected. The fraction of light absorbed varies with wavelength according to the physical and chemical structure of the sample. To be absorbed, light must penetrate the surface of the sample a short distance and transfer energy to molecular bonds. The energy is transferred when the frequency of the incident radiation is the same as the frequency of molecular vibrations. The frequencies of these vibrations are specific to the molecular structure of the material and thus absorption is characteristic of the chemical attributes of the substance. Absorption of near-infrared light occurs because of interaction with overtone and combination frequencies of these vibrations.

The vibrational overtones in the near-infrared originate with vibrations involving strong chemical bonds between light atoms. If the chemical bonds were weak or the atoms heavy, the vibrational frequency would be too low for overtones to be seen in the near-infrared. The result of this is that we see primarily chemical bonds containing hydrogen attached to atoms such as nitrogen, oxygen, and carbon. These weak overtone vibrational bands are influenced more by their environment than are the fundamental modes of the same vibrations. Thus a slight perturbation in the bonding scheme which causes small changes in the position of fundamental bands can lead to drastically large shifts in the near-infrared. This results in an unexpectedly sensitive response to alterations in the molecular environment.

The sensitivity of near-infrared spectroscopic techniques for elucidating the chemical composition of materials has been known for many years. It is only with the development of high speed optics and powerful, inexpensive microcomputers that NIR-DR analysis has become a practical tool. With the more traditional approach to spectral analysis, it was tedious to decipher the broad overlapping bands typically found in this wavelength region. Computer assisted techniques that pro-

vide the correlations between spectral features and composition are responsible for the recent success of NIR–DR methods.

In this section, we discuss some preliminary work undertaken to examine the application of NIR–DR analysis for evaluating the composition of oil sand samples. Spectral features characteristic of the components present in the material and the simple relationships between absorbance and bitumen content are described. The detailed analysis of oil sand samples contained within a length of core using more sophisticated calibration procedures is dealt with in a future chapter.

Exploratory studies designed to assess the utility of NIR–DR analysis for oil, water, solids assay determination and for the detection of clay minerals in oil sand samples were first pursued by Dougan (19). Results were based in large part on spectra obtained at Purdue University (Laboratory for Applications of Remote Sensing) on samples submitted from a variety of sources within the Athabasca deposit. Findings indicated that:

- Spectral features characteristic of the individual bitumen, water, and clay constituents can be seen in the spectra of an oil sand.
- Reasonable correlations appear to exist between bitumen content and measures of absorbance peak height at several wavelengths.
- Subtle discrepancies in baseline curvature and band intensities among oil sand samples of similar composition may be ascribed to differences in depositional environment.

The latter result is very significant in that criteria can perhaps be established (based on peculiarities in the spectral patterns) for categorizing ores with respect to origin. It also demonstrates the need to classify samples before interpreting near–infrared reflectance data. Separate calibration curves relating absorbances to component concentrations would be required for estuarine and marine type ores.

More recent study regarding the application of NIR–DR techniques for oil sand

analysis has been conducted and is reported here. Results obtained using a Nicolet 7199 FT–IR and Cary 17 UV–VIS–NIR spectrophotometer, each especially adapted for diffuse reflectance work, are described. Data generated were intended to augment previous findings, thereby further establishing the utility of the procedure.

## 2.1 Studies With a Nicolet 7199 FT–IR Spectrophotometer

A specialized diffuse reflectance attachment was mounted in the open sample compartment of the spectrophotometer. The optical system and relative positioning of the sample within the device is schematically illustrated in Figure 4. The sample holder, a shallow cup approximately 1 cm in diameter by 0.2 cm deep, is threaded into a guide base and can be moved up or down by rotation. Upon ensuring proper registration of the guide base within the diffuse reflectance attachment, the sample cup was turned to position it such that detector signal to noise ratio was maximized.

Incident radiation was provided from a tungsten source with the diffuse reflected light measured using a lead sulfide detector. Wavelengths scanned covered the region 1200–2550 nm (3920–8330 $cm^{-1}$). Instrumental resolution was a nominal 16 $cm^{-1}$. All spectra were recorded in absorbance mode using a total of 50 scans. Spectra were ratioed against a background response obtained with powdered KBr.

Component spectra obtained for bitumen, water, quartz, and a variety of clays are shown in Figures 5 and 6. Specific features of each spectrum and tentative band assignments based on the information presented in (20,21) are summarized in Table II.

The bitumen spectrum shows two distinctive sets of doublets, one with major peaks at 2285 nm and 2330 nm and the other with peaks at 1725 nm and 1760 nm. These absorbances, along with the much weaker bands at 2400 nm and 2460 nm, can be ascribed to overtones and combinations of the fundamental vibration frequencies within constituent methyl and methylene groups. The bitumen used for this analysis was a typical coker feed material. Although the absorbance peak noted at 2160 nm may signify the presence of aromatic hydrocarbon species, it could also be attributed

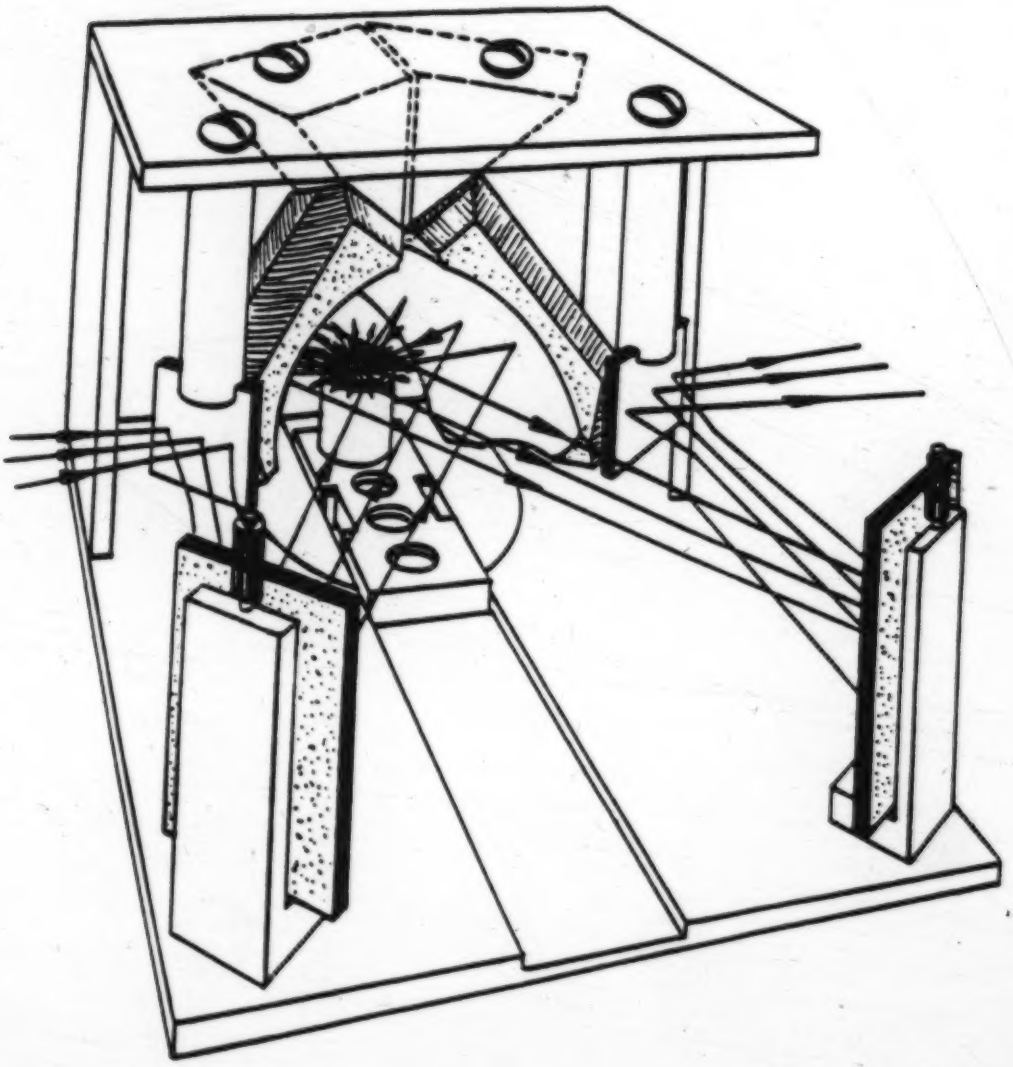

**Figure 4.** NIR diffuse reflectance attachment for Nicolet 7199 FT–IR spectrophotometer. The device is mounted in the sample compartment of the instrument.

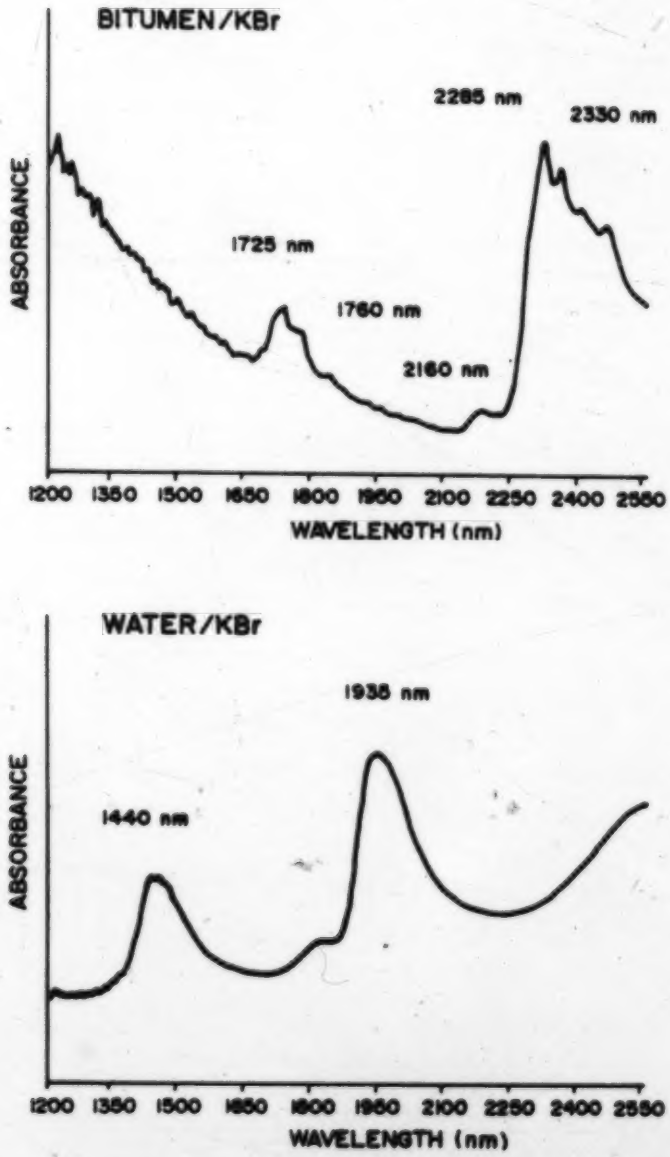


**Figure 5.** NIR diffuse reflectance spectra for bitumen and water dispersed in KBr powder.

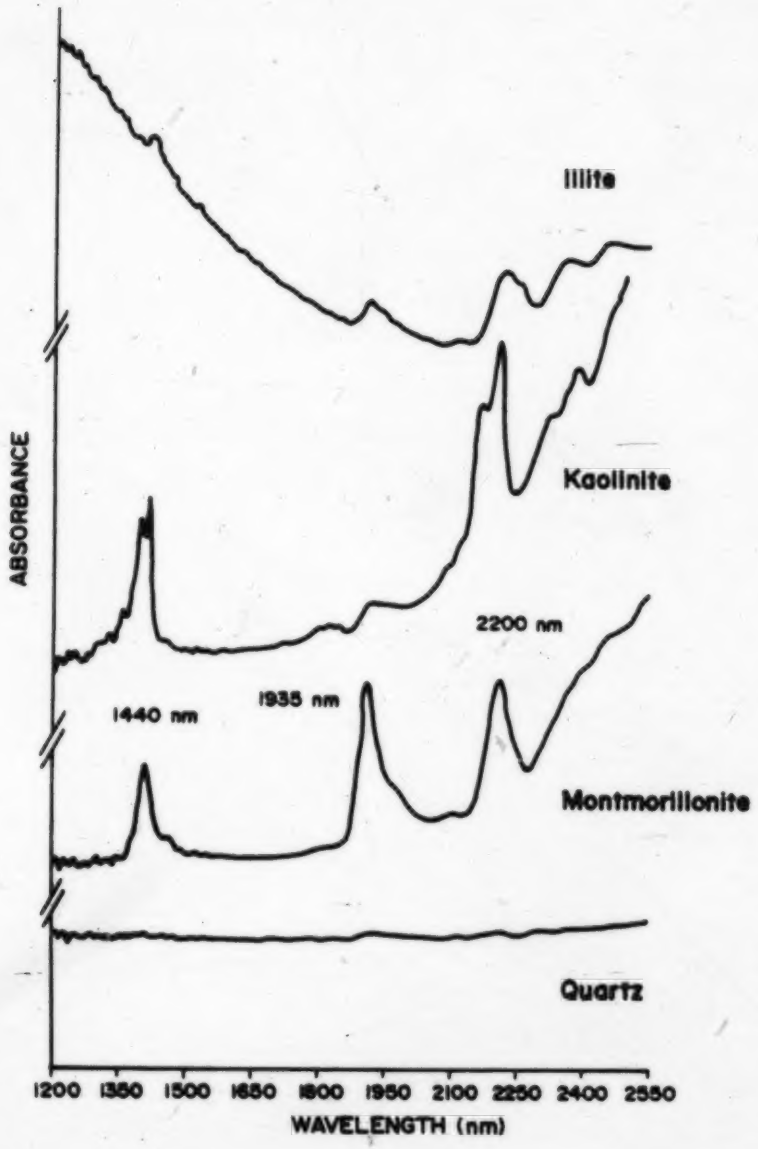


**Figure 6.** NIR diffuse reflectance spectra for various clay minerals and quartz.

**Table II.** Positions and assignments for NIR absorbance bands in the component spectra of oil sands. Adapted from Fysh *et.al.* (20) and Fredericks *et.al.* (21).

| COMPONENT | BAND POSITION | TENTATIVE ASSIGNMENT |
|---|---|---|
| Bitumen | 1725 nm<br>1760 nm | Overtone of symmetric $CH_3$ and $CH_2$ bending modes. |
| | 2160 nm | Combination of aromatic $C$–$H$ stretch and $C$–$C$ stretch. |
| | 2285 nm | Combination of $CH_2$ asymmetric stretch and symmetric bend. |
| | 2330 nm | Combination of $CH_3$ asymmetric stretch and symmetric bend; may also be a combination of $CH_3$ symmetric stretch and symmetric bend. |
| Water | 1440 nm | Free water combination band. |
| | 1935 nm | Free water combination band. |
| Clays | 2200 nm | Combination $Al$–$OH$ vibration band. |

to a contamination by clay, most probably kaolinite.

The diffuse reflectance spectrum for water indicates two strong absorbance peaks at 1440 nm and 1935 nm. These bands, representing combinations of fundamental vibrations associated with free water molecules, are also seen in the spectra obtained for illite, kaolinite, and montmorillonite. The latter spectra also show a major band in the region around 2200 nm which tends to be diagnostic of aluminum-bearing clays. It is apparent from the spectrum obtained for quartz that silica has no significant absorbance bands in the near-infrared.

Differences in the spectral patterns for the various clays appear to be significant. In the spectrum of kaolinite, for example, peaks centered at 1440 nm and 2200 nm are resolved as doublets. Only single peaks at these wavelengths are observed for illite and montmorillonite. One can speculate that the splitting of the 1440 nm absorbance band may be indicative of differences in coupling between the vibrational frequencies of free hygroscopic water and those associated with the water of hydration. In contrast with the spectrum for montmorillonite, the free water absorbance at 1935 nm for kaolinite and illite are relatively weak. Further, illite exhibits a progressive increase in absorbance (diminishing reflectance) towards the shorter wavelengths in a manner very similar to that of bitumen. A completely opposite trend is evident in the spectra for other types of clay.

The near-infrared diffuse reflectance spectra for a fresh and dehydrated sample of high grade oil sand (approximately 13% bitumen content) are shown in Figure 7. Many of the significant features of the individual component spectra appear to be present. The free water absorbance band situated at 1935 nm is clearly absent in the spectrum for the dehydrated sample. It is interesting to note that overall reflectivity is affected by the water content of the material. Moisture in the fresh oil sand sample contributes to an increase in absorbance readings at all wavelengths, presumably due to internal reflections within thin films of water. To eliminate uncertainties in absorbance measurements, all subsequent spectra herein discussed have been obtained using aged oil sand samples which have dried upon exposure to the atmosphere. Samples were ground to a fine powder using a mortar and pestle

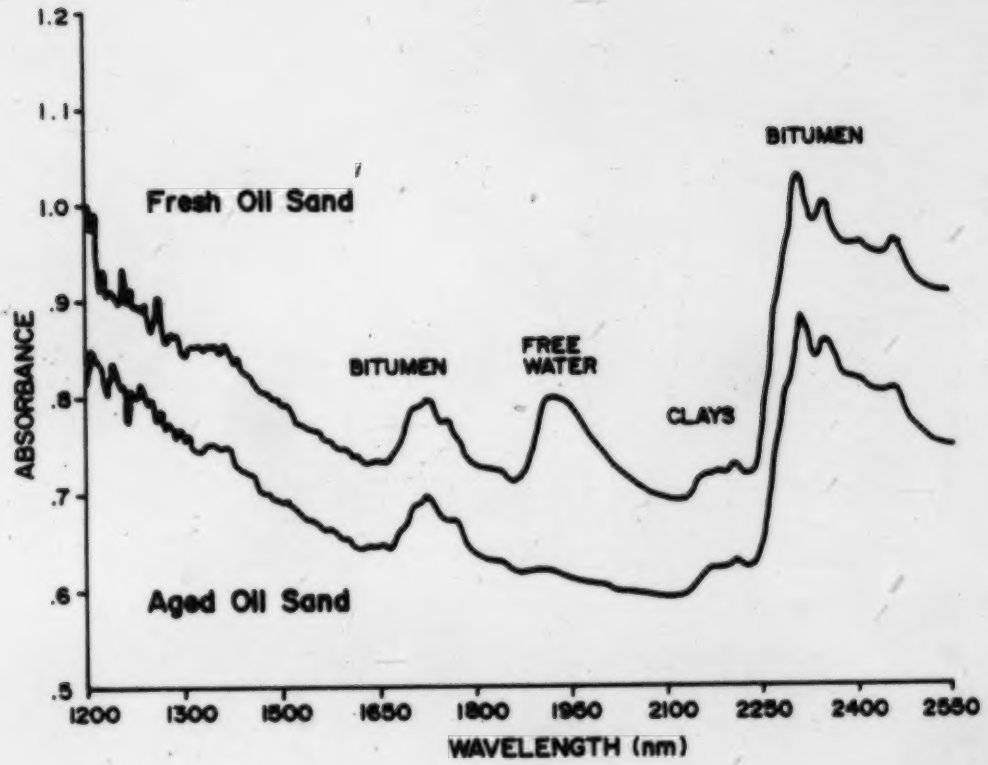


**Figure 7.** Comparison of NIR diffuse reflectance spectra for fresh and aged samples of oil sand.

and placed in the sample cup without compaction.

Figure 8 presents sample spectra obtained for rich, medium, and low grade oil sands. The reduction in the peak heights of the major bitumen absorbance bands (relative to an imposed baseline) with decreasing oil saturation is evident. Note that the absorbance scales for these spectra have been offset for the purposes of clarity.

Subtle differences in the spectral patterns among ores of marine and estuarine origin can be seen in the NIR diffuse reflectance spectra presented in Figure 9. Although the two samples of oil sand depicted here are comparable in terms of bulk composition (approximately 13% bitumen content), the total amount of light reflected from the marine sample is markedly less than that from the estuarine material. Further, the trace for the marine ore tends to have a shallower slope at short wavelengths, leading to a less pronounced curvature in the spectrum towards the higher wavelength region. The ratio of the absolute absorbance at 1200 nm to that of the bitumen peak at 2285 nm is near unity for the estuarine ore and somewhat greater for the marine ore. Conceivably, these traits can be used to establish a discriminant function that allows one to distinguish oil sands with respect to depositional environment.

The reproducibility of diffuse reflectance measurements can be affected by the nature of the sample surface presented for analysis. Replicate spectra recorded for a sample of oil sand under various conditions of surface preparation are shown in Figure 10. The original surface is that obtained by placing the powdered material into the sample cup without compaction. The surface was levelled by screeding the sample with a straight edge blade. The spectrum for the sample generated after packing the material into the sample cup (by tamping with a spatula) shows a general decrease in absolute reflectance over much of the wavelength range. At first glance, this would not constitute a serious problem since quantitative analysis is concerned with the relative absorbance from a baseline that is drawn with respect to the shape and positioning of the curve. Closer inspection of the spectrum however, reveals that the peak height of the absorbance band at 2285 nm is diminished in

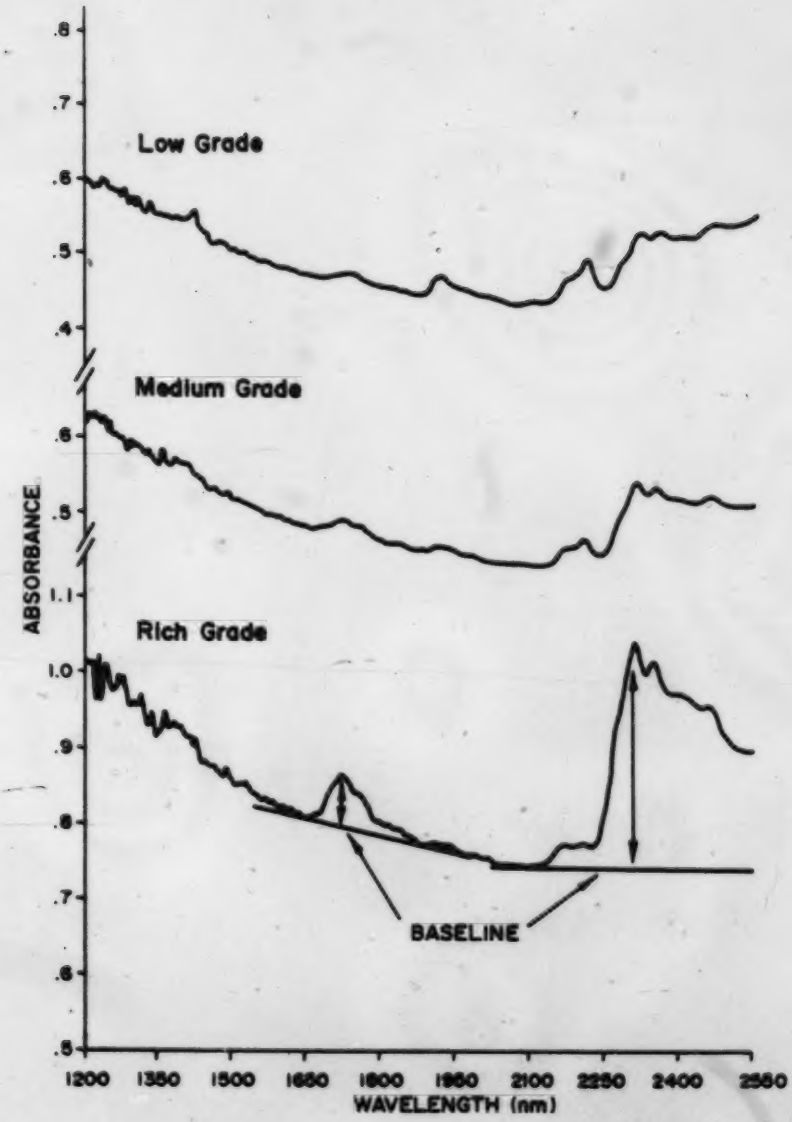


**Figure 8.** Comparison of NIR diffuse reflectance spectra for oil sands of varying bitumen content.

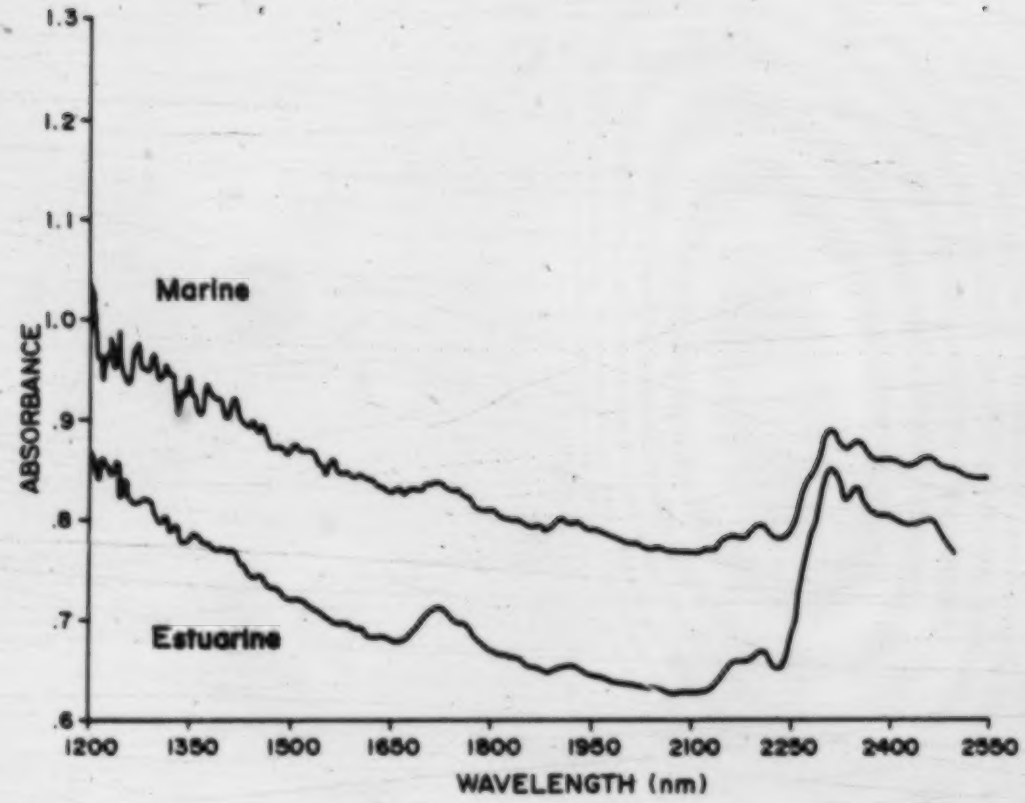


**Figure 9.** Comparison of NIR diffuse reflectance spectra for oil sands of marine and estuarine origin.

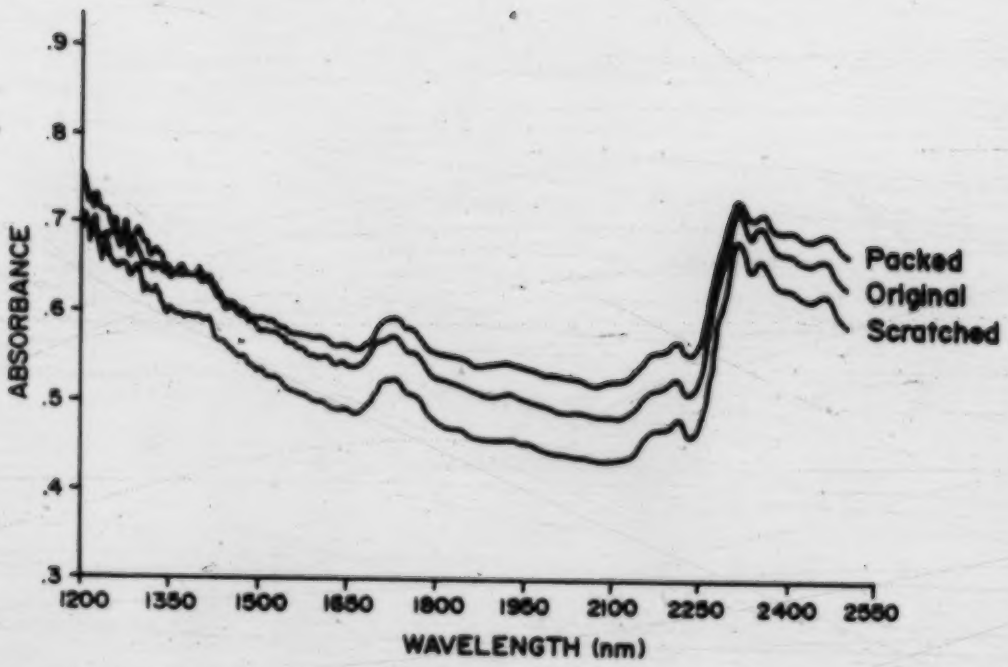


**Figure 10.** Effect of surface preparation procedure on the diffuse reflectance spectra of an oil sand sample.

relation to that of the original, uncompacted sample surface. This would lead to an underestimation of bitumen content if a calibration curve had been developed using the initial sample handling procedure. Roughening of the packed sample by simply scratching the surface with a pin appears to restore the integrity of the spectrum (albeit with a higher overall reflectivity). Results indicate that methods used to prepare samples for diffuse reflectance analysis must be consistent from sample to sample.

A series of replicate NIR–DR measurements were made for a variety of oil sand samples covering a wide range of compositions. Sample descriptions and relative absorbances determined at wavelengths selected to represent the bitumen and clay components are listed in Table III. Assay data is reported on an anhydrous basis.

Relationships between the bitumen content of these samples and the absorbance for peaks centered at 1725 nm and 2285 nm are shown in Figures 11 and 12. Differences in the slope of the calibration curves for oil sands of marine and estuarine origin are clearly evident. The correlation between clay content of the sample (as measured in terms of the –5.5 micron particle size fraction) and absorbance in the region of 2200 nm is presented in Figure 13. The plot suggests that NIR–DR analysis at this wavelength would be inappropriate for the quantitative determination of clays. This observation should be tempered, however, by the realization that much of the solids in this fraction could be silica. Without more detailed mineralogical information, the actual amount of clay present in the material cannot be assessed.

Although the correspondence between the –5.5 micron particle size fraction and absorbance peak height is poor, the data has significant influence in terms of predicting the sample bitumen content. Correlation between independently measured bitumen assays and those derived by considering a linear combination of spectral readings over the three selected wavelengths is illustrated in Figure 14. Regression statistics presented in Table IV indicate that bitumen content can be adequately determined using only two absorbance measurements, namely those obtained at the 2285 nm bitumen peak and the 2200 nm clay peak. Redundant information provided by the bitumen absorbance at 1725 nm serves little to improve the overall

**Table III.** Assay data and replicate absorbance measurements obtained for a variety of oil sand samples.

| SAMPLE TYPE | BITUMEN (wt %) | SOLIDS (wt %) | -8.8 μm SOLIDS (wt %) | ABSORBANCE RELATIVE TO BASELINE | | |
|---|---|---|---|---|---|---|
| | | | | 1738 nm | 2286 nm | 2200 nm |
| Marine | 12.96 | 87.04 | 11.6 | 0.020 | 0.111 | 0.027 |
| | | | | 0.028 | 0.126 | 0.034 |
| Marine | 8.61 | 91.39 | 9.0 | 0.019 | 0.085 | 0.017 |
| | | | | 0.015 | 0.080 | 0.025 |
| Marine | 5.38 | 94.62 | 13.3 | 0.011 | 0.089 | 0.017 |
| | | | | 0.011 | 0.041 | 0.021 |
| Estuarine | 10.70 | 89.30 | N.A. | 0.047 | 0.035 | 0.029 |
| | | | | 0.041 | 0.178 | 0.033 |
| | | | | 0.040 | 0.193 | 0.023 |
| | | | | 0.034 | 0.174 | 0.024 |
| | | | | 0.036 | 0.174 | 0.023 |
| Estuarine | 12.47 | 87.53 | 6.4 | 0.046 | 0.225 | 0.043 |
| | | | | 0.048 | 0.240 | 0.045 |
| Estuarine | 3.68 | 96.32 | 14.5 | 0.007 | 0.067 | 0.051 |
| | | | | 0.007 | 0.049 | 0.046 |
| Estuarine | 4.83 | 95.17 | 14.0 | 0.011 | 0.100 | 0.063 |
| | | | | 0.016 | 0.111 | 0.068 |
| | | | | 0.015 | 0.093 | 0.052 |
| | | | | 0.013 | 0.094 | 0.053 |
| | | | | 0.012 | 0.090 | 0.060 |
| Estuarine | 0.40 | 99.60 | 26.6 | 0.000 | 0.014 | 0.038 |
| | | | | 0.000 | 0.022 | 0.043 |
| Estuarine | 13.03 | 86.97 | 9.0 | 0.084 | 0.259 | 0.059 |
| | | | | 0.068 | 0.304 | 0.041 |
| | | | | 0.064 | 0.270 | 0.029 |
| | | | | 0.068 | 0.591 | 0.040 |
| | | | | 0.068 | 0.271 | 0.030 |
| Estuarine | 16.14 | 83.86 | 3.8 | 0.070 | 0.301 | 0.035 |
| | | | | 0.072 | 0.287 | 0.027 |
| Estuarine | 0.15 | 99.85 | 26.9 | 0.000 | 0.031 | 0.058 |
| | | | | 0.000 | 0.031 | 0.060 |
| Estuarine | 8.15 | 91.85 | 12.4 | 0.020 | 0.113 | 0.035 |
| | | | | 0.021 | 0.102 | 0.027 |
| | | | | 0.030 | 0.135 | 0.039 |
| | | | | 0.022 | 0.109 | 0.023 |
| | | | | 0.024 | 0.129 | 0.040 |

Assay data reported on an anhydrous basis.
-8.8 μm solids content expressed as a fraction of original solids concentration.

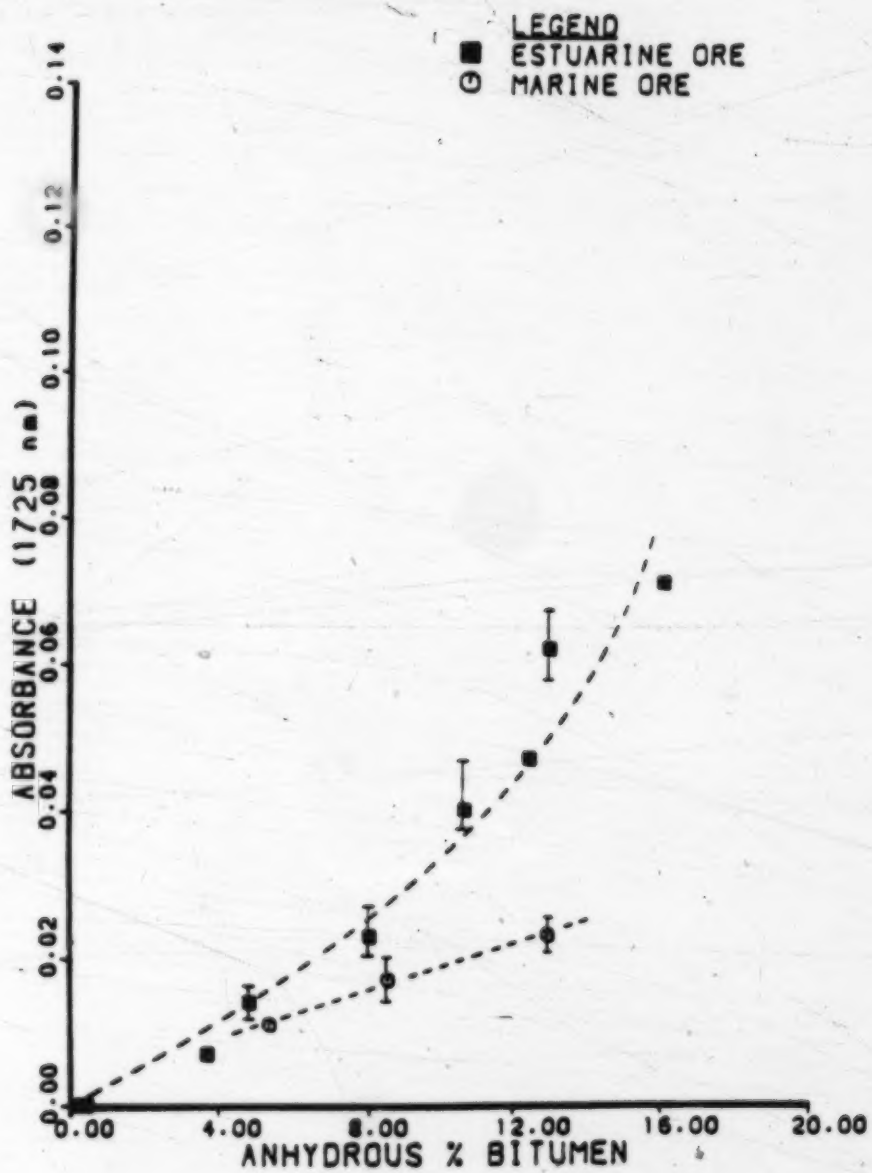


**Figure 11.** Correlation between mean relative absorbance at 1725 nm and anhydrous bitumen content for oil sand samples of marine and estuarine origin. Error bands depict the range observed among replicate sample absorbance measurements.

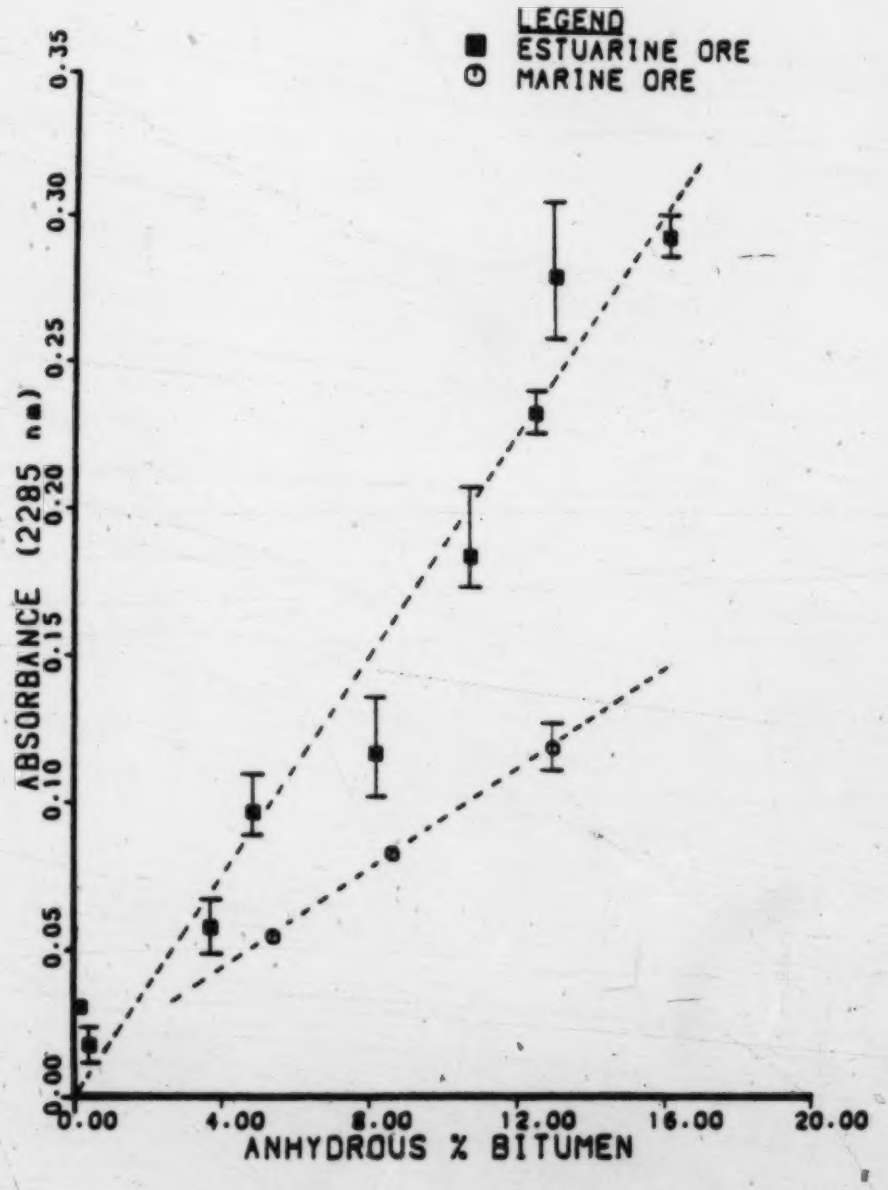


**Figure 12.** Correlation between mean relative absorbance at 2285 nm and anhydrous bitumen content for oil sand samples of marine and estuarine origin. Error bands depict the range observed among replicate sample absorbance measurements.

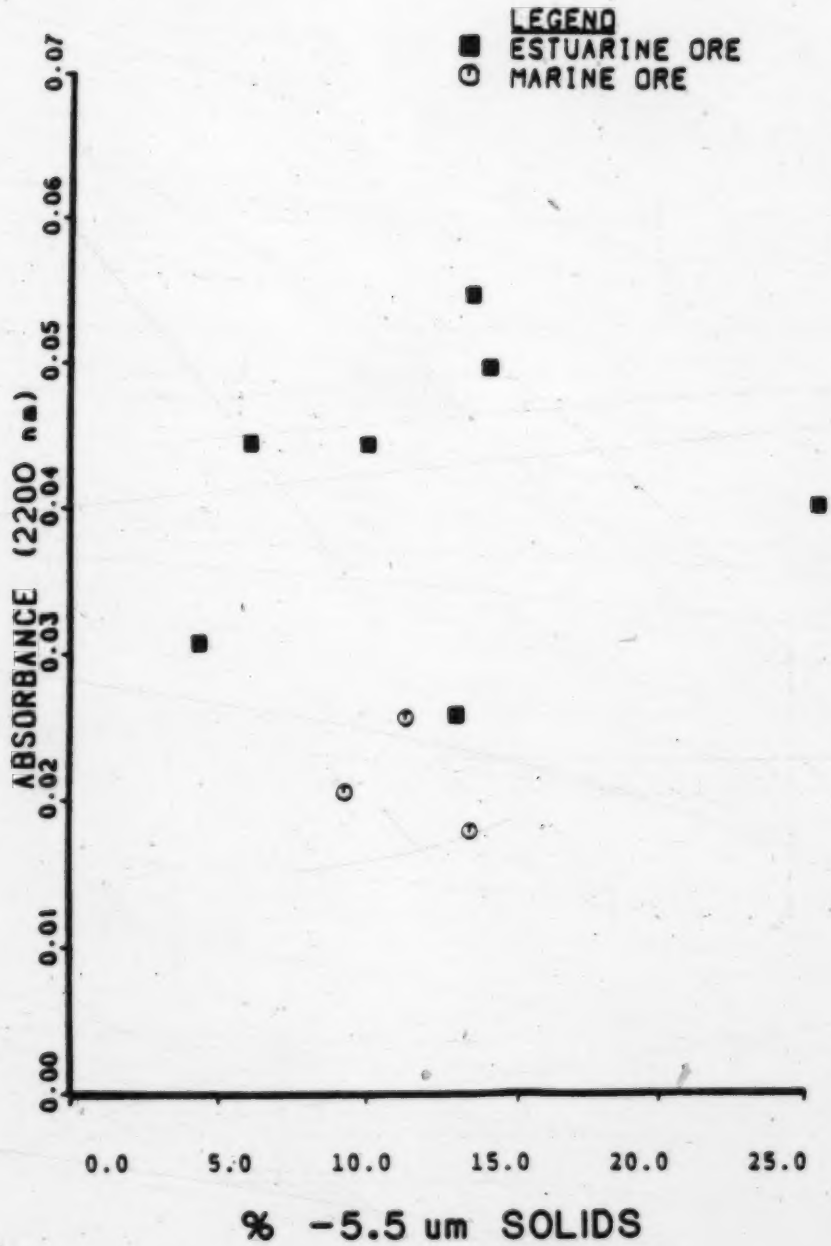


**Figure 13.** Correlation between mean relative absorbance at 2200 nm and -5.5 micron solids content for oil sand samples of marine and estuarine origin.

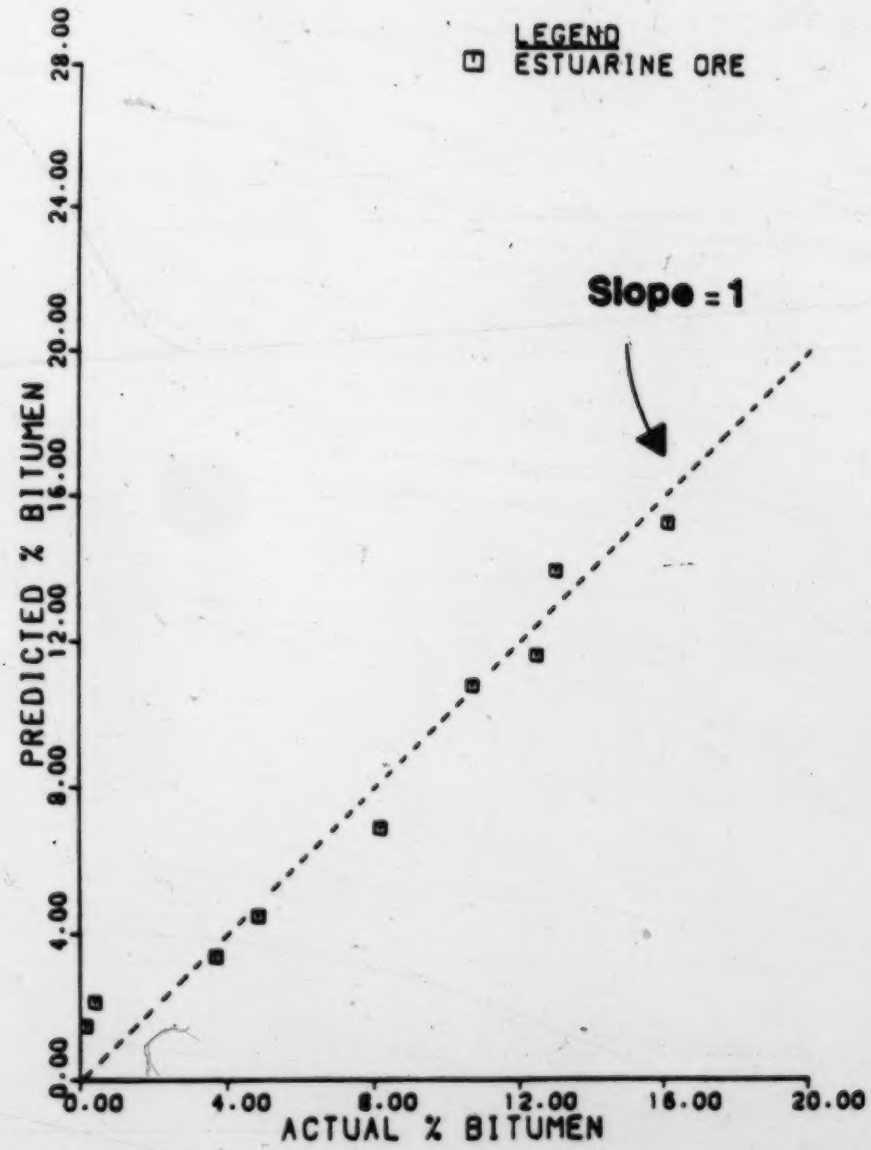


**Figure 14.** Correlation between measured bitumen assays for an estuarine oil sand sample and those predicted from a linear model based on absorbance readings at 1725, 2200, and 2285 nm. The dashed line represents an ideal fit.

**Table IV.** Regression statistics for a linear model relating spectral features and sample bitumen content for an estuarine oil sand.

| | | |
|---|---|---|
| Dependent Variable | $Y$ | Anhydrous Bitumen Content (wt %) |
| Independent Variables | $X1$ | Absorbance at 2285 nm |
| | $X2$ | Absorbance at 1725 nm |
| | $X2$ | Absorbance at 2200 nm |

| | |
|---|---|
| PERCENT VARIATION EXPLAINED | 94.88 |
| MEAN OF THE RESPONSE | 8.308 |
| DEGREES OF FREEDOM | 26 |
| MULTIPLE CORRELATION COEFFICIENT | 0.9741 |

| VARIATION SOURCE | SUM OF SQUARES | DEGREES OF FREEDOM | VARIANCE | STANDARD DEVIATION | F-VALUE |
|---|---|---|---|---|---|
| TOTAL | 659.0 | 29 | | | |
| REGRESSION | 625.3 | 3 | 208.4 | 14.44 | 160.6 |
| RESIDUAL | 33.75 | 26 | 1.298 | 1.139 | |

| INDEPENDENT VARIABLE | PARAMETER ESTIMATE | STD ERROR | t-VALUE |
|---|---|---|---|
| X1 | 63.86 | 22.57 | 2.830 |
| X2 | -75.72 | 92.60 | -0.818 |
| X3 | -80.04 | 23.44 | -3.414 |
| CONSTANT TERM | 4.097 | | |

correlation.

The fact that absorbances at 2200 nm constitute a significant term in a function predicting bitumen concentration implies that measures for the amount of clay in a sample can provide an ancillary estimate of hydrocarbon saturation. For reasons cited above, this is not a simple artifact of the inverse relationship between solids content and bitumen assay. The relative proportion of clay in the solids fraction extracted from a variety of oil sands is not necessarily a constant.

## 2.2 Studies With a Cary 17 UV–VIS–NIR Spectrophotometer

Diffuse reflectance spectra for oil sand samples were also obtained using a Cary 17 UV–VIS–NIR spectrophotometer equipped with an integrating sphere type accessory affixed to the sample compartment of the instrument. The device and optical arrangement are schematically illustrated in Figure 15. Incident radiation reflected from the sample is captured by the sphere and directed to the detector. The internal surface of the integrating sphere is coated with a thin film of MgO. Note that the collection of all diffuse reflectance from the sample enables a large signal to reach the detector. Further, any directional dependence of the reflected light is eliminated since the sphere collects energy from all directions. Specular reflectance (glare from the sample) is essentially negligible. The specular component is directed back through the entrance port.

Incident radiation was provided from a tungsten halogen source with the reflected light measured using a lead sulfide detector. Wavelengths scanned covered the range 2000–2500 nm. All spectra were recorded in absorbance mode (span 0–1.0 absorbance units).

Replicate spectra obtained for samples of lean, average, and rich grade ore (approximately 6%, 10%, and 12% bitumen content, respectively) are shown in Figures 16–18. From previous studies, one would expect to see strong absorbance peaks (doublets) due to bitumen centered at 2285 and 2330 nm as well as a much weaker band at 2200 nm depicting the presence of clays. Further, the relative peak height

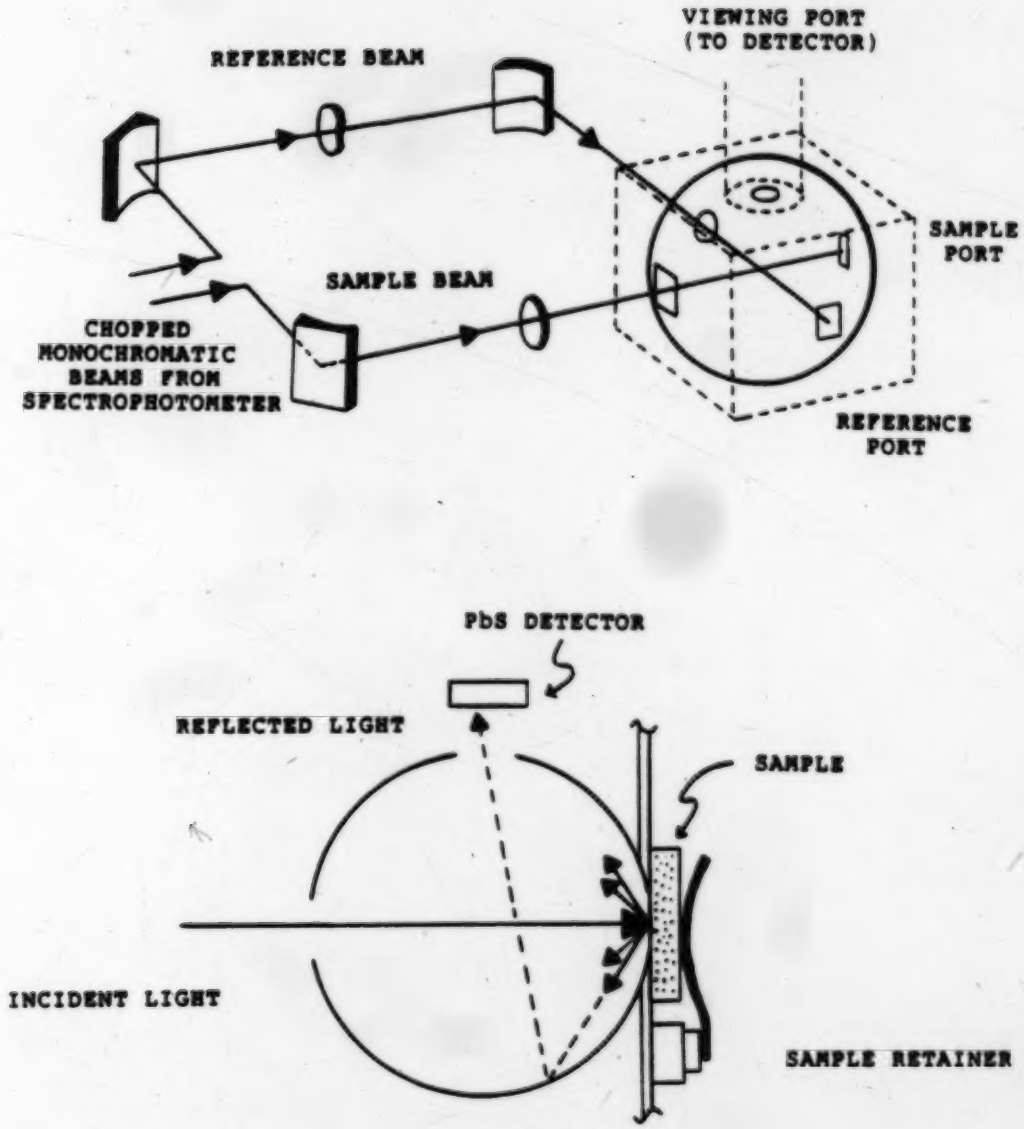


**Figure 15.** Optical diagram of an integrating sphere used for diffuse reflectance measurements.

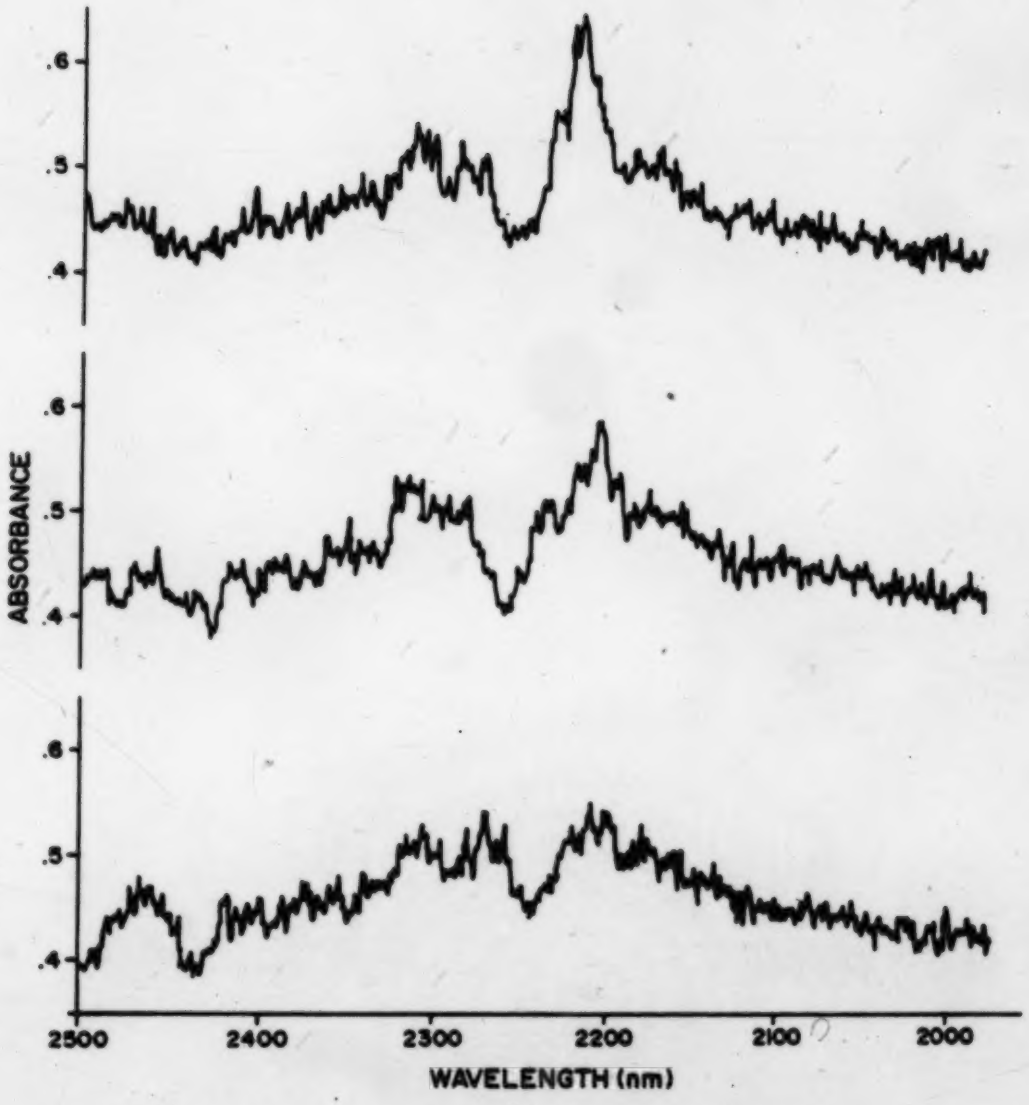


**Figure 16.** NIR diffuse reflectance spectra obtained for a lean grade oil sand sample using a Cary 17 UV–VIS–NIR spectrophotometer and integrating sphere.

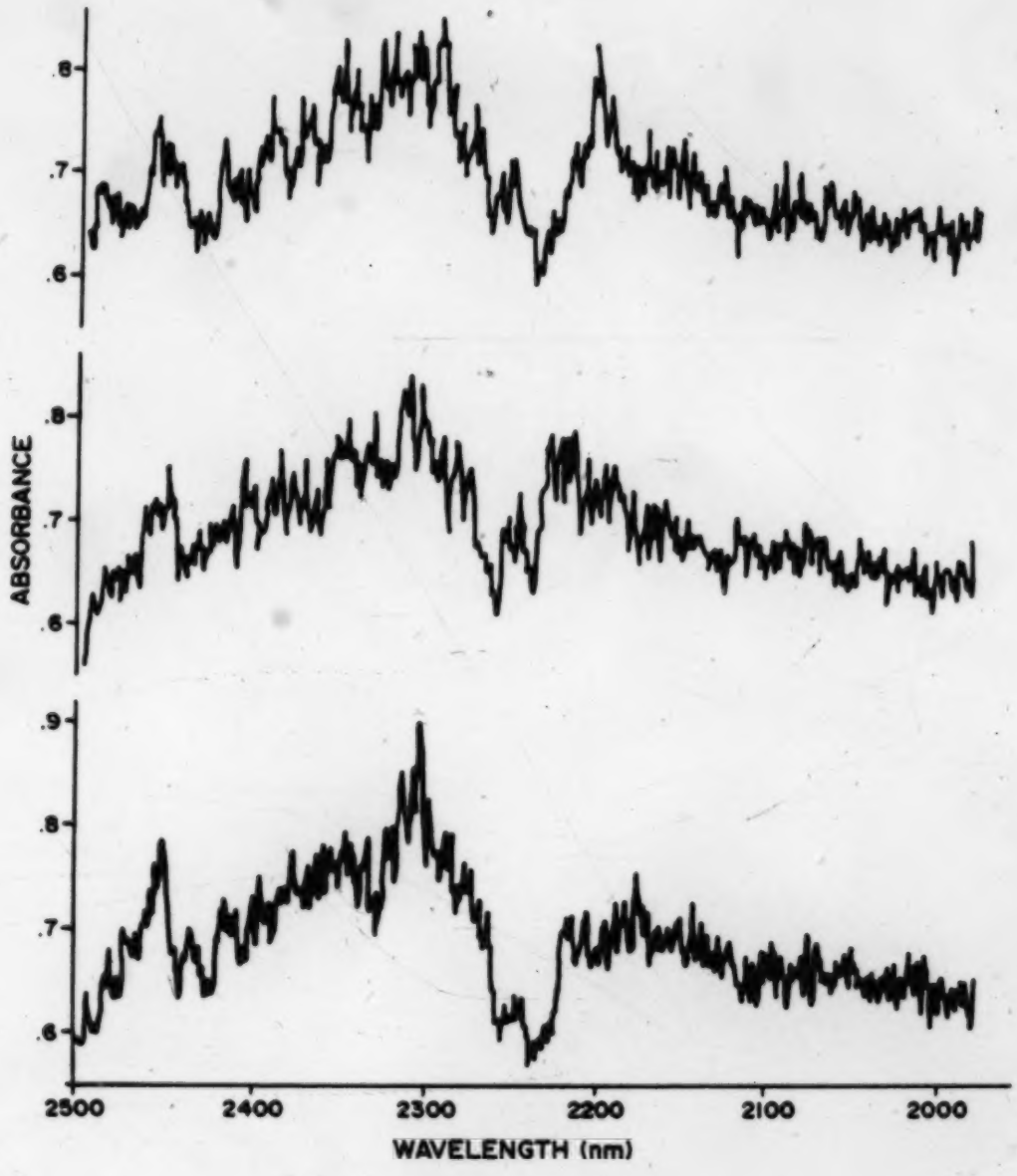


**Figure 17.** NIR diffuse reflectance spectra obtained for an average grade oil sand sample using a Cary 17 UV-ViS-NIR spectrophotometer and integrating sphere.

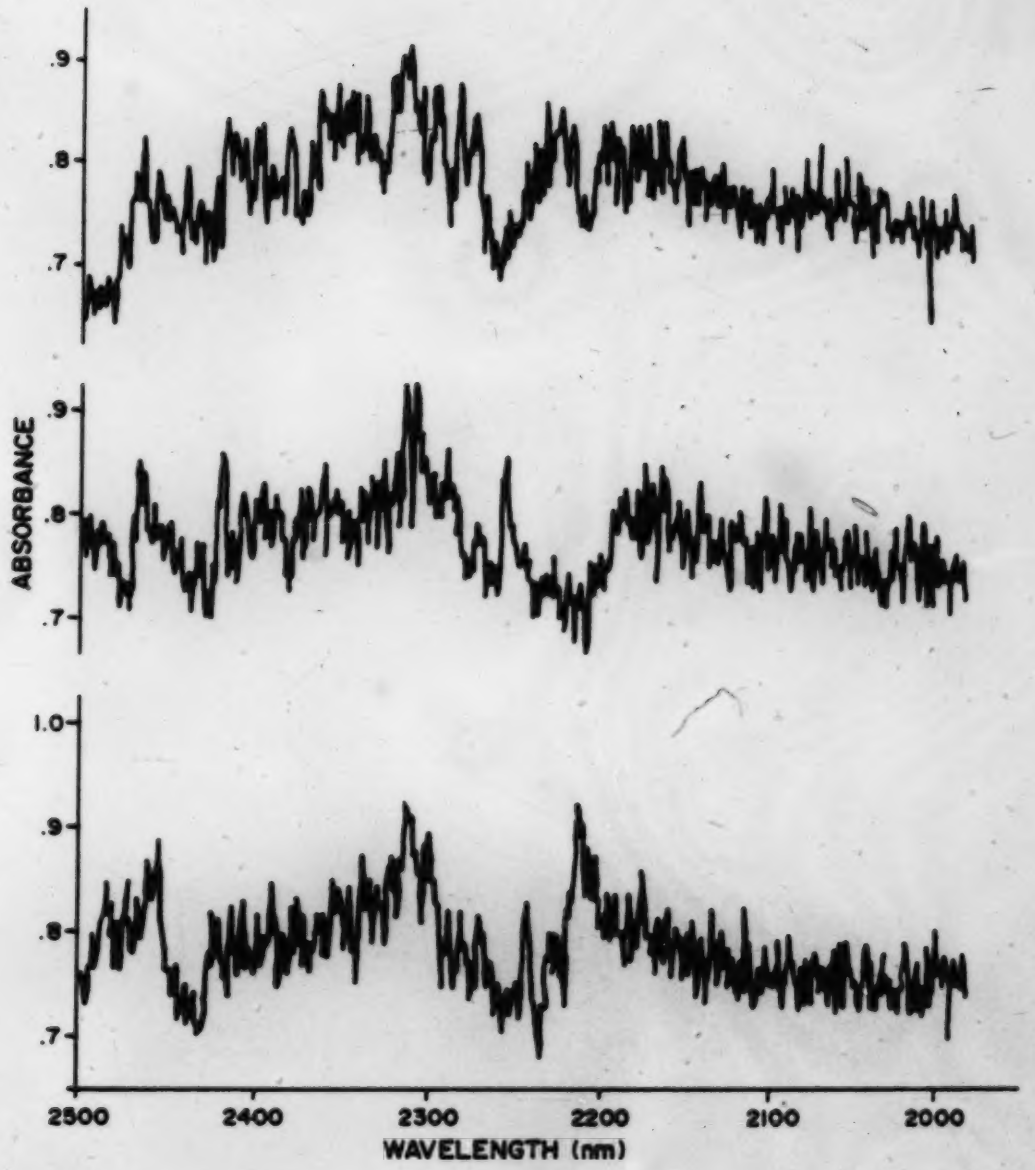


**Figure 18.** NIR diffuse reflectance spectra obtained for a rich grade oil sand sample using a Cary 17 UV–VIS–NIR spectrophotometer and integrating sphere.

of the bitumen bands should increase with increasing hydrocarbon saturation. Overall reflectance will typically increase (*ie.* lower baseline absorbance) as the grade of the sample decreases.

Unfortunately, the spectra generated with the Cary 17 were severely corrupted with noise, owing to the low sensitivity of the detector system. Only general features could be discerned. As such, the spectra did not merit further interpretation. It was concluded that use of this spectrophotometer and integrating sphere should not be considered for quantitative NIR–DR analysis of oil sands. Although the integrity of the spectra could be enhanced by using multiple scans and digital processing of detector signal, the approach would be tedious. The use of other NIR–DR instruments which already include these facilities is clearly preferred.

Although the spectra obtained with the Cary 17 are not useful for the analysis of oil sand samples, the earlier results generated using the Nicolet FT–IR were encouraging. The data indicates that the bitumen content of oil sand samples can be determined from near–infrared absorbance measurements. Combining the basic technique with more sophisticated data handling and multivariable statistical analysis procedures for correlating spectral response and bitumen assay could greatly enhance the utility of the method. The remainder of this report deals with the analysis of oil sand in a core using a microprocessor based instrument specifically designed for NIR–DR analysis.

# 3. NIR–DR MEASUREMENTS FOR THE GRADE OF OIL SAND CONTAINED WITHIN A CORE

Aside from establishing the applicability of an instrumental technique for determining the bitumen content of oil sand samples, an objective of this work is to evaluate the compositional variability of an oil sand deposit in vertical cross–section. Results are based on NIR–DR measurements obtained at 1 cm intervals along a length of core. The high resolution profile depicting the fluctuations in oil sand grade as a function of depth will be used to establish a semi–variogram for modelling compositional trends. The study is designed to provide a foundation for the development of sampling protocols for materials wherein the variable of interest is regionalized and changes as a function of spatial location.

In order to provide the extensive data base required for such an assessment (and to accomplish this within a reasonable time frame) it is desirable that analyses be performed using a spectrophotometer having rapid data acquisition and processing capabilities. These qualities are met in the design of the Quantum 1200 Near–Infrared Analyzer marketed by LT Industries Inc. One of these instruments was recently purchased by Syncrude Canada Ltd. and made available for core analysis.

## 3.1 Description of the Equipment

The LTI Quantum 1200 Near–Infrared Analyzer is a dedicated, micro–processor controlled NIR–DR spectrophotometer developed for on–line and laboratory applications. Spectral response covers the range 1200–2400 nm (grating monochromator). The high speed optics permit spectra to be obtained at the rate of 5 scans per second with a spectral resolution of 1 nm. Sample illumination is provided with a tungsten–halogen lamp. Reflected light is monitored with a pair of lead sulfide detectors. The arrangement of the optical system is shown in Figure 19.

The instrument was interfaced with a Compaq Deskpro 286 computer to run the accompanying LT SpectraMetrix Software Package. These algorithms drive the data acquisition, mathematical processing, modelling, and graphing functions for

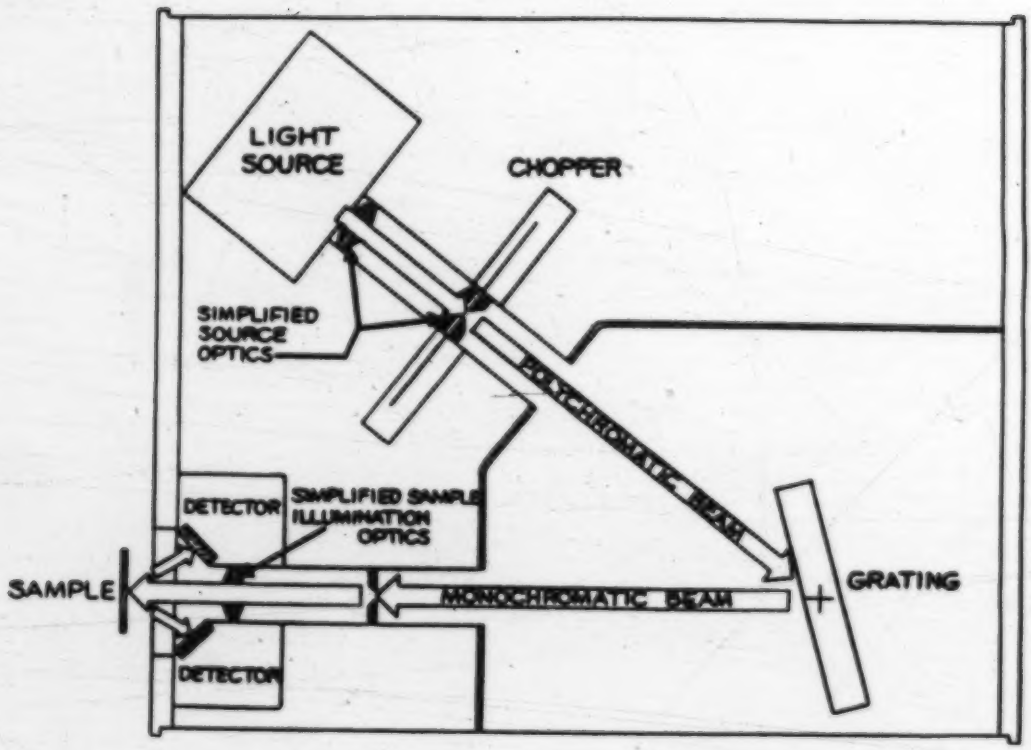


**Figure 19.** Optical arrangement within the LTI Quantum 1200 NIR Analyzer.

the analyzer. A number of diagnostic routines are included to verify the operation and performance of the unit.

An important feature of the LTI Quantum 1200 Near-Infrared Analyzer is its relatively small size. The unit is extremely rugged and can be conveniently operated in any desired spatial orientation. For analyzing oil sand samples contained within a section of core, the instrument was positioned on end such that the incident radiation could be directed downward onto the surface of the sample. A specialized sampling table, consisting of a core holder, registration guide, and bridge assemply for mounting the spectrophotometer, was constructed to permit core to be rastered beneath the viewing port at discrete 1 cm intervals. The viewing port itself was masked to provide a square sample window measuring 1 cm on a side. A schematic of the sampling table is provided in Figure 20. The overall arrangement of the equipment is illustrated in Figure 21.

### 3.2 Test Section of Core

As previously introduced, the core sample made available for this study represents a vertical transect of the Athabasca oil sand deposit in a region known as Syncrude Canada Ltd. Lease 22. The core is approximately 120 metres in length and was originally encased in a plastic core barrel having an inside diameter of approximately 6.4 cm and wall thickness of 0.1 cm. As the result of earlier processing, the core has been cut in half longitudinally and a V-notch sample removed from along the center line. The core has been stored under ambient conditions since it was first analyzed. Consequently, the oil sand contained within the core is virtually devoid of water.

A small section of this core, just over 4 metres in length, was selected for detailed NIR-DR analysis. The section was chosen to represent what appeared to be typical of grade variations seen over the entire length of core. Photographs of the sample, indicating the elevation at which the sample was taken and the geological environments from which the material originated, are shown in Figures 22 and 23.

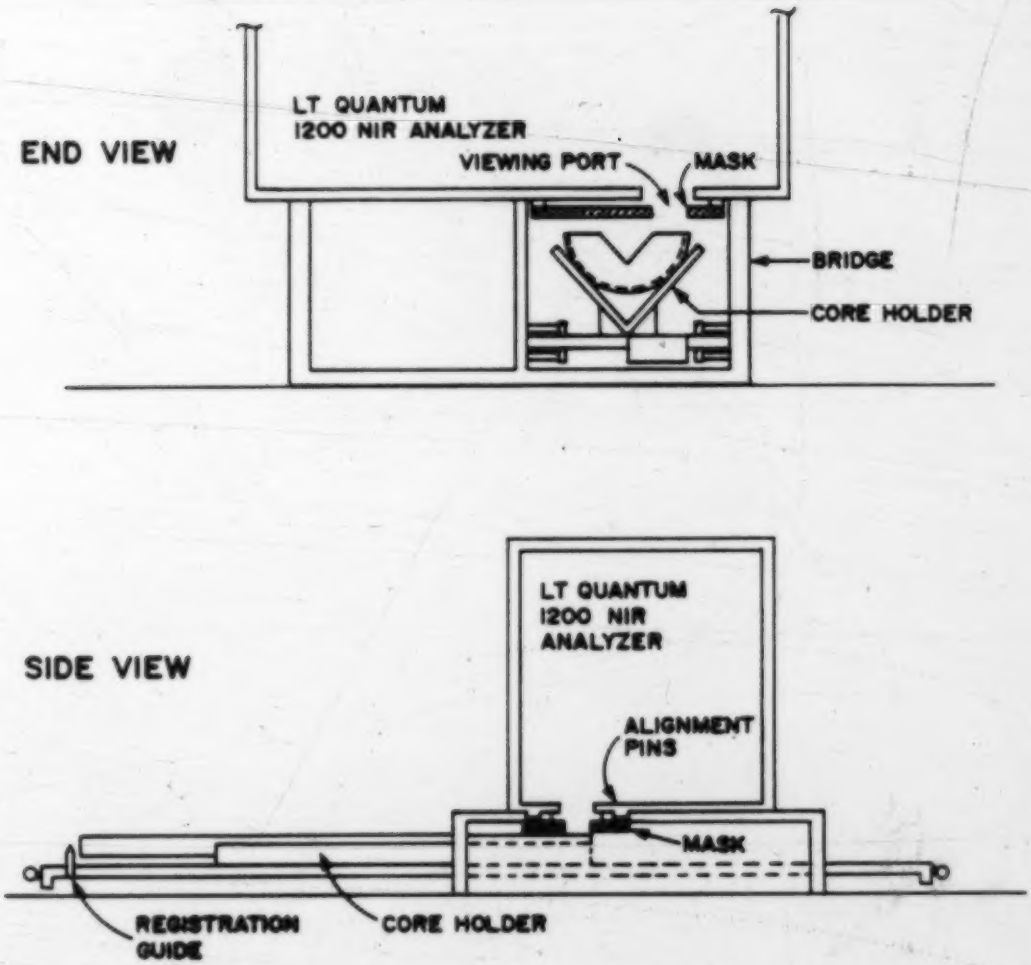


**Figure 20.** Schematic illustration of sampling table constructed for core analysis.

**Figure 21.** General arrangement of LTI Quantum 1200 NIR Analyzer, sampling table, and peripheral equipment.

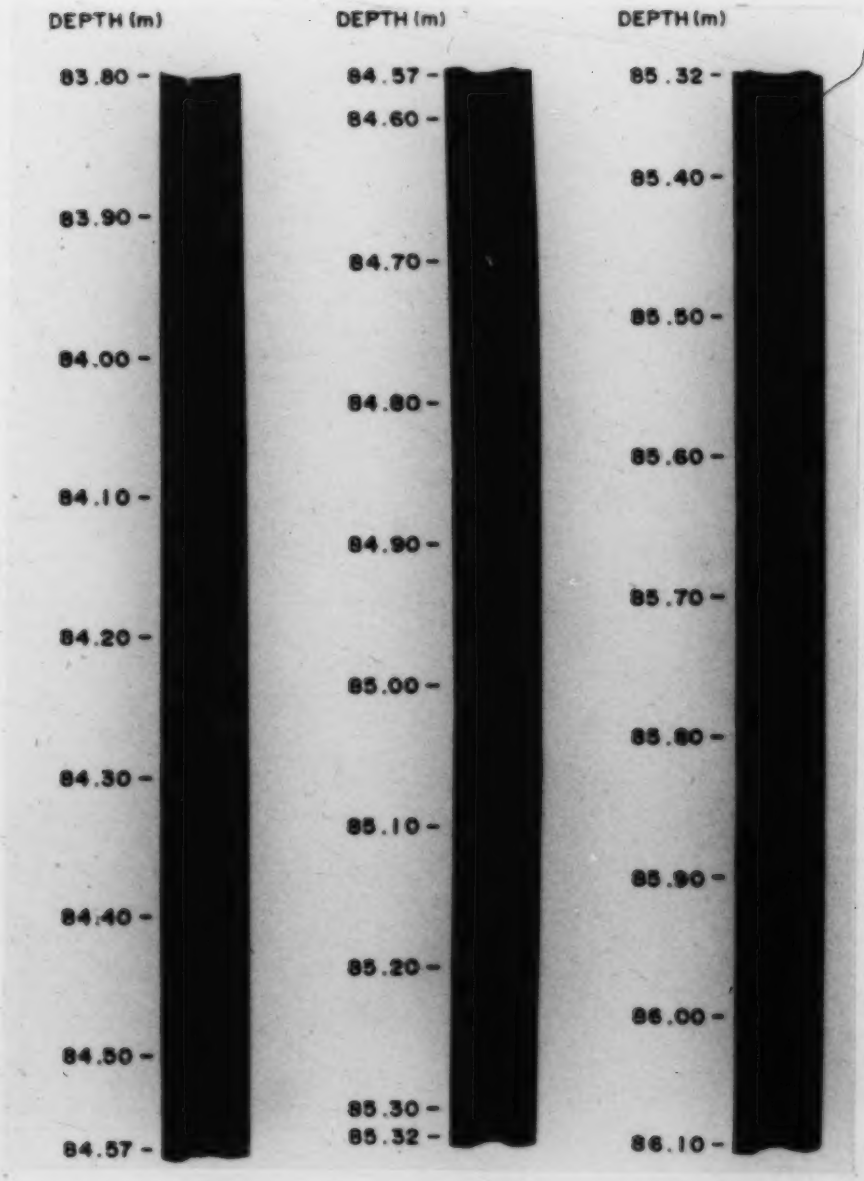


**Figure 22.** Photographs of the test core section over the depth interval 83.8 – 86.1 metres.

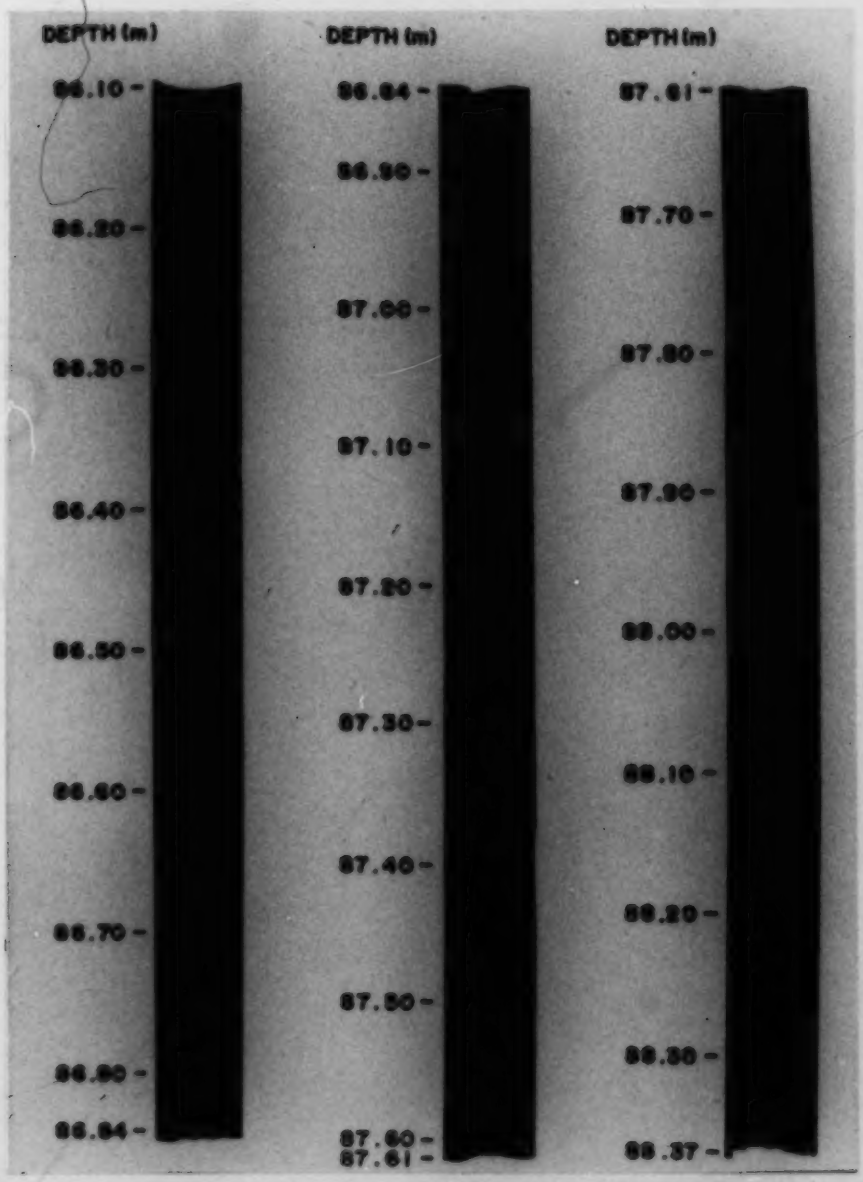


**Figure 23.** Photographs of the test core section over the depth interval 86.1 – 88.4 metres.

## 3.3 Instrumental Conditions

Before proceeding with a comprehensive study of the test core section, a series of experiments were conducted to evaluate the operation of the NIR–DR analyzer and determine the optimal instrumental conditions for oil sand analysis. Procedural notes and a discussion of these results follows.

### 3.3.1 Sample Window

A test was undertaken to determine the location and area of the sample window when viewing core samples. Proper orientation of the core in relation to the optical path of the NIR analyzer is obviously essential for consistent and accurate results.

A paper test pattern consisting of light and dark areas of known geometry was used to evaluate the alignment and dimensions of the optical window. The template was overlayed on the core barrel and registered as indicated in Figure 24. The surface of the template was positioned parallel to the sample table and normal to the optical path (horizontal checked with a line level). Overall reflectivity and other spectral features of the light and dark areas differ. Reference spectra are shown in Figure 25.

NIR data were collected at regular intervals as the sample table was rastered beneath the viewing port. Template location was recorded from the vernier. All spectra were obtained by averaging 10 scans over the wavelength region 1200–2400 nm. Spectra were corrected for a background response measured at the 3 cm mark (light area of template).

Original reflectance data were transformed as $Log(1/R)$. Absorbance data obtained at 1800 nm (a reasonably flat region in the spectra thought to be indicative of transitions from light to dark regions) is presented in Table V. Results are plotted as a function of measured template location in Figure 26.

The geometry of the sample window was determined on the basis of peak half heights as shown in Figure 27. Results indicate that the area viewed is square,

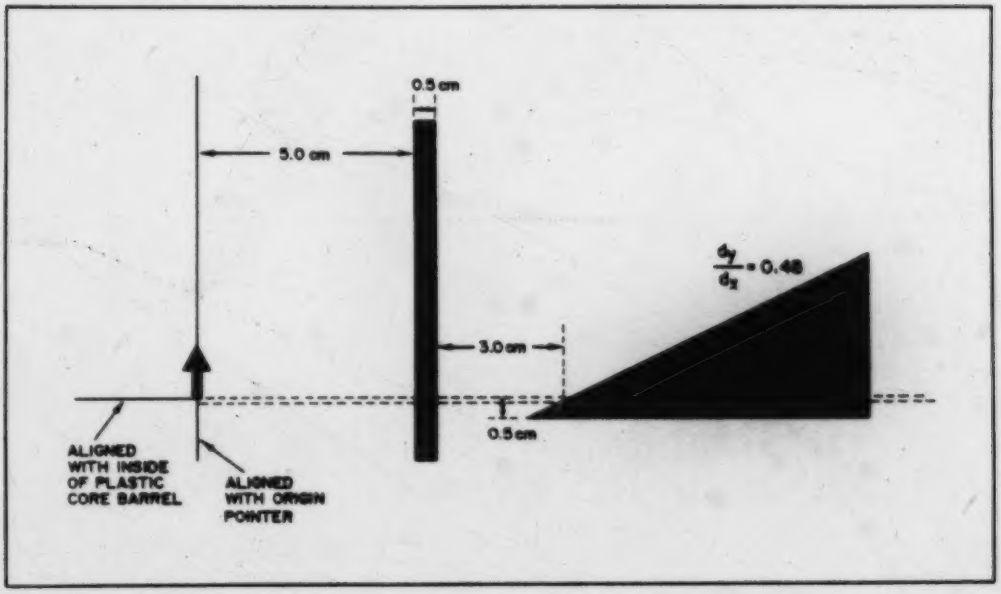


**Figure 24.** Optical template used to evaluate the alignment and dimensions of the sample window for diffuse reflectance measurements.

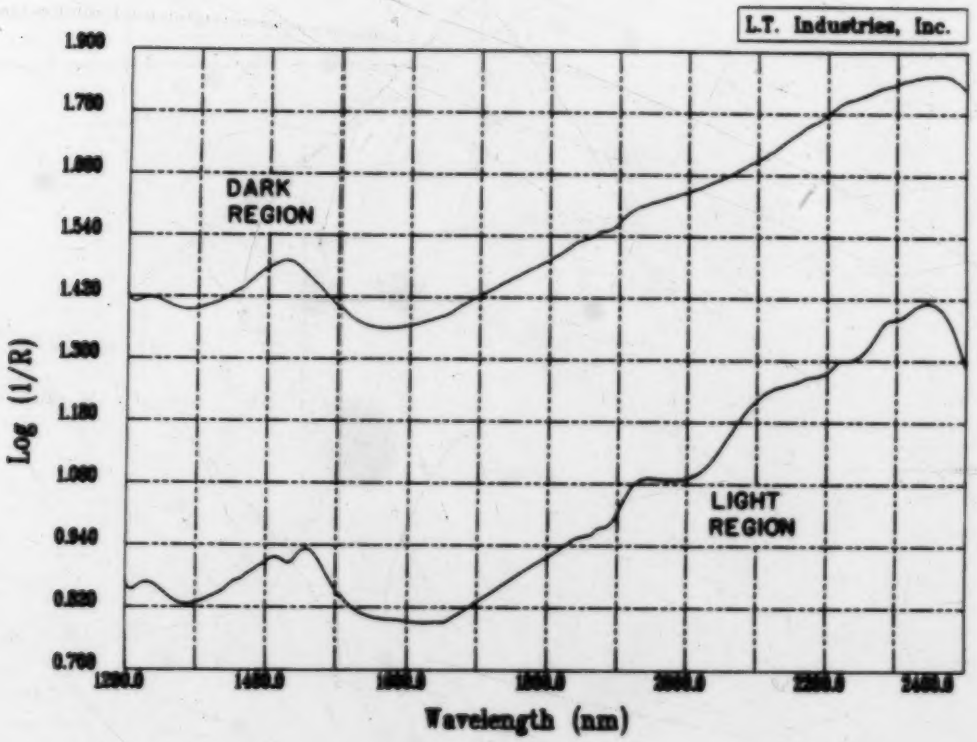


**Figure 25.** Diffuse reflectance spectra of the light and dark regions of the optical template (Background = 1.0).

**Table V.** Absorbance measurements obtained from the optical template as a function of location along the sampling table.

| VERNIER READING (cm) | ABSORBANCE AT 1800 nm | VERNIER READING (cm) | ABSORBANCE AT 1800 nm |
|---|---|---|---|
| 3.00 | 0.000 | 6.40 | 0.009 |
| 3.10 | 0.001 | 6.50 | 0.011 |
| 3.20 | 0.000 | 6.60 | 0.012 |
| 3.30 | 0.000 | 6.70 | 0.012 |
| 3.40 | 0.000 | 6.80 | 0.014 |
| 3.50 | 0.002 | 6.90 | 0.016 |
| 3.60 | 0.002 | 7.00 | 0.018 |
| 3.70 | 0.004 | 7.20 | 0.020 |
| 3.80 | 0.004 | 7.40 | 0.027 |
| 3.90 | 0.005 | 7.60 | 0.034 |
| 4.00 | 0.007 | 7.80 | 0.040 |
| 4.10 | 0.004 | 8.00 | 0.045 |
| 4.20 | 0.035 | 8.20 | 0.048 |
| 4.30 | 0.073 | 8.40 | 0.051 |
| 4.40 | 0.121 | 8.60 | 0.053 |
| 4.50 | 0.168 | 8.80 | 0.056 |
| 4.60 | 0.207 | 9.00 | 0.060 |
| 4.70 | 0.224 | 9.20 | 0.068 |
| 4.80 | 0.226 | 9.40 | 0.082 |
| 4.90 | 0.220 | 9.60 | 0.105 |
| 5.00 | 0.202 | 9.80 | 0.135 |
| 5.10 | 0.169 | 10.00 | 0.186 |
| 5.20 | 0.114 | 10.20 | 0.233 |
| 5.30 | 0.095 | 10.40 | 0.310 |
| 5.40 | 0.049 | 10.60 | 0.372 |
| 5.50 | 0.019 | 10.80 | 0.451 |
| 5.60 | 0.005 | 11.00 | 0.507 |
| 5.70 | 0.006 | 11.20 | 0.536 |
| 5.80 | 0.007 | 11.40 | 0.558 |
| 5.90 | 0.009 | 11.60 | 0.562 |
| 6.00 | 0.009 | 11.80 | 0.562 |
| 6.10 | 0.007 | 12.00 | 0.563 |
| 6.20 | 0.008 | 12.20 | 0.564 |
| 6.30 | 0.008 | 12.40 | 0.565 |

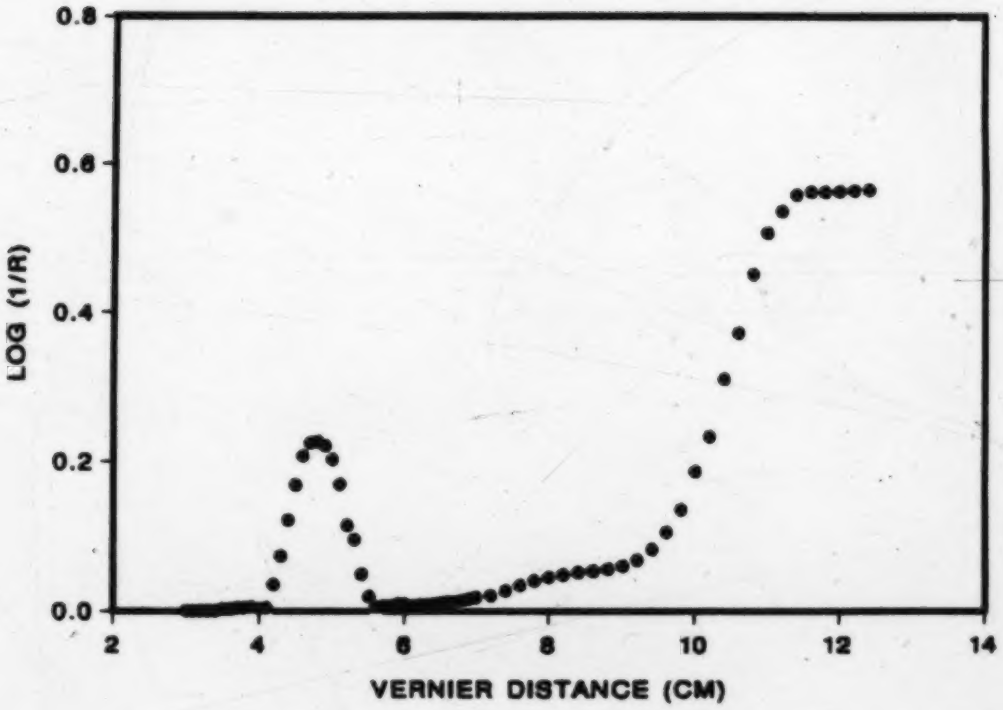


**Figure 26.** Plot of absorbance readings obtained from the optical template as a function of location along the sampling table.

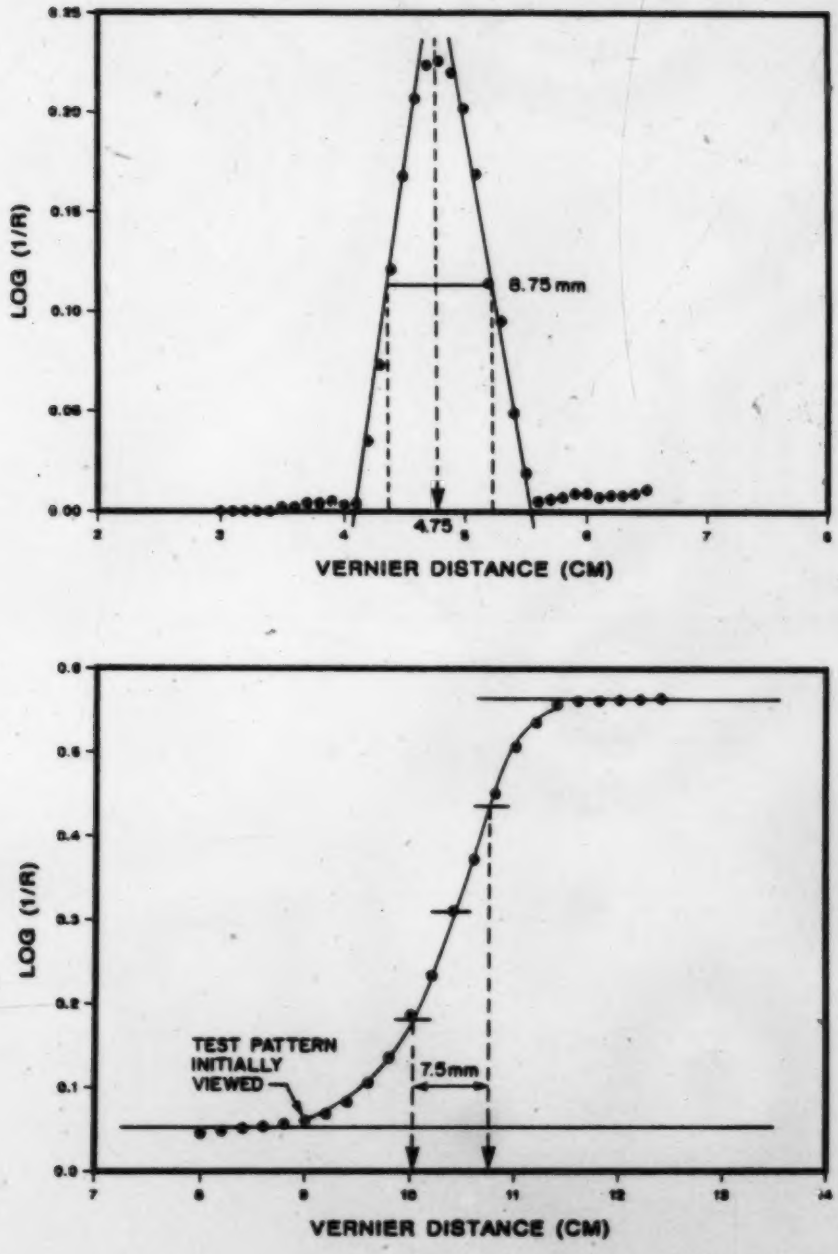


**Figure 27.** Plot of absorbance readings as a function of optical template location indicating the measurements used to establish the geometry of the sample window.

approximately 0.8 cm along a side. The sample window does not overlap the plastic core barrel. A clearance of approximately 2 mm is provided. Given that the face of the core presented for analysis is nominally 1 cm wide, a portion of the V-notch is viewed.

Based on the actual position and dimensions of the vertical bar on the template, a maximum in absorbance data is expected to occur at a distance of 5.25 cm from the origin. The vernier reading at this maximum is 4.75 cm. Thus, when registering core samples, a given vernier reading corresponds to a sample centered at that distance plus 0.5 cm. For a vernier reading of 1.0 cm, the sample window viewed is 1.1-1.9 cm along the sample table axis.

### 3.3.2 Selection of Background Reference Material

The objective of this work was to select a suitable reference material for background corrections. The desired qualities of a reference material are that it be relatively devoid of spectral features and exhibit a low overall reflectivity.

Spectra were obtained for a variety of proposed reference materials. These included:

- Silica Sand (-50 +80 Mesh)
- KBr Powder (Spectral Grade)
- White Paper Test Card
- Black Paper Test Card
- Ceramic (Alumina)
- Ceramic (LTI Standard Reference)
- Carbon Black (Darco G-60 Activated Carbon)

Samples were positioned in the optical path of the instrument at a constant elevation from the sample table. The plane of the sample surface was at the same height as that of a core when placed in the horizontal position. Particulate samples were placed in a small tray. The surface of these material was prepared by simply

screeding with a straight edge.

Spectra were recorded using 10 scans over the wavelength region 1200–2400 nm (Background = 1.0). Results, transformed as $Log(1/R)$, are presented in Figures 28–30. Spectra obtained in like manner for a typical oil sand and clay region in a core sample are shown in Figure 31.

Carbon black appears to be the most suitable reference material. It exhibits a high absorptivity (low reflectance) and is relatively featureless over most of the wavelength range. The broad absorption band centered at approximately 1430 nm in the spectrum of carbon black is also prevalent in the spectrum of the oil sand sample. The spectrum of clay is more like that of the silica sand and ceramics, showing two absorbance bands at 1410 nm and 1460 nm.

Spectra of oil sand and clay when ratioed against carbon black exhibit the signature absorbances characteristic of the hydrocarbon and mineral components. Data is presented in Figure 32. For comparison, the spectrum of oil sand corrected for a silica sand background is shown in Figure 33. It is not as well defined. A spectrum of silica sand ratioed against carbon black is also illustrated.

Discontinuities in the spectra observed over the wavelength range 1400–1500 nm (water absorbing region) are the result of over and under compensation by the background. This could present difficulties when attempting to correlate NIRA response and component assay data using the modelling programs available on the system. It is recommended that spectra be collected over the limited range of 1500–2400 nm.

### 3.3.3 Sample Elevation

A study was conducted to evaluate the sensitivity of detector response to changes in sample elevation. Spectra were obtained for samples of carbon black and oil sand, each contained within a split core barrel.

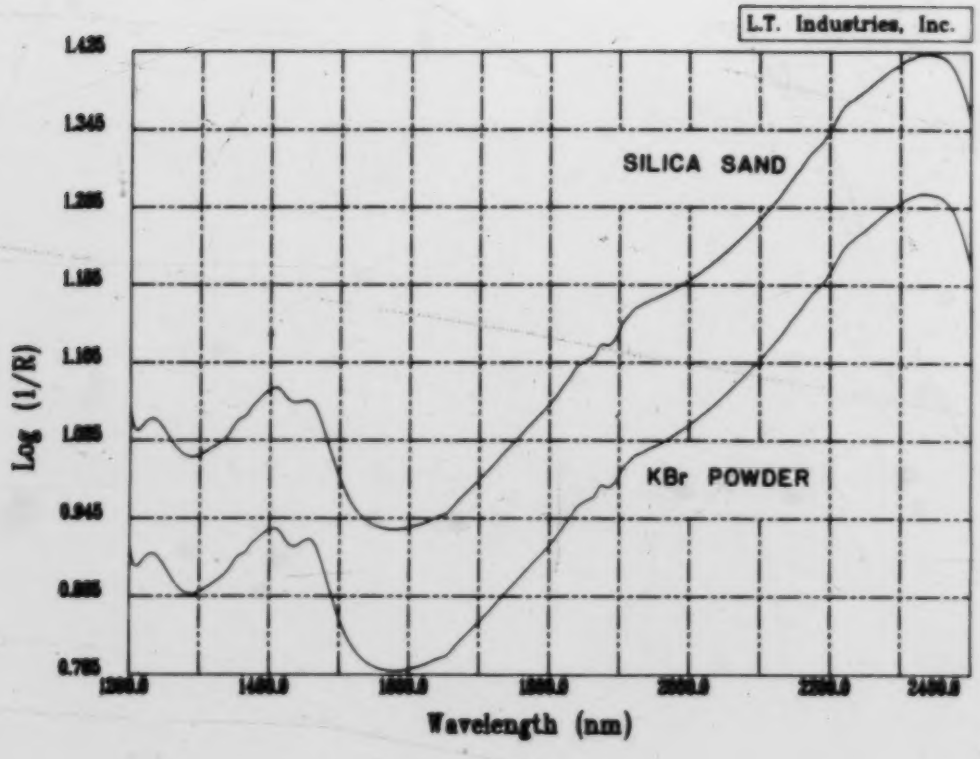


**Figure 28.** Diffuse reflectance spectra of silica sand and KBr powder (Background = 1.0).

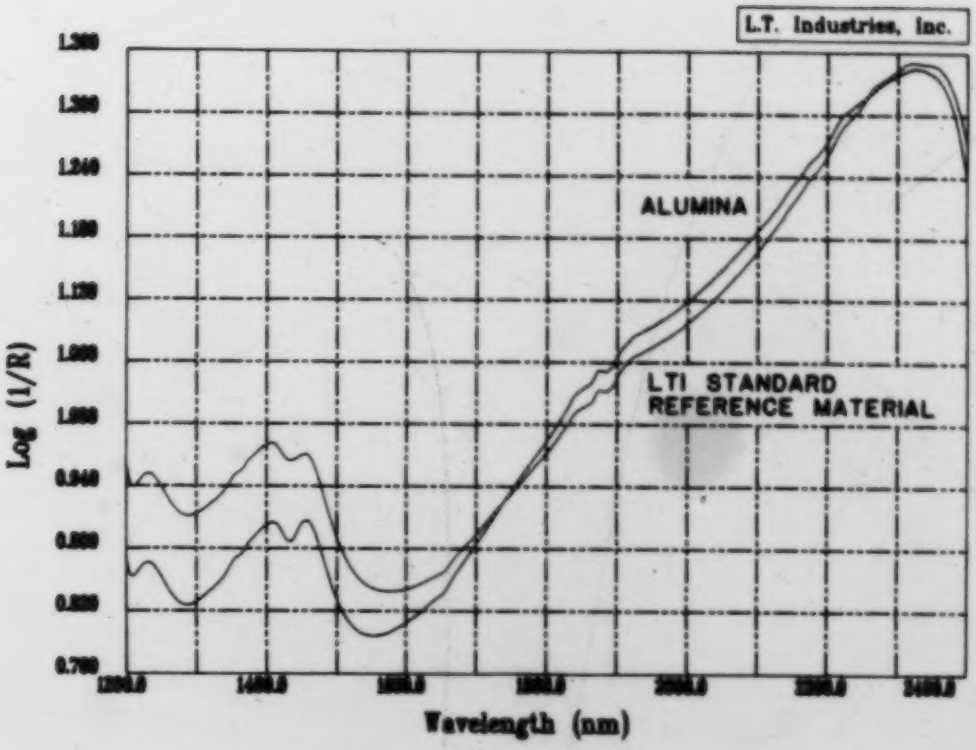


**Figure 29.** Diffuse reflectance spectra of various ceramic materials (Background = 1.0).

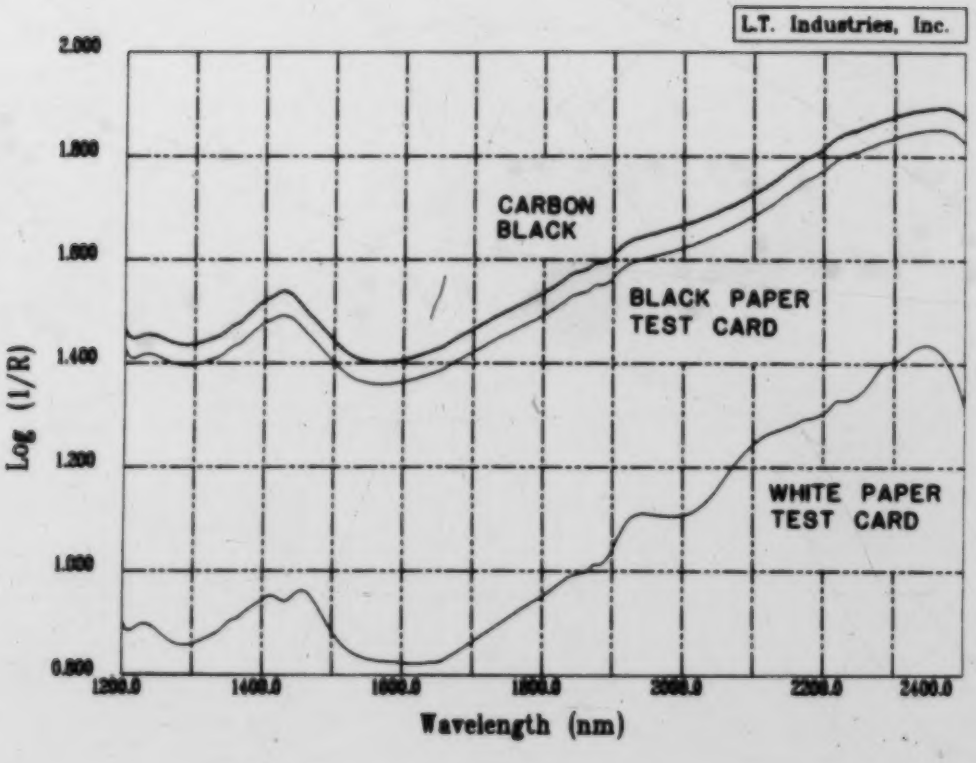


**Figure 30.** Diffuse reflectance spectra of carbon black and various paper test cards (Background = 1.0).

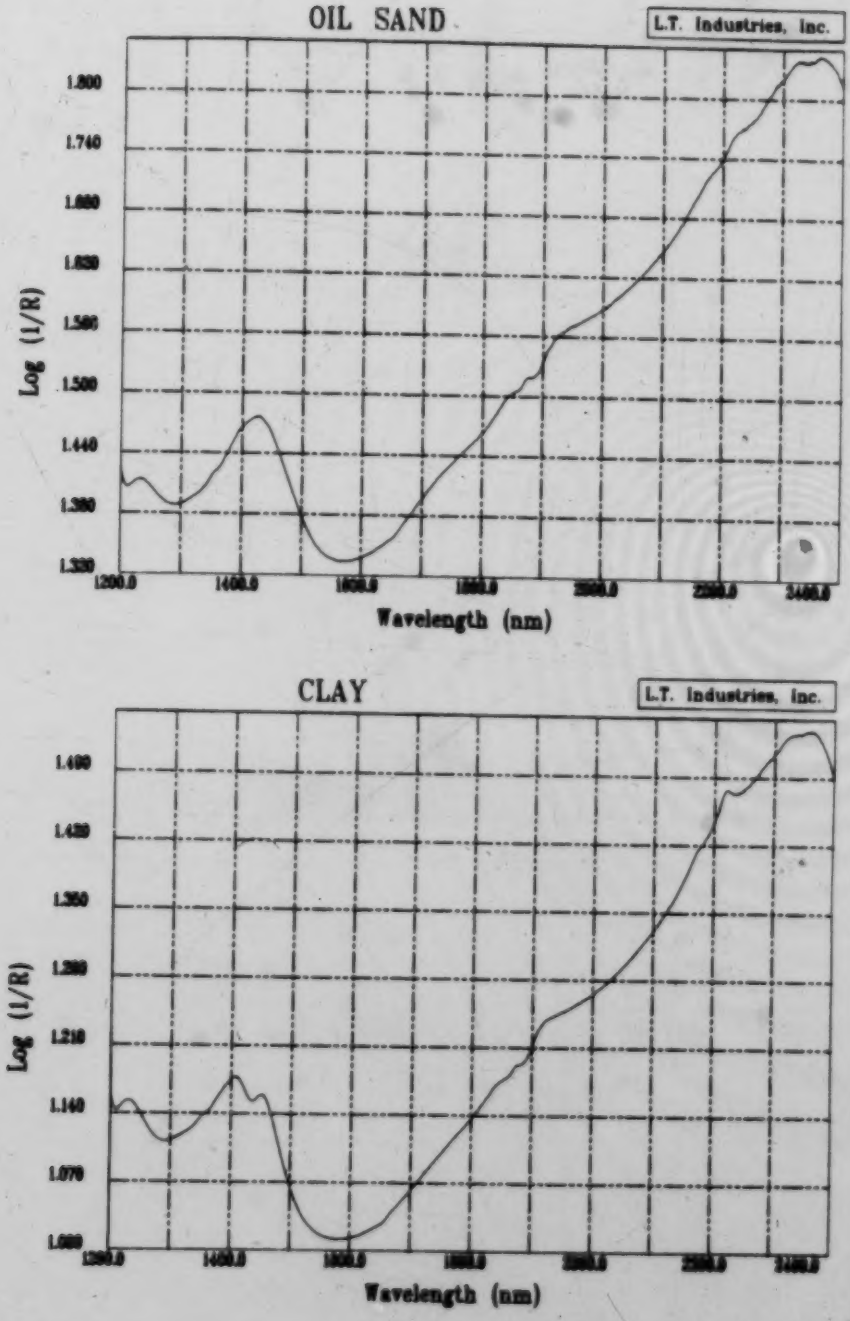


**Figure 31.** Diffuse reflectance spectra of oil sand and clay (Background = 1.0).

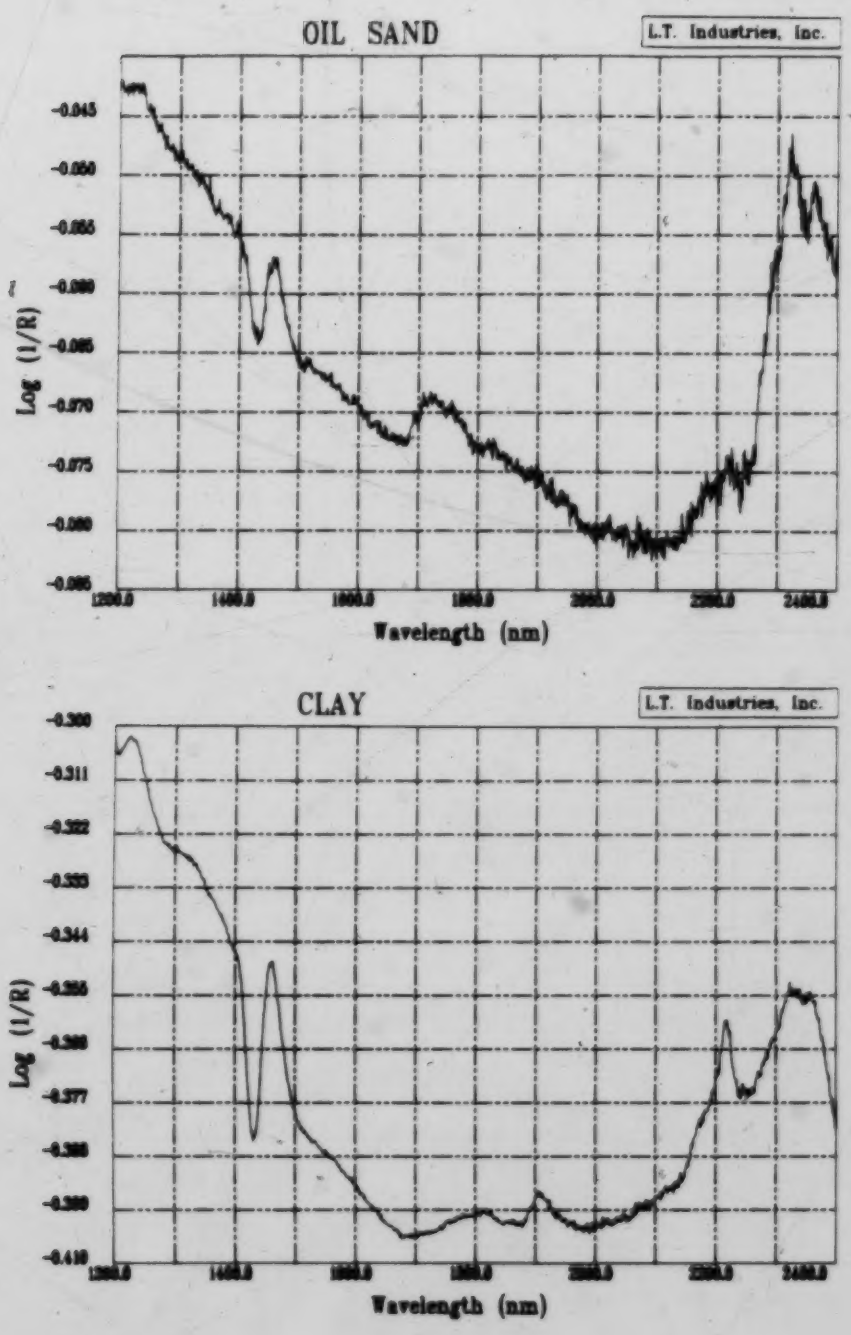


**Figure 32.** Diffuse reflectance spectra of oil sand and clay (Background = carbon black).

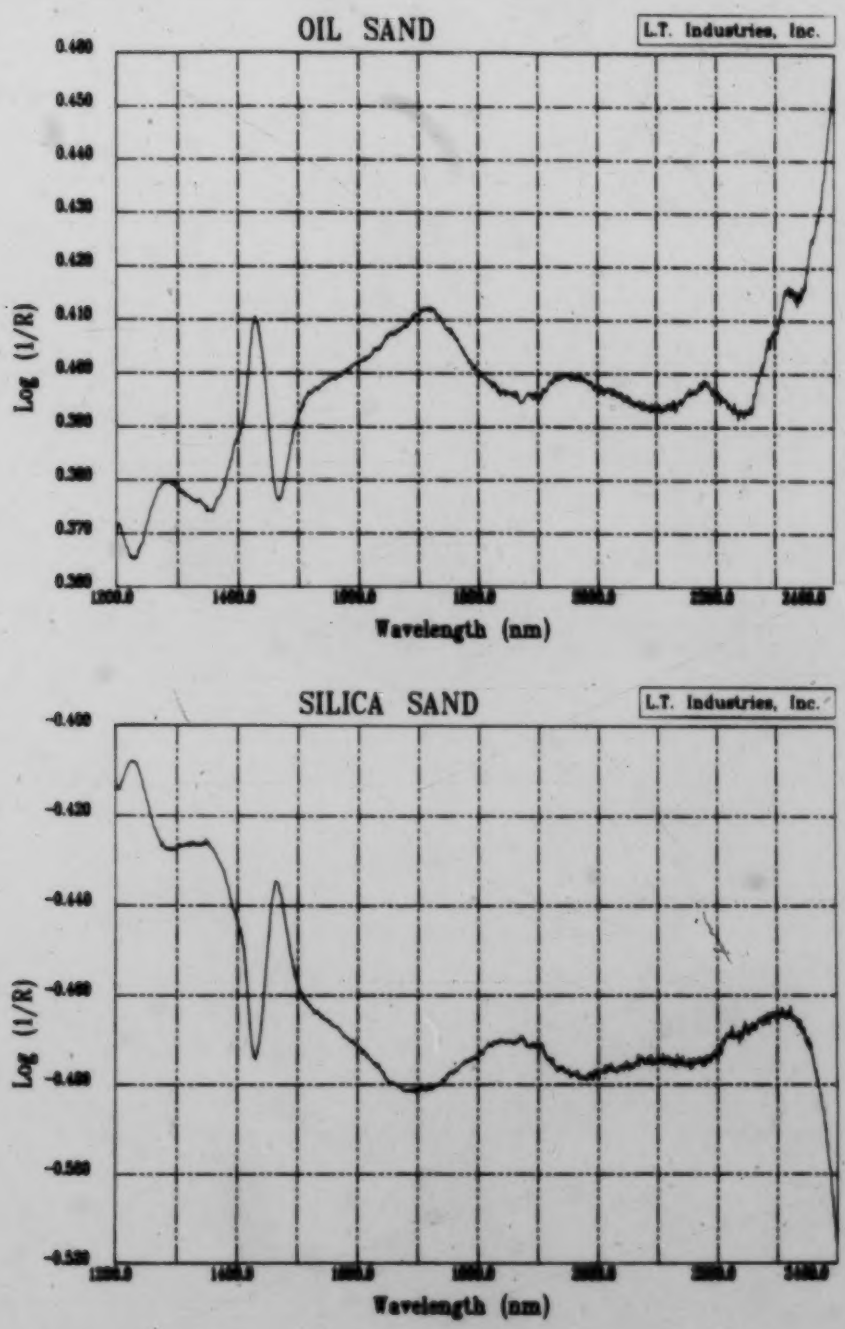


**Figure 33.** Diffuse reflectance spectra of oil sand (Background = silica sand) and silica sand (Background = carbon black).

| | |
|---|---|
| Number of scans | 10 |
| Wavelength Range | 1200–2400 nm |
| Background | Carbon Black |

Samples were placed at a reference elevation (52 mm above sample table) with surface plane normal to the optical path. Comparative spectra were then recorded after moving the sample surfaces up and down 2 mm from the original position. Note that this operation imparts an angular deflection to the surface of approximately 5 degrees from the normal.

Absorbance spectra for carbon black are presented in Figure 34. It would appear that minor changes in sample elevation significantly alter the intensity of light reflected back to the detectors. Results suggest that moving the sample surface up or down 2 mm from the reference elevation affects the gain by approximately 2% relative. This was determined as follows:

Define:

| | |
|---|---|
| $S(0)$ | Reflectance spectrum of sample at the reference elevation. |
| $G(0)$ | Instrumental gain for detector response at the reference elevation. |
| $S(X)$ | Reflectance spectrum of sample at $\pm$2mm from the reference elevation. |
| $G(X)$ | Instrumental gain at either of these positions. |

Assuming gains to be constant over all wavelengths, the following equality holds:

$$\frac{S(X)}{G(X)} = \frac{S(0)}{G(0)} \quad \text{and hence} \quad S(X) = \frac{G(X)}{G(0)} S(0)$$

Taking Logs of reciprocal terms leads to the expression:

$$Log \frac{1}{S(X)} = Log \frac{G(0)}{G(X)} + Log \frac{1}{S(0)}$$

Substituting mean absorbance values as the characteristic feature of the spectra yields the relationship:

$$A(X) = Log \frac{G(0)}{G(X)} + A(0) \quad \text{and thus} \quad Log \frac{G(0)}{G(X)} = A(X) - A(0)$$

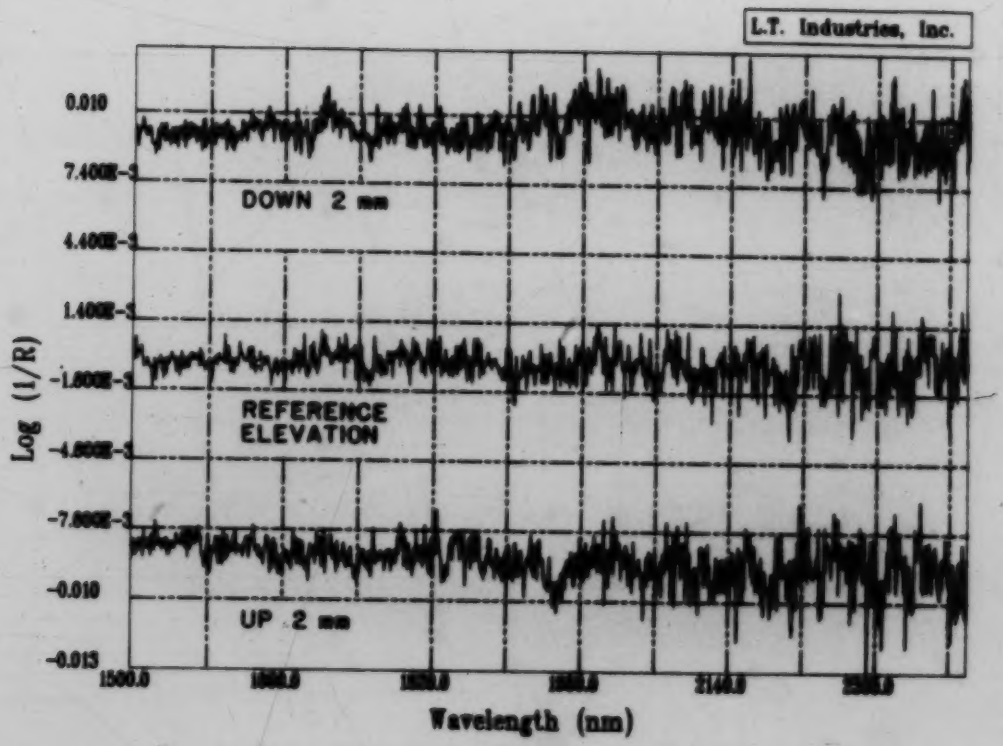


**Figure 34.** Diffuse reflectance spectra for carbon black determined at various sample elevations (Background = carbon black).

Measured Values:

$A(0)$ = 0.000
$A(X)$ = –0.0089 at +2 mm Elevation
$A(X)$ = +0.0094 at –2 mm Elevation

Solving for $G(X)$:

$G(X)$ = 1.0207 $G(0)$ at +2 mm Elevation
$G(X)$ = 0.9786 $G(0)$ at –2 mm Elevation

The apparent asymmetry about unity gain may be due to slight errors in the measurement of sample elevation.

Inspection of the oil sand spectra shown in Figure 35, on the other hand, reveals that the peak heights of absorption bands change as the sample is moved closer to or farther from the detector. This is not consistent with a simple gain function. As illustrated in Figure 36, one would expect absorbance bands to be of equivalent peak height (albeit offset from one another by a factor corresponding to the Log of the gain ratio). Peak heights for the oil sand sample measured at 2320 nm relative to a baseline at 2060 nm are noted below:

| SAMPLE POSITION | ABSORBANCE | | PEAK HEIGHT |
|---|---|---|---|
| | 2320 nm | 2060 nm | |
| Horizontal | –0.0521 | –0.0872 | 0.0351 |
| Up 2 mm | –0.0842 | –0.1360 | 0.0518 |
| Down 2 mm | –0.0190 | –0.0400 | 0.0210 |

Conceivably, other factors such as:

- Changes in light scattering properties as they relate to the shape and orientation of fine particles in the oil sand
- Changes in the specular component of the reflected light
- Changes in the area of the sample actually viewed (a function of proximity to the mask) and hence composition of the material

may serve to explain these results. Use of the Kubelka–Munk transform (an algorithm designed to diminish the effects of differences in particle scattering phenomena

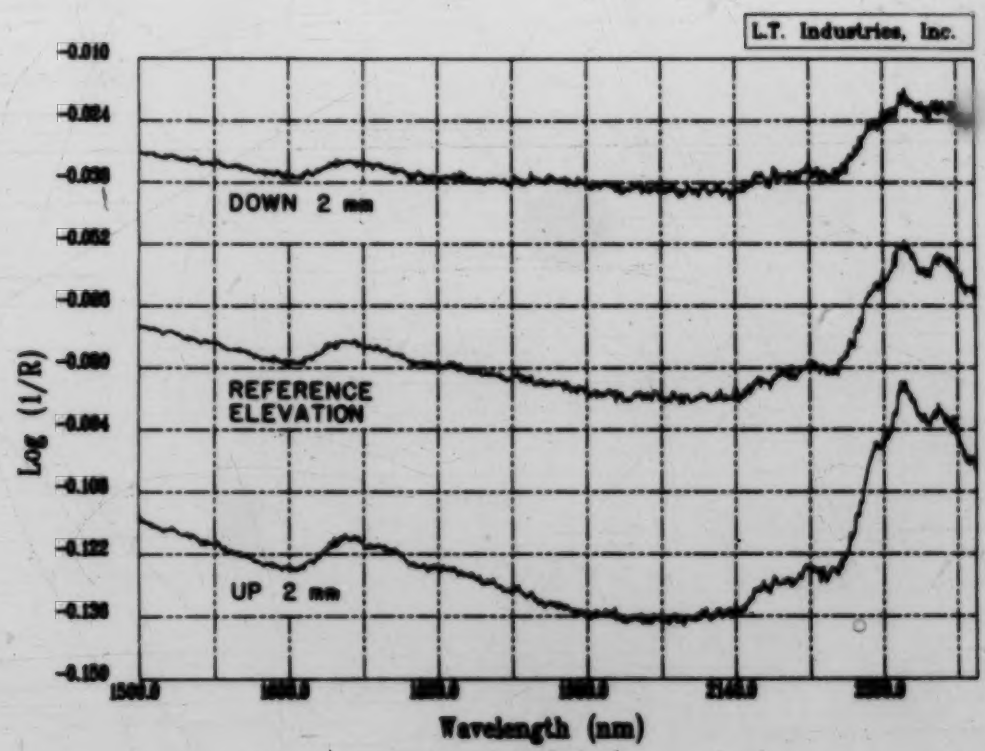


**Figure 35.** Diffuse reflectance spectra for an oil sand sample determined at various sample elevations (Background = carbon black).

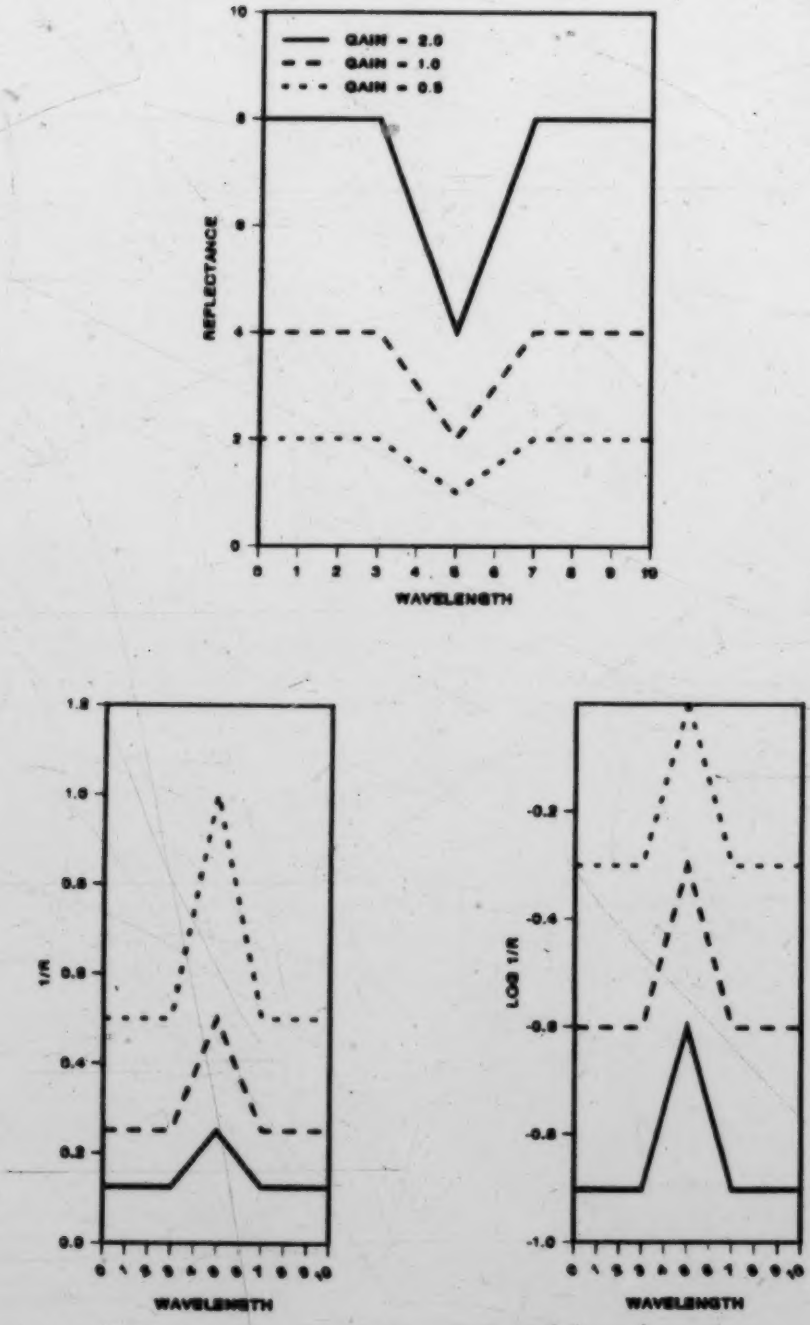


**Figure 36.** Effect of instrumental gain on spectral features.

among samples) seems to bring the spectra more in line with each other. Results are shown in Figure 37. It would seem unlikely that differences observed in peak height actually represent changes in sample composition. Normalized absorbance spectra are shown in Figure 38. Changes in sample composition would be revealed by displacements in the relative peak heights of the hydrocarbon and mineral components.

Given that detector response is extremely sensitive to sample elevation, it is imperative that great care be taken to ensure consistent positioning of the sample. To ensure adequate clearance between the core barrel and mask, a standard elevation of 52 mm above the sample table was used for all subsequent measurements on core.

### 3.3.4 Number of Scans

The purpose of this experiment was to examine the relationship between spectral noise and number of scans. Spectra of an oil sand sample were obtained by varying the number of scans used for signal averaging. Background corrections in each case were based on the same number of scans as that used to generate the sample spectra.

| | |
|---|---|
| Number of scans | Range 10 – 500 |
| Wavelength Range | 1200–2400 nm |
| Background | Carbon Black |

The sample and background material were positioned at the reference elevation with surface plane normal to the optical path.

Estimates for the level of noise in the sample spectra were determined by calculating the standard deviation of the mean absorbance as measured over the wavelength range 2060–2100 nm (a reasonably flat region in the spectra).

The relationship between spectral noise (evaluated in terms of the relative RMS deviation from mean response) and number of scans is shown in Figure 39. Experimental data is presented in Table VI. The trend in the data follows the statistical expectation that noise is a linear function of the reciprocal of $\sqrt{N}$, where $N$ is the

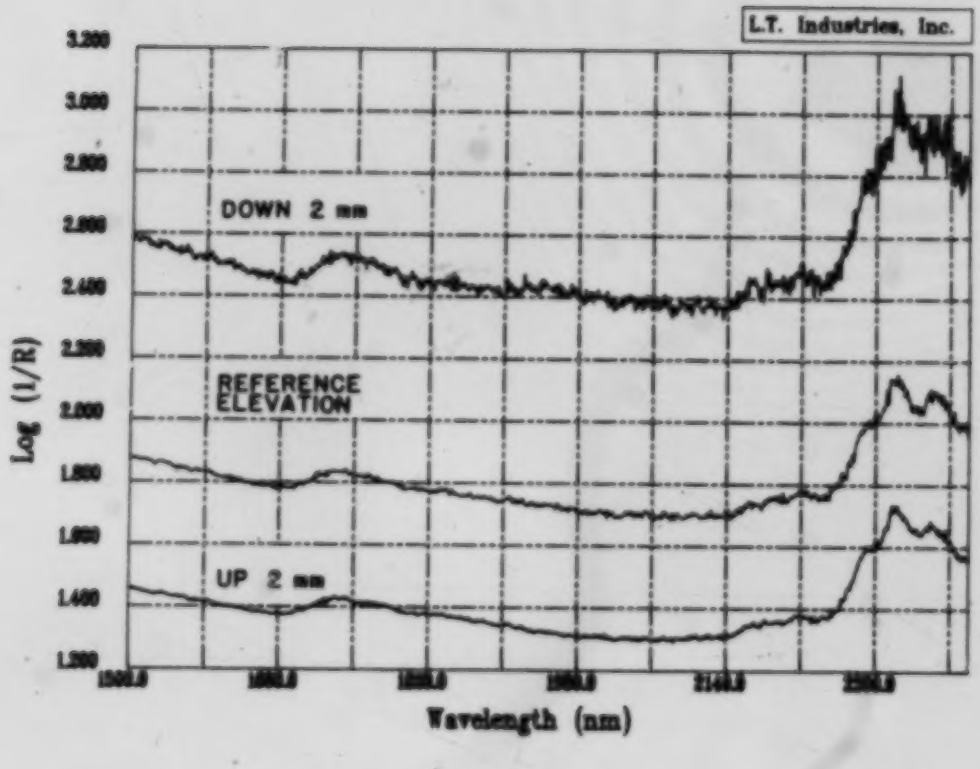


**Figure 37.** Diffuse reflectance spectra (Kubelka–Munk transform) for an oil sand sample determined at various surface elevations (Background = carbon black).

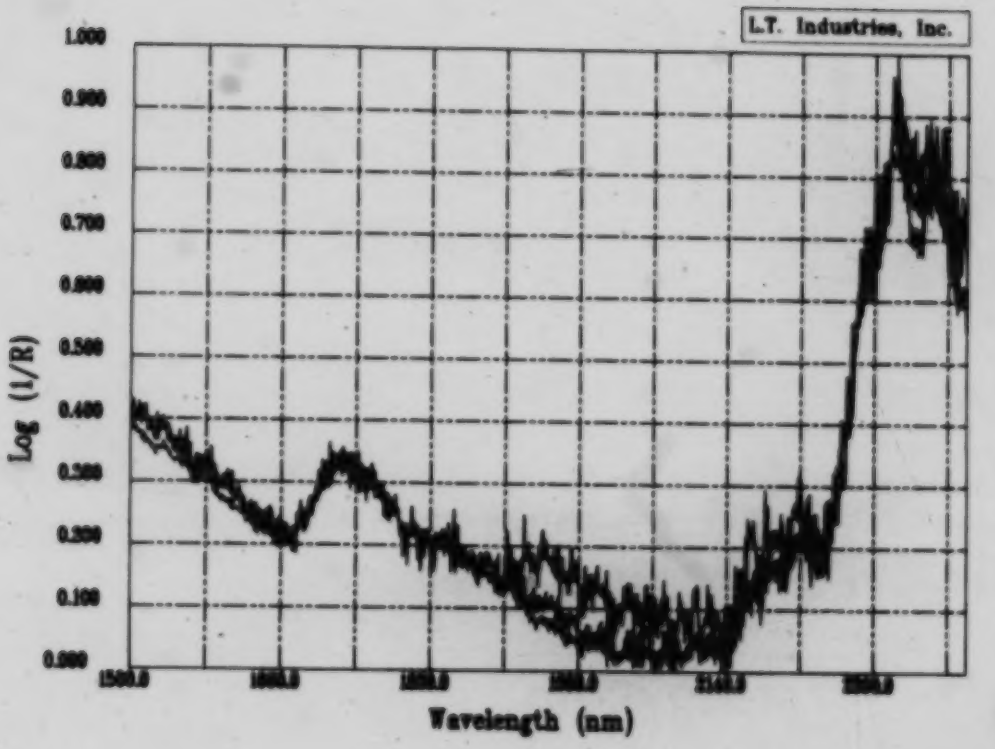


**Figure 38.** Normalized diffuse reflectance spectra for an oil sand sample determined at various surface elevations (Background = carbon black). Spectra recorded for samples in the horizontal, up, and down positions are largely superimposed.

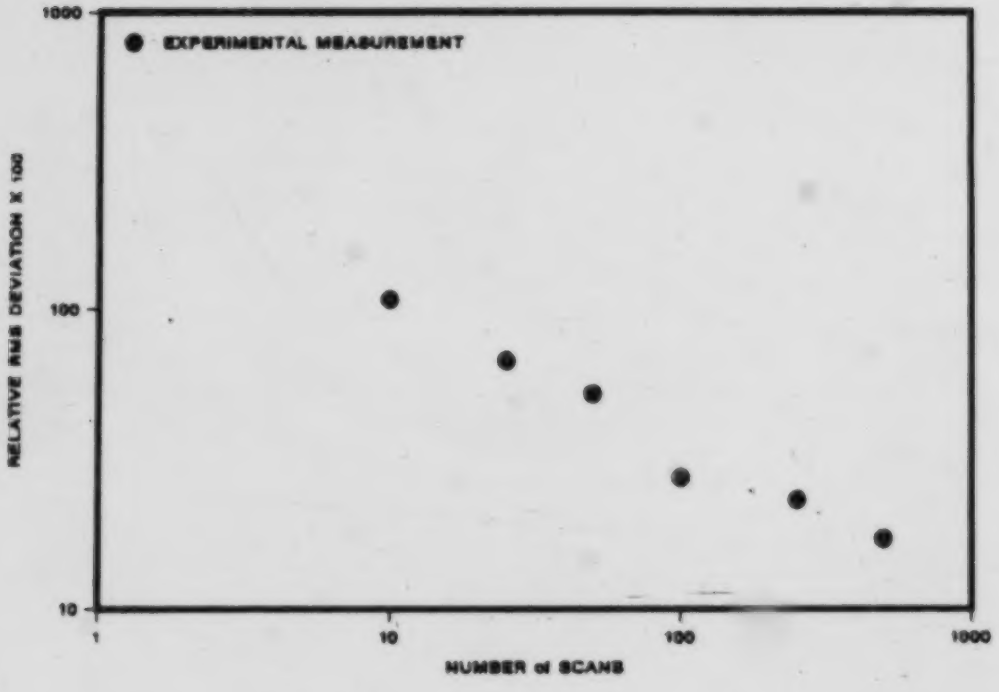


**Figure 39.** Relationship between spectral noise and number of scans.

**Table VI.** Absorbance readings obtained from the spectra of an oil sand sample upon varying the number of scans used for signal averaging. Absorbance data has been coded using the multiplicative factor $-10^{-4}$

| WAVELENGTH (nm) | NUMBER of SCANS | | | | | |
|---|---|---|---|---|---|---|
| | 10 | 25 | 50 | 100 | 250 | 500 |
| 2060 | 801 | 796 | 788 | 797 | 781.3 | 783.3 |
| 2061 | 813 | 799 | 792 | 797 | 778.7 | 783.5 |
| 2062 | 796 | 796 | 786 | 793 | 780.7 | 782.5 |
| 2063 | 799 | 790 | 792 | 793 | 779.8 | 783.6 |
| 2064 | 818 | 794 | 793 | 783 | 780.7 | 783.1 |
| 2065 | 811 | 792 | 789 | 795 | 780.8 | 783.2 |
| 2066 | 810 | 786 | 788 | 799 | 781.7 | 782.3 |
| 2067 | 810 | 788 | 788 | 796 | 782.0 | 783.7 |
| 2068 | 809 | 793 | 785 | 797 | 780.4 | 782.9 |
| 2069 | 793 | 785 | 790 | 795 | 779.4 | 785.4 |
| 2070 | 801 | 795 | 791 | 797 | 779.2 | 784.5 |
| 2071 | 791 | 790 | 796 | 799 | 779.4 | 784.3 |
| 2072 | 794 | 798 | 791 | 796 | 779.6 | 785.5 |
| 2073 | 784 | 796 | 792 | 794 | 778.5 | 784.6 |
| 2074 | 792 | 789 | 792 | 794 | 781.5 | 784.7 |
| 2075 | 787 | 793 | 785 | 798 | 781.6 | 784.0 |
| 2076 | 807 | 792 | 788 | 800 | 779.8 | 783.6 |
| 2077 | 795 | 792 | 792 | 796 | 783.1 | 784.4 |
| 2078 | 813 | 790 | 785 | 800 | 781.5 | 783.8 |
| 2079 | 804 | 789 | 786 | 794 | 779.3 | 783.1 |
| 2080 | 811 | 787 | 786 | 794 | 779.7 | 785.2 |
| 2081 | 809 | 801 | 790 | 795 | 778.9 | 783.3 |
| 2082 | 802 | 801 | 784 | 797 | 779.7 | 785.0 |
| 2083 | 792 | 788 | 789 | 797 | 779.7 | 783.3 |
| 2084 | 798 | 781 | 793 | 796 | 778.4 | 784.9 |
| 2085 | 804 | 796 | 794 | 796 | 779.5 | 780.5 |
| 2086 | 799 | 793 | 786 | 799 | 781.2 | 783.1 |
| 2087 | 790 | 791 | 785 | 795 | 781.3 | 784.1 |
| 2088 | 803 | 790 | 789 | 795 | 780.6 | 784.0 |
| 2089 | 809 | 797 | 787 | 796 | 781.2 | 784.3 |
| 2090 | 794 | 797 | 783 | 797 | 781.3 | 785.5 |
| 2091 | 794 | 789 | 795 | 794 | 783.1 | 784.5 |
| 2092 | 787 | 799 | 790 | 794 | 784.7 | 785.9 |
| 2093 | 798 | 789 | 791 | 794 | 786.0 | 785.0 |
| 2094 | 805 | 794 | 791 | 802 | 783.3 | 787.0 |
| 2095 | 795 | 784 | 788 | 796 | 781.6 | 786.9 |
| 2096 | 800 | 791 | 778 | 798 | 781.0 | 787.0 |
| 2097 | 800 | 793 | 793 | 795 | 779.1 | 785.3 |
| 2098 | 815 | 793 | 788 | 794 | 777.7 | 785.7 |
| 2099 | 795 | 781 | 787 | 795 | 777.6 | 784.3 |
| 2100 | 812 | 780 | 781 | 793 | 777.9 | 782.5 |
| MEAN | 800.98 | 791.46 | 787.95 | 796.02 | 780.55 | 784.20 |
| STD DEV | 8.60 | 5.31 | 4.09 | 2.17 | 1.80 | 1.34 |
| RSD | 1.07% | 0.67% | 0.52% | 0.27% | 0.23% | 0.17% |

number of scans used for signal averaging. This is illustrated in Figure 40. The equation:

$$y = 3.380(x) + 0.002, \qquad r = 0.994$$

where $y$ = Relative RMS Deviation (% of Response), and $x = 1/\sqrt{N}$ derived by linear regression best describes this relationship.

Actual spectra obtained over the wavelength range 1500–2400 nm for $N$ equal to 10, 50, 100, and 500 scans are shown in Figures 41 and 42. Spectra recorded in expanded scale over the region of interest are shown in Figures 43 and 44. Spectra generated by averaging the signal over 50 scans limits noise to approximately 0.5% relative. This was considered adequate for all subsequent work.

### 3.3.5 Reproducibility of Sample Spectra

A total of 10 replicate analyses were performed on samples of core (oil sand, clay, and interbedded material) and carbon black to evaluate the precision of absorbance measurements.

| | |
|---|---|
| Number of scans | 50 |
| Wavelength Range | 1200–2400 nm |
| Background | Carbon Black (Core Samples) |

The core and background samples were removed from the sample table and repositioned between scans. Care was taken to ensure that all samples were placed at the reference elevation and aligned with the origin pointer.

The mean, minimum, and maximum absorbance spectra for each of the core samples, along with corresponding estimates for the uncertainty (standard deviation) of absorbance readings as a function of wavelength, are presented in Figures 45–47. Features characteristic of the hydrocarbon and mineral components of the samples are clearly evident in the spectra. It is also apparent that differences in the overall reflectivity of a sample can be used to distinguish oil sand and clay. The spectra of

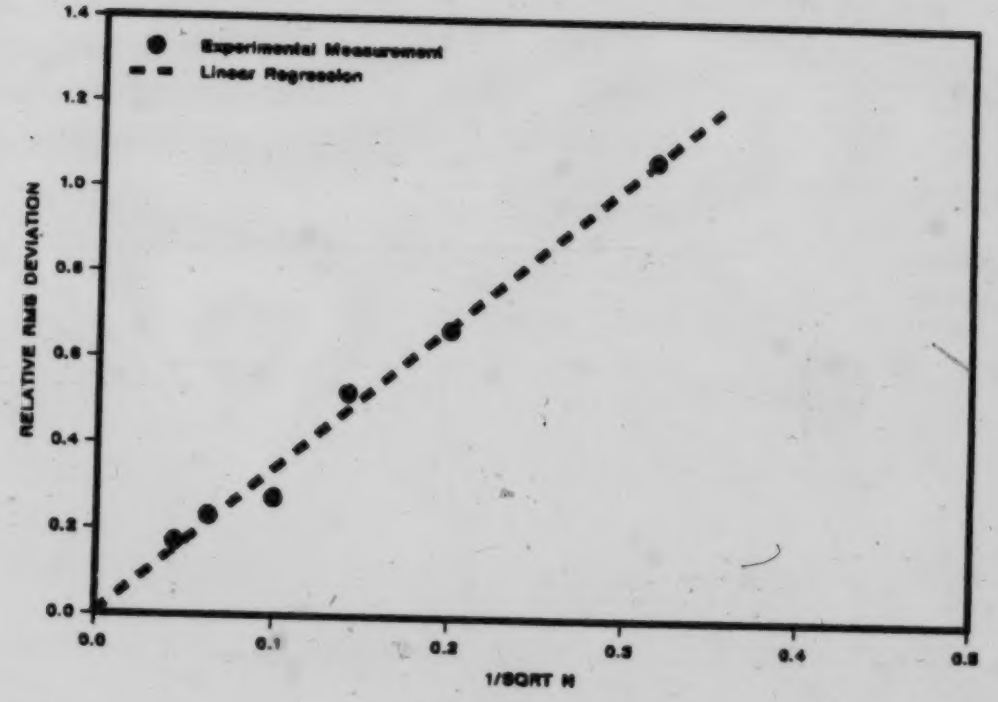


**Figure 40.** Relationship between spectral noise and number of scans used for signal averaging.

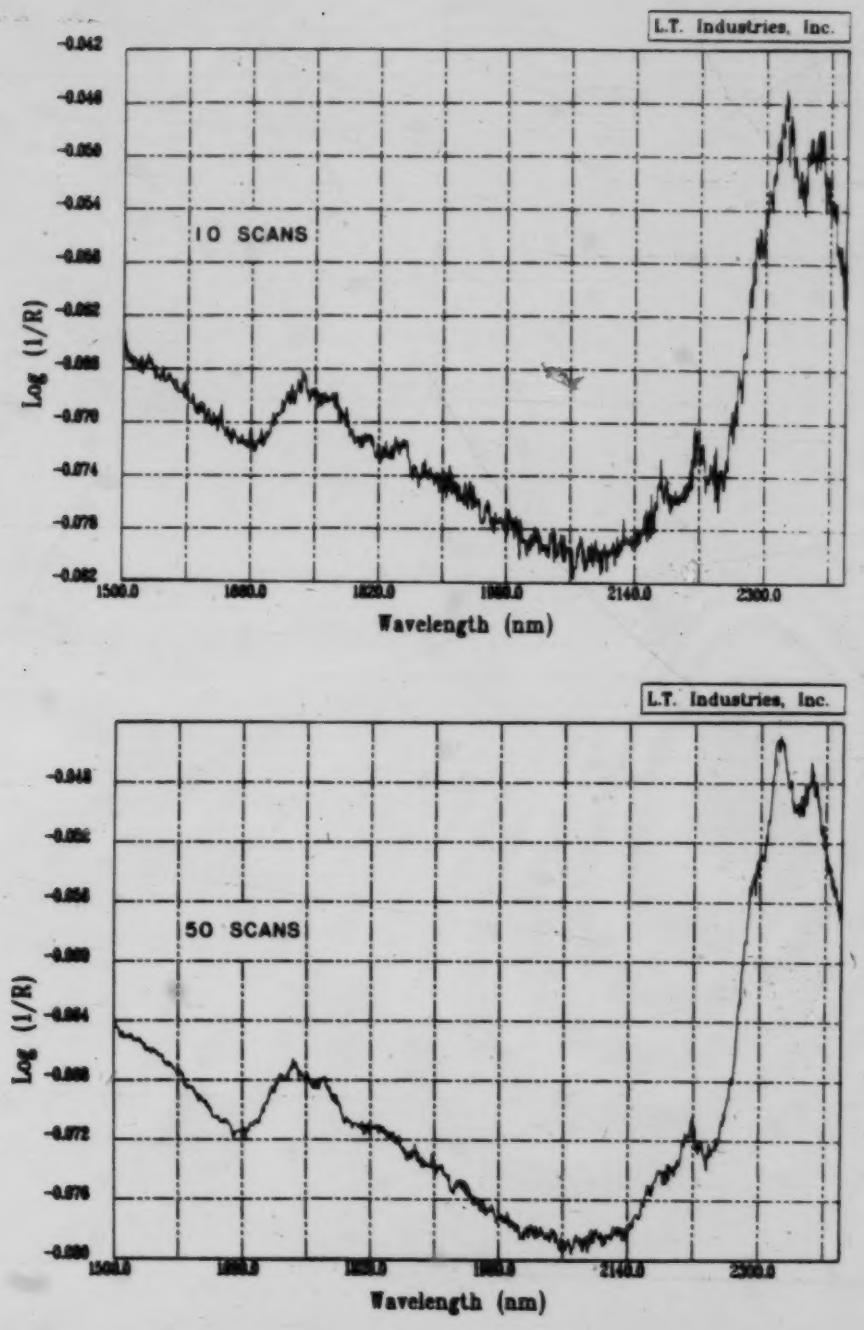


**Figure 41.** Diffuse reflectance spectra of an oil sand sample illustrating the reduction in noise as a function of increasing the number of scans used for signal averaging (Background = carbon black).

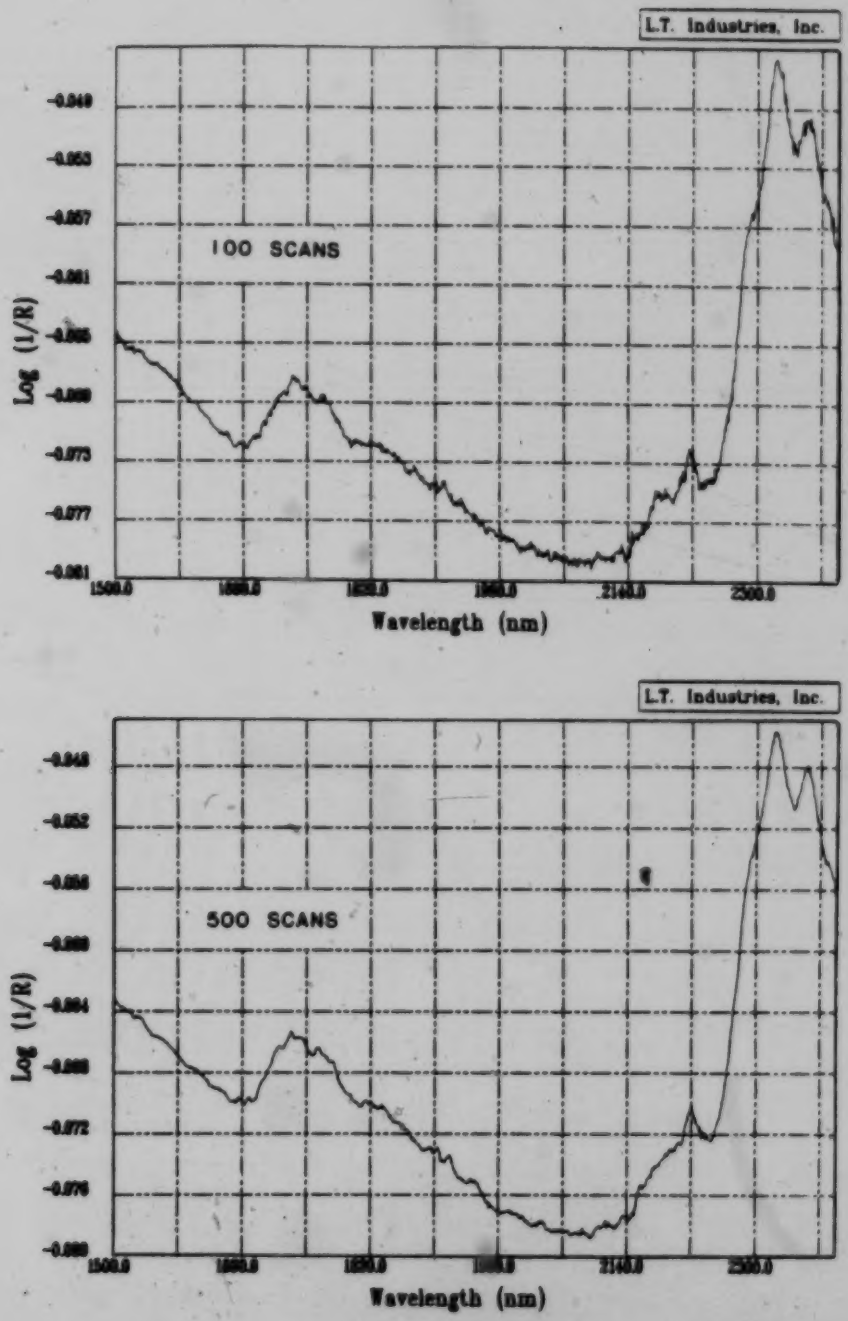


**Figure 42.** Diffuse reflectance spectra of an oil sand sample illustrating the reduction in noise as a function of increasing the number of scans used for signal averaging (Background = carbon black).

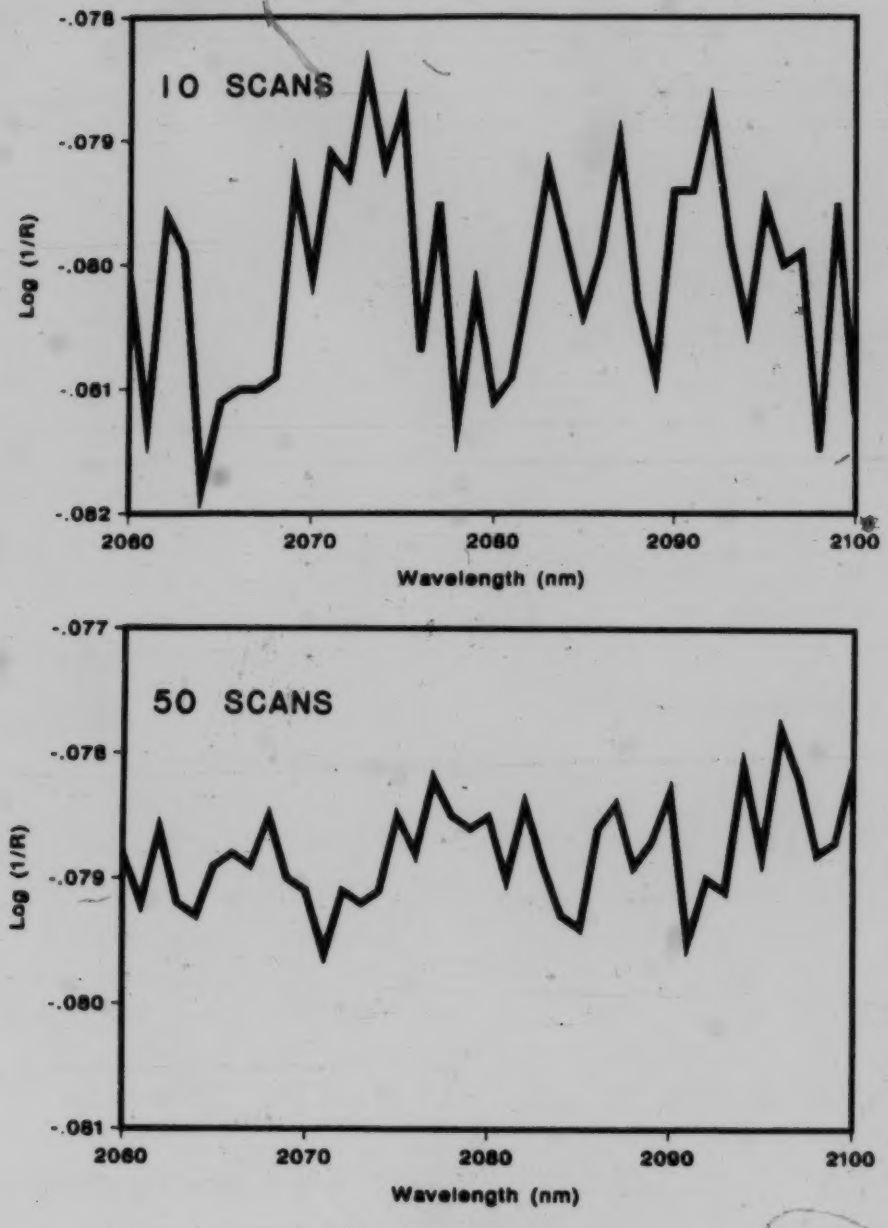


**Figure 43.** Diffuse reflectance spectra of an oil sand sample obtained over the expanded wavelength region 2060–2100 nm illustrating the reduction in noise as a function of increasing the number of scans used for signal averaging (Background = carbon black).

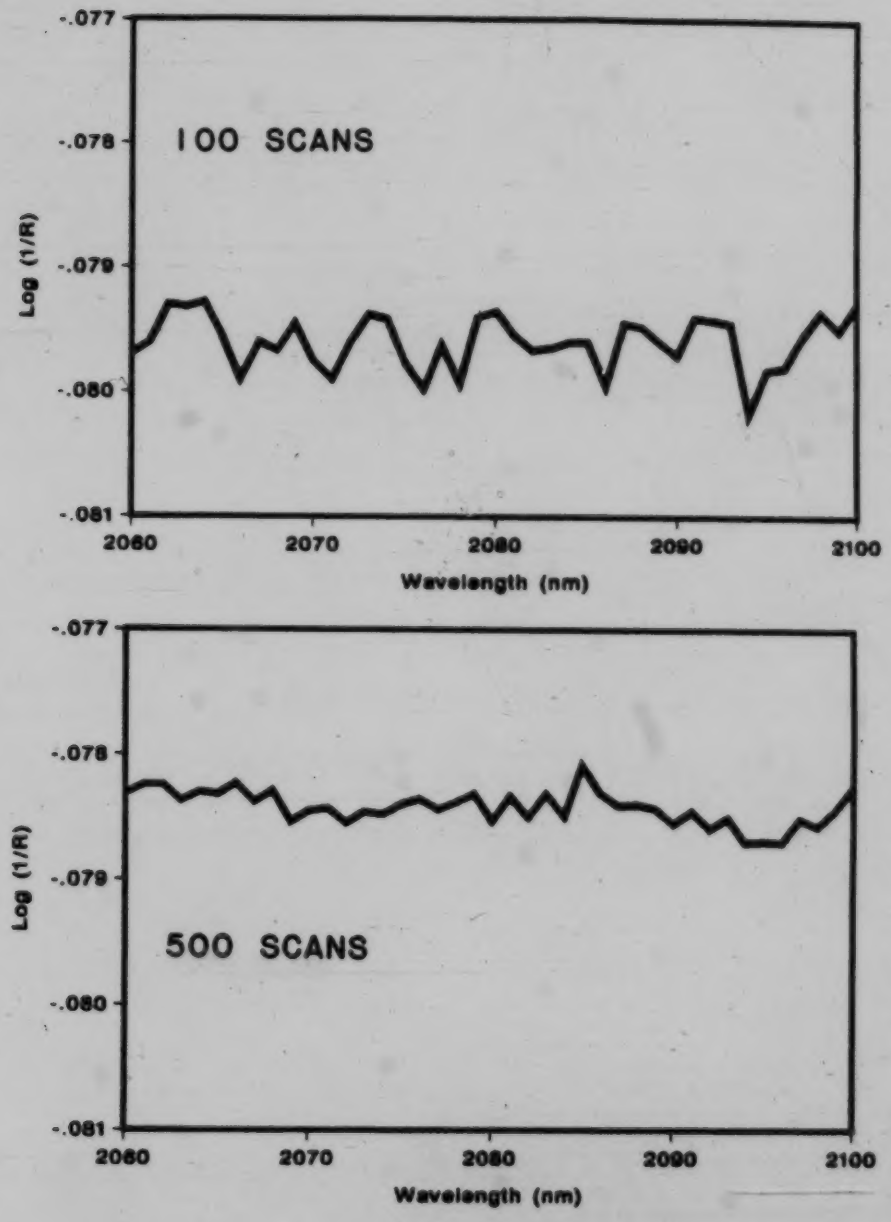


**Figure 44.** Diffuse reflectance spectra of an oil sand sample obtained over the expanded wavelength region 2060–2100 nm illustrating the reduction in noise as a function of increasing the number of scans used for signal averaging (Background = carbon black).

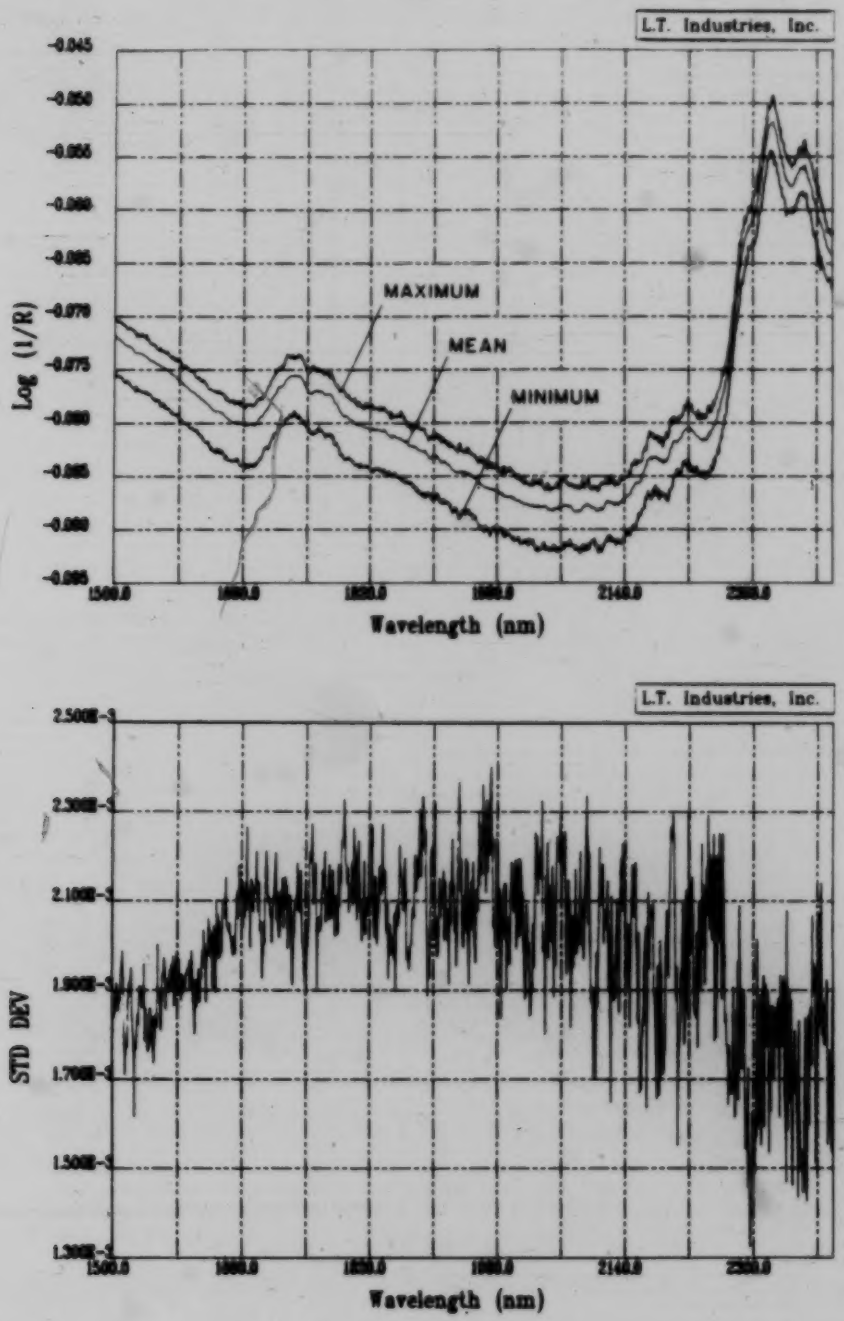


**Figure 45.** Reproducibility of diffuse reflectance spectra for an oil sand sample (Background = carbon black). Results are based on 10 replicate analyses.

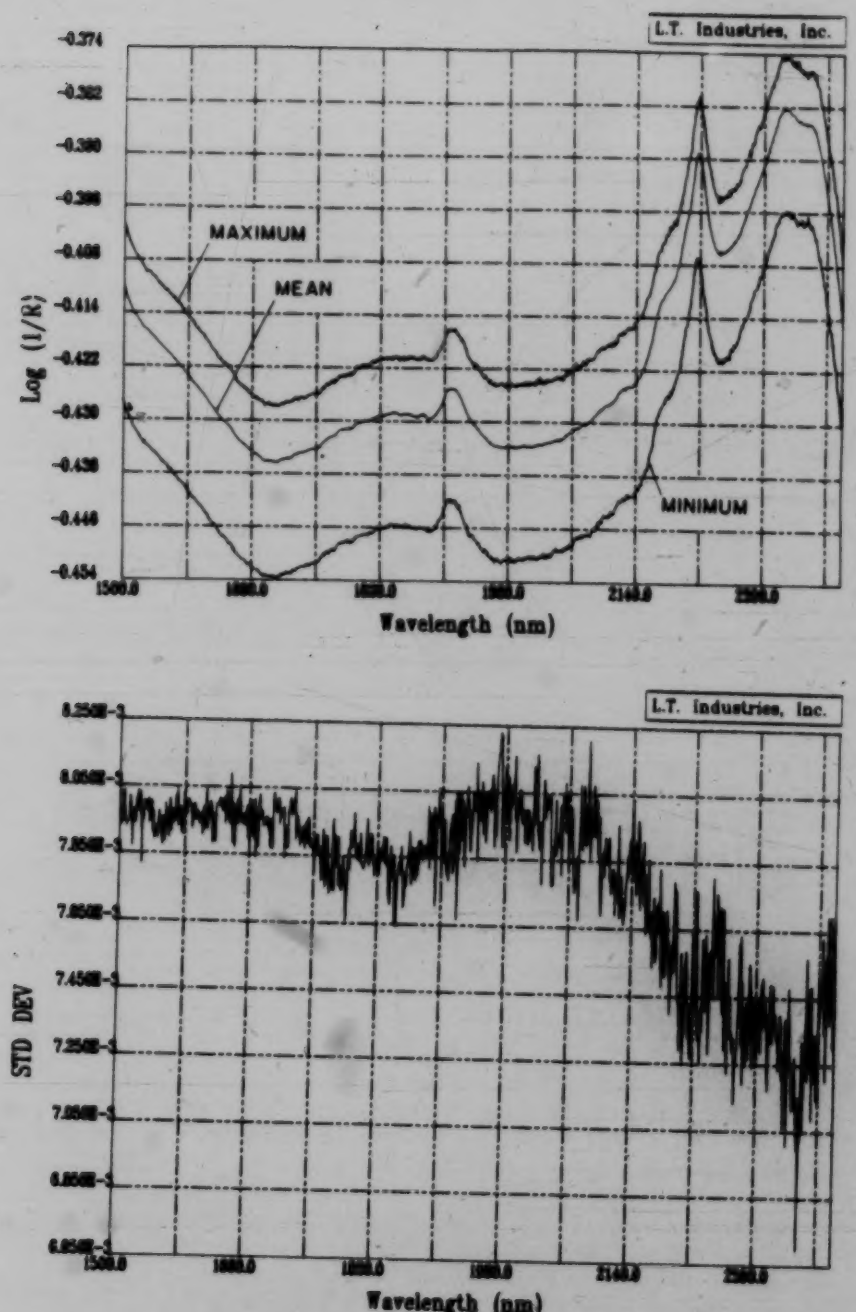


**Figure 46.** Reproducibility of diffuse reflectance spectra for a sample of clay (Background = carbon black). Results are based on 10 replicate analyses.

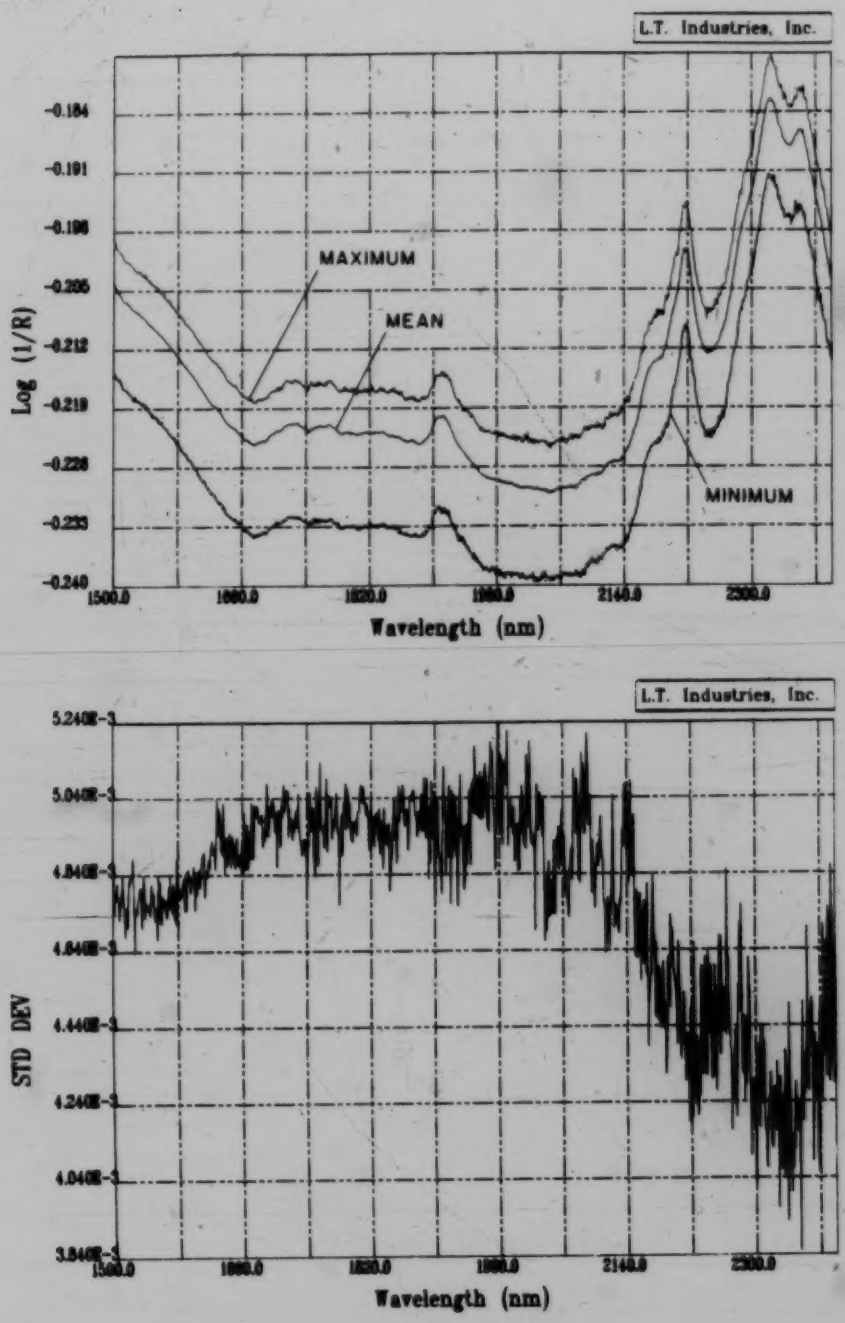


**Figure 47.** Reproducibility of diffuse reflectance spectra for an interbedded sample of oil sand and clay (Background = carbon black). Results are based on 10 replicate analyses.

the interbedded sample (a stratified mixture of oil sand and clay) reveals the traits of both parent materials.

The curvature in the traces of standard deviation *versus* wavelength indicate that the precision of absorbance values for a particular sample is not constant. The magnitude of the uncertainty varies with wavelength and tends to be inversely related to absorbance.

In order to provide a common basis for comparing the variability among spectra for each type of core sample analyzed, mean spectra were characterized in terms of an average absorbance calculated over the wavelength range 1500–2400 nm (based on data points taken at 50 nm intervals). In similar fashion, average values for the standard deviation among sample spectra were also determined. Data is reported in Table VII and summarized below:

| MEAN VALUE | OIL SAND | INTERBEDDED MATERIAL | CLAY |
|---|---|---|---|
| Absorbance | −0.0780 | −0.2161 | −0.4203 |
| Standard Deviation | 0.0019 | 0.0047 | 0.0077 |
| Percent RSD | 2.44 | 2.17 | 1.83 |

Typically, the uncertainty among replicate sample spectra is on the order of 2% relative. The implications of this variability in terms of the correlations between spectral response and sample assay are yet to be determined (a sensitivity analysis could be performed after selecting an appropriate model).

The variability among spectra for a particular sample is thought to arise from two contributing sources:

- Uncertainties associated with the background correction
- Inconsistencies in the positioning of the sample surface (spatial displacements, both lateral and vertical)

Given an independent estimate for the standard deviation among replicate absorbance spectra of the reference material, it is possible to determine the relative

**Table VII.** Absorbance measurements and associated uncertainty values obtained from the mean spectrum of various core samples. Data has been coded using multiplicative factors of $-10^4$ for absorbance readings and $10^4$ for estimates of standard deviation.

| WAVELENGTH (nm) | OIL SAND | | INTERBEDDED MATERIAL | | CLAY | |
|---|---|---|---|---|---|---|
| | ABS | STD DEV | ABS | STD DEV | ABS | STD DEV |
| 1500 | 717 | 19 | 2043 | 47 | 4098 | 79 |
| 1550 | 744 | 18 | 2099 | 47 | 4192 | 79 |
| 1600 | 772 | 18 | 2156 | 48 | 4262 | 79 |
| 1650 | 799 | 20 | 2217 | 49 | 4336 | 79 |
| 1700 | 772 | 20 | 2224 | 50 | 4359 | 79 |
| 1750 | 770 | 20 | 2218 | 48 | 4332 | 77 |
| 1800 | 799 | 20 | 2224 | 49 | 4300 | 78 |
| 1850 | 812 | 20 | 2227 | 50 | 4288 | 78 |
| 1900 | 829 | 22 | 2216 | 48 | 4262 | 78 |
| 1950 | 851 | 21 | 2261 | 51 | 4323 | 80 |
| 2000 | 870 | 21 | 2285 | 48 | 4335 | 79 |
| 2050 | 882 | 20 | 2295 | 48 | 4322 | 79 |
| 2100 | 879 | 17 | 2274 | 48 | 4276 | 77 |
| 2150 | 862 | 21 | 2233 | 47 | 4217 | 77 |
| 2200 | 821 | 22 | 2091 | 45 | 4017 | 74 |
| 2250 | 806 | 21 | 2128 | 46 | 4040 | 77 |
| 2300 | 607 | 14 | 1941 | 40 | 3910 | 72 |
| 2350 | 577 | 17 | 1885 | 42 | 3845 | 72 |
| 2400 | 643 | 17 | 2042 | 46 | 4138 | 75 |

contribution of each source of error to the total based on the additivity of variances. This was arrived at by considering the following fundamental expressions:

Let $R$ represent a background corrected sample spectrum recorded in reflectance mode

$$R = \frac{R(S)}{R(B)}$$

where $R(S)$ = absolute reflectance spectrum of the sample, and $R(B)$ = absolute reflectance spectrum of the reference

It follows that:

$$Log\frac{1}{R} = Log\frac{1}{R(S)} - Log\frac{1}{R(B)}$$

This is analogous to:

$$A = A(S) - A(B)$$

where $A$, $A(S)$, and $A(B)$ represent the corresponding absorbance spectra.

In terms of the propagation of random error:

$$\sigma_A^2 = \left[\frac{\partial A}{\partial A(S)}\right]^2 \sigma_{A(S)}^2 + \left[\frac{\partial A}{\partial A(B)}\right]^2 \sigma_{A(B)}^2$$

$$\frac{\partial A}{\partial A(S)} = \frac{\partial A}{\partial A(B)} = 1$$

$$\text{Therefore,} \quad \sigma_A^2 = \sigma_{A(S)}^2 + \sigma_{A(B)}^2$$

The reproducibility of absorbance spectra for carbon black (Background = 1.0) is illustrated in Figure 48. The magnitude of the standard deviation is reasonably

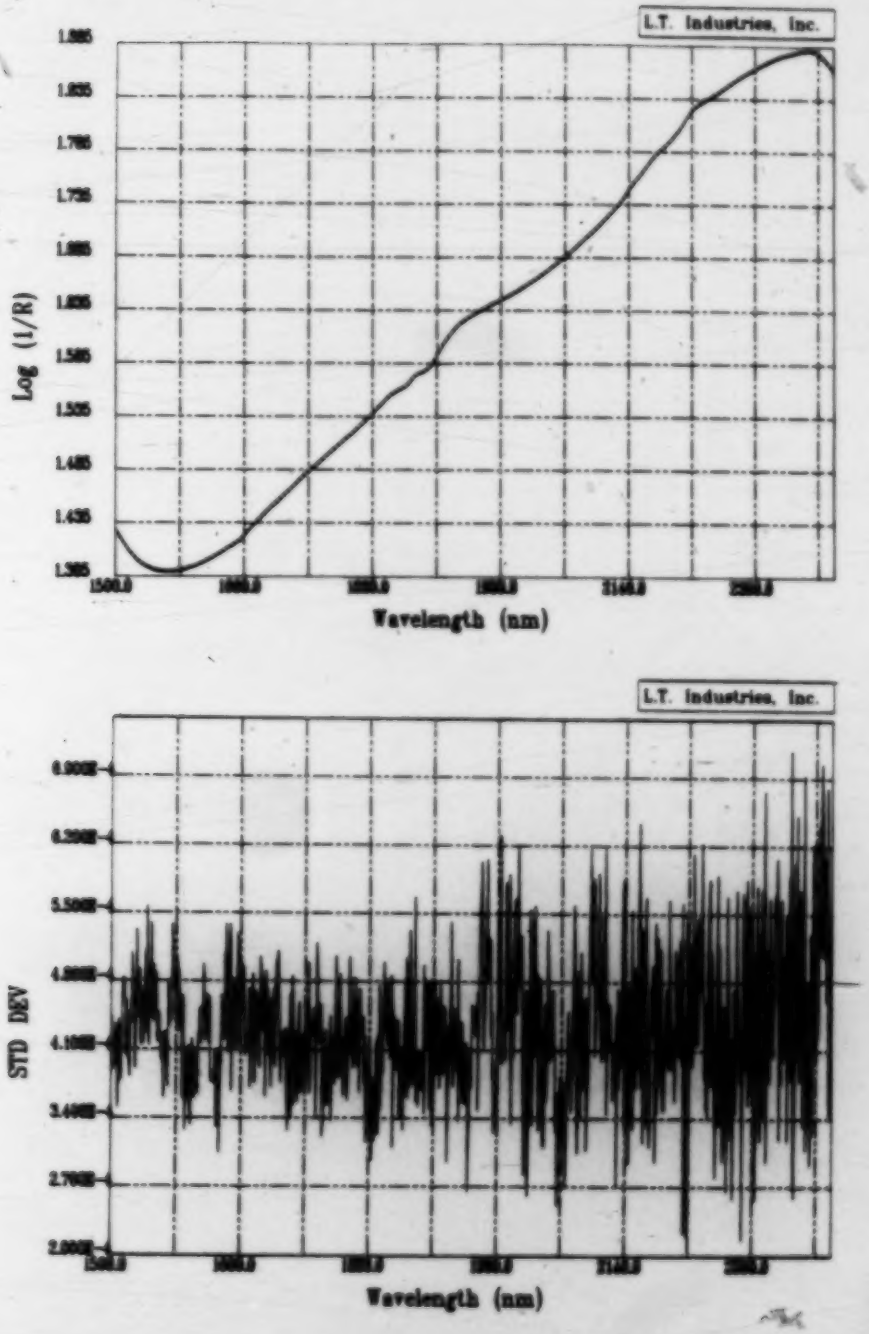


**Figure 48.** Reproducibility of diffuse reflectance spectra for carbon black (Background = carbon black). Results are based on 10 replicate determinations. In the upper spectra, mean, minimum, and maximum values are superimposed.

constant over the wavelength range 1500–2400 nm, averaging 0.00045 absorbance units (obtained in the same manner as previously discussed for the core samples). Since this value is small in comparison to the standard deviations calculated for the background corrected spectra of core samples, it is clear that uncertainties due to sample positioning are the dominant source of error.

A test was also done to evaluate the effect of instrumental drift on the reproducibility of sample spectra. Spectra were obtained for a sample of core (interbedded material) and carbon black on each of 5 consecutive days to examine the stability of instrumental response.

| | |
|---|---|
| Number of scans | 50 – |
| Wavelength Range | 1200–2400 nm |
| Background | Carbon Black (Core Samples) |

Sample spectra and corresponding estimates for the standard deviation among the daily values are shown in Figures 49 and 50. Results indicate that the magnitude of the variability in absorbance readings for the core sample is comparable to that previously obtained in an evaluation of spectral measurement precision. Although some degree of instrumental drift is present (as evidenced by the relatively high standard deviation among spectra of the reference material), it is masked by the uncertainties that arise due to subtle changes in sample positioning.

### 3.3.6 Wavelength Calibration

The reflectance spectrum for a standard reference material (NBS SRM 1920) was obtained to establish the accuracy of the wavelength scale for the NIR analyzer. This standard consists of a mixture of rare earth oxides of dysprosium, erbium, and holium contained in a small aluminum cup. The material is sealed behind an infrared transmitting window. The standard reflectance spectrum provided for this material is illustrated in Figure 51. Certified wavelengths for the reflectance bands are listed in Table VIII.

The standard was run with the LTI Quantum 1200 spectrophotometer using 50

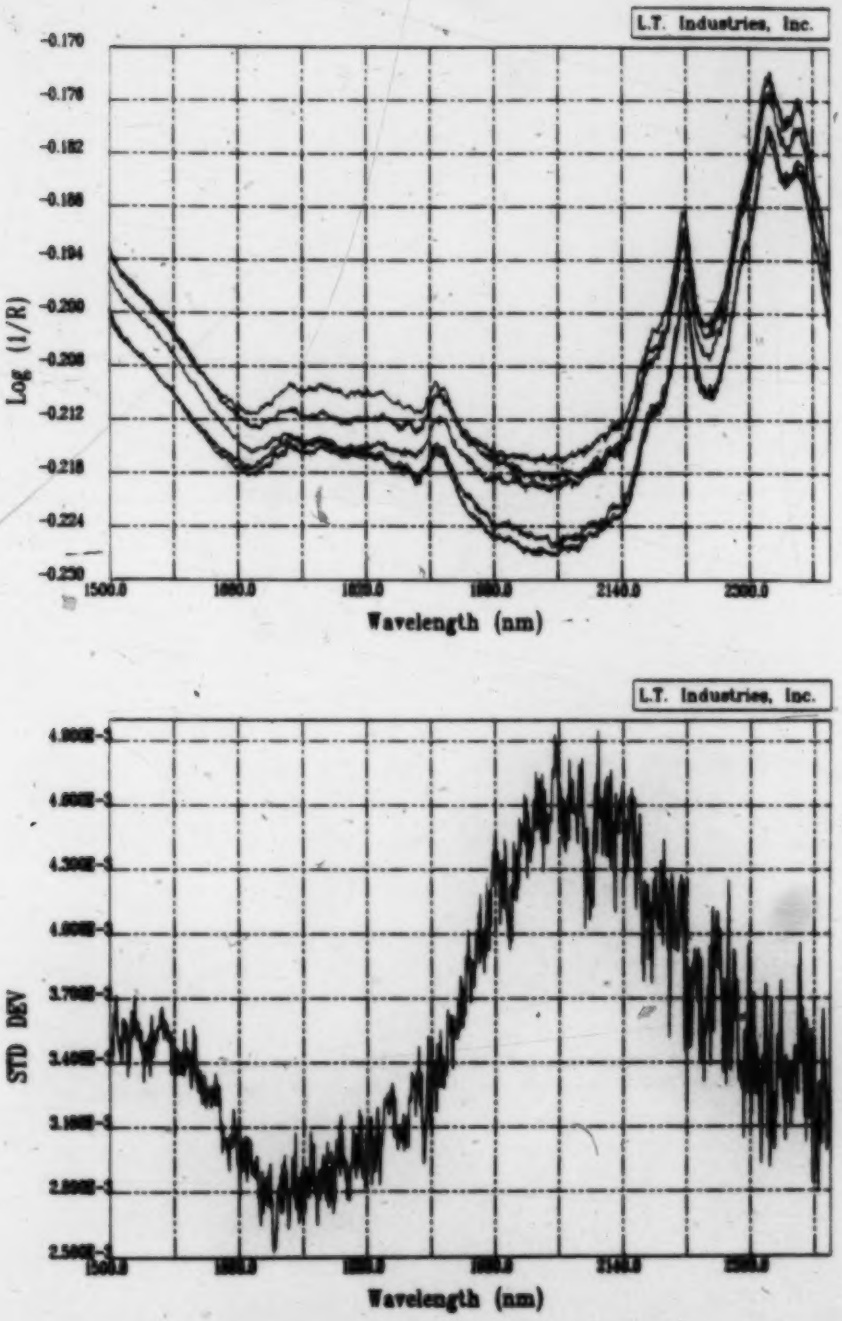


**Figure 49.** Reproducibility of diffuse reflectance spectra for a sample of interbedded oil sand and clay illustrating the effect of instrumental drift (Background = carbon black). Spectra were obtained on each of 5 consecutive days.

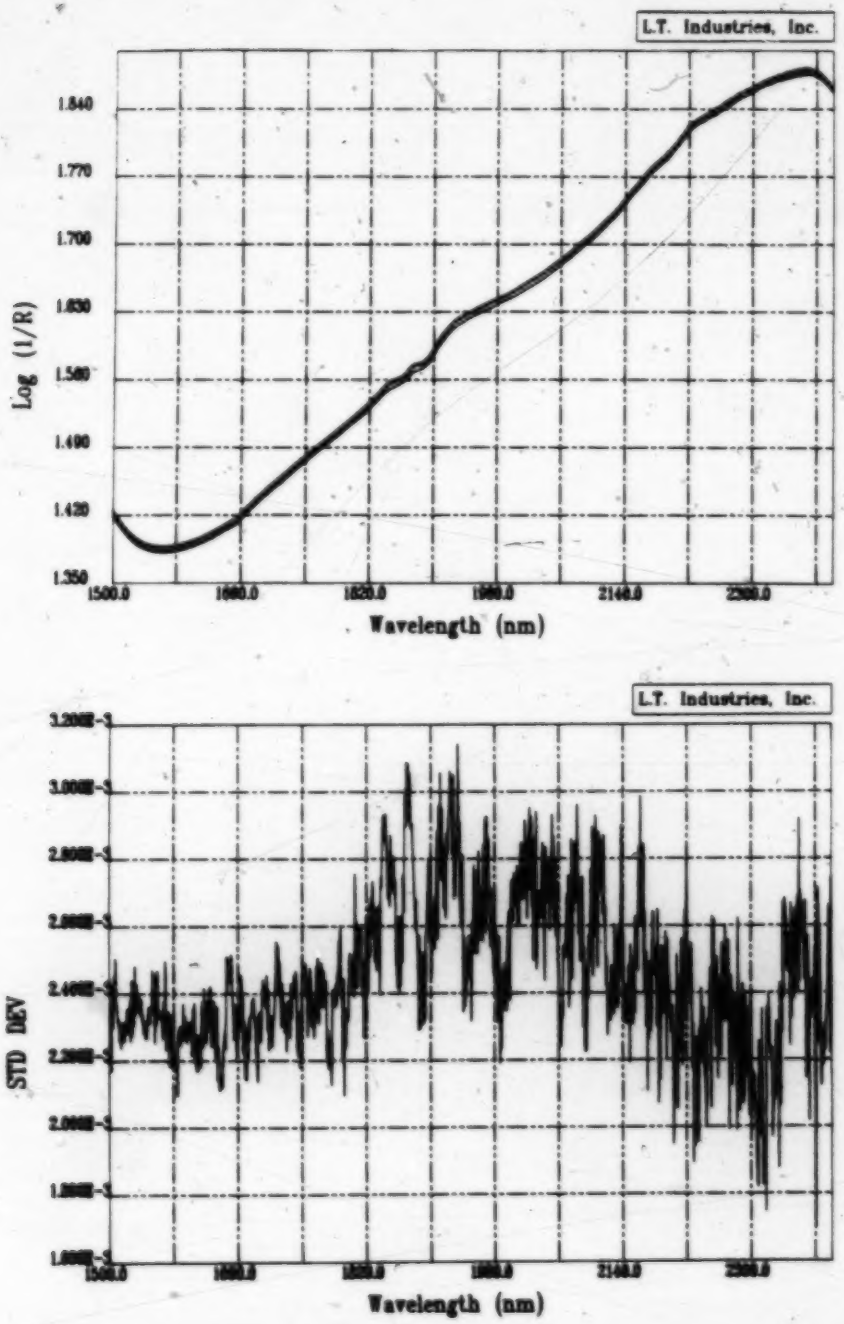


**Figure 50.** Reproducibility of diffuse reflectance spectra for carbon black illustrating the effect of instrumental drift (Background = carbon black). Spectra were obtained on each of 5 consecutive days.

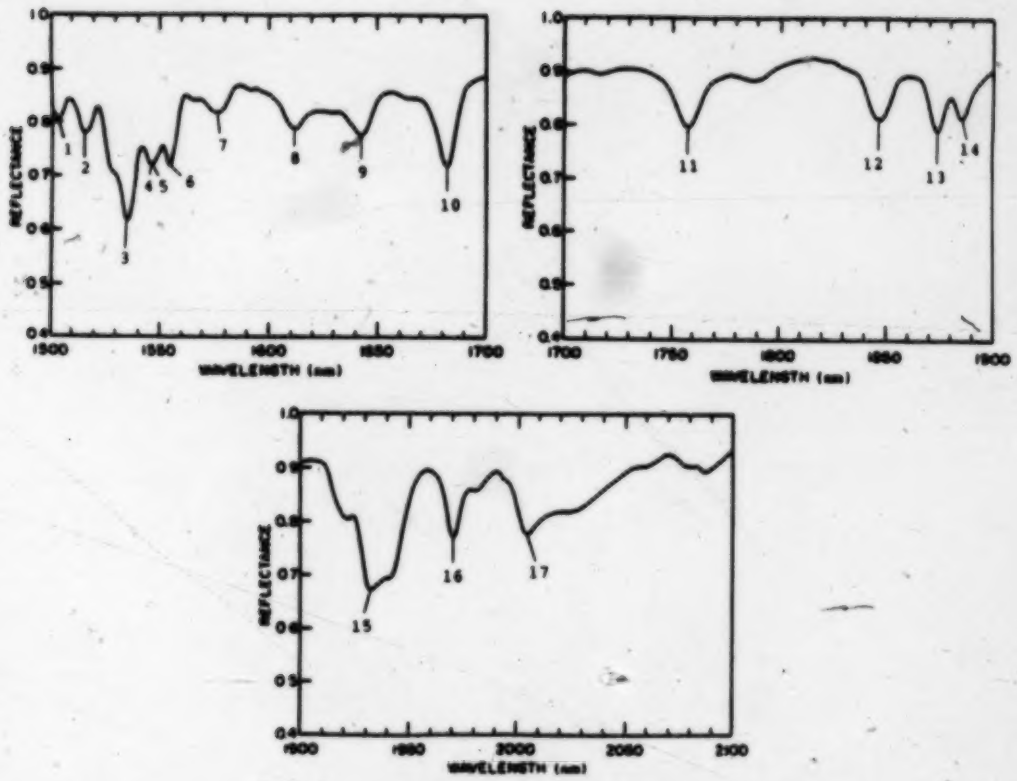


**Figure 51.** Diffuse reflectance spectrum of NBS SRM 1920 (Near-Infrared Reflectance Wavelength Standard).

**Table VIII.** Adopted wavelengths of minimum reflectance for NBS SRM 1920 (Near-Infrared Reflectance Wavelength Standard) at various selected spectral bandwidths.

| RARE-EARTH OXIDE | BAND NUMBER | SPECTRAL BAND WIDTH | | | | |
|---|---|---|---|---|---|---|
| | | 2 nm | 3 nm | 4 nm | 5 nm | 10 nm |
| $Er_2O_3$ | 1 | 1503.4 | 1503.5 | 1503.5 | – | – |
| | 2 | 1516.0 | 1516.0 | 1515.9 | 1515.7 | – |
| | 3 | 1535.5 | 1535.6 | 1535.6 | 1535.4 | 1535.6 |
| | 4 | 1544.7 | – | – | – | – |
| | 5 | 1548.1 | – | – | – | – |
| | 6 | 1555.1 | 1555.0 | 1554.8 | – | – |
| | 7 | 1577.1 | 1577.2 | 1577.2 | – | – |
| $Dy_2O_3$ | 8 | 1611.8 | 1611.7 | 1611.7 | 1611.9 | – |
| | 9 | 1642.7 | 1642.7 | 1642.5 | 1642.5 | – |
| | 10 | 1682.6 | 1682.3 | 1682.2 | 1682.2 | 1681.4 |
| | 11 | 1757.6 | 1757.8 | 1757.9 | 1757.8 | 1757 6 |
| $Ho_2O_3$ | 12 | 1847.5 | 1847.3 | 1846.9 | 1847.0 | 1847.3 |
| | 13 | 1874.3 | 1874.0 | 1873.8 | 1874.0 | – |
| | 14 | 1885.0 | 1885.3 | 1885.7 | 1885.5 | – |
| | 15 | 1930.9 | 1931.6 | 1932.2 | 1932.5 | 1932.5 |
| | 16 | – | 1970.6 | 1970.7 | 1970.8 | 1970.8 |
| | 17 | – | 2004.5 | 2005.9 | 2005.8 | 2006.3 |

scans (referenced to carbon black) over the range 1500–2100 nm. The spectrum, shown in Figure 52, shows band positions in close agreement with those defined for the standard.

## 3.4 Micro Soxhlet Extraction Procedure for Reference Assay Determination

Near–infrared diffuse reflectance measurements for the bitumen content of oil sand samples confined within a core need to be calibrated against some reference method which provides direct assay information. Since we are concerned with evaluating the grade of material in a core at intervals of 1 cm, it is necessary to perform these reference analyses on very small quantities of sample. A micro–Soxhlet extraction technique would seem ideally suited for this application. Studies were pursued to examine the precision and accuracy of oil sand assay\data obtained using a micro–Sohxlet extraction procedure.

The analysis involves a separation of the bitumen and solids components of the sample by refluxing toluene in a solvent extraction assembly. The extraction apparatus is schematically shown in Figure 53. The sample to be analyzed is placed in a tared single–thickness cellulose thimble and positioned within the extractor column. During reflux, condensed toluene is continually delivered to the thimble to extract bitumen from the sample. In contrast with larger scale extraction assemblies, the solvent does not percolate and drain through the sample. Rather, the solvent accumulates in the extractor column until its level approaches the top of the thimble. The solvent then siphons back to the flask and the process is repeated. This eliminates channelling of the solvent through the sample and greatly reduces the time required to dissolve and wash all the bitumen from the solids. A photograph of some extraction assemblies in operation is provided in Figure 54.

When the extraction is complete, the thimble containing clean solids is dried and reweighed. The resultant extract (solvent and dissolved bitumen) is quantitatively transferred to a tared evaporating dish and allowed to dry. The amount of bitumen in the original sample is determined gravimetrically. It is important to note that the

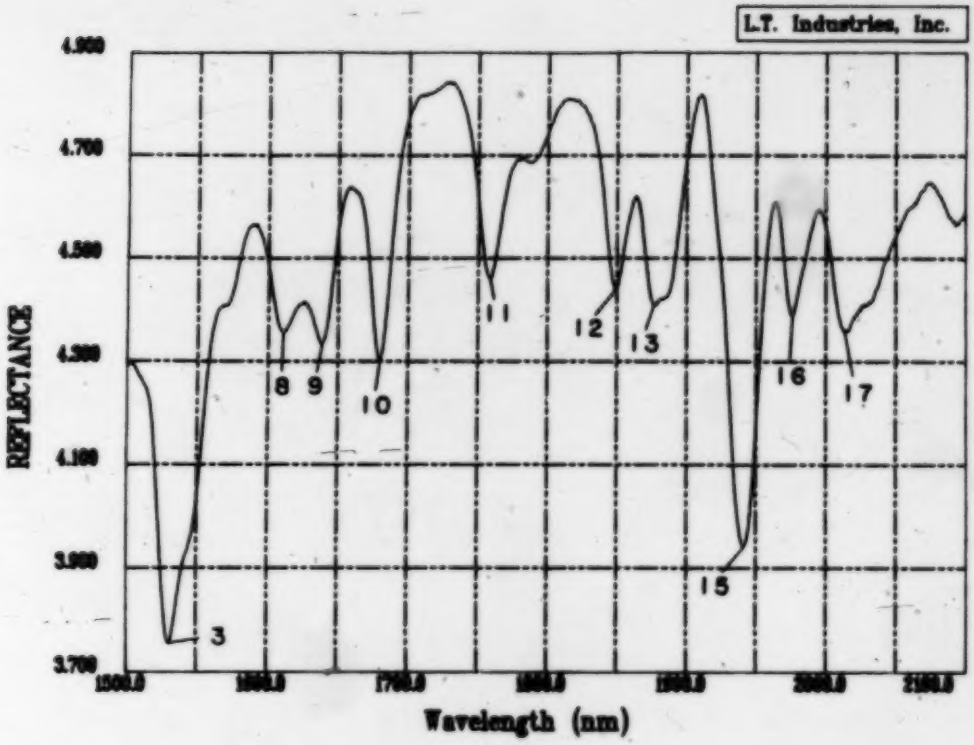


| BAND NUMBER | MEASURED WAVELENGTH (nm) | BAND NUMBER | MEASURED WAVELENGTH (nm) |
|---|---|---|---|
| 3 | 1531 | 12 | 1849 |
| 8 | 1611 | 13 | 1878 |
| 9 | 1639 | 15 | 1941 |
| 10 | 1680 | 16 | 1977 |
| 11 | 1759 | 17 | 2013 |

**Figure 52.** Diffuse reflectance spectrum of NBS SRM 1920 (Near-Infrared Reflectance Wavelength Standard) obtained with the LTI Quantum 1200 NIR Analyzer (Background = carbon black).

| | |
|---|---|
| THIMBLE SIZE | 10mm X 50 mm |
| SAMPLE WEIGHT | 1.5 g |
| SOLVENT VOLUME | 20 mL (Toluene) |
| EXTRACTION TIME | 30 minutes |

**Figure 53.** Micro-Soxhlet extraction assembly used for the analysis of bitumen and solids contents of oil sand.

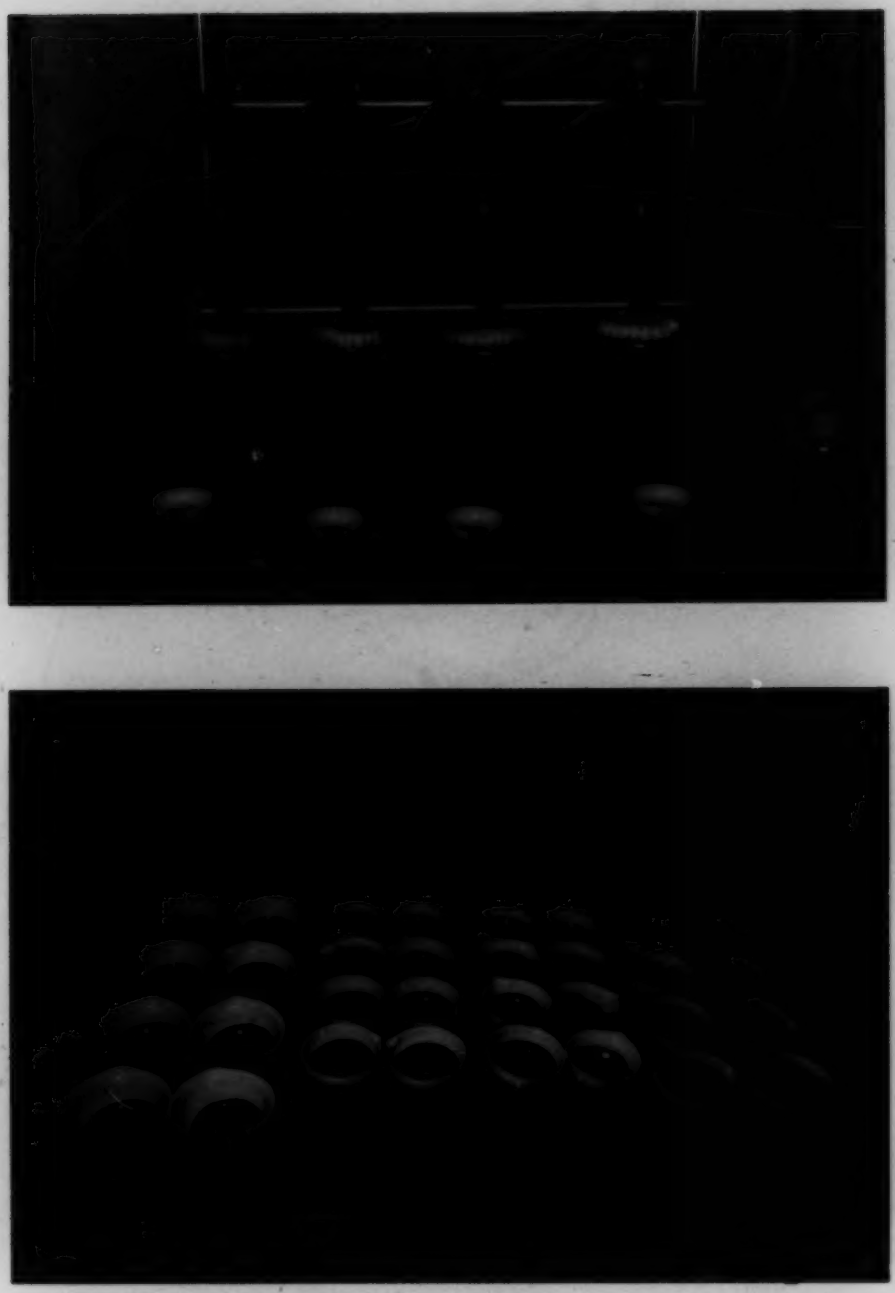

**Figure 54.** Micro–Soxhlet extraction equipment used for the analysis of oil sand samples. Lower photograph shows bitumen residue after evaporation of solvent.

samples to be analyzed over the course of this study are relatively free of connate water. As such, corrections to compensate for moisture loss need not be applied.

Preliminary assay results obtained for replicate determinations on a variety of oil sand samples are given in Table IX. For these analyses, both the thimbles and evaporating dishes were dried in a forced draft oven for 24 hours at 120 °C. Results indicate that there is a significant bias in the analysis. The consistently low mass closures (the ratio of the sum of the measured bitumen and solids mass to the original sample mass) imply that measures for the bitumen and/or solids content of the sample are under–estimates of the true composition.

Systematic error in the analysis procedure may be attributed to a number of sources, including:

- Loss of bitumen light ends upon drying the solvent extract at elevated temperatures.
- Loss of hygroscopic water from thimbles and oil sand samples.
- Incomplete retention of fine particles in the thimble.

The first two sources of bias would lead to low recoveries. The latter problem, if present, would not be detected by examining mass closure data. Solids lost through the thimble would ultimately report to the extract and be accounted for (albeit erroneously) as bitumen. The toluene used for extraction contained no measurable residue upon evaporation.

Tests were performed to evaluate the sources of systematic error thought responsible for the low mass closure results. A comparison of bitumen weights obtained from sample extracts evaporated under ambient conditions and subsequently dried in an oven are shown in Table X. The average weight loss upon heating the bitumen for 16 hours at 120 °C was on the order of 0.01–0.02 g, a significant value when we consider that the original sample of oil sand analyzed typically contains less than 0.2 g of bitumen. Blank thimble extractions were also done to see if hygroscopic water could have a detrimental influence on assay results. Weight loss data obtained

**Table IX.** Preliminary estimates for the precision of bitumen and solids analyses performed on samples of lean, medium, and rich grade oil sand using the micro-Soxhlet extraction procedure.

| SAMPLE | | BITUMEN (wt %) | SOLIDS (wt %) | MASS CLOSURE |
|---|---|---|---|---|
| LEAN GRADE | MEAN | 3.15 | 94.48 | 0.9763 |
| (n = 4) | STD DEV | 0.35 | 0.44 | 0.0033 |
| LEAN GRADE | MEAN | 3.36 | 95.15 | 0.9851 |
| (n = 2) | STD DEV | 0.34 | 0.21 | 0.0013 |
| MEDIUM GRADE | MEAN | 10.22 | 86.81 | 0.9704 |
| (n = 3) | STD DEV | 0.22 | 0.42 | 0.0044 |
| RICH GRADE | MEAN | 13.14 | 84.28 | 0.9742 |
| (n = 4) | STD DEV | 0.67 | 0.70 | 0.0029 |

$$Mass\ Closure = \frac{\%Bitumen + \%Solids}{100}$$

**Table X.** Data obtained for evaluating the effect of systematic errors in the analysis of oil sand samples by micro–Soxhlet extraction.

LOSSES OF BITUMEN LIGHT ENDS
MEDIUM GRADE OIL SAND

| WEIGHT BITUMEN (g) Extract Evaporated Under Ambient Conditions (24 Hours at 20 °C) | WEIGHT BITUMEN (g) Extract Dried in Forced Draft Oven (16 Hours at 120 °C) |
|---|---|
| 0.1150 | 0.0979 |
| 0.1086 | 0.0930 |
| 0.1145 | 0.0988 |
| 0.1300 | 0.1103 |
| 0.1061 | 0.0940 |
| 0.1238 | 0.1112 |
| 0.1117 | 0.0981 |
| 0.1385 | 0.1213 |

BLANK THIMBLE EXTRACTIONS

| | | |
|---|---|---|
| Weight Loss Upon Drying in Forced Draft Oven for 1.5 Hour at 120 °C | MEAN | 0.0152 g |
| | STD DEV | 0.0020 g |
| Weight Loss Upon Extraction | MEAN | 0.0002 g |
| | STD DEV | 0.0002 g |

by simply drying the thimbles for 1.5 hours at 120 $^{0}$C indicate that the magnitude of bias introduced by not accounting for residual moisture is comparable to that associated with the loss of bitumen light ends.

These findings suggest that considerable care must be exercized when performing micro–Soxhlet extractions. To minimize the effects of systematic error, sample thimbles must be dried prior to analysis. Further, extract solutions should be evaporated to dryness at room temperature. As shown by the replicate sample analysis data presented in Table XI, recoveries of better than 99% can be achieved under these conditions. The precision of the analytical method is acceptable and, based on preliminary investigations, comparable to that which can be attained from NIR–DR measurements. It should be noted that differences among these replicate sample analyses probably reflect sampling variability more than actual analytical variability. Sampling uncertainties when dealing with small quantities of heterogeneous material are most likely the dominant source of error in an analysis.

### 3.5 Training Set and Data Modelling

Having specified the operating conditions for the analyzer, sample spectra were obtained for oil sand at 1 cm intervals along the entire length of the test core section. The spectra were digitized and stored on hard disc in the computer.

To establish a model relating the spectral features of these samples to oil sand composition, it is necessary to develop a reference library of spectra for which assays of the oil sand samples are known. Since the spectra of all samples in the core were already on file, it became a simple matter of analyzing a number of the samples to provide the requisite assay information. This training set, once developed, would be used to generate correlations between spectral characteristics and sample composition.

A total of 48 samples were selected to represent the broad compositional range of material contained within the test section of core. Samples, each weighing on the

**Table XI.** Precision of replicate micro-Soxhlet extraction analyses for samples of lean, medium, and rich grade oil sand.

| SAMPLE | BITUMEN (wt %) | SOLIDS (wt %) | MASS CLOSURE |
|---|---|---|---|
| LEAN | 5.99 | 93.56 | 0.9955 |
| GRADE | 6.35 | 93.24 | 0.9959 |
| | 6.19 | 93.36 | 0.9955 |
| | 6.30 | 93.29 | 0.9959 |
| | 6.02 | 93.70 | 0.9972 |
| | 6.03 | 93.60 | 0.9964 |
| | 5.85 | 93.82 | 0.9968 |
| | 5.89 | 93.94 | 0.9963 |
| MEAN | 6.05 | 93.56 | 0.9962 |
| STD DEV | 0.22 | 0.25 | 0.0006 |
| RSD | 3.68 % | 0.27 % | 0.06 % |
| MEDIUM | 8.34 | 90.80 | 0.9914 |
| GRADE | 8.10 | 91.11 | 0.9921 |
| | 8.51 | 90.81 | 0.9932 |
| | 8.49 | 90.82 | 0.9931 |
| | 8.51 | 90.70 | 0.9921 |
| | 8.63 | 90.73 | 0.9936 |
| | 8.83 | 90.26 | 0.9909 |
| | 8.90 | 90.28 | 0.9918 |
| MEAN | 8.54 | 90.69 | 0.9923 |
| STD DEV | 0.26 | 0.29 | 0.0009 |
| RSD | 3.0 % | 0.3 % | 0.10 % |
| RICH | 16.67 | 82.88 | 0.9955 |
| GRADE | 16.67 | 82.90 | 0.9957 |
| | 17.00 | 82.53 | 0.9953 |
| | 16.99 | 82.48 | 0.9947 |
| | 16.86 | 82.84 | 0.9950 |
| | 16.59 | 82.86 | 0.9945 |
| | 16.88 | 82.73 | 0.9961 |
| | 16.48 | 83.00 | 0.9948 |
| MEAN | 16.74 | 82.78 | 0.9952 |
| STD DEV | 0.19 | 0.18 | 0.0005 |
| RSD | 1.14 % | 0.22 % | 0.05 % |

order of 1–2 grams, were removed from the core using a scalpel. The samples were identified with respect to their position along the core. Care was taken to ensure that samples withdrawn matched the exact area viewed when taking the NIR–DR spectra.

Each of these training set samples was ground in a mortar and pestle. A subsample of the homogenized material was then analyzed using the micro–Soxhlet extraction procedure. Assay data, along with a qualitative description of the samples, is presented in Table XII.

Representative spectra for some of the samples included in the training set are illustrated in Figures 55–63. The first and second derivative spectra were generated from the absorbance spectra (*i.e.*, the $Log(1/R)$ transformed data). Note that the training set includes samples of coal. This material was found to be relatively abundant in the test section of core, oftentimes interbedded with oil sand. As evidenced in the spectra for these samples (and further substantiated in the mass closure results from the sample analysis), these sediments contain an appreciable amount of water.

It became apparent when analyzing the samples in this training set that our current understanding of the structure of oil sand may not be adequate to explain the range of grades found within the deposit. As postulated by Takamura (22), oil sand is thought to consist of a matrix of small sand and clay particles held within a continuum of bitumen and water. This structure is shown in Figure 64. The bitumen content of an oil sand sample is presumably governed by the size distribution of the solids (and hence related to the interstitial volume). It is believed that this model of an oil sand applies only to samples which can be unequivocally classified as oil rich material and containing perhaps 12% bitumen or more. Oil sands of lower grade are thought to be the result of dilution with relatively oil–free sediments (clay or coal). Thus, an oil sand containing less than 12% bitumen is not a homogeneous dispersion of bitumen, water, and solids, but rather a mixture of discrete bitumen–rich and bitumen–lean materials.

**Table XII.** Description and analytical data for training set samples. Assay results were obtained using the micro–Soxhlet extraction procedure.

| SAMPLE DEPTH (metres) | SAMPLE DESCRIPTION | BITUMEN (wt %) | SOLIDS (wt %) | MASS CLOSURE | ANHYDROUS BITUMEN (wt %) |
|---|---|---|---|---|---|
| 84.10 | Oil Sand | 13.60 | 86.62 | 0.9923 | 13.71 |
| 84.21 | Interbedded Oil Sand and Coal | 10.47 | 87.41 | 0.9787 | 10.6. |
| 84.28 | Oil Sand | 16.28 | 83.08 | 0.9937 | 16.39 |
| 84.31 | Interbedded Oil Sand and Clay | 8.07 | 91.34 | 0.9942 | 8.13 |
| 84.36 | Coal | 1.98 | 93.67 | 0.9646 | 2.07 |
| 84.43 | Oil Sand | 13.48 | 86.34 | 0.9879 | 13.61 |
| 84.53 | Interbedded Oil Sand and Clay | 4.09 | 94.91 | 0.9900 | 4.13 |
| 84.56 | Interbedded Oil Sand and Clay | 9.89 | 89.49 | 0.9908 | 9.68 |
| 84.59 | Coal | 0.96 | 94.01 | 0.9496 | 1.00 |
| 84.72 | Oil Sand | 9.51 | 89.93 | 0.9943 | 9.56 |
| 84.76 | Interbedded Oil Sand and Clay | 5.69 | 93.77 | 0.9946 | 5.72 |
| 84.82 | Oil Sand | 14.96 | 84.06 | 0.9899 | 15.10 |
| 84.94 | Oil Sand | 14.48 | 84.79 | 0.9925 | 14.57 |
| 85.01 | Interbedded Oil Sand and Clay | 4.76 | 94.54 | 0.9930 | 4.79 |
| 85.03 | Interbedded Oil Sand and Clay | 4.56 | 94.70 | 0.9926 | 4.60 |
| 85.06 | Interbedded Oil Sand and Clay | 8.15 | 91.09 | 0.9924 | 8.21 |
| 85.36 | Oil Sand | 16.11 | 83.44 | 0.9955 | 16.18 |
| 85.50 | Oil Sand | 17.66 | 81.89 | 0.9955 | 17.74 |
| 85.58 | Oil Sand | 14.06 | 85.53 | 0.9960 | 14.12 |
| 85.62 | Interbedded Oil Sand and Coal | 12.54 | 85.42 | 0.9796 | 12.80 |
| 85.71 | Interbedded Oil Sand and Coal | 9.09 | 88.71 | 0.9780 | 9.30 |
| 85.78 | Oil Sand | 15.83 | 83.68 | 0.9951 | 15.91 |
| 85.99 | Oil Sand | 16.32 | 83.09 | 0.9941 | 16.42 |
| 86.06 | Interbedded Oil Sand and Clay | 5.24 | 92.53 | 0.9777 | 5.36 |
| 86.15 | Coal | 2.11 | 92.89 | 0.9500 | 2.22 |
| 86.36 | Clay | 2.01 | 97.24 | 0.9935 | 2.03 |
| 86.38 | Clay | 1.86 | 97.32 | 0.9919 | 1.88 |
| 86.41 | Clay | 3.31 | 95.94 | 0.9914 | 3.23 |
| 86.46 | Interbedded Oil Sand and Clay | 3.14 | 96.13 | 0.9927 | 3.16 |
| 86.58 | Interbedded Oil Sand and Clay | 4.28 | 95.03 | 0.9931 | 4.31 |
| 86.62 | Interbedded Oil Sand and Clay | 6.45 | 92.95 | 0.9940 | 6.49 |
| 86.66 | Interbedded Oil Sand and Clay | 5.47 | 93.92 | 0.9939 | 5.51 |
| 86.69 | Interbedded Oil Sand and Clay | 6.43 | 92.88 | 0.9931 | 6.48 |
| 86.73 | Interbedded Oil Sand and Clay | 5.83 | 93.54 | 0.9936 | 5.86 |
| 86.90 | Oil Sand | 14.49 | 84.84 | 0.9933 | 14.59 |
| 86.75 | Interbedded Oil Sand and Clay | 7.13 | 92.26 | 0.9938 | 7.16 |
| 86.88 | Oil Sand | 16.07 | 83.21 | 0.9927 | 16.18 |
| 86.92 | Interbedded Oil Sand and Clay | 8.18 | 91.06 | 0.9924 | 8.24 |
| 87.14 | Interbedded Oil Sand and Clay | 6.50 | 92.90 | 0.9940 | 6.54 |
| 87.29 | Oil Sand | 13.58 | 86.91 | 0.9949 | 13.64 |
| 87.38 | Oil Sand | 13.41 | 86.06 | 0.9949 | 13.48 |
| 87.48 | Oil Sand | 13.71 | 85.73 | 0.9944 | 13.78 |
| 87.67 | Oil Sand | 13.53 | 85.78 | 0.9931 | 13.63 |
| 87.88 | Oil Sand | 10.03 | 88.64 | 0.9907 | 10.17 |
| 87.96 | Coal | 0.94 | 97.39 | 0.9838 | 0.96 |
| 88.06 | Oil Sand | 13.55 | 86.86 | 0.9941 | 13.63 |
| 88.09 | Interbedded Oil Sand and Coal | 9.48 | 88.44 | 0.9793 | 9.68 |
| 88.27 | Interbedded Oil Sand and Clay | 7.50 | 91.88 | 0.9838 | 7.64 |

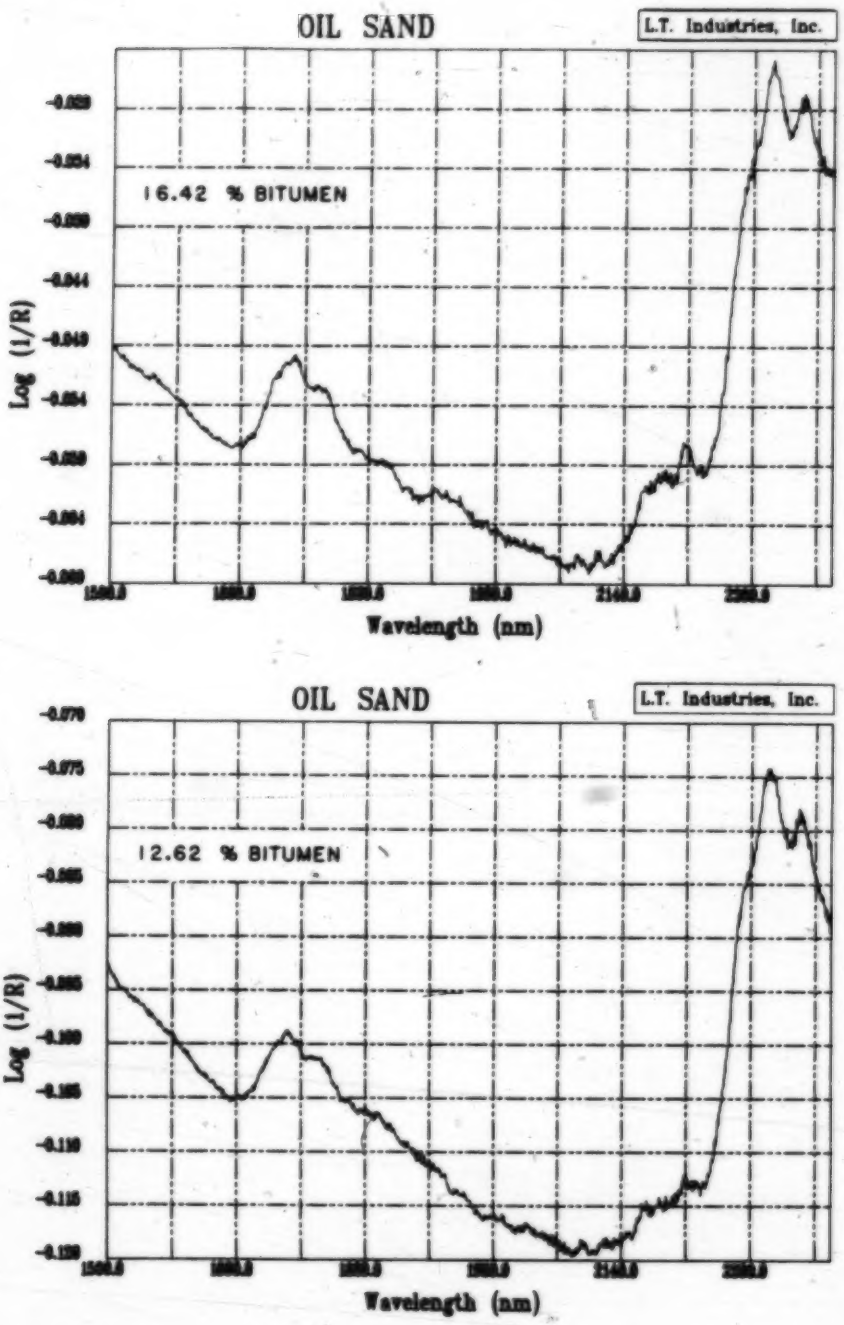


**Figure 55** Representative diffuse reflectance spectra for samples of oil sand in the training set (Background = carbon black).

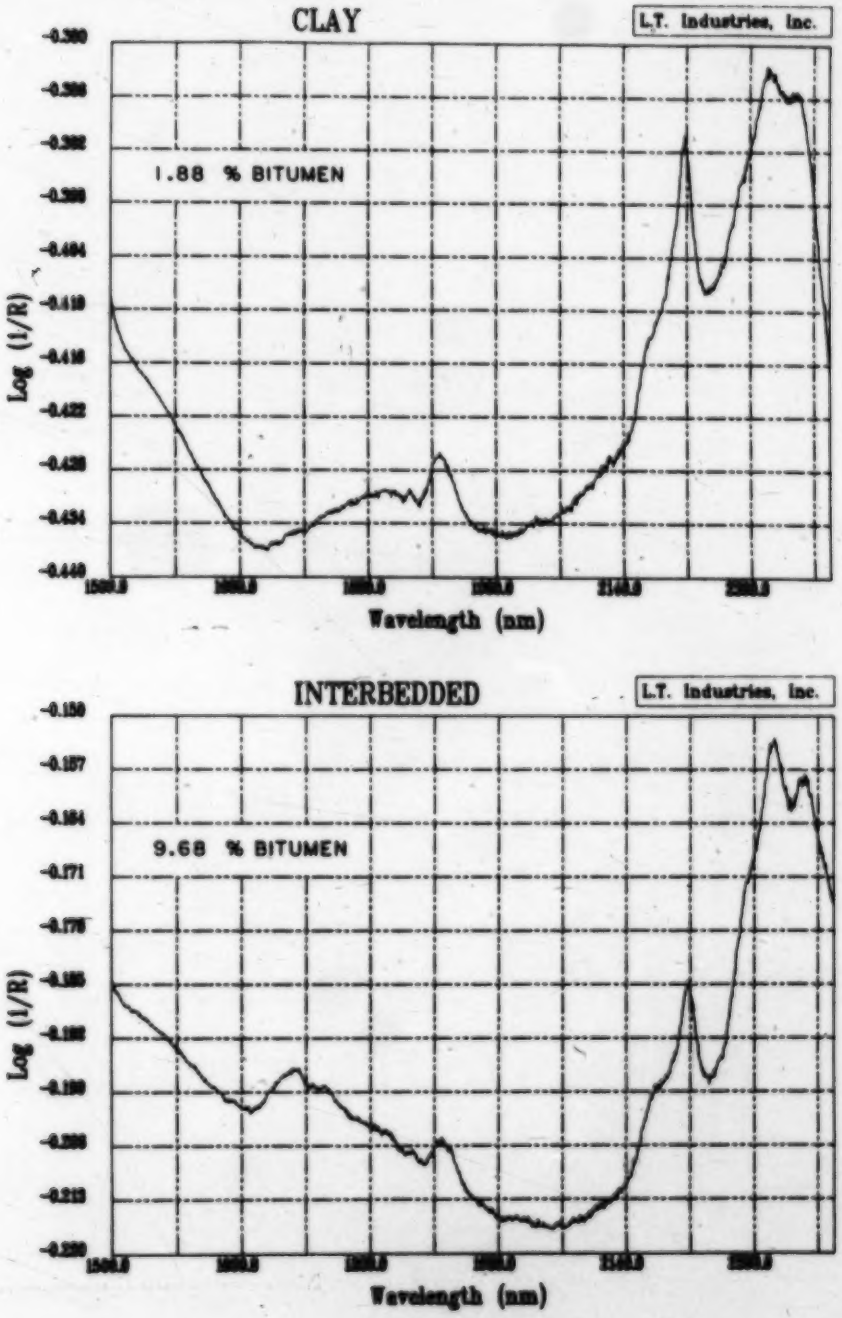


**Figure 56.** Representative diffuse reflectance spectra for samples of clay and interbedded oil sand and clay in the training set (Background = carbon black).

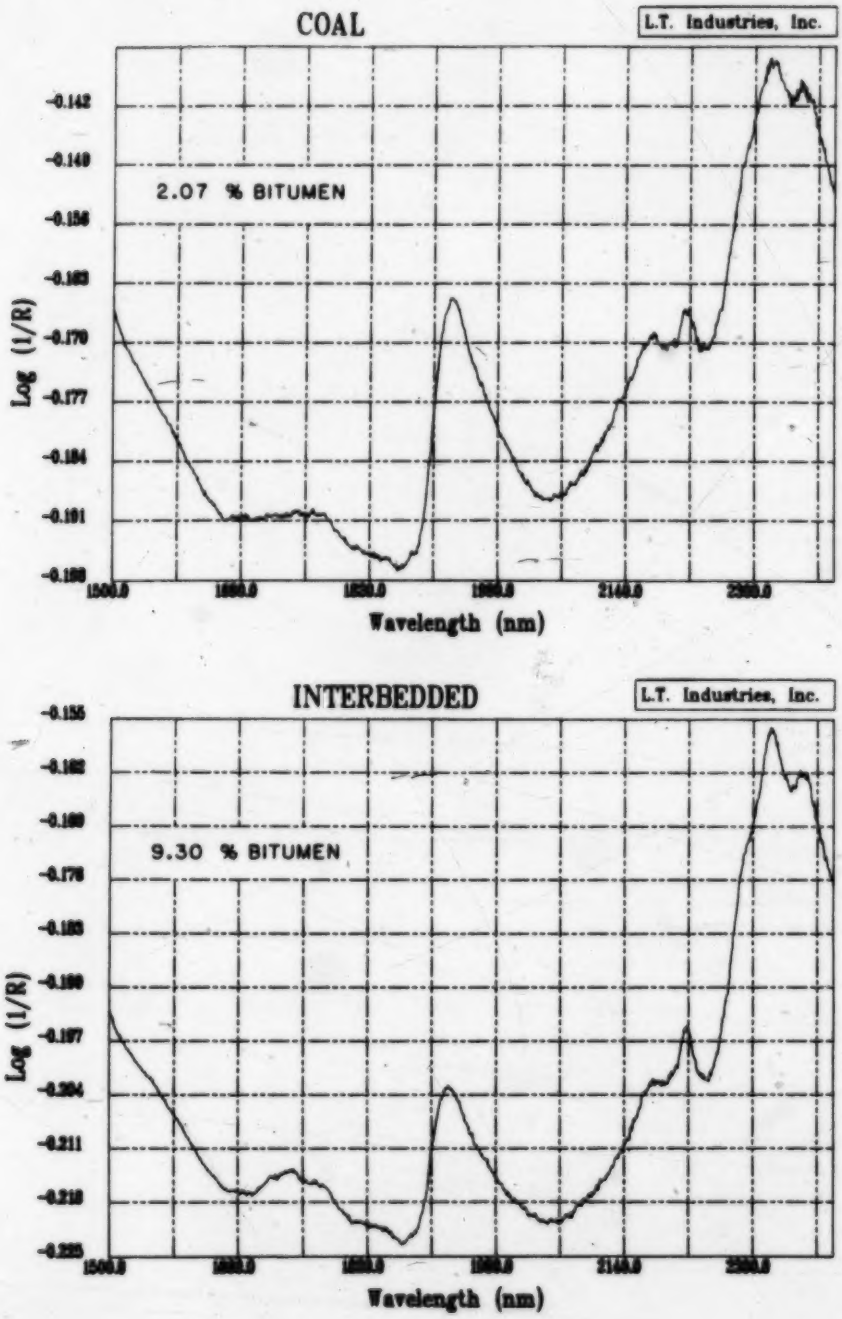


**Figure 57.** Representative diffuse reflectance spectra for samples of coal and interbedded oil sand and coal in the training set (Background = carbon black).

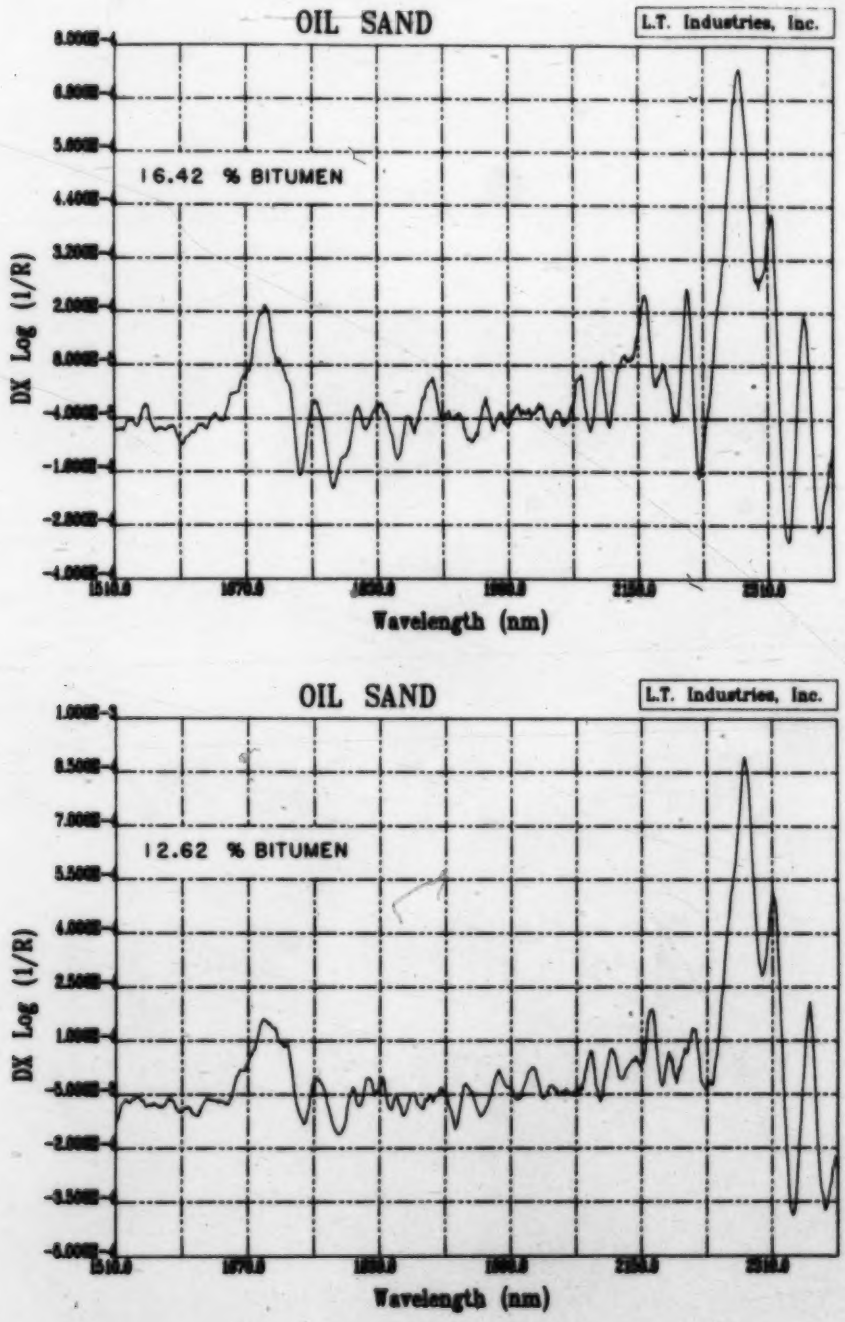


**Figure 58.** Representative diffuse reflectance spectra (first derivative of $Log(1/R)$ data) for samples of oil sand in the training set (Background = carbon black).

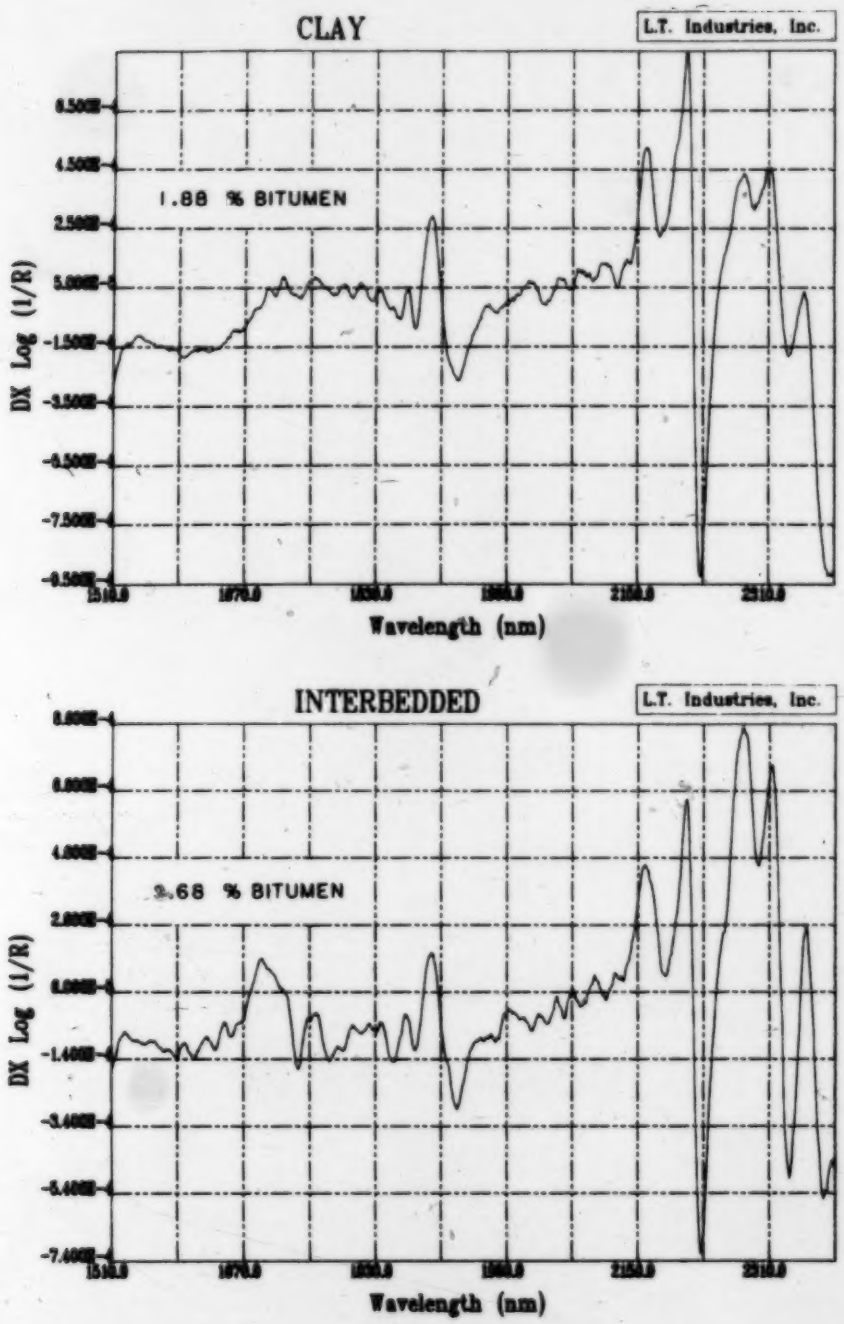


**Figure 59.** Representative diffuse reflectance spectra (first derivative of $Log(1/R)$ data) for samples of clay and interbedded oil sand and clay in the training set (Background = carbon black).

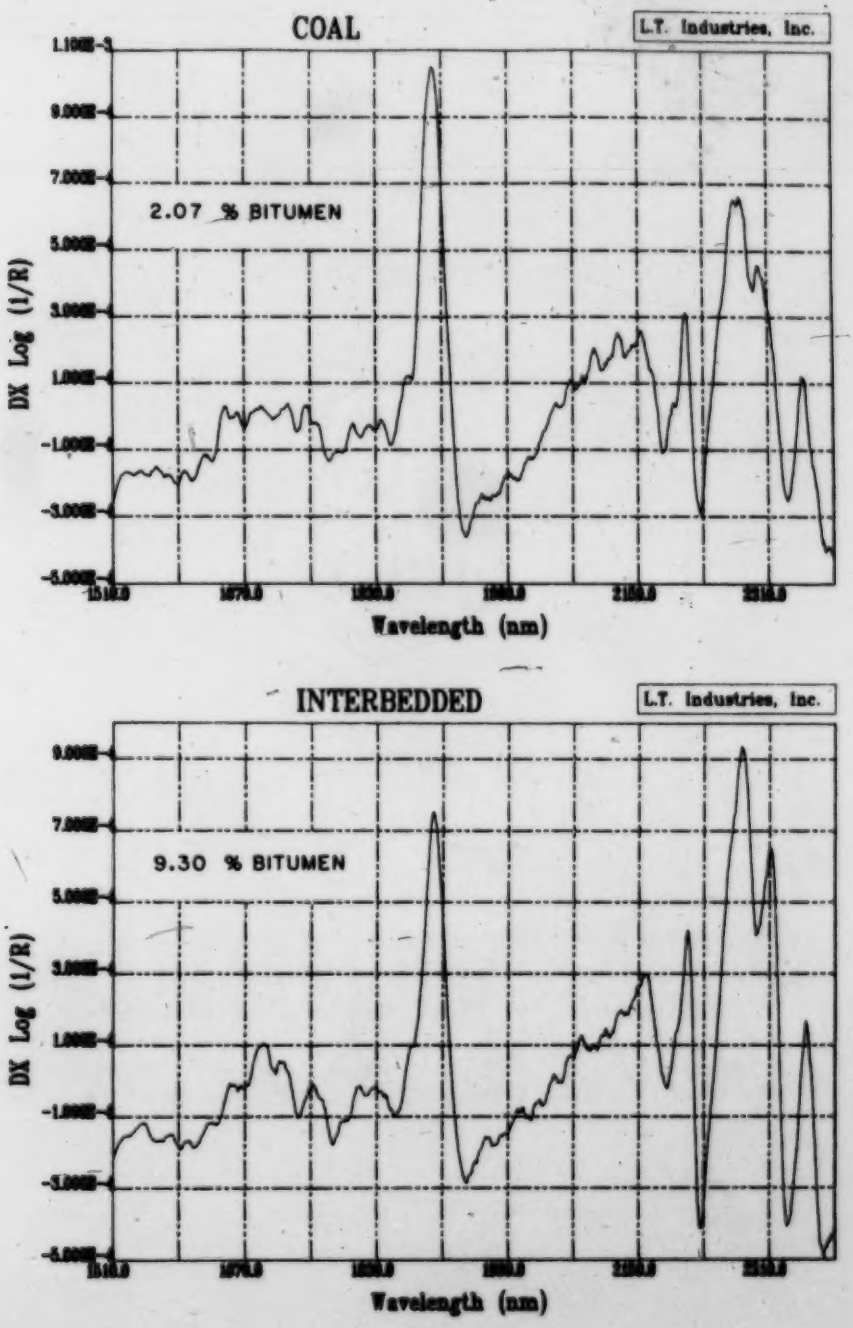


**Figure 60.** Representative diffuse reflectance spectra (first derivative of $Log(1/R)$ data) for samples of coal and interbedded oil sand and coal in the training set (Background = carbon black).

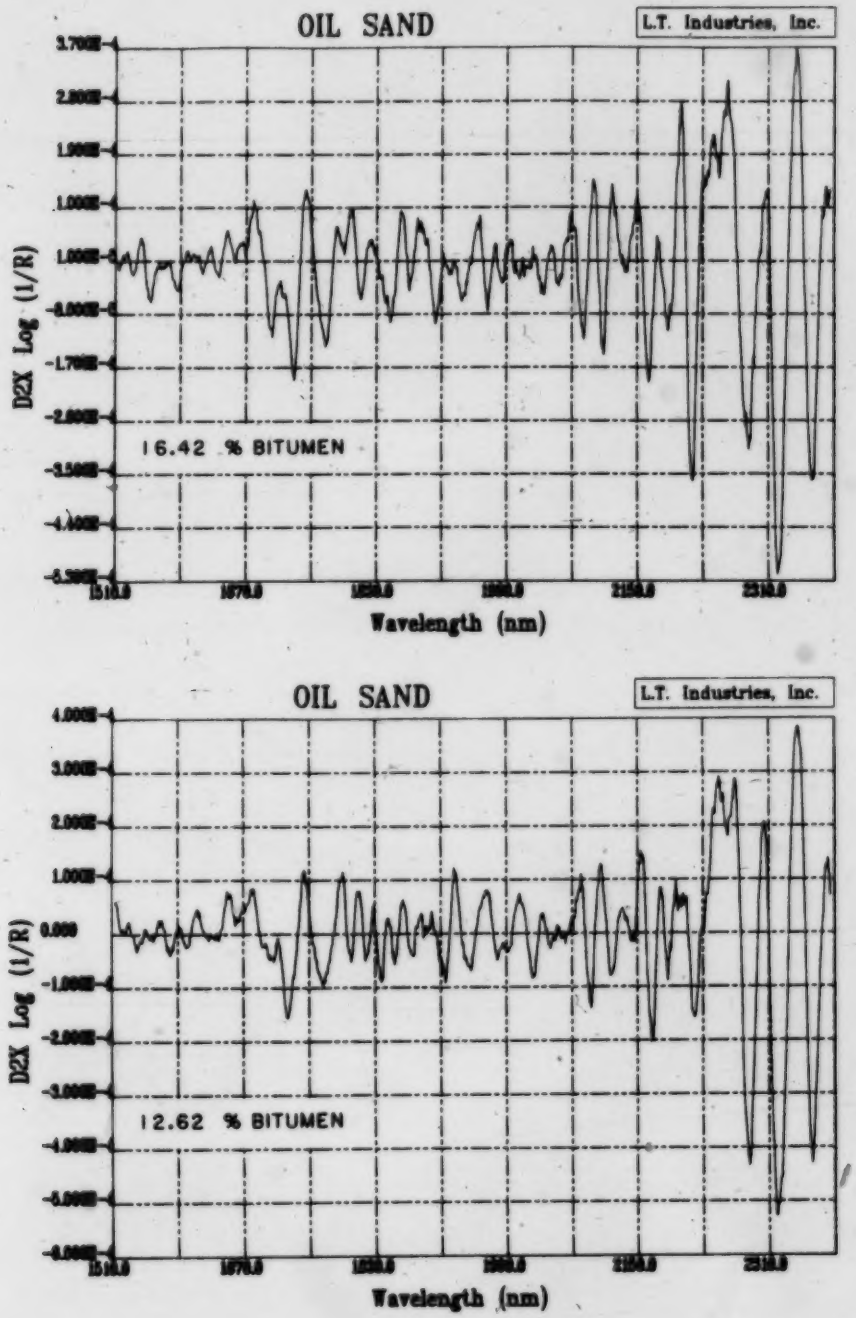


**Figure 61.** Representative diffuse reflectance spectra (second derivative of $Log(1/R)$ data) for samples of oil sand in the training set (Background = carbon black).

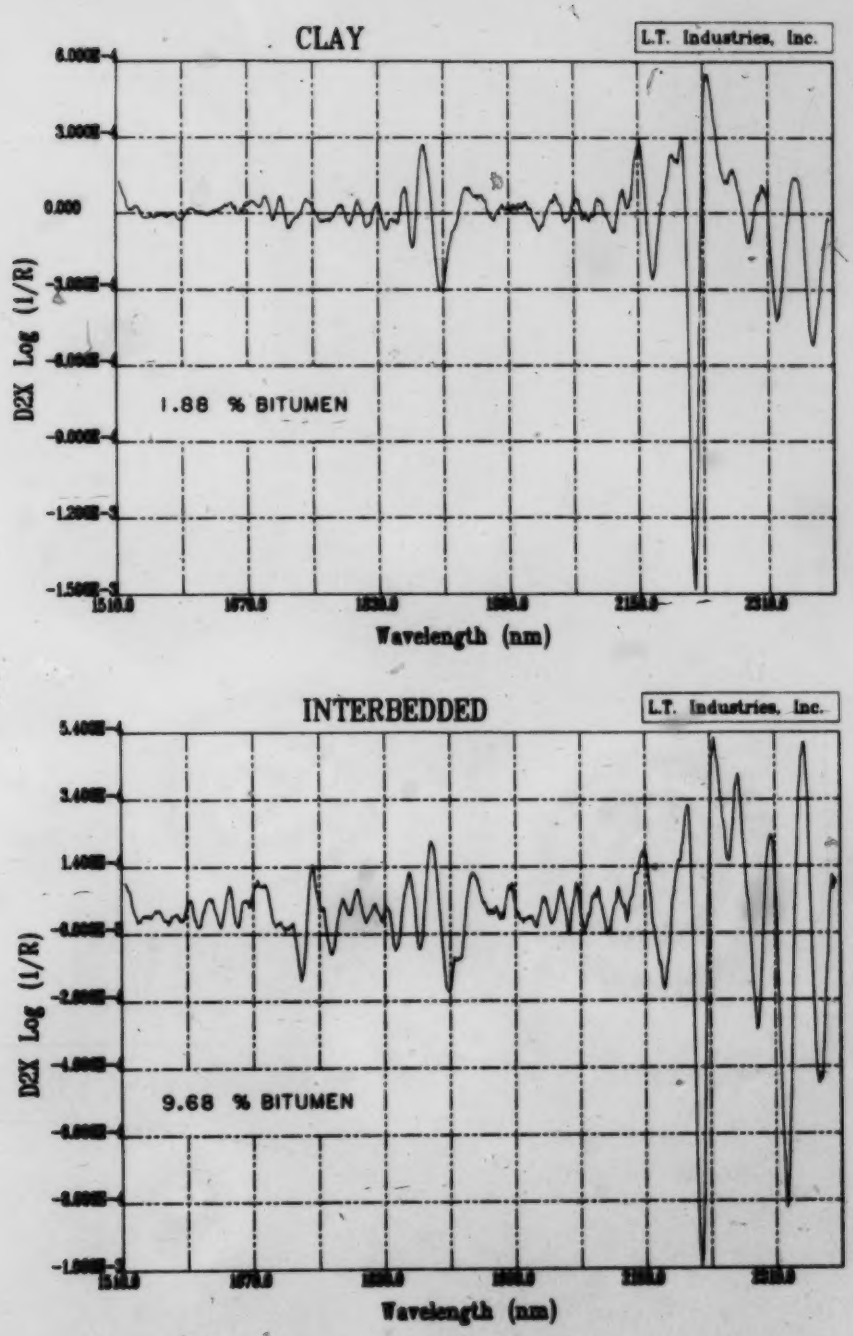


**Figure 62.** Representative diffuse reflectance spectra (second derivative of $Log(1/R)$ data) for samples of clay and interbedded oil sand and clay in the training set (Background = carbon black).

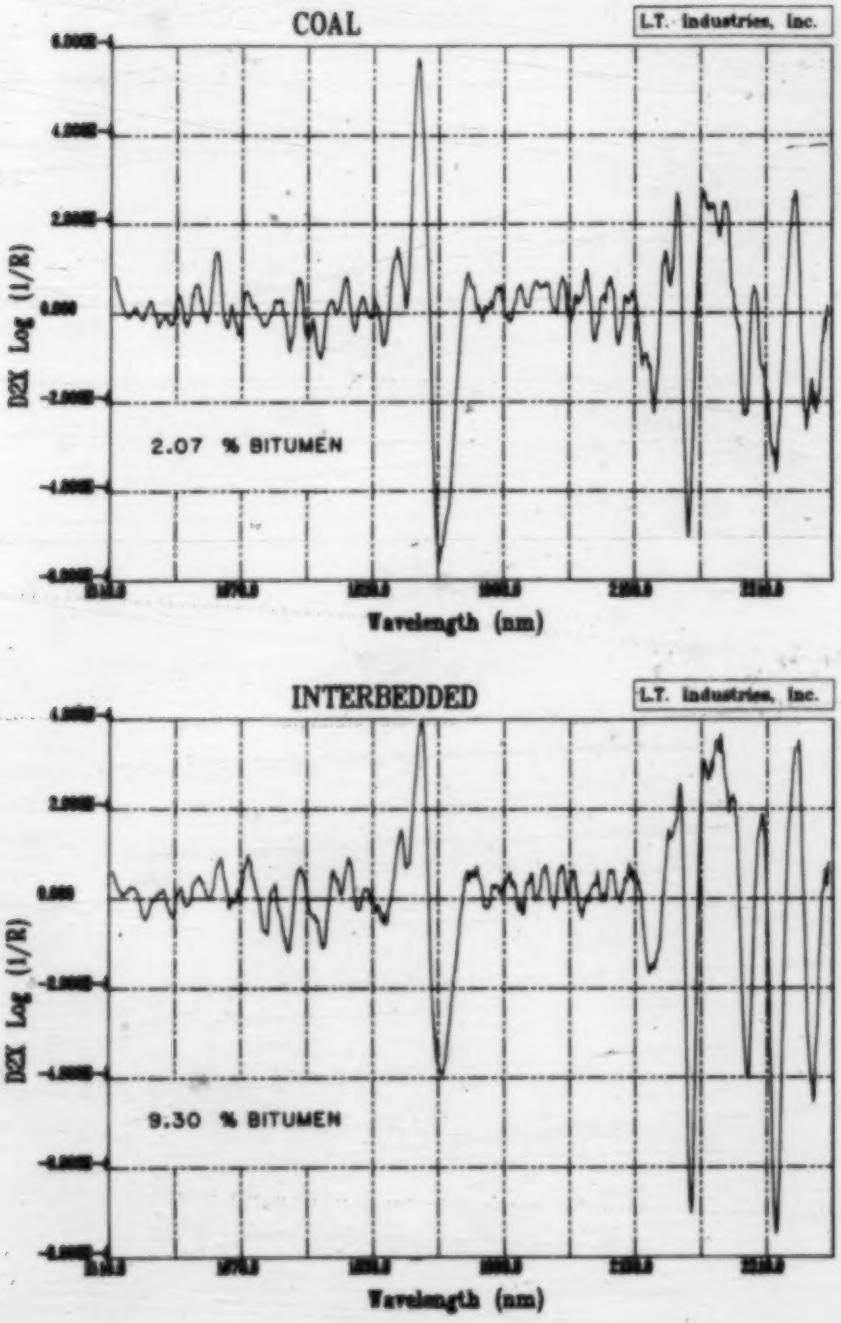


**Figure 63.** Representative diffuse reflectance spectra (second derivative of $Log(1/R)$ data) for samples of coal and interbedded oil sand and coal in the training set (Background = carbon black).

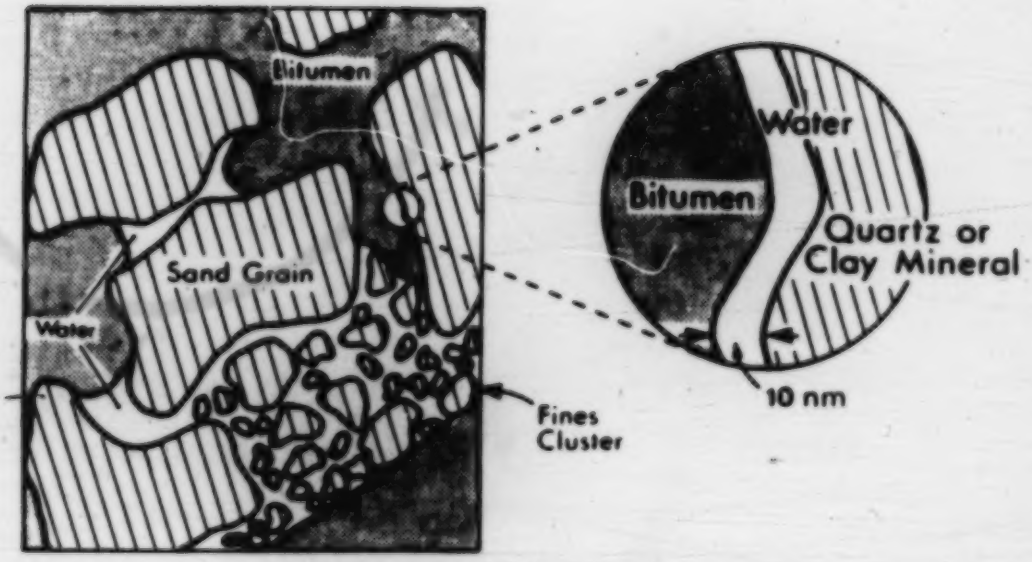


**Figure 64.** Structural model of an oil sand contained within the Athabasca deposit. Adapted from Takamura (22).

The correlations between compositional data and spectral features as a function of wavelength for samples in the training set is graphically shown in Figures 65–67. There appears to be a direct relationship between absolute absorbance and bitumen content over virtually all wavelengths in the range 1500–2400 nm. From these results, it would seem that a model relating sample bitumen content and absorbance could be predicated simply on the intensity of light reflected from the sample surface at any given wavelength. Note that, unlike the preliminary correlations established during studies with the Nicolet FT-IR, we are not looking at the peak height of absorbance bands from some imposed baseline.

Correlations based on the first or second derivative of the absorbance spectrum are considerably more discriminating than those based on absolute reflectivity. By virtue of the mathematical processing, differences in the baseline intensities of the reflected light have are normalized. Thus, the derivative spectra are descriptive of the actual absorbance peaks. In these instances, there is a strong dependency between the correlation coefficient and wavelength. Models based on derivative spectra are likely to provide a better relationship between spectral features and sample composition.

A statistical procedure known as stepwise linear regression was used to model the data provided from the training set. The objective of the analysis is to derive a model of the form:

$$Y = C_0 + C_1(W_1) + C_2(W_2) + \cdots + C_n(W_n)$$

where $Y$ is the parameter of interest (in our case % bitumen content) and $W_1$, $W_2$ through $W_n$ represent the magnitude of a spectral feature (absolute absorbance or derivative value) at wavelengths for which there is correspondence with sample composition. The coefficients $C_0$, $C_1$, $C_2$ through $C_n$ are the associated weighting factors.

In order to reduce the problem of solving this model to a manageable level, it is assumed that the magnitude of a spectral feature at a wavelength for which there

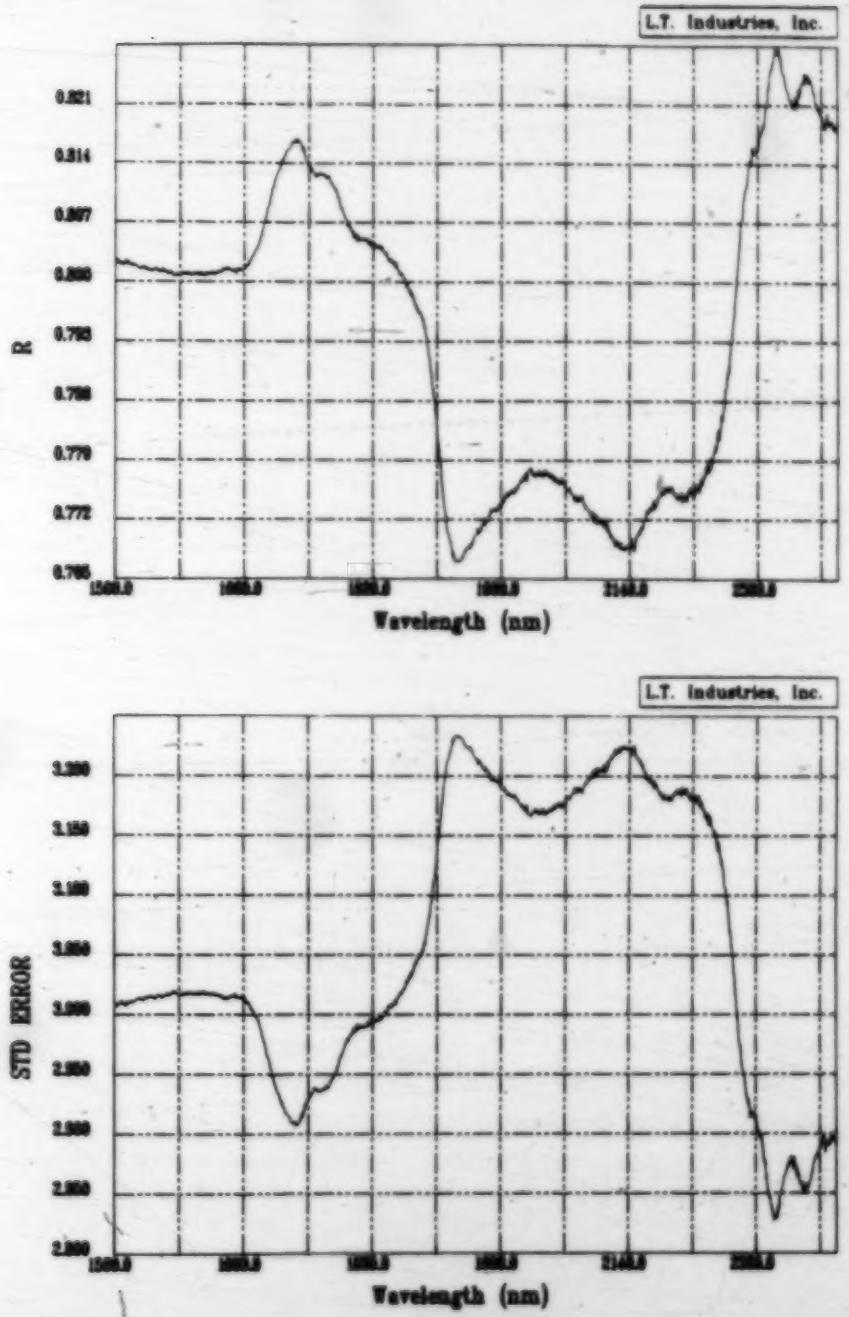


**Figure 65.** Correlation coefficient and its associated standard error for the relationship between compositional data and spectral features ($Log(1/R)$, Background = carbon black) as a function of wavelength for samples in the training set.

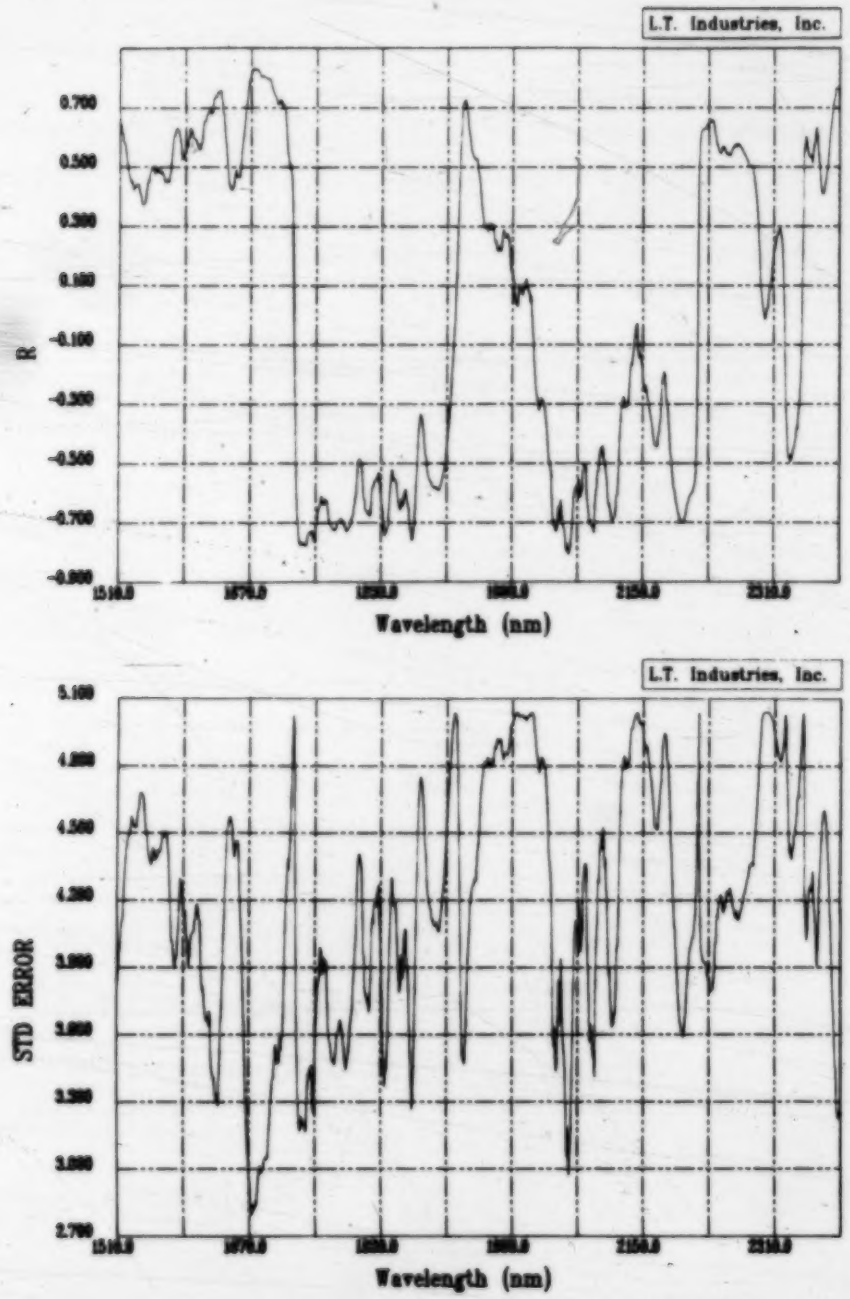


**Figure 66.** Correlation coefficient and its associated standard error for the relationship between compositional data and spectral features (first derivative of $Log(1/R)$, Background = carbon black) as a function of wavelength for samples in the training set.

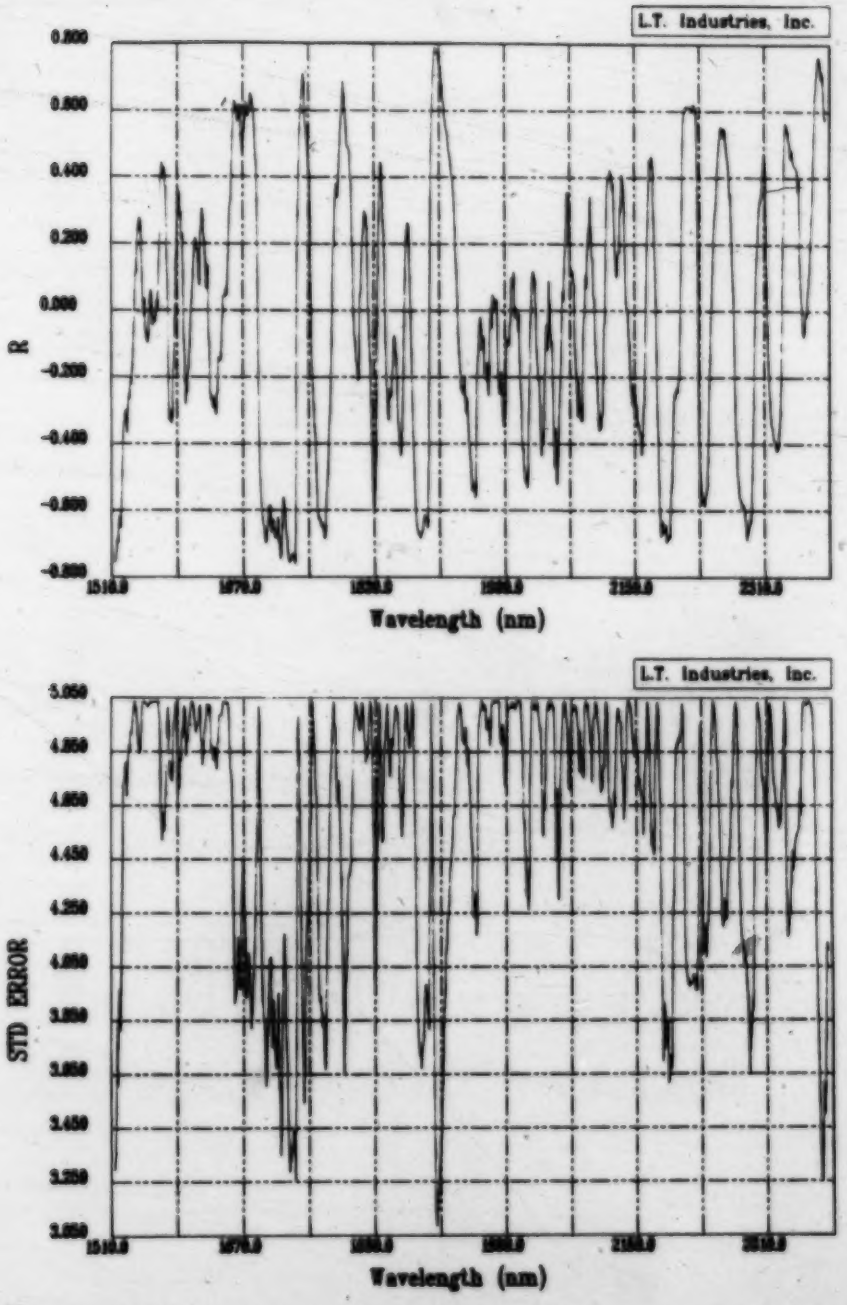


**Figure 07.** Correlation coefficient and its associated standard error for the relationship between compositional data and spectral features (second derivative of $Log(1/R)$, Background = carbon black) as a function of wavelength for samples in the training set.

exists a high correlation between response and sample assay serves to explain most of the variability in the data. This simple model is given by the expression:

$$Y = C_0 + C_1(W_1)$$

Any lack of fit is caused by second order effects which can be modelled using additional wavelengths. The selection and addition of subsequent terms is based on their ability to reduce the residual error (determined by means of an F–test) and is directly related to an improvement in the multiple correlation coefficient.

Composite models were developed for the training set spectra obtained in absorbance, first derivative, and second derivative mode. In all cases, the primary relationship between assay data and spectral feature was determined for each of ten starting wavelengths. These wavelengths correspond to the ten best positions at which there is high correlation between sample assay and spectral response. Having established this, additional terms were added (up to a maximum of 4 wavelengths) in order to reduce the sum of residual errors. The various models generated by this procedure are tabulated in Appendix A. The best model obtained (highest multiple correlation coefficient) for each series of training set spectra is described in Table XIII. Plots of predicted grade *versus* the actual measured bitumen content of training set samples are shown in Figures 68–70.

Results would suggest that the best model for the calibration of spectral response is that based on the first derivative of absorbance data. This model was used to establish the bitumen content of all samples analyzed by NIR–DR in the test section of core. The resulting grade profile will be interpreted using geostatistical analysis and the concepts of fractal dimension.

**Table XIII.** Statistical summary of the best fit models developed from the training set for relating the bitumen content of core samples and their diffuse reflectance spectra.

*Log*(1/*R*) SPECTRA

| | |
|---|---|
| MULTIPLE CORRELATION COEFFICIENT | 0.9615 |
| STD ERROR OF ESTIMATE | 1.603 |
| SUM OF SQUARED ERRORS | 110.6 |
| F-TEST | 102.9 |

| WAVELENGTH | MODEL COEFFICIENT | STD ERROR | t-VALUE |
|---|---|---|---|
| 2399.0 | 0.2900E+03 | 0.2711E+01 | 0.1103E+02 |
| 1923.0 | -0.7888E+03 | 0.9470E+01 | 0.8013E+01 |
| 2129.0 | 0.9734E+03 | 0.1558E+03 | 0.6252E+01 |
| 2191.0 | -0.4920E+03 | 0.1115E+03 | 0.4413E+01 |
| INTERCEPT | 0.1306E+01 | | |

FIRST DERIVATIVE OF *Log*(1/*R*) SPECTRA

| | |
|---|---|
| MULTIPLE CORRELATION COEFFICIENT | 0.9673 |
| STD ERROR OF ESTIMATE | 1.323 |
| SUM OF SQUARED ERRORS | 752.6 |
| F-TEST | 156.1 |

| WAVELENGTH | MODEL COEFFICIENT | STD ERROR | t-VALUE |
|---|---|---|---|
| 1964.0 | 0.7302E+06 | 0.4606E+04 | 0.1586E+03 |
| 2234.0 | 0.1268E+06 | 0.1176E+04 | 0.1078E+03 |
| 1790.0 | -0.4686E+06 | 0.4949E+04 | 0.9466E+01 |
| 2030.0 | -0.3884E+06 | 0.5540E+04 | 0.6098E+01 |
| INTERCEPT | 0.1397E+01 | | |

SECOND DERIVATIVE OF *Log*(1/*R*) SPECTRA

| | |
|---|---|
| MULTIPLE CORRELATION COEFFICIENT | 0.9611 |
| STD ERROR OF ESTIMATE | 1.440 |
| SUM OF SQUARED ERRORS | 89.23 |
| F-TEST | 130.9 |

| WAVELENGTH | MODEL COEFFICIENT | STD ERROR | t-VALUE |
|---|---|---|---|
| 1906.5 | 0.2975E+06 | 0.1666E+04 | 0.1434E+02 |
| 1714.5 | -0.6786E+06 | 0.7977E+04 | 0.8506E+01 |
| 1874.5 | 0.2537E+06 | 0.3509E+04 | 0.7230E+01 |
| 2023.5 | 0.2512E+06 | 0.4096E+04 | 0.6133E+01 |
| INTERCEPT | 0.1493E+01 | | |

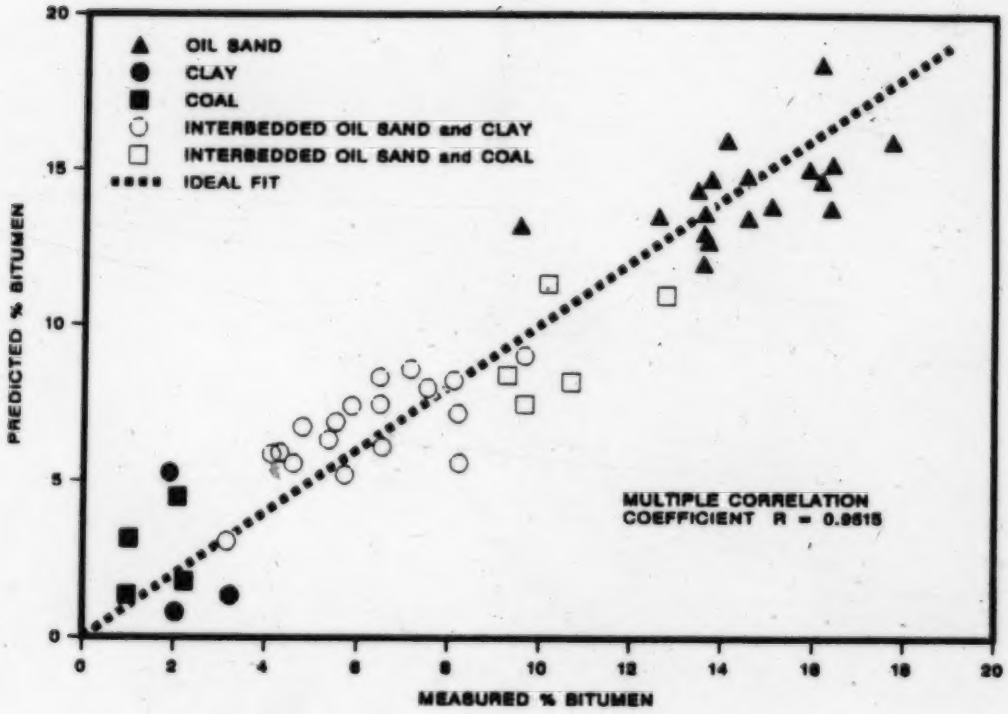


**Figure 68.** Comparison of predicted *versus* measured bitumen content for core samples in the training set using the best fit model based on $Log(1/R)$ spectral data.

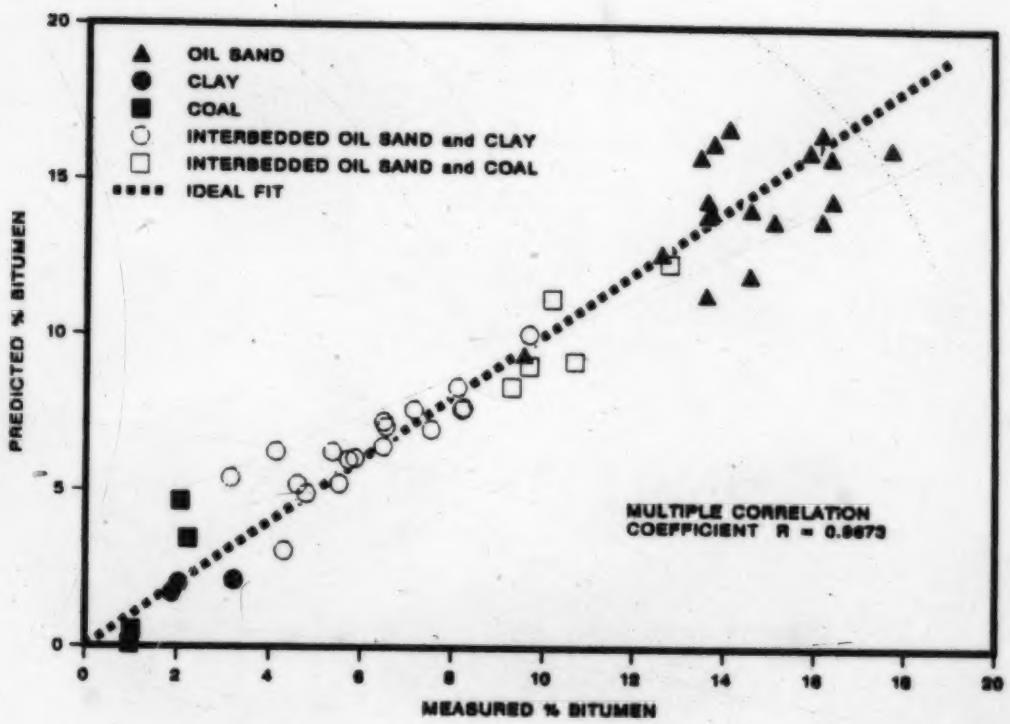


**Figure 69.** Comparison of predicted *versus* measured bitumen content for core samples in the training set using the best fit model based on the first derivative of $Log(1/R)$ spectral data.

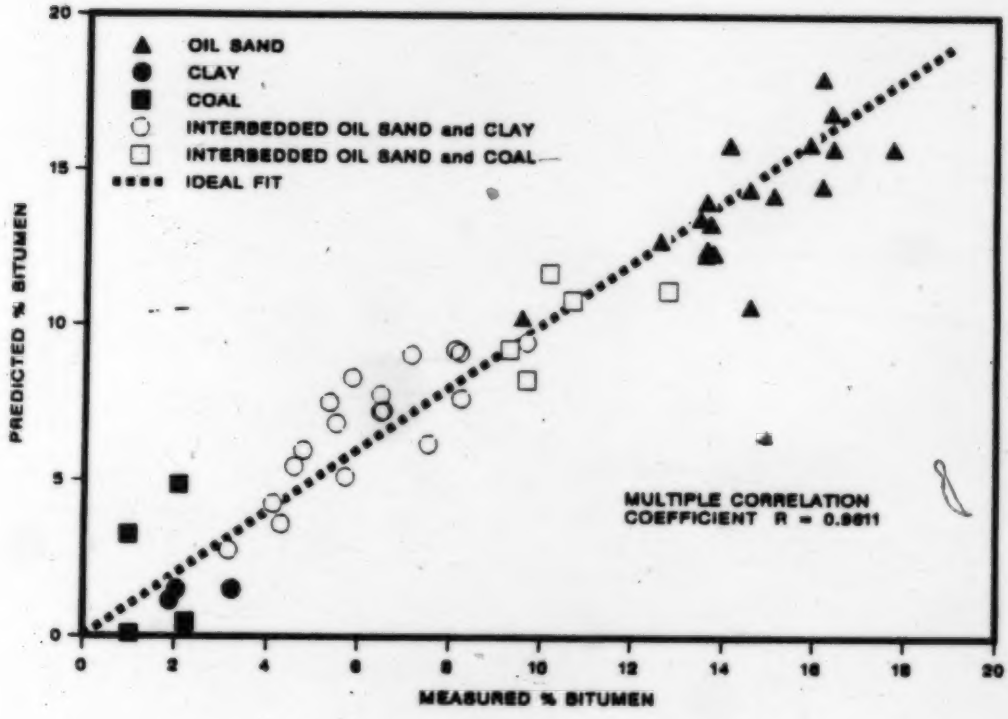


**Figure 70.** Comparison of predicted *versus* measured bitumen content for core samples in the training set using the best fit model based on the second derivative of $Log(1/R)$ spectral data.

# 4. FRACTAL DIMENSION OF RUGGED CURVES

## 4.1 General Concepts

Based on an extensive study of the mathematical properties of rugged curves and surfaces, Mandelbrot introduced the concept of fractal dimension to describe the disorder or irregularity of such contours (23,24). In particular, he examined a class of functions which are continuous but not differentiable. A curve generated using a polynomial function, for example, is differentiable because it can resolved as an infinite number of straight lines. A non–differentiable curve cannot be so resolved. Every attempt to split it into smaller parts results in the resolution of still more structure.

A classic example of a non–differentiable curve is known as Koch's triadic island. As illustrated in Figure 71, this curve can be created by successively constructing equilateral triangles of decreasing size around the perimeter of the basic unit. This process can be repeated an infinite number of times. An interesting property of Koch's triadic island is that it confines a finite area within a limitless boundary. This paradox has challenged the thinking of traditionally trained mathematicians.

In order to describe the structure of rugged curves (similar to those of Koch's triadic island) and, upon extension, the character of irregular surfaces, Mandelbrot suggested adding a fractional value to the topological dimension of an object to provide a measure of its relative space–filling ability. This new quantity is termed the Hausdorf–Besicovitch dimension $D$, or more commonly, the fractal dimension. Formally,

$$d < D < n \quad \text{where:} \quad \begin{array}{lcl} d & = & \text{topological dimension} \\ D & = & \text{fractal dimension} \\ n & = & \text{dimension of the space in which the object is immersed} \end{array}$$

Note that both $d$ and $n$ are integers. The fractal dimension of a curve can vary between 1 (a straight line) and 2 (a line so tortuous that it effectively occupies the

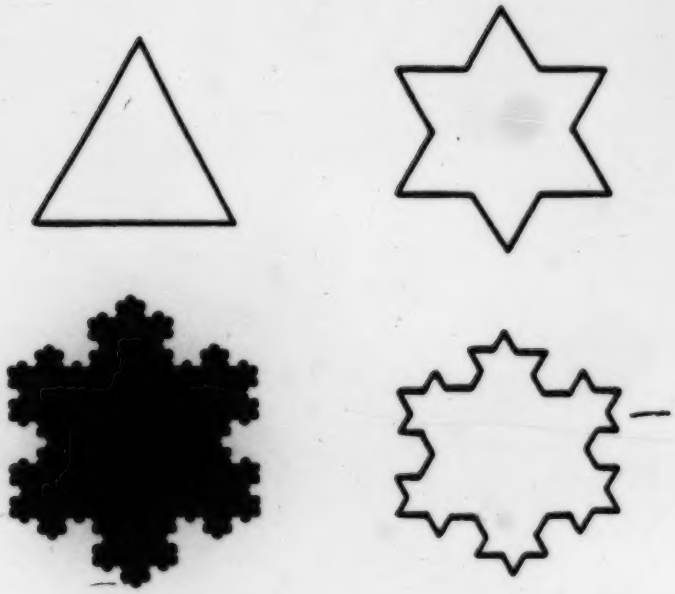

**Figure 71.** Koch's Triadic Island, a fractal object that confines a finite area within an infinite boundary. Adapted from Beddow (25) and Kaye (26).

whole of two–dimensional topological space). For surfaces, the corresponding range of fractal dimension lies between 2 (absolutely smooth) and 3 (infinitely rugged).

Aside from its peculiar fractional dimensionality, fractal objects generally exhibit self similarity, meaning that the geometric features of the structure are indistinguishable as a function of scale or measurement resolution. In other words, patterns observed at one level of detail are comparable to those seen under a higher or lower degree of scrutiny. A fragment of a fractal object has the same structure as the whole. Koch's triadic island depicts this self–similarity as do the fractal objects shown in Figure 72. Although scale invariant structure is not a mathematical requirement for fractal behaviour, rugged curves or surfaces that exhibit self–similarity are by definition fractal objects.

The utility of the fractal concept lies in the argument that structure which seems to be of random nature can be described within a geometric mathematical framework. Fractal dimension permits a quantitative interpretation of the appearance of any rugged boundary. Previously, these would have been described in a less tangible fashion using adjectives such as rough, textured, tangled, convoluted, *etc.*

The ideas advanced by Mandelbrot have gained wide acceptance over the last few years. Indeed, the recent literature abounds with applications of fractal dimension to describe the attributes of many natural phenomena. A considerable number of these publications are relevent to the field of chemistry and typically address the use of fractal dimension for characterizing the shape of fine particles (25,26) and surface properties of adsorbents (27–30).

## 4.2 Measurement of Fractal Dimension

Mandelbrot's major contribution to the art of describing the structure a rugged curve was to demonstrate a technique for allocating a numerical fractal dimension to a natural boundary. To provide a foundation for Mandelbrot's methodology, it is first useful to examine the problem of measuring the shoreline of an island. Mandelbrot (31) describes the work of Richardson who explored this problem on

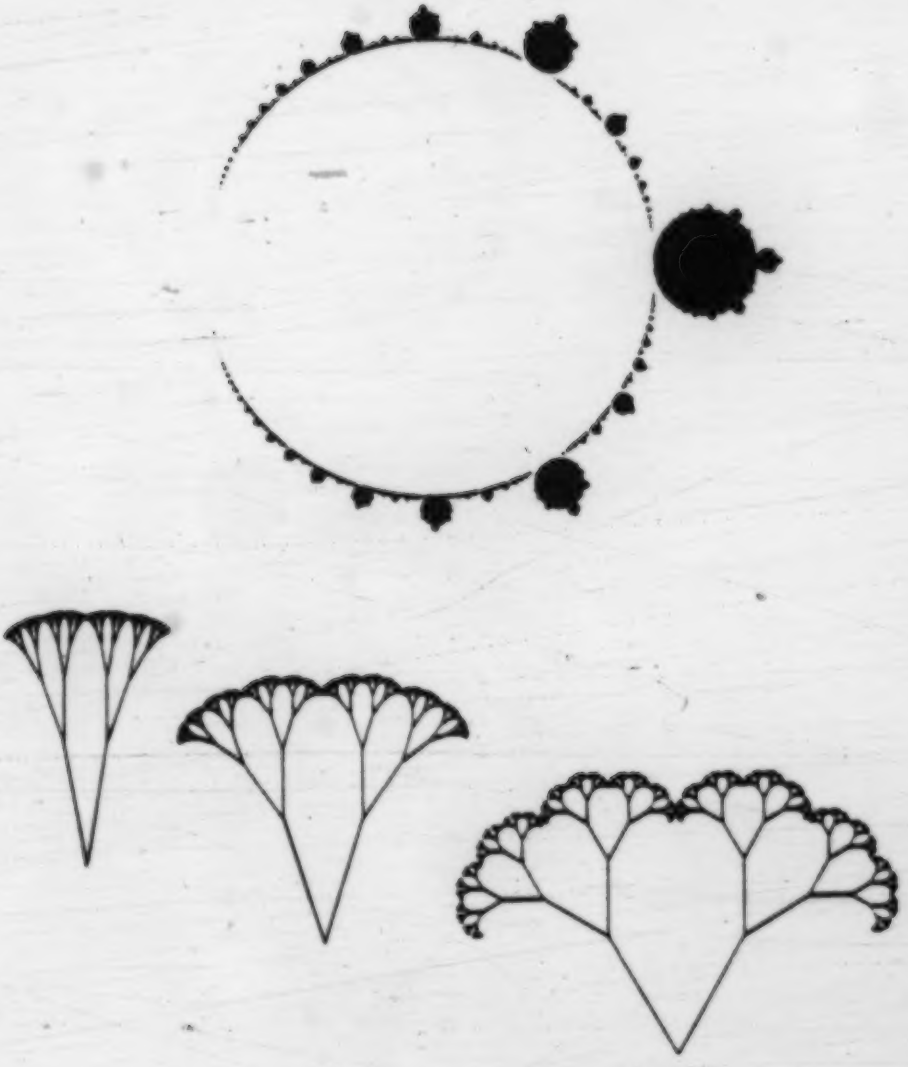

**Figure 72.** Examples of fractal objects that exhibit self–similarity over many scales. Adapted from Mandelbrot (24).

an experimental basis. He discovered that if one estimated the extent of a coastline by constructing a polygon of side length $x$ within the coastline boundary, then the boundary estimate based upon the perimeter of the polygon was dependent on the magnitude of $x$ according to the relations:

$$L = q(x)^p$$

$$Log\ L = Log\ q + p\ Log\ x$$

where $L$ = length of the coastline, $x$ =length of the polygon side, $q$ = proportionality constant, and $p$ = exponential factor. This relation is known as Richardson's Law. The construction of a polygon around the shore boundary is analogous to walking around the boundary with a stride of magnitude $x$. From the perspective of such a structured walk, stride length is in essence a yardstick and hence defines a degree of measurement resolution. Thus, a plot of coastline length *versus* measurement resolution graphed on a log–log scale will conform to a straight line having negative slope $p$.

What appeared to be distinctive about the various coastlines studied by Richardson was the rate at which the boundaries tended toward infinity. He noted that boundaries, all of which are essentially infinite, can be characterized by the rate at which they approach infinity. Mandelbrot showed that Richardson's Law holds for natural rugged boundaries other than coastlines and that in fact it is a widely occurring phenomenon. Furthermore, he suggested that the slope of the data line on a Richardson's plot could be related to the fractal dimension as:

$$D = 1 + |\,p\,|$$

Thus, data depicting the value of some result as a function of yardstick length or measurement resolution permits one to evaluate the fractal dimension of the system.

The structured walk technique is conceptually the simplest way of measuring the fractal dimension of a rugged curve. To illustrate the use of this technique, let us consider an assessment of the irregular profile of a crystal as shown in Figure 73.

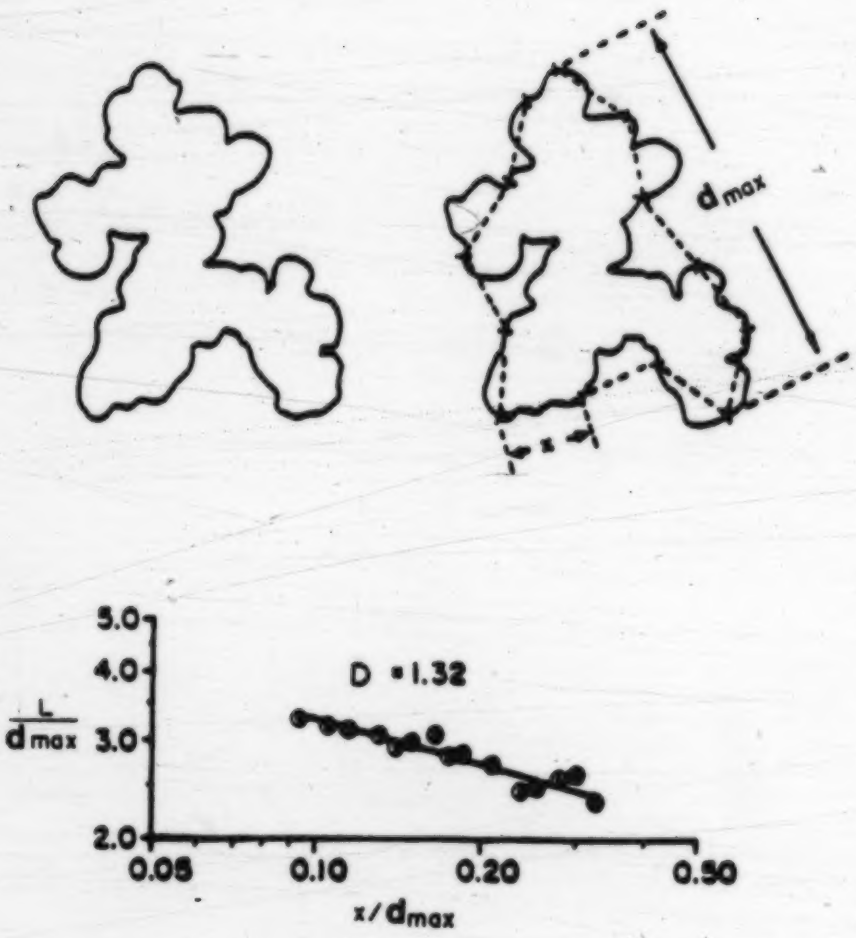


**Figure 73.** Application of the structured walk technique to evaluate the fractal dimension of a rugged profile. The slope of the relationship between *Log L* and *Log x* is –0.32. Adapted from Kaye (26).

The perimeter of the polygon drawn around the outline of the particle is an estimate of the length of the boundary at resolution $x$. As the magnitude of $x$ is changed, so does the perceived length of the crystal boundary. The plot of *Log L versus Log x* follows a straight line relationship from which the fractal dimension is readily deduced. For this particular example, both $L$ and $x$ have been normalized with respect to the longest projected length of the contour.

In this report, we are concerned about the variability in oil sand bitumen content in a deposit as a function of depth. The data base consists of a series of estimates of % bitumen obtained at 1 cm spacings in the vertical direction along a section of core. We can envision a line connecting the individual points in the data series as a "coastline" or rugged curve. Thus, an evaluation of the irregularity of the trace (representative of the variance among samples) could be pursued using the structured walk technique. For extensive data bases, however, the procedure is very time consuming and tedious to implement. As will be described in more detail later, an alternative method for calculating the fractal dimension of the system based on some principles of geostatistics provides a more convenient approach.

## 4.3 Fractal Dimension of Serial Data

An application of fractal analysis which is crucial to our discussion of sampling theory as it pertains to regionalized variables lies in the modelling of data obtained as a sequence of points in either the temporal or spatial domain.

A caveat of current sampling theory is that sampling uncertainties (ascribed to segregation or otherwise) result from random variations in the distribution of components throughout the bulk. As a consequence, stringent requirements are imposed on how samples should be collected in order to ensure an accurate represention of the parent material. Sample increments must be obtained in random fashion with all increments having an equivalent probability of selection. Systematic sampling is not condoned.

In many instances however, the systematic sampling of materials cannot be

avoided. Oftentimes, for economic reasons or perhaps because of some physical constraint of the sampling system, increments must be obtained at regularly spaced intervals within the bulk material. Without prior knowledge of how the component of interest is distributed throughout the bulk, the application of sampling equations to prescribe the number of samples and size of increments required to confidently estimate bulk composition may be invalidated.

It is of interest to determine whether the use of fractal dimension to characterize the structure of contours derived from serial data may be of benefit in defining sampling protocols for bulk materials in which sample increments are regionalized (and hence identifiable in terms of time or location). Further, the relation between segregation within bulk materials and concepts based on fractal dimension will be examined in the following sections.

### 4.3.1 Fractional Gaussian Noise

Data collected at regularly spaced time intervals constitute a time series conventionally analyzed using the methods of Box and Jenkins (32). Equations designed to model the trends in the data and provide the capability for predicting some future result in the series can be determined from the autocorrelation function. The autocorrelation function is defined as the set of correlation coefficients $r(k)$ obtained by linear regression of a value at time $t$ with its corresponding value at time $t + k$ where $k$ represents the time lag between data points.

Mandelbrot and co-workers (33,34) have demonstrated that time series data can also be modelled in terms of fractal dimension. Time series that display a characteristic fractal dimension are termed fractional gaussian noise models. In the more formal sense, fractional Gaussian noise is that generated from white noise by fractional differentiation or integration.

Let us consider a Gaussian random process $B(t)$ which satisfies the conditions:

$$B(0) = 0, \quad E[B(t)] = 0, \quad E[B^2(t)] = \mid t \mid^{2H}$$

where $E$ denotes expectation, $t$ is time, and $H$ is an exponential factor. A further condition which must be imposed is that the distribution of $B(t+k)$–$B(t)$ be independent of $t$, where $k$ again represents the interval time lag between the samples of interest. If we confine our attention to discrete instants of time, the difference between successive values in the series, $W(t)$,

$$W(t) = B(t+1) - B(t)$$

is stationary, has zero mean, and has an autocorrelation function given by

$$r(k) = 0.5(\mid k+1 \mid^{2H} -2k^{2H} + \mid k-1 \mid^{2H})$$

The values of $H$ are restricted and must lie within the range of zero to one. The case for which $H = 0.5$ represents a purely random phenomenon or white noise process.

The parameter $H$ provides the connection between the time series and the concept of fractional dimension. The graph of a realization of $B(t)$ has a fractal dimension of $D = 2 - H$. Thus, a fractal dimension of 1.5 would indicate that the variable under consideration is randomly distributed as a function of time.

A further use of the parameter $H$ lies in its relationship to the idea of persistence. Values of $H$ greater than 0.5 (for which $D < 1.5$) are associated with processes that exhibit trends in the data. These time series are termed persistent and are formed by the fractional integration of white noise. Values of $H$ less than 0.5 (for which $D > 1.5$) signify antipersistent processes formed by fractional differentiation of white noise. These time series tend to fluctuate between high and low values more than would be expected with a purely random variable. Examples of time series that reflect white noise, persistent, and antipersistent processes are shown in Figure 74.

In analogous fashion, serial data obtained in the spatial domain can also be modelled in terms of fractal dimension. The approach is based on geostatistical techniques that rely on the development of an experimental semi–variogram. The procedures involved in such an evaluation are described in the next section.

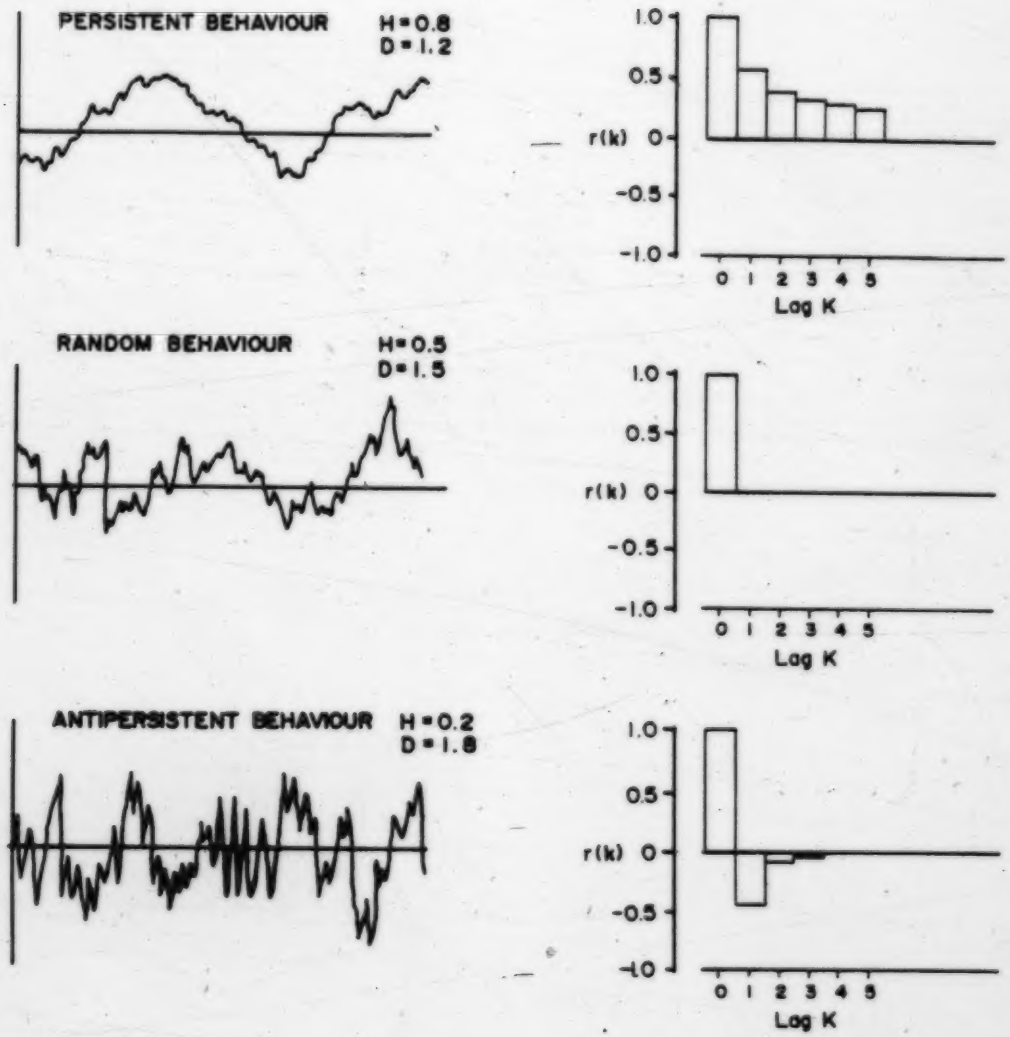


**Figure 74.** Rugged curves of differing fractal dimension generated under equivalent scales of resolution. Autocorrelation functions depict ideal behaviour.

### 4.3.2 Relationship to the Semi-Variogram

Before proceeding with a discussion on the inter-relationship between fractal dimension and the structure of curves depicting the spatial variability in the composition of a given bulk material, it will be useful to first introduce some of the fundamental principles of geostatistical analysis.

A prerequisite in the geostatistical evaluation of an ore reserve involves the investigation and modelling of the physical structure of the deposit. Measures of spatial variability and continuity within the deposit are embodied in the interpretation of experimental semi-variograms. An understanding of the semi-variogram provides the foundation for global reserve estimation, a procedure known as kriging.

The semi-variance, $Y(h)$, is defined as half of the mean squared difference among point grade estimates, $g$, separated by a distance $h$:

$$Y(h) = \frac{1}{2n} \sum [g(x) - g(x+h)]^2$$

where $x$ denotes position and $n$ is the number of paired data points used for the evaluation. Results are normally plotted as a function of the spatial separation. The graph is called a semi-variogram.

Geostatistics assumes that the distribution of the difference between two point samples is the same over the entire deposit and that it depends only on the distance between and orientation of the points. Normally, points close together will be more related than points farther apart. In geostatistical terms, if the points are highly correlated, then the variance of the distribution of differences will be low. Conversely, if the points are not highly correlated, and can therefore be considered independent, the variance of the distribution of differences will be high. Thus, this variance is a measure of the influence of samples over neighboring areas within the deposit. In this discussion, we need not concern ourselves with the aspect of orientation since the data base of interest has but one degree of freedom (oil sand assay data is regionalized with respect to the vertical direction).

As previously introduced, the mean squared differences between samples can be used to construct an experimental semi–variogram depicting the variability in composition or other attribute of a material as a function of increasing distance between sample points. The total variance in the distribution of differences among point grade estimates can be considered the sum of two variance components. One represents the spatial variance determined by the differences in sample values at increasingly larger distances. The other represents the localized or short range variance determined by differences in sample quality at points separated by very small distances. This latter component is termed the nugget effect. A typical semi–variogram, shown in Figure 75, serves to illustrate these points.

While a calculated semi–variogram based on experimental results may assist in determining the structure of a deposit, it is merely a data summary technique. Further, it is specific to the data base upon which the semi–variogram was produced. To draw conclusions regarding the nature of the entire reserve, it must be related to some theoretical model that describes, on a more general basis, the underlying patterns of variability and continuity. Just as there are few distributions available to the practitioner of classical statistics, there are only a few simple models for a theoretical semi–variogram. These models can be categorized as:

- Those in which the semi–variance increases as the distance between samples increases (generalized linear model)
- Those in which the semivariance increases at first and then tends to level off at a constant value, termed the sill (exponential or spherical model)

The characteristic shape of these theoretical semi–variograms are shown in Figure 76. Although other models exist to describe the underlying patterns in regionized variables, the ones described above are by far the most common. The spherical model in particular is widely used to approximate the trends typically observed in geological and environmental data.

One useful characteristic of models that possess a sill is that the plateau value

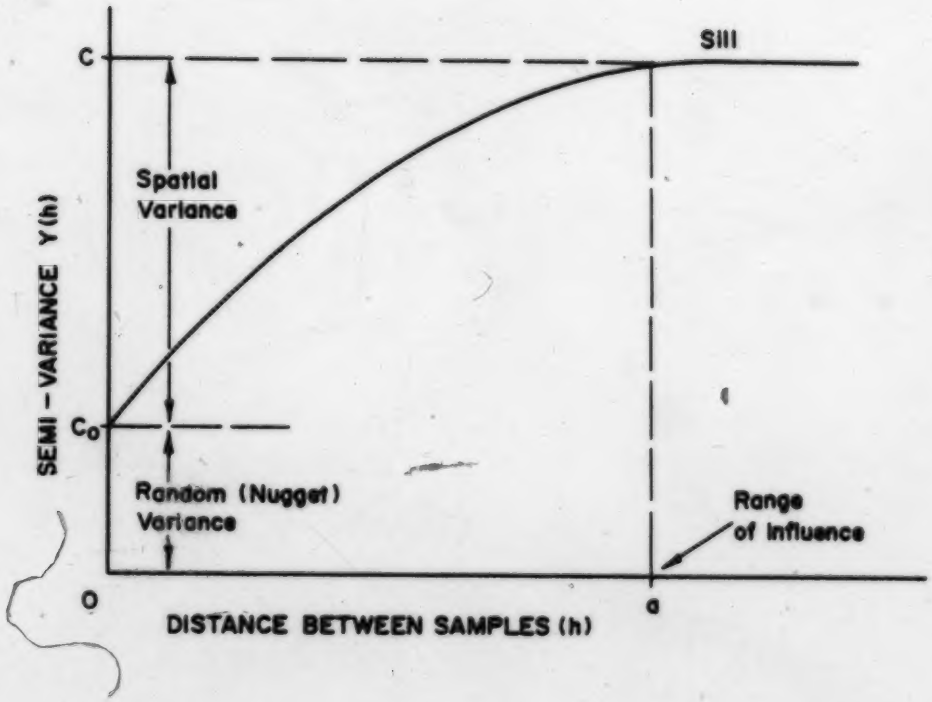


**Figure 75.** A typical semi-variogram possessing a sill, $C$, and nugget variance, $C_0$. The range of influence is denoted by $a$.

**MODELS WITHOUT SILLS**

**GENERALIZED LINEAR MODEL**

$$Y(h) = ph^{\lambda}$$

where $0 \leq \lambda < 2$

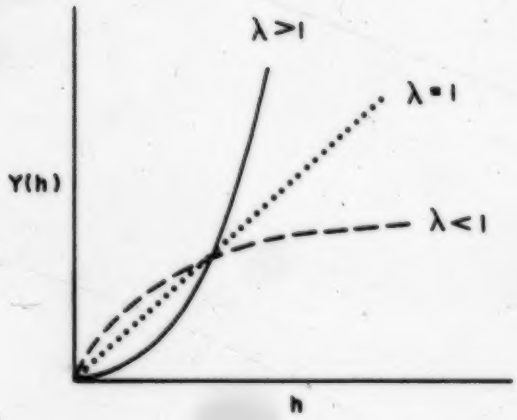


**MODELS WITH SILLS**

**EXPONENTIAL MODEL**

$$Y(h) = C\left(1 - e^{-\frac{h}{a}}\right)$$

**SPHERICAL MODEL**

$$Y(h) = C\left(\frac{3h}{2a} - \frac{h^3}{2a^3}\right)$$

for $h \leq a$

$Y(h) = C$ for $h \geq a$

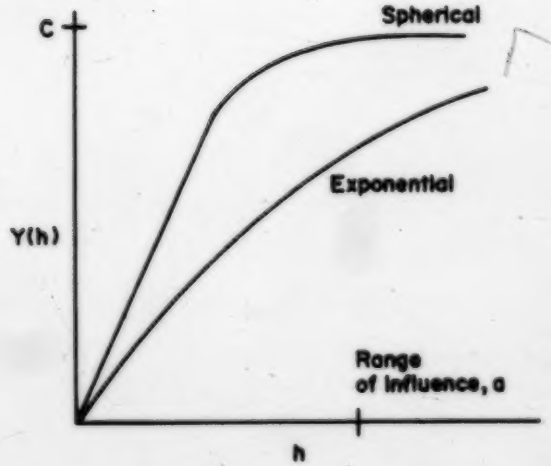


**Figure 76.** Theoretical semi-variograms. Note that the spherical and exponential models as shown have the same sill, $C$, and range of influence, $a$.

of $Y(h)$ provides a measure of the variance in the set of sample values used to construct the semi–variogram. Thus the variance of the data set can be determined without first having to calculate the mean value. Of further interest is that the distance at which the sill occurs denotes the point at which the correlation among sample values has diminished to zero. This separation distance is referred to as the range of influence. Beyond this distance, samples no longer resemble each other and can therefore be considered independent. A more comprehensive discussion of the procedures used to generate experimental semi–variograms and to deduce theoretical models for the structure of a given ore deposit is provided by Clark (35).

Having briefly described the development and modelling of experimental semi–variograms, let us now pursue the idea of calculating the fractal dimension of a rugged curve subtended by a spatial data series. The form of the equation for calculating the semi–variogram is very similar to that previously given for the differences between successive values in a time series. Not surprisingly then, it would seem likely that a relationship also exists between the semi–variogram and the concept of fractal dimension. Indeed, Burrough (36) shows that the squared differences among samples which are separated by some distance $h$ will vary as $h^{4-2D}$ as the lag approaches zero. This allows us to evaluate the fractal dimension from the semi–variogram. The slope of a plot of *Log* $Y(h)$ *versus Log* $h$ near the origin is $4 - 2D$. From this relationship, calculation of $D$ is a simple matter.

For data obtained as a spatial series (as is the case for oil sand grades determined as a function of depth), it is conjectured that a measure of persistence, or conversely antipersistence, can be implored as an indicator of sample consistency. Data contours that have a fractal dimension less than 1.5 are persistent in nature, implying that sample increments taken close together are likely to be of similar composition or quality. This is evidenced by trending in the data which may persist for quite some distance, that is, over several adjacent sample increments. The sample can be considered heterogeneous only in terms of long range effects. On the other hand, data contours that have a fractal dimension exceeding 1.5 are antipersistent. Sample increments taken in proximity of each other are likely to be extremely variable

in composition. This suggests that heterogeneity is dominant over the short range. Thus, the fractal dimension provides a measure of the scale over which segregation becomes of concern.

Note that, as the value of $D$ increases, more of the range of compositional data is seen among samples of a fixed increment size. A corrollary is that the number of samples required to provide a given confidence interval for estimates of mean value decrease with $D$. Although the effects of sample segregation are not addressed, the results fit well with classical statistics wherein the reliability of a mean value increases as the number of independent estimates increase.

## 4.4 Application to the Geostatistical Analysis of an Oil Sand Deposit

In Burrough's paper, a diversity of environmental data was examined to see if features could be modelled in terms of an intrinsic fractal dimension. Fortuitously, the fractal dimension of oil sand grades obtained through vertical sections of the Athabasca deposit was included in his study. The value $D = 1.7$ was reported based on evaluation of a semi-variogram originally published by Dowd and Royle (37). This semi-variogram, further discussed by Journel and Huijbregts (38) as a case study in geostatistical analysis, was developed from estimates of the average bitumen content of core samples obtained at 60 cm spacings in the vertical direction. The data base encompassed more than 40 cores drilled through the reserve, each averaging about 107 metres in depth. The exact location of the lease area examined was not reported. The experimental semi-variogram is illustrated in Figure 77. The curve depicting a best fit spherical model with nugget effect is also shown.

The relatively high fractal dimension suggests that the variability among adjacent samples is not a random function. Differences among samples separated by short lags (multiples of 60 cm) can be ascribed to the dominating effect of localized segregation. Burrough questions the wisdom of interpolation mapping of oil sand grades with depth given the high value for fractal dimension.

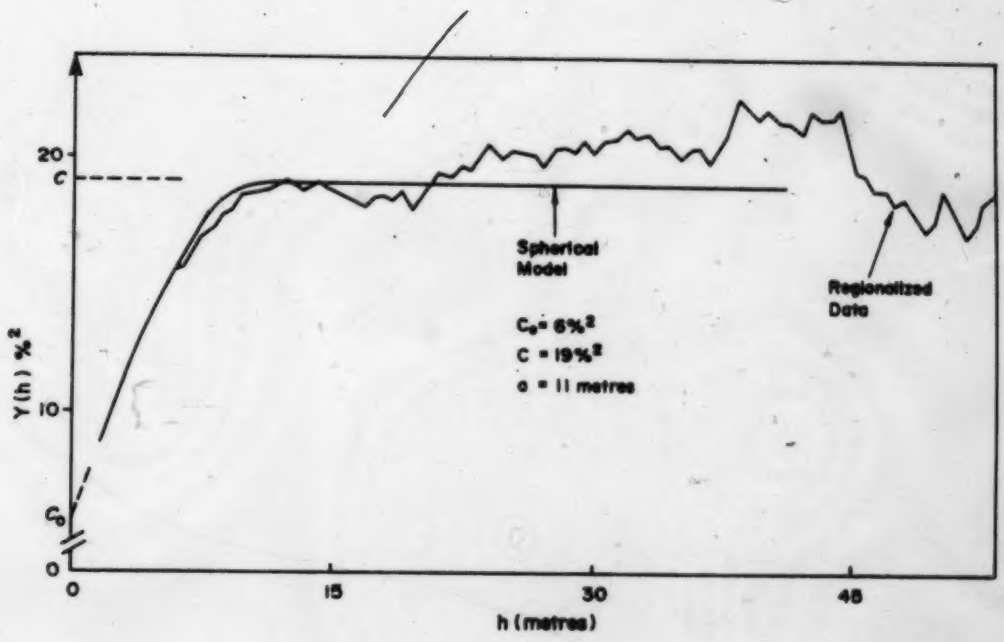


**Figure 77.** Experimental semi-variogram for oil sand grades obtained at 60 cm spacings in the vertical direction. Adapted from Journel and Huijbregts (38).

An objective of the current research work was to determine the fractal dimension of regionalized oil sand assay data based on a sampling resolution of 1 cm. If the resulting value is comparable to that calculated from Dowd and Royle's data, then it can be assumed with some degree of certainty that vertical contours exhibit self-similarity. Stated another way, the structure of the grade profile at high resolution is the same as that obtained at a lower level of resolution. This could have significant implication in terms of how the geology of the region should be viewed, especially as it pertains to understanding the patterns by which the sediments were originally deposited and explaining the intrusion of hydrocarbon within the sand particle matrix.

Should the calculated value for fractal dimension differ from that based on Dowd and Royle's data, it could be construed that several scales of variability may exist within the formation. If this is reasonable, an examination of $D$ values would be useful for trying to separate scales of variation that might be the result of particular natural processes. Moreover, identifying such scales could be of enormous practical value because one could then tailor sampling plans to the specific phenomenon in question.

## 5. FRACTAL ANALYSIS OF EXPERIMENTAL NIR-DR DATA

### 5.1 Variability in a Spatial Series of Oil Sand Grades Obtained at High Sampling Resolution

Having selected a model to relate the bitumen content of a sample to its near infrared diffuse reflectance spectra (based on the first derivative of $Log1/R$ data), sample assays were obtained from the spectra previously generated for the remainder of the test core section. Results represent predicted measures for anhydrous bitumen saturation at spacings of 1 cm along the length of core. Data is plotted as a function of depth in Figure 78 and tabulated in Appendix B. Results are summarized below:

| | | |
|---|---|---|
| Number of Samples | 427 | |
| Mean Grade | 10.56 | % Bitumen |
| Variance | 19.596 | |
| Standard Deviation | 4.427 | |

Assay values span a wide range from zero to almost 20% by weight bitumen.

The autocorrelation function and semivariogram for the data series are illustrated in Figures 79 and 80. Data are tabulated in Appendix C. A listing of the Fortran program used to generate these results is also provided.

The pattern in the correlation coefficients as a function of distance lag is similar to that of a damped sine wave and signifies the presence of long term trends in the data. Oil sand grades measured at spacings on the order of 100 cm apart tend to be inversely related whereas data obtained at more or less distant intervals show positive correlations. This periodicity in the data is also revealed upon closer inspection of the grade *versus* depth profile. Assay results appear to cycle between high and low values at a frequency corresponding to a 2 metre sampling interval.

The existence of a systematic trend in the data is also reflected in the experimental semi-variogram. In this instance, the magnitude of $Y(h)$, representing half of the mean squared difference between grade estimates a distance $h$ apart, increases with increasing separation lags of up to approximately 100 cm. Thereafter, the

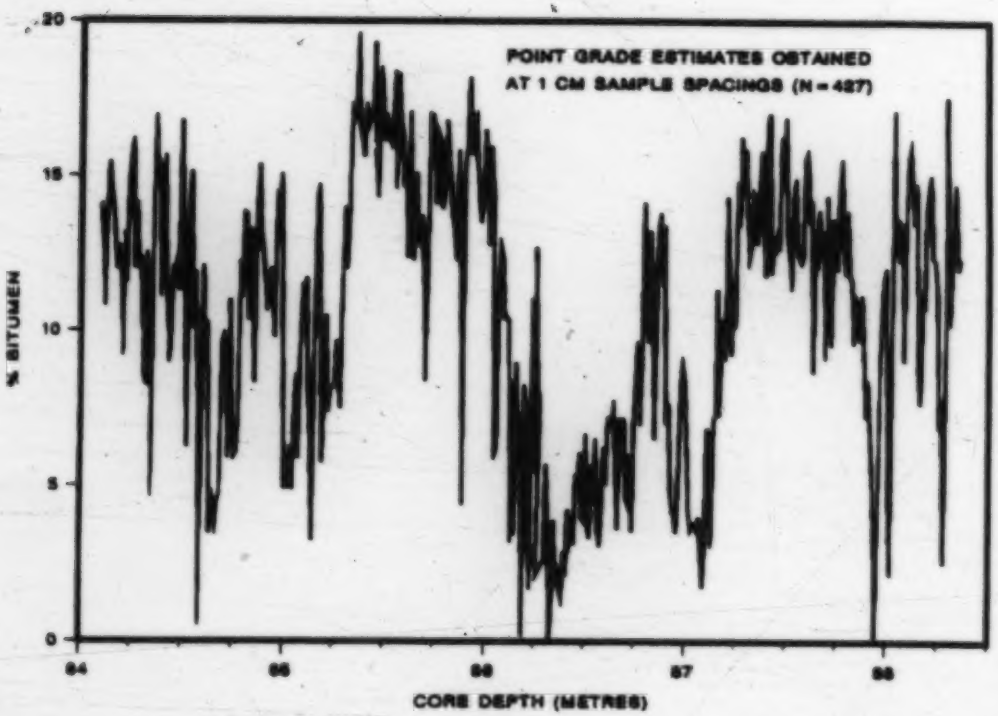


**Figure 78.** Variability in bitumen content as a function of depth for the test core section. Point grade estimates obtained at 1 cm sample spacings.

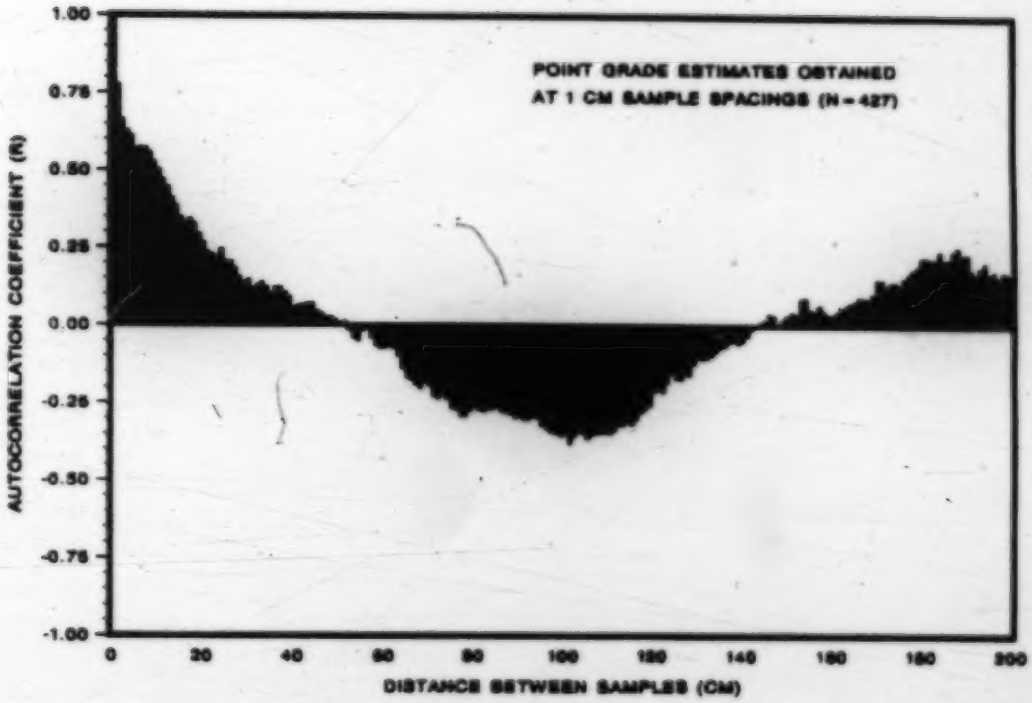


**Figure 79.** Autocorrelation function for point grade estimates obtained at 1 cm sample spacings.

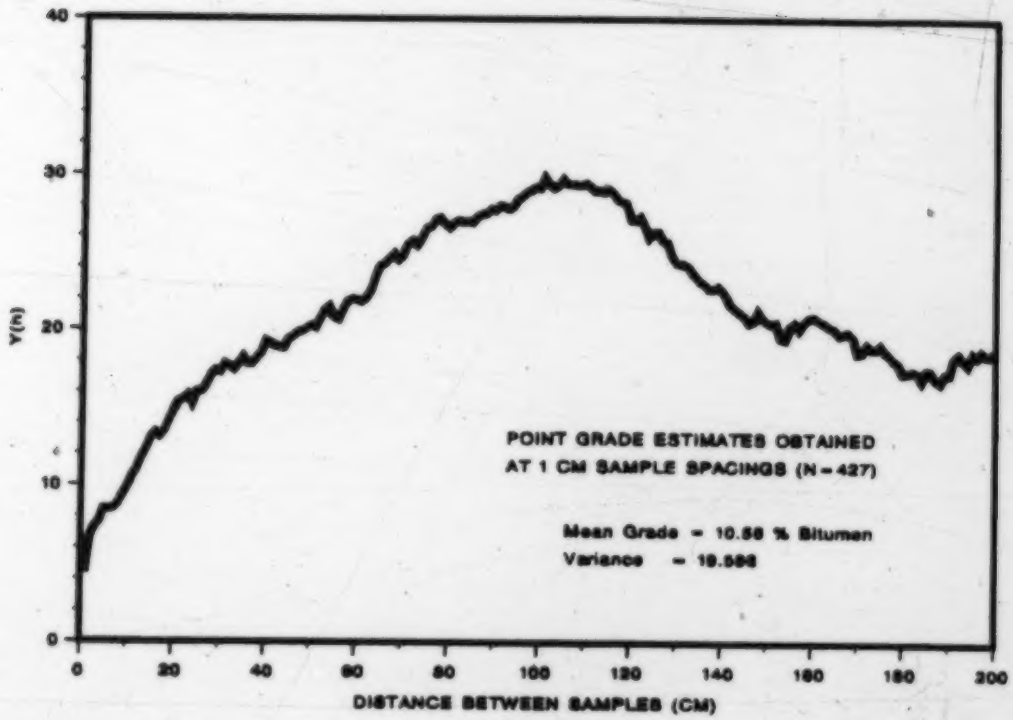


**Figure 80.** Experimental semi-variogram for point grade estimates obtained at 1 cm sample spacings.

semi–variogram tapers off and tends towards a constant value of $Y(h)$ comparable to the calculated variance of the total data set.

Since we are ultimately interested in deriving the fractal dimension of the data series (based on the relationship between *Log* $Y(h)$ and *Log* $h$ as separation distance approaches zero), we need not be concerned with the implications of long range periodic trends in the data. The apparent periodicity in the results may be unique to this particular section of core. Given that the length of core examined is short relative to the frequency of the periodic trend, it can not be determined whether this behaviour is manifest over longer sections.

We will consider the data obtained over the range of lags having $Y(h)$ values less than or equal to the sill value as representing a stationary process. Under this pretext, it is expected that the sill value would be reached at much shorter distance spacings. The separation distance at which this would occur is in the vicinity of the intersection of a line drawn through the first few points of the semi–variogram and the line extended through points of the sill. Treating the data in this manner permits one to use a simple model for evaluating the theoretical semi–variogram.

The experimental semi–variogram for sample spacings of up to 50 cm can be described nicely in terms of a spherical model with nugget effect. This is illustrated in Figure 81. The equations defining the model are noted below:

$$Y(h) = C_0 + C_1\left(\frac{3h}{2a} - \frac{h^3}{2a^3}\right) \quad \text{for} \quad h \leq a$$

$$Y(h) = C \quad \text{for} \quad h \geq a$$

where $C_0$ = nugget variance, $C$ = sill, $C_1 = C - C_0$, $h$ = distance between samples, and $a$ = range of influence. The nugget variance, $C_0$, is an estimate of the random variability among neighboring samples separated by extremely short distances. It is calculated as the intercept of a best fit straight line drawn through the first few values of $Y(h)$. To provide a consistent criterion for interpretation of experimental semi–variograms, the nugget effect is determined using $Y(h)$ results evaluated for

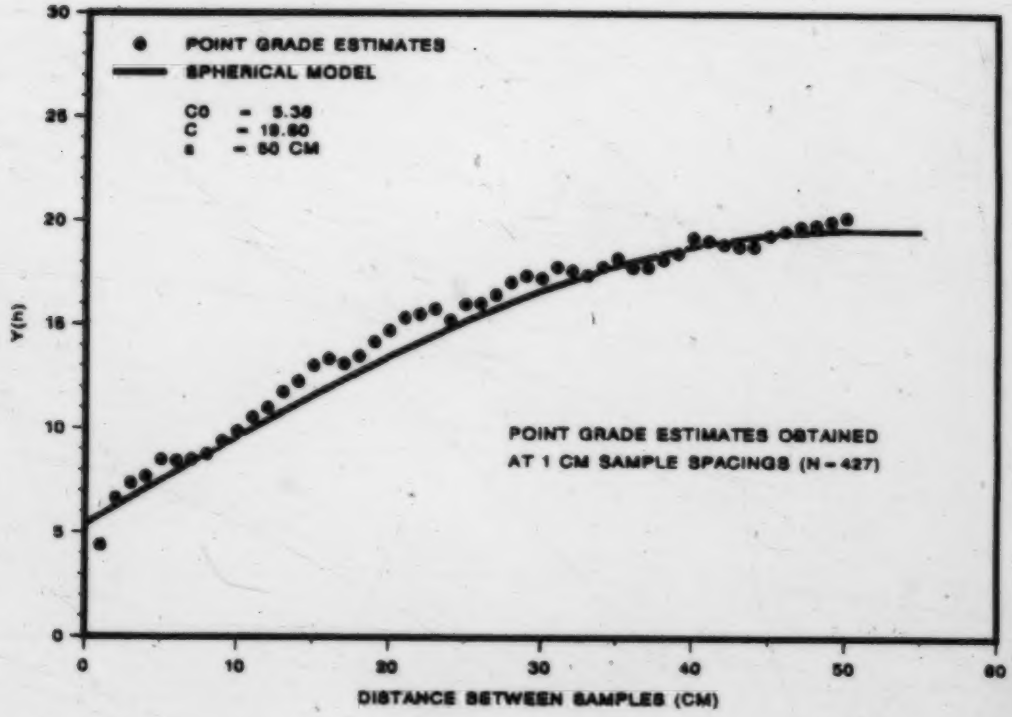


**Figure 81.** Spherical model of the experimental semi-variogram for point grade estimates obtained at 1 cm sample spacings.

distance spacings in the range $1 < h < 20$ cm. Based on the results from a linear regression, this best fit line intersects the ordinate at $C_0 = 5.38$.

The sill of the semi-variogram, $C$, is defined as the assymptotic value at which there is no further trend in $Y(h)$ values as a function of separation distance. For a stationary series, the value of $C$ is equal to the variance in the data. Thus, $C = 19.596$.

The range of influence, $a$, defines the distance between samples within which samples may be assumed to bear some relationship to one another. Points separated by a distance greater than $a$ are unrelated and independent. Thus $a$ corresponds to the separation distance at which the sill is reached. For a spherical model, the range of influence is normally calculated from the expectation that a straight line drawn through the first few points of the experimental semi-variogram will intersect the sill at $h = 2/3a$. Given the linear regression line previously developed to evaluate the nugget effect, and solving for $h$ at $Y(h) = 19.596$, it can be determined that the sill is reached at a separation distance of approximately 30 cm. Therefore, $a \approx 45$ cm.

An alternative means for deducing the range of influence can be based on the autocorrelation function. Since $a$ represents the spacing at which samples become independent, it can be evaluated as the separation distance at which the autocorrelation function is zero. This occurs at $h = 50$ cm. This procedure for obtaining a value for the range of influence is convenient and deemed to provide a more reliable estimate over that obtained by conventional means.

A plot of *Log* $Y(h)$ *versus Log* $h$ for separation distances of 50 cm or less is presented in Figure 82. As introduced earlier, the fractal dimension of the data series can be determined from the slope of a straight line drawn through the points. Based on the results of a linear regression, the value $D = 1.80$ is obtained. The result is comparable to that determined from Dowd and Royle's data ($D = 1.7$) and suggests that the structure of the variability in down hole grade estimates at a sampling resolution of 1 cm is similar to that at a sampling resolution of 60 cm.

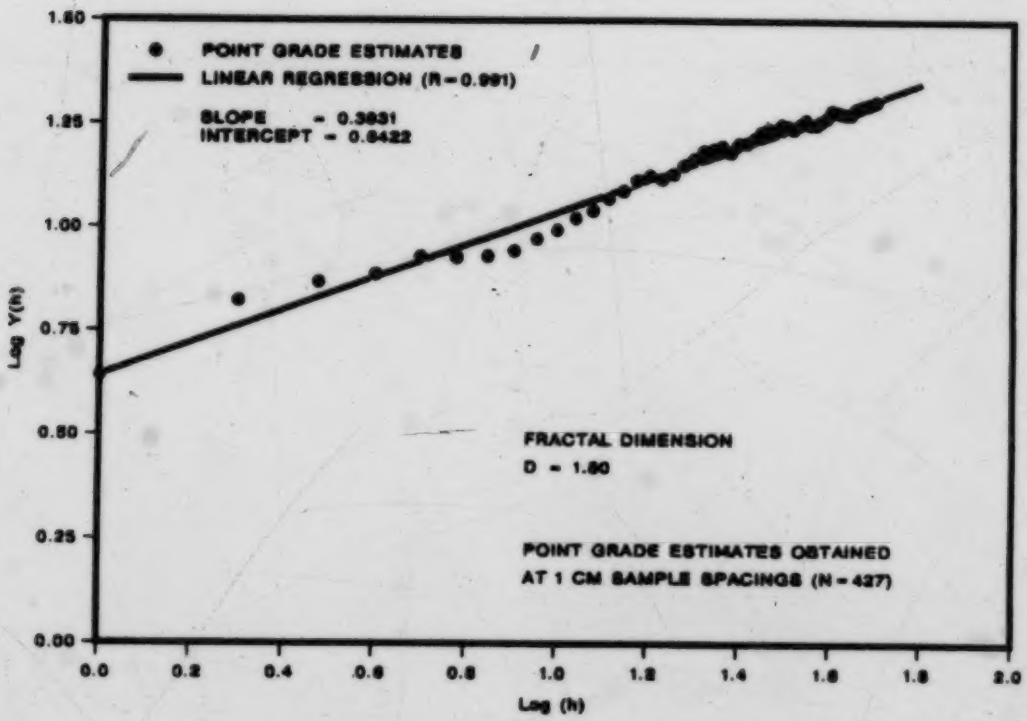


**Figure 82.** Evaluation of fractal dimension from the experimental semi–variogram for point grade estimates obtained at 1 cm sample spacings.

Recalling that values of $D > 1.5$ signify antipersistent behaviour, results imply that oil sand is extremely heterogeneous and can be considered segregated at both scales of observation. With reference to material confined within a core, increasing sample size by a factor of 60 or so does little to reduce sampling uncertainties ascribed to segregation effects.

Outwardly, it would appear that variability in vertical grade profiles of an oil sand deposit could be characterized in terms of an intrinsic fractal dimension that lies somewhere in the range $1.7 < D < 1.8$. It becomes of interest to see whether the fractal dimension of such data series obtained at some intermediate sampling resolution falls within the expected range. This point is discussed in the following section.

## 5.2 Effect of Sample Size on the Structure of Vertical Grade Contours

Estimates for the fractal dimension of the grade profile in our test section of core at sampling resolutions other than 1 cm were obtained in a somewhat artificial manner by averaging results over multiple sample spacings. Point grades representing the composition of the oil sand at 2 cm intervals, for example, were determined by averaging results for consecutive pairs of sampled values. As a result, the new data series contains only half the number of points of the original data base. In similar fashion, sample values for yet lower degrees of resolution were obtained by grouping the data over the increment range of interest and calculating the mean values for those particular sets of samples.

At this point, there may be some confusion as to how samples obtained over various lengths of core may be related to sample size. To clarify this issue, let us define the volume of a sample increment, $V$, as follows:

$$V = AL$$

where $L$ is the length of the sample and $A$ is the cross-sectional area of the core. In

the more general case, these dimensions would normally be governed by the type of sampling tool used to withdraw an increment from a quantity of bulk material. For samples of equivalent density, $d$, the weight of a sample increment, $W$, is given by

$$W = dAL = kL$$

for a given cross–sectional area. Thus, the weight of a sample increment obtained from material confined within a section of core is directly proportional to the linear dimension of the sampling unit. Further, if we assume that sample composition is invariant along the plane of cross–sectional area (in our case across the width of the core), then the variance among samples of weight $W$ is the same as the variance among samples of length $L$.

Grade profiles based on sample increments obtained at 2, 5, 10, and 20 cm spacings along the length of the core section are illustrated in Figures 83–90. Corresponding results from a geostatistical analysis, including the plots for evaluating the fractal dimension of these contours, are also provided. Data is tabulated in Appendices B and C. Due to limitations in size of the data set as a result of the averaging process, it is unrealistic to pursue an evaluation for the variability among samples at spacings greater than 20 cm.

The data indicates that the fractal dimension of grade profiles decreases as sample size increases. Similarly, the nugget variance diminishes as the amount of sample used to establish point grade estimates becomes larger. These results were unexpected. It would seem that patterns in the variability of oil sand grades with depth are not self–similar as previously thought. The data further suggests that samples in the spatial series become more homogeneous with increasing sample size. Segregation effects decrease and the variability among adjacent sample increments approaches that expected for a random distribution.

The relationship between fractal dimension and sample size for this test section of core is shown in Figure 91. The fractal dimension appears to be inversely related to the log of the sample size. By extrapolating a best fit line through the points, it

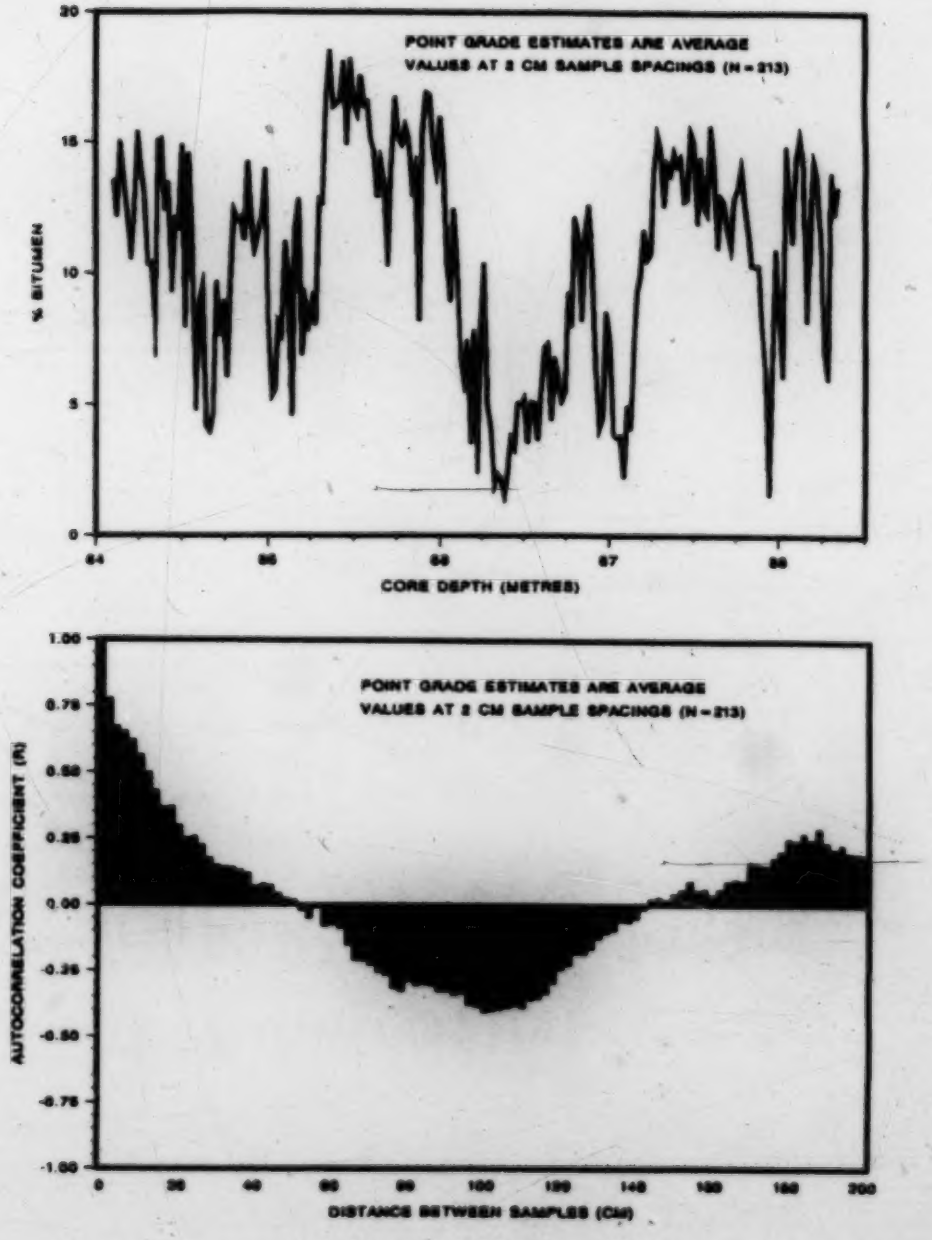
POINT GRADE ESTIMATES ARE AVERAGE
VALUES AT 2 CM SAMPLE SPACINGS (N = 213)
% BITUMEN
CORE DEPTH (METRES)
POINT GRADE ESTIMATES ARE AVERAGE
VALUES AT 2 CM SAMPLE SPACINGS (N = 213)
AUTOCORRELATION COEFFICIENT (R)
DISTANCE BETWEEN SAMPLES (CM)

**Figure 83.** Grade profile and autocorrelation function for point grade estimates obtained at 2 cm sample spacings.

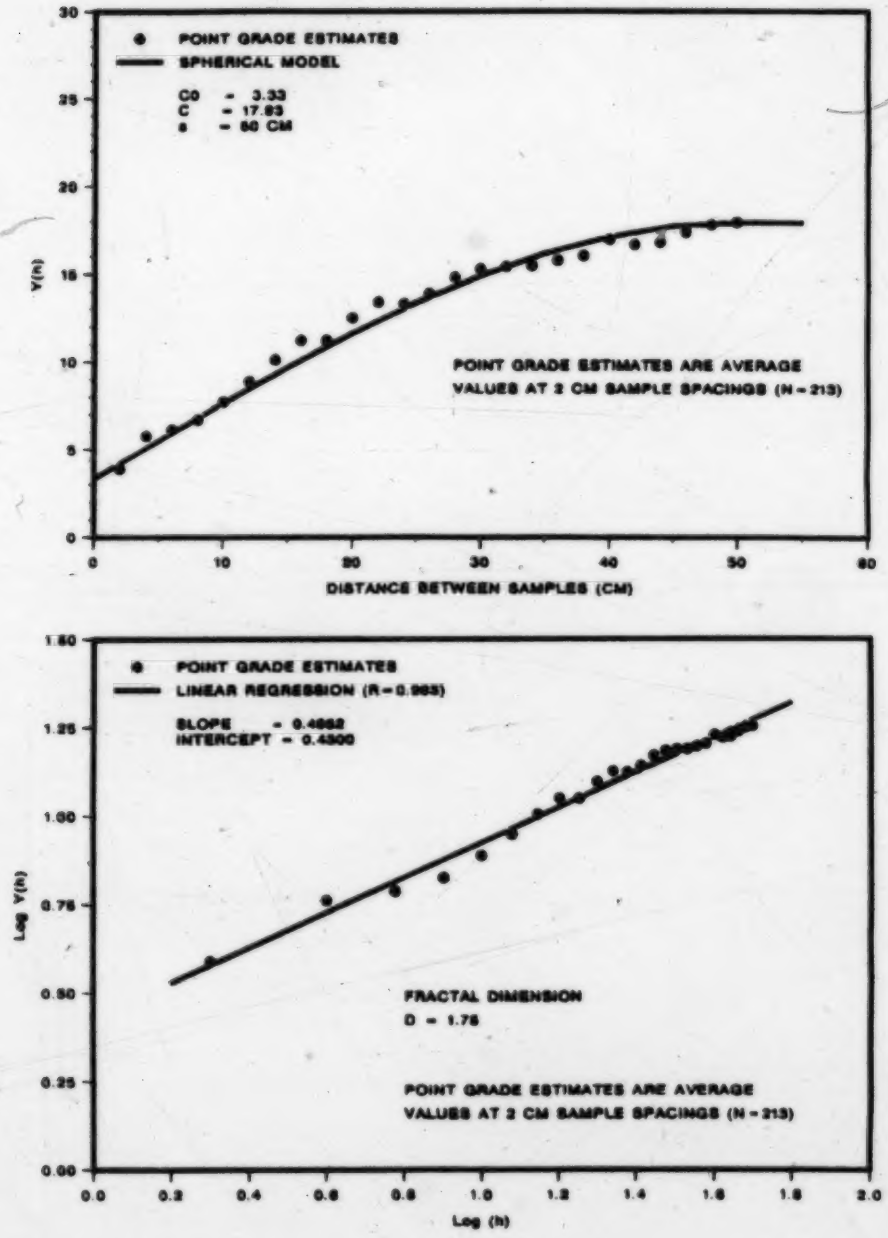


**Figure 84.** Experimental semi-variograms for point grade estimates obtained at 2 cm sample spacings.

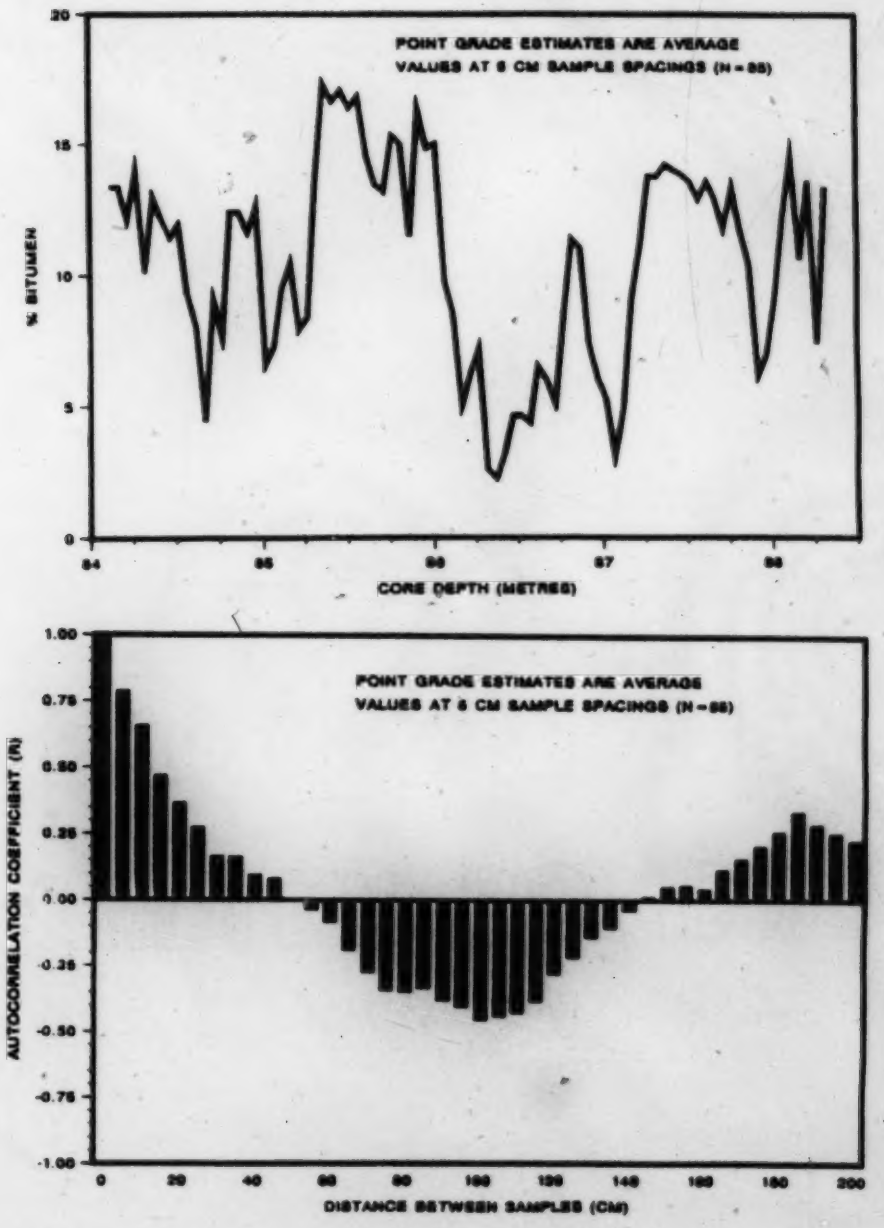
POINT GRADE ESTIMATES ARE AVERAGE
VALUES AT 5 CM SAMPLE SPACINGS (N = 88)
% BITUMEN
CORE DEPTH (METRES)
POINT GRADE ESTIMATES ARE AVERAGE
VALUES AT 5 CM SAMPLE SPACINGS (N = 88)
AUTOCORRELATION COEFFICIENT (Ri)
DISTANCE BETWEEN SAMPLES (CM)

**Figure 85.** Grade profile and autocorrelation function for point grade estimates obtained at 5 cm sample spacings.

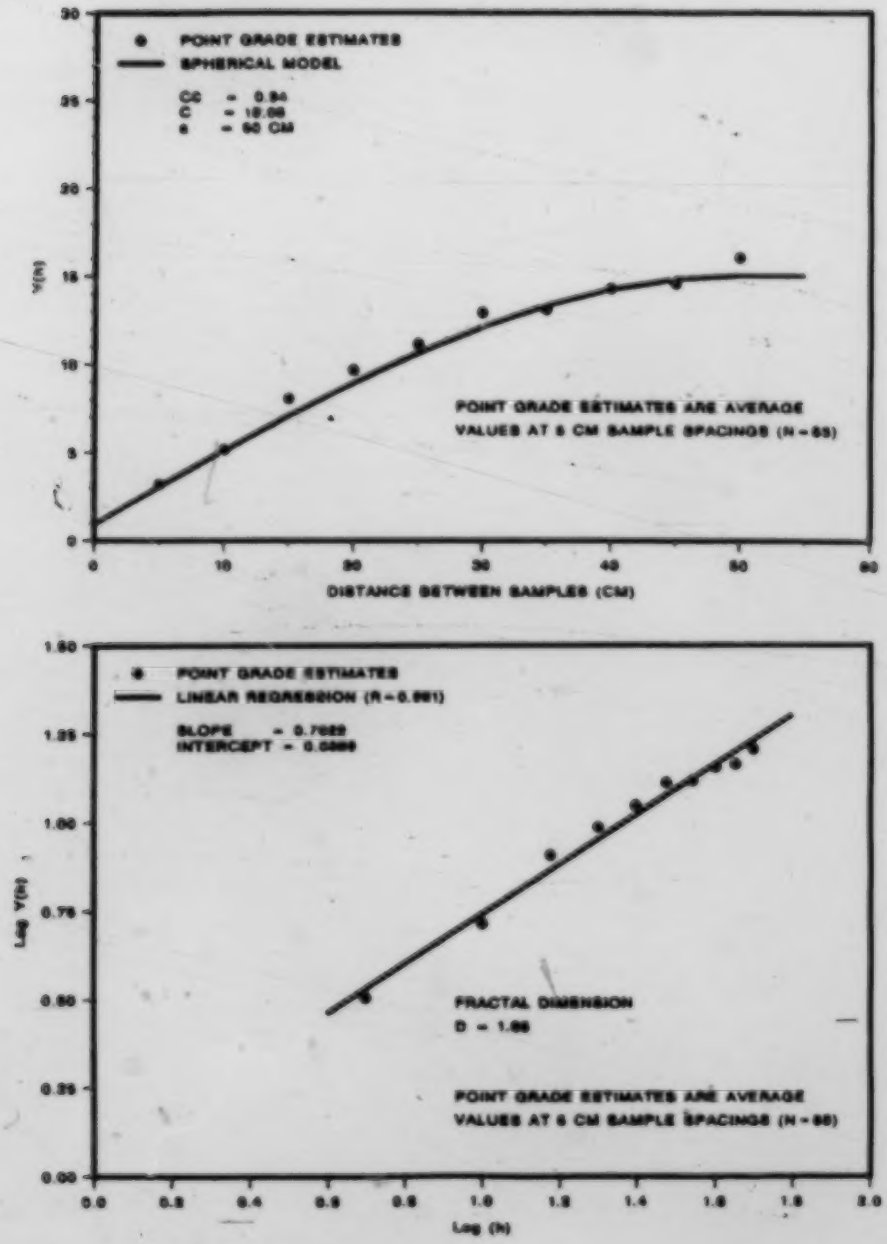
POINT GRADE ESTIMATES
SPHERICAL MODEL
POINT GRADE ESTIMATES ARE AVERAGE
VALUES AT 5 CM SAMPLE SPACINGS (N = 65)
DISTANCE BETWEEN SAMPLES (CM)
POINT GRADE ESTIMATES
LINEAR REGRESSION
FRACTAL DIMENSION
POINT GRADE ESTIMATES ARE AVERAGE
VALUES AT 5 CM SAMPLE SPACINGS (N = 65)

**Figure 86.** Experimental semi-variograms for point grade estimates obtained at 5 cm sample spacings.

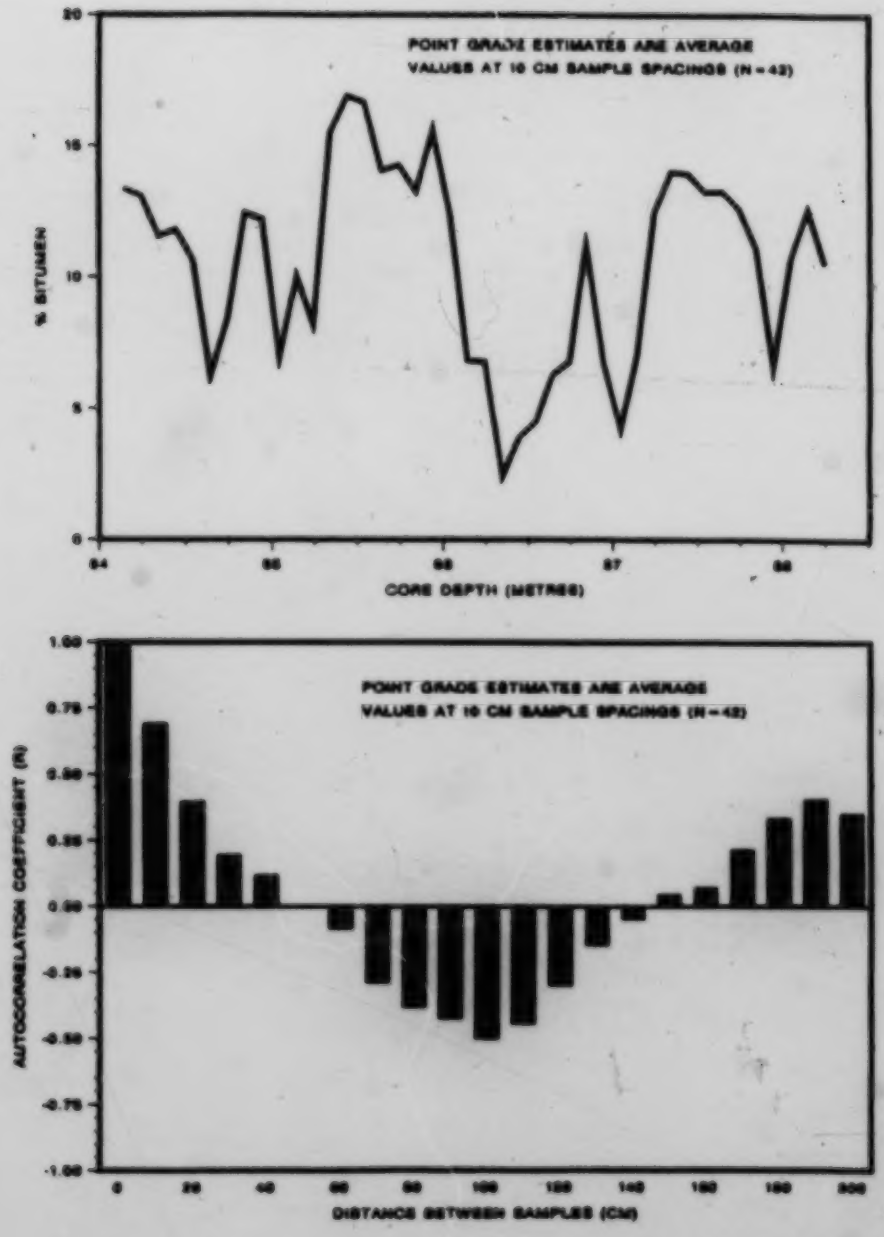
POINT GRADE ESTIMATES ARE AVERAGE
VALUES AT 10 CM SAMPLE SPACINGS (N = 42)
% BITUMEN
CORE DEPTH (METRES)
POINT GRADE ESTIMATES ARE AVERAGE
VALUES AT 10 CM SAMPLE SPACINGS (N = 42)
AUTOCORRELATION COEFFICIENT (R)
DISTANCE BETWEEN SAMPLES (CM)

**Figure 87.** Grade profile and autocorrelation function for point grade estimates obtained at 10 cm sample spacings.

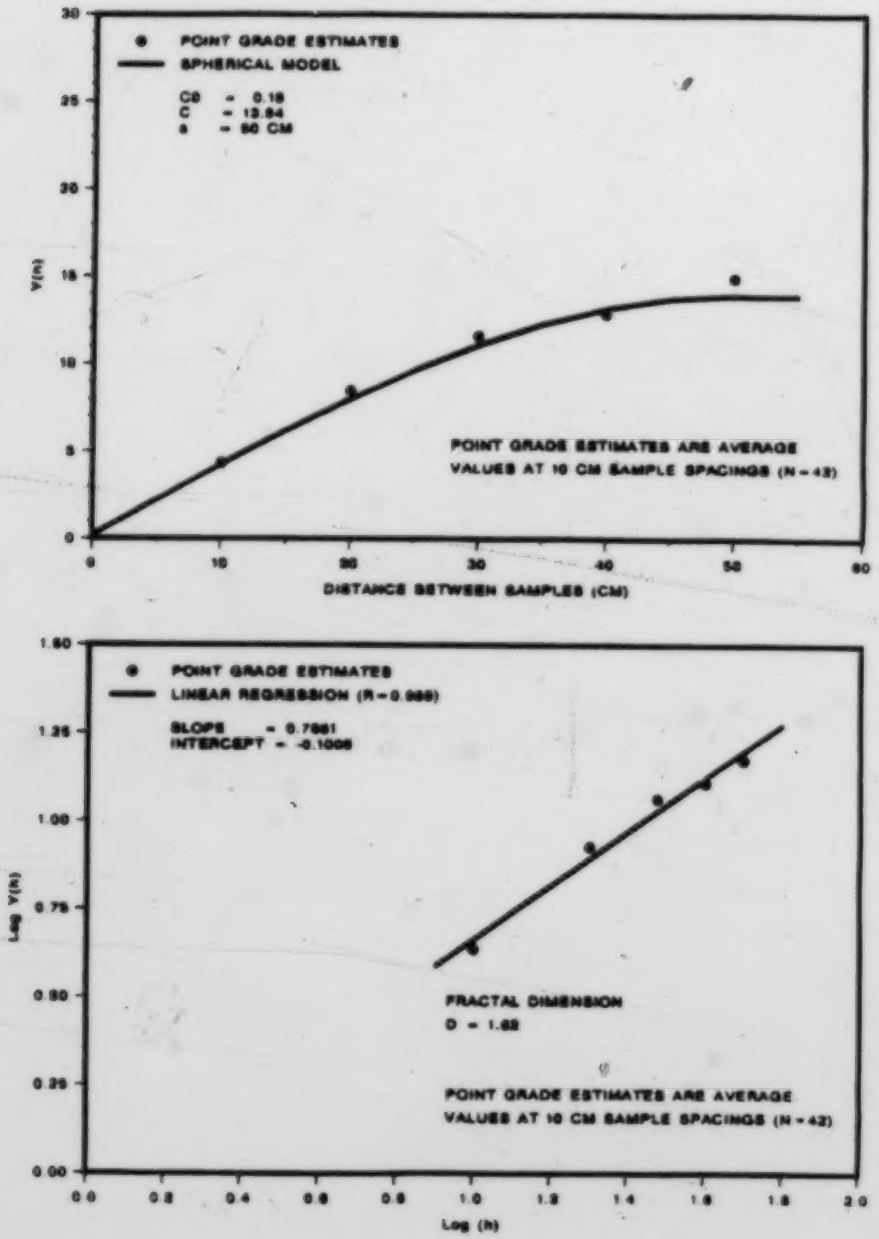


**Figure 88.** Experimental semi-variograms for point grade estimates obtained at 10 cm sample spacings.

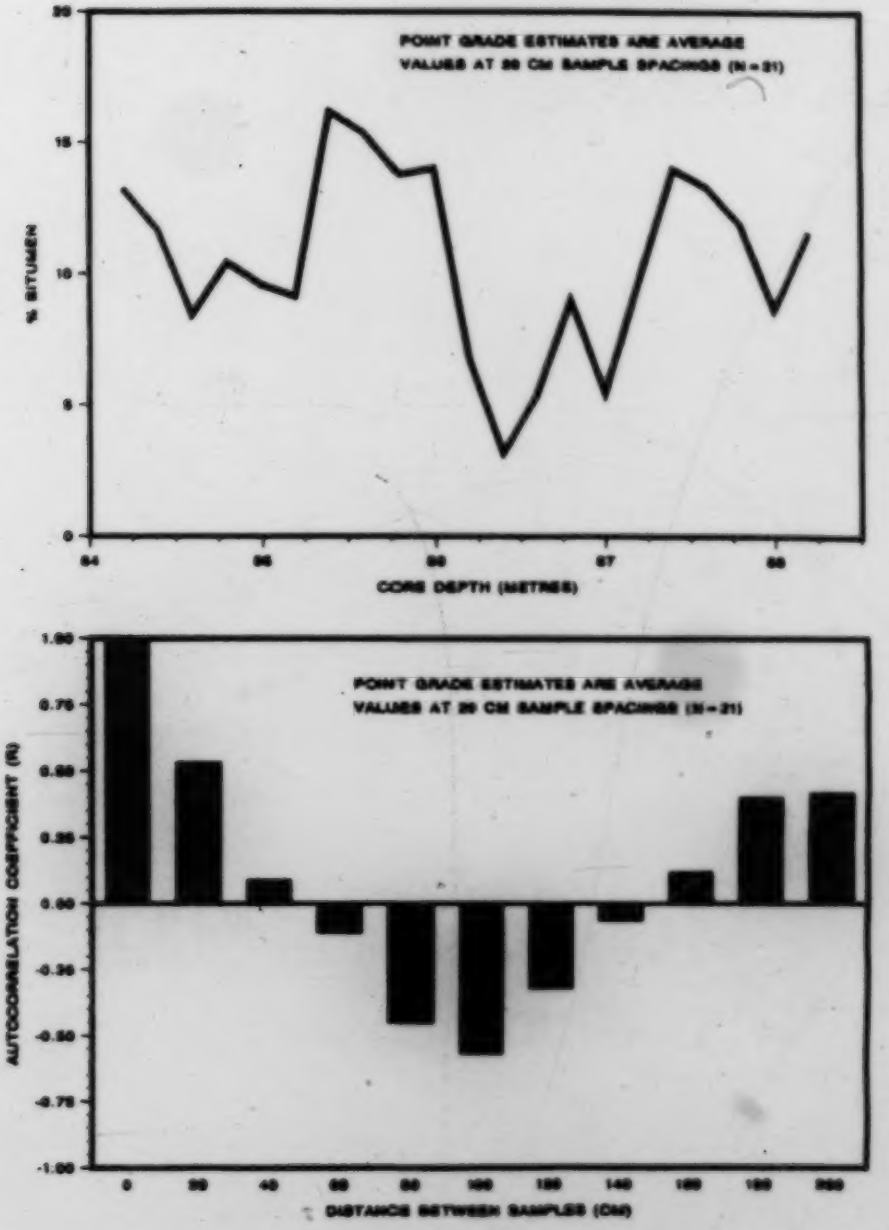
POINT GRADE ESTIMATES ARE AVERAGE
VALUES AT 20 CM SAMPLE SPACINGS (N=21)
% BITUMEN
CORE DEPTH (METRES)
POINT GRADE ESTIMATES ARE AVERAGE
VALUES AT 20 CM SAMPLE SPACINGS (N=21)
AUTOCORRELATION COEFFICIENT (R)
DISTANCE BETWEEN SAMPLES (CM)

**Figure 89.** Grade profile and autocorrelation function for point grade estimates obtained at 20 cm sample spacings.

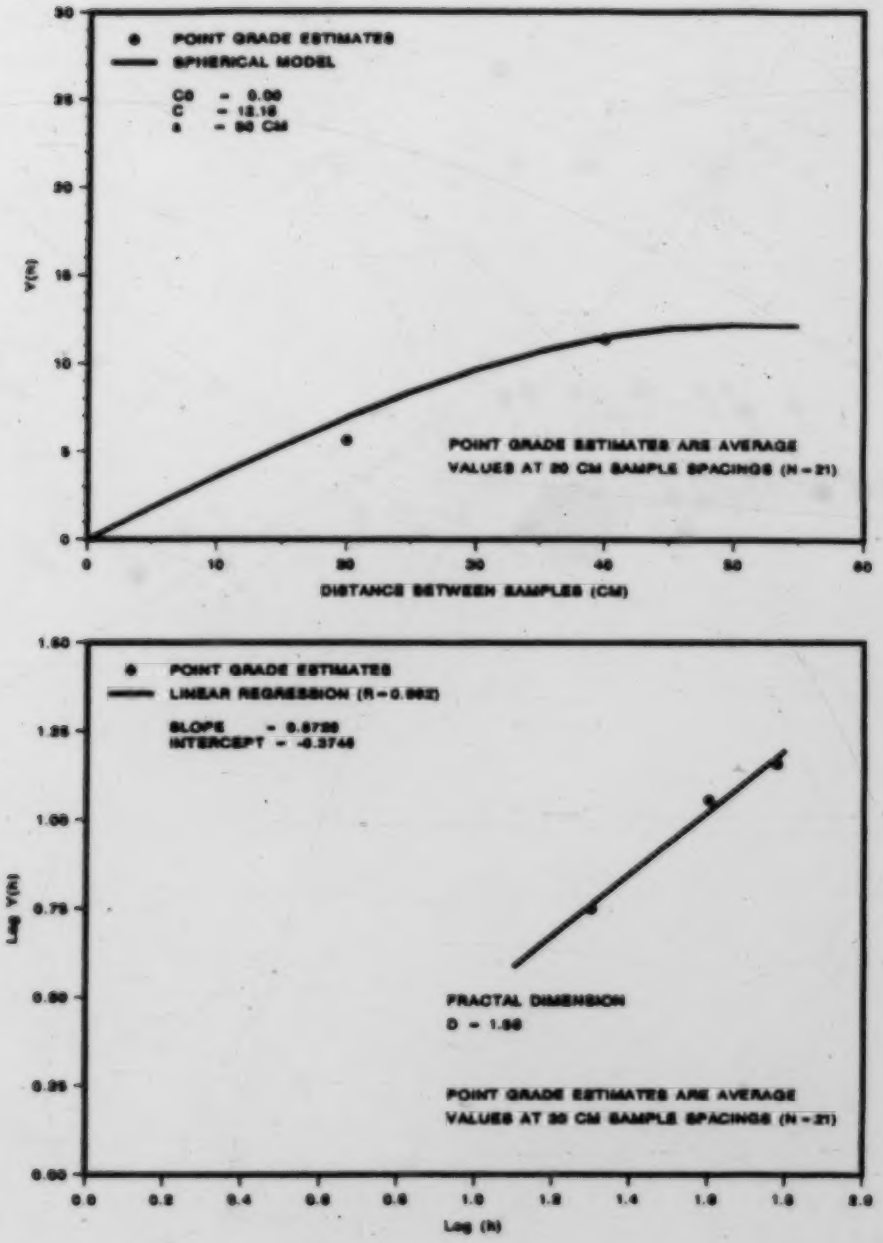


**Figure 90.** Experimental semi-variograms for point grade estimates obtained at 20 cm sample spacings.

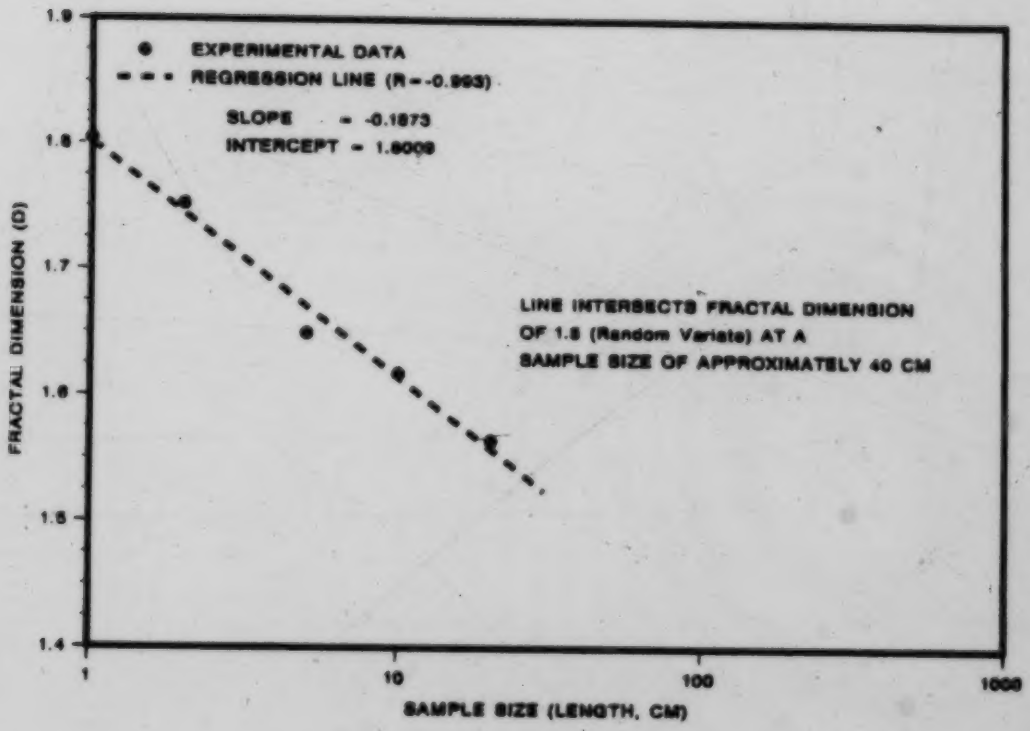


**Figure 91.** Relationship between fractal dimension and sample size for regularized core assay data.

can be shown that the value $D = 1.5$ (signifying purely random behaviour) is achieved at a sample size of length approximately equal to 40 cm. Thus, compositional data obtained for samples of this particular size will be randomly distributed as a function of depth. Consequently, a representative estimate for the grade of an oil sand deposit could be determined by selecting any number of these samples and averaging the results. The reliability of the estimate, as measured by the sampling uncertainty (expressed as variance), would improve by a factor of $1/n$, where $n$ is the number of samples used to generate the mean. The number of samples required to ensure a given confidence interval for the estimate could easily be determined. Samples of size less than 40 cm do not vary at random due to the effects of localized segregation.

The findings from this work indicate that there are different scales of variation in the data depending on the resolution used for measurement. To explore this further, the variability in the composition of oil sand within the parent core sample (from which our test core section is but a small fraction of the total length) was examined. Unfortunately, assay data originally obtained for this core was not determined at regularly spaced intervals. Samples varied in length between 0.3 and 3.3 metres and were selected on the basis of common geological feature. The average sample spacing was 1.8 metres.

It is possible to regularize the data at some constant sample spacing by a procedure known as reconstitution. In this method, data obtained at irregular sample spacings are averaged over some specified sampling interval in order to create a new image of the spatial series. The size of the sampling interval must exceed the average distance spacing of the original series. It must be noted that restoration of the data base using this linear interpolation process smooths out some of the variation in the spatial series and hence must not be carried out indefinitely.

The variability in oil sand grade as a function of depth for this core based on sample values reconstituted at regular 2 metre spacings is shown in Figure 92. Data is tabulated in Appendix B. The corresponding autocorrelation function and semivariogram, for which the data is provided in Appendix C, along with the graph

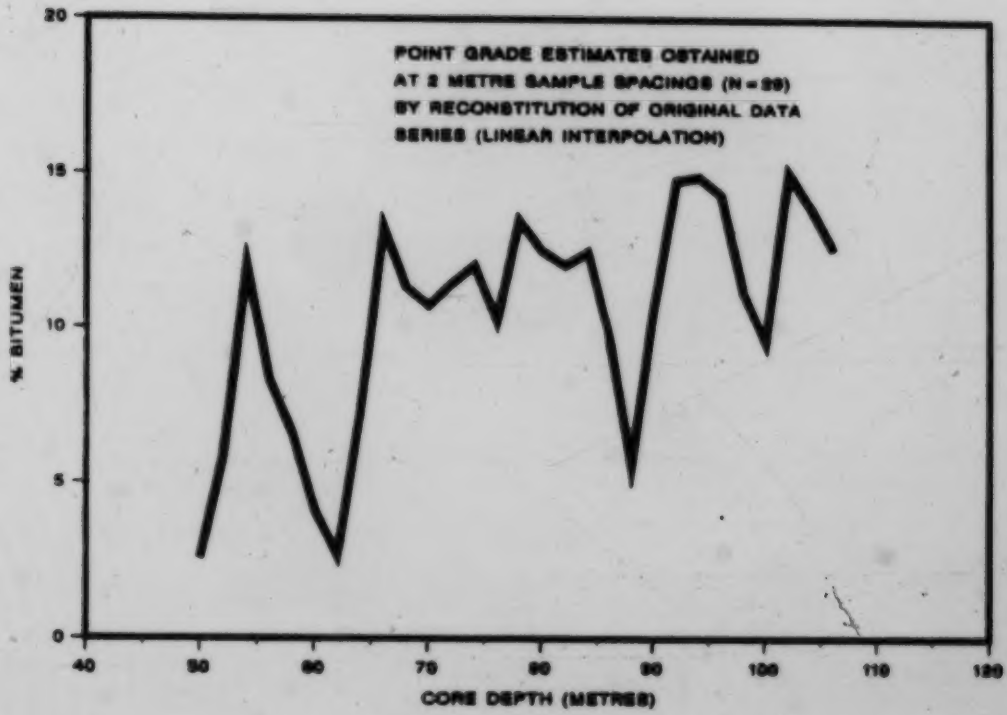


**Figure 92.** Variability in bitumen content as a function of depth for core hole 22-38-60-0-0-0.

relating *Log* $Y(h)$ and *Log* $h$, are presented in Figures 93 and 94. From the slope of this latter plot, the fractal dimension of the spatial series is found to be 1.61. Clearly, this value depicts behaviour intermediate between that seen at other levels of sampling resolution and confirms the idea that variability differs as a function of measurement scale.

It is interesting to note that a line joining this estimate of fractal dimension and the value obtained from Dowd and Royle's data has a slope similar to that for the results obtained at much higher sampling resolutions. Data is plotted in Figure 95. There appears to be a transition zone separating distinct states of sample heterogeneity. Material considered homogeneous at one scale of measurement resolution is suddenly a segregated mixture when resolved at the next scale of measurement. These findings suggest that sampling protocols must be tuned to a particular scale range of the phenomenon in question. Moreover, an estimate for the sampling uncertainty associated with a value for the composition of a bulk material may not be applicable at other scales of observation.

## 5.3 Implications With Respect to Sampling Theory for Segregated Bulk Materials

When estimating the composition of a bulk material from subsamples withdrawn from the lot, it is imperative that the magnitude of sampling uncertainties be known such that a rational inference can be made regarding the integrity of the result. To control these sampling uncertainties, a sampling protocol must be developed that takes into account the variability in the bulk property being measured. An introduction to the concepts of sampling theory and the factors which must be considered in the design of sampling plans is provided by Kratochvil and Taylor (39). More detailed treatments of sampling theory and a review of practical applications can be found in the extensive bibliography prepared by Kratochvil, Wallace,and Taylor (40).

Sampling equations for bulk solids, such as those proposed by Gy (41) and Ingamells (42) for well mixed materials and Visman (43) for the more general case

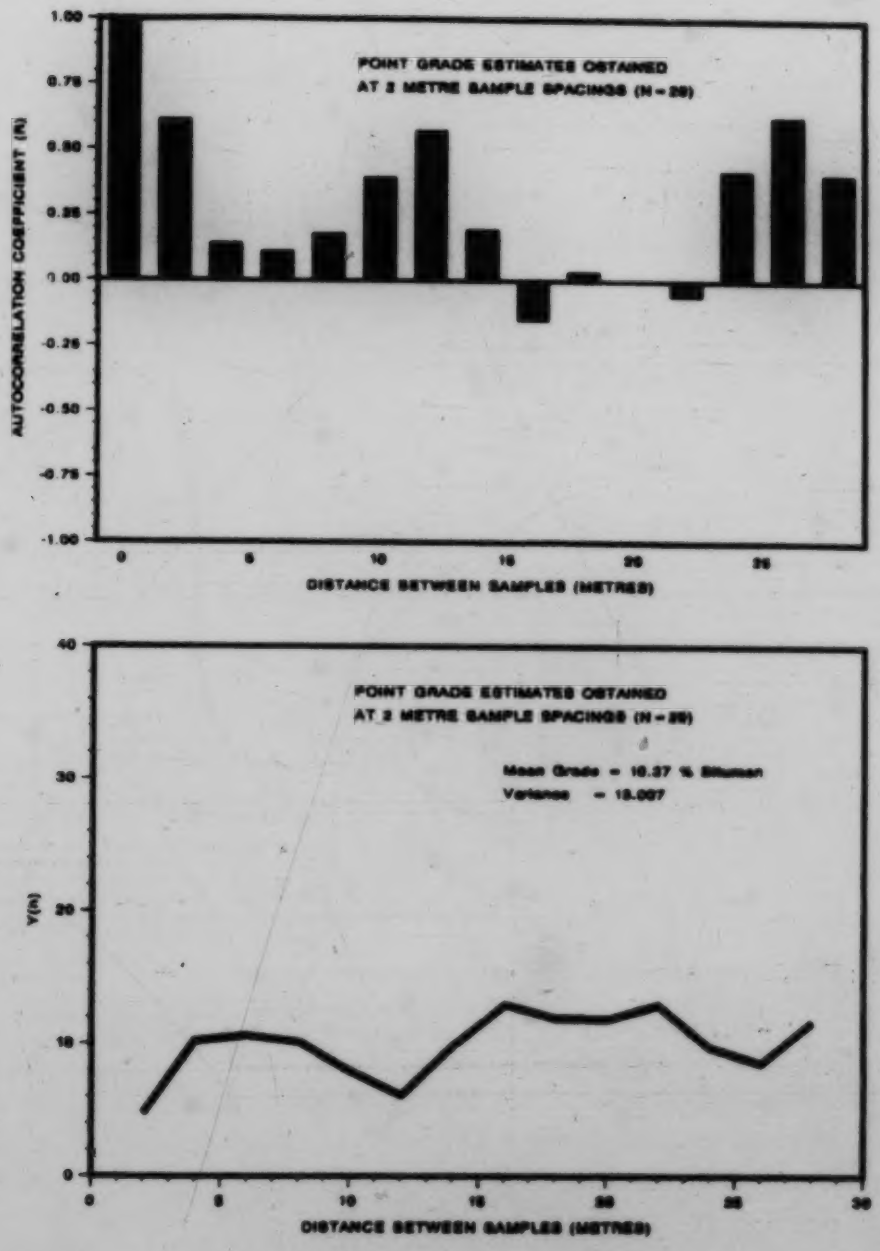


**Figure 93.** Autocorrelation function and experimental semi-variogram for core hole 22-38-60-0-0-0. Point grade estimates obtained at 2 metre sample spacings by reconstitution of original data series.

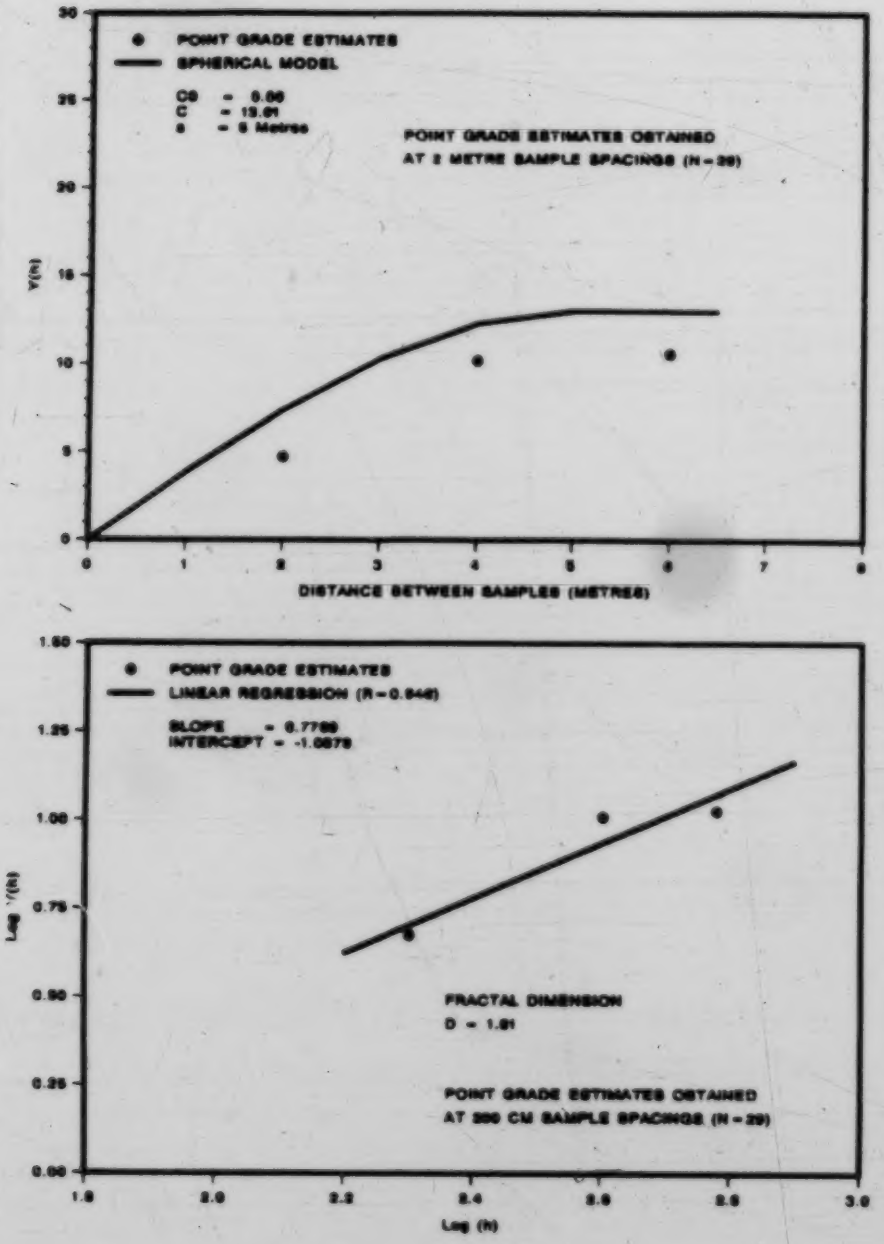


**Figure 94.** Experimental semi-variograms for core hole 22-38-60-0-0-0. Point grade estimates obtained at 2 metre sample spacings by reconstitution of original data series.

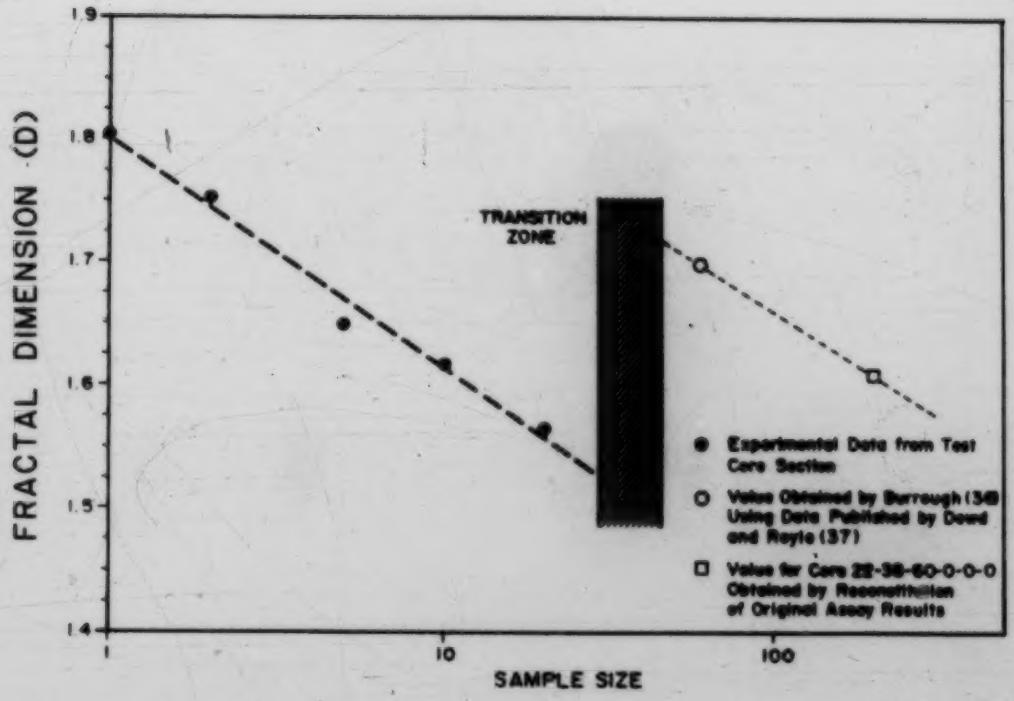


**Figure 95.** Relationship between fractal dimension and sample size for regularized core assay data indicating possible transition zone between scales of sample heterogeneity.

of segregated materials, may be used to calculate the number and size of sample increments required to hold sampling uncertainty at a specified level. For a given population, values for the above sampling constants are obtained by initial testing until they are considered typical of all samples likely to be encountered. The previous section shows that this could become a monumental task for materials which must be characterized in terms of a spatial series of samples. With regard to regionalized oil sand grades, for example, sampling variability appears to change depending on the scale of measurement resolution used to estimate the quality of the bulk.

Visman presents a general sampling model that includes a term for variability due to trend or segregation phenomena. The basic ideas of his sampling theory have been incorporated in the design of sampling plans for coal (44). Visman's sampling equation describes sampling uncertainty, $s^2$, as a sum of random and segregation variance components:

$$s^2 = \frac{A}{wn} + \frac{B}{n}$$

where $A$ = sampling constant for random variance, $B$ = sampling constant for segregation variance, $w$ = weight of a sample increment, and $n$ = number of sample increments. In this expression, sampling uncertainty attributed to the random distribution of assay values can be reduced by increasing either the size or number of samples withdrawn from the bulk. Uncertainties resulting from trend or segregation effects, however, can only be reduced by increasing the number of sample increments collected to represent bulk material composition. The application of this theory as it pertains to the characterization of a bulk oil sand sample has been discussed by Wallace and Kratochvil (45,46).

A deficiency in the application of Visman's equation has to do with the evaluation of the sampling constants $A$ and $B$ in bulk materials for which there exist serial correlations among consecutive sample increments. Rose (47) addressed this problem from a theoretical perspective and introduced a model to evaluate sampling uncertainties for data obtained at regularly spaced intervals in either the time

or spatial domain. As reported by Merks (48), variance estimates based on this model when sampling a stream of coal are in close agreement with values obtained using Visman's equation in which $A$ and $B$ were estimated from a narrow range of sample increment sizes. Neither of these models, however, consider the implications of extenuating segregation effects that change depending on the scale of resolution used to sample the bulk material.

Estimates for Visman's sampling constants for some specified lot of material are obtained by analyzing sets of large and small sample increments. For a well mixed material, the magnitude of sampling variances obtained among samples of different mass will obey the relation:

$$s_L^2(w_L) = s_S^2(w_S)$$

where the subscripts $S$ and $L$ refer to the small and large sample increments, respectively. This equation is formulated from basic statistical principles. Here, sample weight is indicative of the total number of sampling units used to obtain a given mass of material. Thus, variance decreases with increasing $n$.

If equality does not hold, implying that

$$s_L > \left(\frac{w_S}{w_L}\right)^{\frac{1}{2}} s_S$$

then the bulk material is considered to be segregated. The values obtained for the sampling uncertainty associated with the large and small increments can be used to determine Visman's sampling constants according to the equations:

$$A = \frac{w_L w_S}{w_L - w_S}\left(s_S^2 - s_L^2\right)$$

and

$$B = s_L^2 - \frac{A}{w_L}$$

or alternatively,

$$B = s_S^2 - \frac{A}{w_S}$$

By definition, segregation exists if $B$ is greater than zero. Should this be the case, sampling equations developed for homogeneous bulk materials could severely misrepresent the level of sampling uncertainty attainable under a prescribed set of conditions. They should not be used to establish analytical protocols for segregated materials.

Implicit in Visman's theory is the assumption that segregation variance is independent of increment size. It is presumed to be a large scale effect that is reflected in the differences observed among samples of weight $w_L$. The selection of $w_L$ in relation to $w_S$, however is arbitrary. As a general guideline, it is recommended that the size of the large increments be at least an order of magnitude greater than the small increments. Duncan (49) has pointed out that estimates for segregation variance may indeed vary depending on the size of increment used to evaluate this term. A better understanding of segregation variance (and its role in the design of sampling plans for serially correlated materials) may be possible in the context of fractal dimension. In the material that follows, it will be shown that segregation variance for data sampled as a spatial series can be described in terms of the rate at which sampling uncertainties diminish as a function of separation distance between consecutive increments.

The selection of large sample increments in relation to the small sample increments when evaluating the Visman sampling constants is crucial for determining segregation variance. As was shown in a previous section, there may exist several scales of variability in bulk samples that are manifested by the resolution at which the material is sampled. For oil sand grades measured along a length of core, it was found that sampling uncertainties decrease with increasing sample size up to a point. There may then exist a transition wherein the variance among samples increases dramatically. A new scale of segregation is encountered. It is possible to obtain a data set in which the variance calculated for small sample increments is considerably less than that for larger sample increments.

Data describing the sampling uncertainties for regionalized oil sand grades as a function of sample size are summarized in the following table.

| SAMPLE SIZE (cm) | SAMPLING UNCERTAINTY (Variance) | $A$ | $B$ | FRACTAL DIMENSION ($D$) |
|---|---|---|---|---|
| 1 | 19.596 | — | — | 1.80 |
| 2 | 17.934 | 3.324 | 16.272 | 1.75 |
| 5 | 15.048 | 5.685 | 13.911 | 1.65 |
| 10 | 13.937 | 6.288 | 13.308 | 1.62 |
| 20 | 12.155 | 7.832 | 11.764 | 1.56 |

These results were obtained from the detailed inspection of a relatively small section of core. Here, sampling uncertainty is defined as the variance among samples at the point where assay results can be considered independent of location, that is, the sill value from the experimental semi-variogram. In this calculation of the Visman sampling constants, samples obtained at 1 cm intervals represent $w_s$ and samples averaged over other distance spacings represent the mass of larger sample increments. Clearly, the sampling constants are far from invariant and can be shown to be directly related to the fractal dimension of the data series. Results are plotted in Figure 96.

In all instances, the fractal dimension of the system is greater than 1.5, indicating that segregation is a localized phenomenon and dominant over these scales of sampling resolution (albeit at different degrees). Further, the value for the sampling constant $A$ always exceeds that obtained for $B$. Lines which could be drawn through the data, however, intersect at a point where $A = B$. On the graph, this occurs at a fractal dimension of 1.5. Here, it is postulated that segregation becomes a random effect which can not be distinguished from other sources of sampling uncertainty. Samples of a size for which the fractal dimension of the system is 1.5 can be considered to vary at random. Thus, an optimal sample weight may be defined as that at which antipersistent behaviour is damped out.

Extrapolation beyond this intersection point, where $D < 1.5$, suggests that values obtained for $A$ should become greater than those for $B$. At these fractal dimensions, segregation effects reappear. Instead of being of a localized nature, however, this type of segregation is persistent and can be ascribed to long range

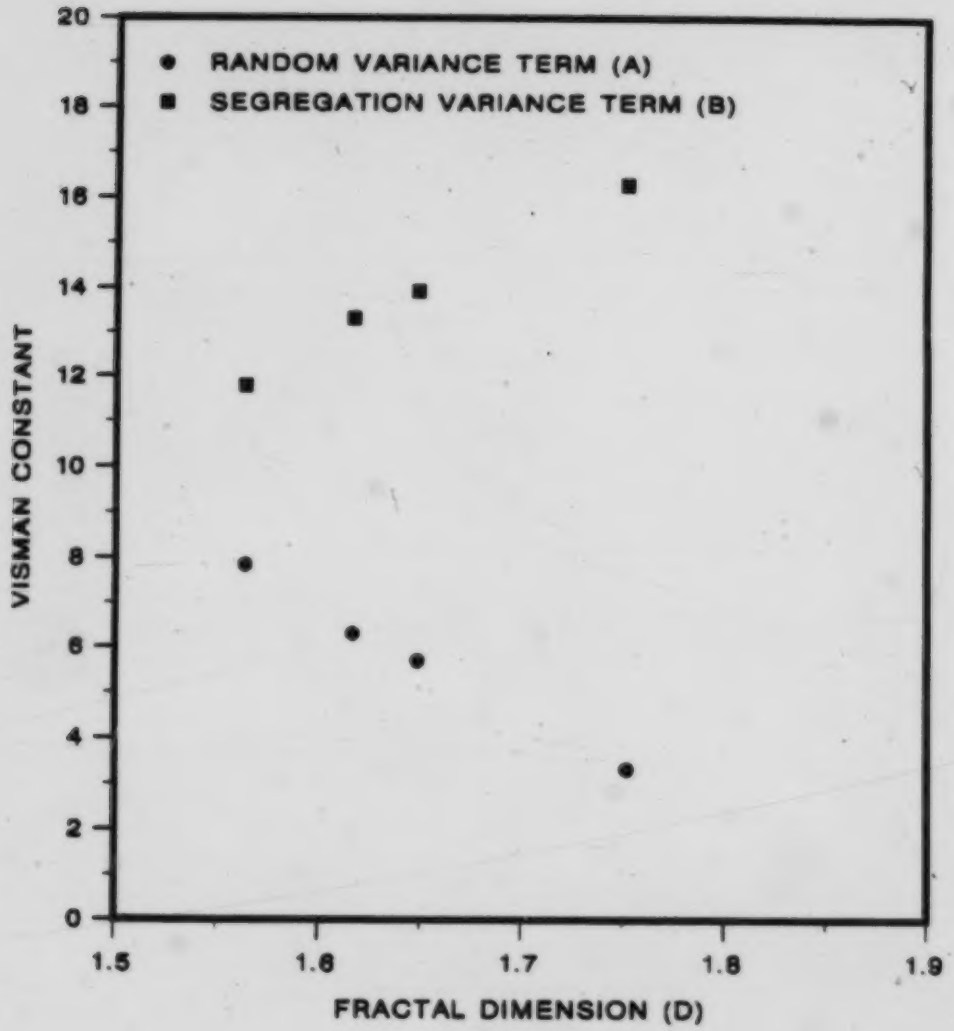


**Figure 96.** Relationship between fractal dimension and Visman sampling constants for segregated materials.

trends in the data. As we have seen earlier though, a discontinuity may exist at which these trends again become antipersistent.

It becomes apparent that an appreciation for the extent of segregation in a bulk sample should based not on the value obtained for $B$ but rather the ratio of $A$ to $B$. For systems that can be characterized in terms of a fractal dimension, the value of $A/B$ serves to define the scale of segregation present in the sample. The point at which $A = B$ establishes the size of increments required to assure that segregation patterns are randomly distributed.

# 6. CONCLUSIONS AND SUGGESTIONS FOR FUTURE WORK

This study was undertaken to examine the application of near–infrared diffuse reflectance spectroscopy for the non–destructive determination of bitumen content in samples of oil sand. Results indicated that reliable measures for hydrocarbon saturation can be obtained using a calibration curve relating spectral response and compositional data for series of known standards. A micro–Soxhlet extraction procedure, especially suited for the analysis of small quantities of oil sand, was developed to provide the reference assay data.

The instrumental technique was used to provide a high resolution profile of grade variability as a function of depth along a section of core representing a vertical transect through the Athabasca deposit. Patterns in the structure of the resulting contour were interpreted from a geostatistical perspective employing the concept of fractal dimension. Implications with respect to the development of sampling protocols for segregated materials which can be described in terms of a spatial series of attributes were addressed.

The significant findings from this work are summarized below:

- Near–infrared diffuse reflectance analysis provides a rapid means for analyzing bitumen content in samples of Athabasca oil sand. A linear model based on the first derivative of absorbance spectra was found to provide an excellent relationship between spectral features and sample composition over the wide range of oil sand grades encountered.

- The advantage of the instrumental procedure lies in the use of sophisticated data handling and multivariable statistical tehniques which have become readily available with the advent of microprocessor based systems.

- Based on the experimental semi–variogram for sample assays obtained at 1 cm intervals along a length of core, it was found that the structure of the vertical grade profile can be characterized as having a fractal dimension greater than

that of a randomly distributed variate. This implies that the material is extremely heterogeneous and can be considered a segregated mixture at the scale of observation used to generate the spatial series.

- Up to a point, the degree of segregation was found to diminish as sample size increased, or alternatively, as the resolution used for sampling decreased. Variations in oil sand composition as a function of location under these conditions appear to become more consistent with that expected for a random phenomenon. Beyond this scale of observation however, a transition zone may exist at which segregation trends again become dominant.

- Findings indicate that there are several scales of variability among regionalized estimates for the bitumen content of an oil sand deposit depending on the resolution used for measurement. Sampling theories that address the contribution of segregation variance to the overall level of sampling uncertainty must take into account the distinct scales of variability which may be present in the quantity of material under consideration. Segregation variance is not independent of increment size.

It has long been appreciated that the recovery of bitumen from an oil sand deposit is governed in large part by the quality of the ore fed to the process. Near-infrared diffuse reflectance analysis has potential for characterizing oil sand not only with respect to bitumen content but also in terms of its mineralogy and depositional environment. Further study in this area is warranted, particularly as it pertains to the development of on-line sensors and control strategies for commercial oil sand extraction plants.

Additional work should also be pursued to confirm the presence of transition zones among scales of segregation for oil sand in the Athabasca deposit. This could be accomplished by examining vertical grade profiles in cores sampled at yet higher or lower resolution than that described in this particular study.

## REFERENCES


1. Wetzel,D.L. "Near-Infrared Reflectance Analysis - Sleeper Among Spectroscopic Techniques." Analytical Chemistry **55** (12) 1165A (1983).

2. Analytical Chemistry. "Near-Infrared Reflectance Spectrometry: Tip of the Iceberg." Analytical Chemistry **56** (8) 933A (1984).

3. McDonald,R.S. "Review: Infrared Spectrometry." Analytical Chemistry **58** (9) 1906 (1986).

4. Stark,E., Luchter,K., and Margoshes,M. "Near-Infrared Analysis (NIRA): A Technology for Quantitative and Qualitative Analysis." Applied Spectroscopy Reviews **22** (4) 335 (1986).

5. Kubelka,P. and Munk,F. Z. Tech. Phys. **12** 593 (1931).

6. Kortum,P., Braun,W., and Herzog,G. Angew. Chem., Int. Ed. Engl. **2** 333 (1963).

7. Fuller,M.P. and Griffiths,P.R. "Diffuse Reflectance Measurements by Infrared Fourier Transform Spectrometry." Analytical Chemistry **50** (13) 1906 (1978).

8. Thompson,G.R. Method and Apparatus for On-Line Monitoring of Bitumen Content in Tar Sand. Canadian Patent 1139702 (1983).

9. Honigs,D.E., Hieftje,G.M., and Hirschfeld,T. "A New Method for Obtaining Individual Component Spectra From Those of Complex Mixtures." Applied Spectroscopy **38** (3) 317 (1984).

10. McClure,W.F. et.al. "Fourier Analysis Enhances NIR Diffuse Reflectance Spectroscopy." Applied Spectroscopy **38** (3) 322 (1984).

11. Hruschka.W.R. and Norris,K.H. "Least Squares Fitting of Near Infrared Spectra Predicts Protein and Moisture Content of Ground Wheat." Applied Spectroscopy **36** (3) 261 (1982).

12. Beebe,K.R. and Kowalski,B.R. "An Introduction to Multivariate Calibration and Analysis." Analytical Chemistry **59** (17) 1007A (1987).

13. Montalvo,J.G., Faught,S.E., and Buco,S.M. "Matching a Sample Constituent to a Sample Property Measured by NIRA." American Laboratory **18** (11) 37 (1986).

14. Mark,H. "Comparative Study of Calibration Methods for Near-Infrared Reflectance Analysis Using a Nested Experimental Design." Analytical Chemistry **58** (13) 2814 (1986).

15. Honigs,D.E., Hieftje,G.M., and Hirschfeld,T. "Number of Samples and Wavelengths Required for the Training Set in Near-Infrared Reflectance Spectroscopy." Applied Spectroscopy **38** (6) 844 (1984).

16. O'Donnell,N.D. and Ostrowski,T.B. "Ore Reserve Estimation at Syncrude Canada Ltd." Applied Mining Geology: Ore Reserve Estimation. Society of Mining Engineers, Inc. Littleton, Colorado, 1986.

17. May,R.W. and Ryan,W.B. "Point Kriging for Isopach Estimation: A Case Study in Reject Assessment." Ibid.

18. Bulmer,J.T. and Starr,J. Syncrude Analytical Methods for Oil Sand and Bitumen Processing. Alberta Oil Sands Technology and Research Authority, Edmonton, Alberta, 1979.

19. Dougan,P.D. "Near-Infrared Analysis: Its Potential Application in Oil Sand Processing." Submitted for Publication in AOSTRA Journal of Research **4** (1988).

20. Fysh,S.A., Swinkels,D.A.J., and Fredericks,P.M. "Near-Infrared Diffuse Reflectance Spectroscopy of Coal." Applied Spectroscopy **39** (2) 354 (1985).

21. Fredericks,P.M., Tattersall,A., and Donaldson,R. "Near-Infrared Reflectance Analysis of Iron Ores." Aplied Spectroscopy **41** (6) 1039 (1987).

22. Takamura,K. "Microscopic Structure of Athabasca Oil Sand." Canadian Journal of Chemical Engineering **60** (4) 538 (1982).

23. Mandelbrot,B.B. Fractals, Form, Chance, and Dimension. Freeman, San Francisco, 1977.

24. Mandelbrot,B.B. The Fractal Geometry of Nature. Freeman, San Francisco, 1982.

25. Beddow,J.K. Particle Characterization in Technology. CRC Press, Inc., Boca Raton, Florida, 1984.

26. Kaye,B.H. "Fractal Dimension and Signature Waveform Characterization of Fine Particle Shape." American Laboratory **18** (3) 55 (1986).

27. Friesen,W.I. and Mikula,R.J. "Fractal Dimensions of Coal Particles." Journal of Colloid and Interface Science **120** (1) 263 (1987).

28. Fairbridge,C., Ng,S.H., and Palmer,A.D. "Fractal Analysis of Gas Adsorption on Syncrude Coke." Fuel **65** (12) 1759 (1986).

29. Avnir,D. and Pfeifer,P. "Fractal Dimension in Chemistry. An Intensive Characteristic of Surface Irregularity." Nouveau Journal de Chemie **7** (2) 71 (1983).

30. Van Damme,H. and Fripiat,J.J. "A Fractal Analysis of Adsorption Processes by Pillared Swelling Clays." J.Chem.Phys. **82** (6) 2785 (1985).

31. Mandelbrot,B.B. "How Long is the Coast of Britain?" Science **156** 636 (1967).

32. Box,G.E.P. and Jenkins,G.M. Time Series Analysis Forecasting and Control. Holden–Day, San Francisco, 1976.

33. Mandelbrot,B.B and Van Ness,J.W. "Fractional Brownian Motions, Fractional Noises, and Applications." SIAM Review **10** 422 (1968).

34. Mandelbrot,B.B. "Statistical Methodology for Nonperiodic Cycles: From the Covariance to R/S Analysis." Annals of Economic and Social Measurement **1** 257 (1972).

35. Clark,I. Practical Geostatistics. Applied Science Publishers Ltd., London, 1979.

36. Burrough,P.A. "Fractal Dimensions of Landscapes and Other Environmental Data." Nature **294** 240 (1981).

37. Dowd,P.A. and Royle,A.G. "Geostatistical Applications in the Athabasca Tar Sands." Proceedings, 15th International APCOM Symposium, Brisbane, Australia (1977).

38. Journel,A.G. and Huijbregts,Ch.J. Mining Geostatistics. Academic Press, New York, 1978.

39. Kratochvil,B. and Taylor,J.K. "Sampling for Chemical Analysis." Analytical Chemistry **53** (8) 924A (1981).

40. Kratochvil,B., Wallace,D., and Taylor,J.K. "Sampling for Chemical Analysis". Analytical Chemistry **56** (5) 113R (1984).

41. Gy,P.M. Sampling of Particulate Matter, Theory and Practice. Elsevier Scientific Publishing Co., Amsterdam, 1979.

42. Ingamells,C.O. "New Approaches to Geochemical Analysis and Sampling." Talanta **21** 141 (1974).

43. Visman,J. "A General Sampling Theory." Materials Research and Standards **9** (11) 9 (1969).

44. ASTM D2234 Method for Collection of a Gross Sample of Coal. American Society for Testing Materials, Philadelphia, PA.

45. Wallace,D. and Kratochvil,B. AOSTRA Journal of Research **2** 233 (1986).

46. Wallace,D. and Kratochvil,B. "Visman Equations in the Design of Sampling Plans for Chemical Analysis of Segregated Bulk Materials." Analytical Chemistry **59** (2) 226 (1987).

47. Rose,C.D. "Variances in Sampling Streams of Coal." Journal of Testing and Evaluation **11** (5) (1983).

48. Merks,J.W. Sampling and Weighing of Bulk Solids. Series on Bulk Materials Handling, Volume 4 (1985). Trans Tech Publications, Clausthal-Zellerfeld, Germany, 1985.

49. Duncan,A.J. Materials Research and Standards **11** 25 (1971).

# APPENDIX A

## TRAINING SET MODELS RELATING

## NEAR-INFRARED DIFFUSE REFLECTANCE SPECTRA

## AND BITUMEN CONTENT FOR SAMPLES OF OIL SAND

- Dependent measures for the bitumen content of oil sand samples were determined using a micro–Soxhlet extraction procedure.
- Training set models were developed from $Log1/R$, first derivative of $Log1/R$, and second derivative of $Log1/R$ spectra using a maximum of four independent variables. Each variable represents a selected spectral feature at some wavelength for which there is correspondence with sample composition.

TRAINING SET MODELS

Log 1/R Diffuse Reflectance Spectra

INITIAL WAVELENGTHS FOR COMPOSITE MODELS
AND ASSOCIATED LOCAL MINIMUM SUM OF
SQUARED ERROR (SSE) VALUES:

| MODEL NUMBER | WAVELENGTH | SSE |
|---|---|---|
| 1 | 2323.0 | 0.3676E+03 |
| 2 | 2359.0 | 0.3734E+03 |
| 3 | 2371.0 | 0.3780E+03 |
| 4 | 2347.0 | 0.3789E+03 |
| 5 | 2311.0 | 0.3804E+03 |
| 6 | 2387.0 | 0.3825E+03 |
| 7 | 2399.0 | 0.3854E+03 |
| 8 | 1727.0 | 0.3887E+03 |
| 9 | 2300.0 | 0.3896E+03 |
| 10 | 1712.0 | 0.3915E+03 |

BEST MODEL FOUND WAS MODEL NUMBER: 7

MODEL NUMBER: 1

| | |
|---|---|
| MULTIPLE CORRELATION (R) | 0.9304E+00 |
| STD ERR OF ESTIMATE (SE) | 0.1889E+01 |
| SUM OF SQUARED ERRORS | 0.1569E+03 |
| F TEST | 0.9452E+02 |
| SUM OF RESIDUALS | -0.9996E-12 |

| WAVE-LENGTH | MODEL COEFFICIENT | STANDARD ERROR COEFF | T-VALUE |
|---|---|---|---|
| 2323.0 | 0.1615E+03 | 0.1902E+02 | 0.8490E+01 |
| 1923.0 | -0.8900E+03 | 0.1717E+03 | 0.5185E+01 |
| 1951.0 | 0.7622E+03 | 0.1679E+03 | 0.4539E+01 |
| INTERCEPT | 0.1152E+02 | | |

ANALYSIS OF VARIANCE FOR THE REGRESSION

| VARIATION SOURCE | DF | SUM OF SQ | MEAN SQ | F VALUE |
|---|---|---|---|---|
| ATTRIB TO REGRESSION | 3 | 0.1011E+04 | 0.3371E+03 | 0.9452E+02 |
| DEV FROM REGRESSION | 44 | 0.1569E+03 | 0.3567E+01 | |
| TOTAL | 47 | 0.1168E+04 | | |

| EXP NUM | ACTUAL | MODEL OUTPUT | PERCENT DIFF | ACTUAL DIFF |
|---|---|---|---|---|
| 1 | 0.9680E+01 | 0.8816E+01 | 8.93 | 0.8641E+00 |
| 2 | 0.4130E+01 | 0.4949E+01 | -19.83 | -0.8189E+00 |
| 3 | 0.1361E+02 | 0.1232E+02 | 9.48 | 0.1290E+01 |
| 4 | 0.2070E+01 | 0.4149E+01 | -100.44 | -0.2079E+01 |
| 5 | 0.8120E+01 | 0.8606E+01 | -5.98 | -0.4855E+00 |
| 6 | 0.1639E+02 | 0.1227E+02 | 25.16 | 0.4123E+01 |
| 7 | 0.1069E+02 | 0.8838E+01 | 17.32 | 0.1852E+01 |
| 8 | 0.1371E+02 | 0.1303E+02 | 4.96 | 0.6795E+00 |
| 9 | 0.8210E+01 | 0.7723E+01 | 5.93 | 0.4871E+00 |
| 10 | 0.4600E+01 | 0.5794E+01 | -25.96 | -0.1194E+01 |
| 11 | 0.4790E+01 | 0.6539E+01 | -36.51 | -0.1749E+01 |
| 12 | 0.1457E+02 | 0.1358E+02 | 6.82 | 0.9943E+00 |
| 13 | 0.1510E+02 | 0.1311E+02 | 13.17 | 0.1989E+01 |
| 14 | 0.5720E+01 | 0.2205E+01 | 61.44 | 0.3515E+01 |
| 15 | 0.9560E+01 | 0.9954E+01 | -4.12 | -0.3936E+00 |
| 16 | 0.1000E+01 | 0.3160E+00 | 68.40 | 0.6840E+00 |
| 17 | 0.5360E+01 | 0.6772E+01 | -26.35 | -0.1412E+01 |
| 18 | 0.1642E+02 | 0.1454E+02 | 11.46 | 0.1882E+01 |
| 19 | 0.1591E+02 | 0.1488E+02 | 6.47 | 0.1029E+01 |
| 20 | 0.9300E+01 | 0.7696E+01 | 17.25 | 0.1604E+01 |
| 21 | 0.1280E+02 | 0.1054E+02 | 17.64 | 0.2258E+01 |
| 22 | 0.1412E+02 | 0.1483E+02 | -5.02 | -0.7088E+00 |
| 23 | 0.1774E+02 | 0.1479E+02 | 16.61 | 0.2947E+01 |
| 24 | 0.1618E+02 | 0.1881E+02 | -16.23 | -0.2627E+01 |
| 25 | 0.1459E+02 | 0.1365E+02 | 6.43 | 0.9381E+00 |
| 26 | 0.7160E+01 | 0.1046E+02 | -46.06 | -0.3298E+01 |
| 27 | 0.5860E+01 | 0.9050E+01 | -54.44 | -0.3190E+01 |
| 28 | 0.6480E+01 | 0.9504E+01 | -46.66 | -0.3024E+01 |
| 29 | 0.5510E+01 | 0.8155E+01 | -48.00 | -0.2645E+01 |
| 30 | 0.6490E+01 | 0.9265E+01 | -42.76 | -0.2775E+01 |
| 31 | 0.4310E+01 | 0.6267E+01 | -45.41 | -0.1957E+01 |
| 32 | 0.3160E+01 | 0.3876E+01 | -22.67 | -0.7163E+00 |
| 33 | 0.3230E+01 | 0.2216E+01 | 31.38 | 0.1014E+01 |
| 34 | 0.1880E+01 | 0.2663E+00 | 85.83 | 0.1614E+01 |
| 35 | 0.2030E+01 | 0.4985E+00 | 75.44 | 0.1531E+01 |
| 36 | 0.2220E+01 | 0.1000E+01 | 54.93 | 0.1220E+01 |
| 37 | 0.1378E+02 | 0.1464E+02 | -6.21 | -0.8558E+00 |
| 38 | 0.1348E+02 | 0.1473E+02 | -9.24 | -0.1246E+01 |
| 39 | 0.1364E+02 | 0.1420E+02 | -4.08 | -0.5563E+00 |
| 40 | 0.6540E+01 | 0.7507E+01 | -14.78 | -0.9668E+00 |
| 41 | 0.8240E+01 | 0.7318E+01 | 11.19 | 0.9223E+00 |
| 42 | 0.1618E+02 | 0.1483E+02 | 8.35 | 0.1351E+01 |
| 43 | 0.7540E+01 | 0.8817E+01 | -16.93 | -0.1277E+01 |
| 44 | 0.9680E+01 | 0.8013E+01 | 17.22 | 0.1667E+01 |
| 45 | 0.1262E+02 | 0.1293E+02 | -2.46 | -0.3107E+00 |
| 46 | 0.9600E+00 | 0.3011E+01 | -213.67 | -0.2051E+01 |
| 47 | 0.1017E+02 | 0.1143E+02 | -12.39 | -0.1260E+01 |
| 48 | 0.1363E+02 | 0.1249E+02 | 8.38 | 0.1142E+01 |

MODEL NUMBER: 2

| | |
|---|---|
| MULTIPLE CORRELATION (R) | 0.9480E+00 |
| STD ERR OF ESTIMATE (SE) | 0.1659E+01 |
| SUM OF SQUARED ERRORS | 0.1183E+03 |
| F TEST | 0.9541E+02 |
| SUM OF RESIDUALS | -0.2442E-13 |

| WAVE-LENGTH | MODEL COEFFICIENT | STANDARD ERROR COEFF | T-VALUE |
|---|---|---|---|
| 2359.0 | 0.1875E+03 | 0.1852E+02 | 0.1012E+02 |
| 1939.0 | -0.2267E+04 | 0.3353E+03 | 0.6760E+01 |
| 1951.0 | 0.2300E+04 | 0.3642E+03 | 0.6315E+01 |
| 2218.0 | -0.2054E+03 | 0.5483E+02 | 0.3747E+01 |
| INTERCEPT | 0.1074E+02 | | |

ANALYSIS OF VARIANCE FOR THE REGRESSION

| VARIATION SOURCE | DF | SUM OF SQ | MEAN SQ | F VALUE |
|---|---|---|---|---|
| ATTRIB TO REGRESSION | 4 | 0.1060E+04 | 0.2625E+03 | 0.9541E+02 |
| DEV FROM REGRESSION | 43 | 0.1183E+03 | 0.2751E+01 | |
| TOTAL | 47 | 0.1168E+04 | | |

| EXP NUM | ACTUAL | MODEL OUTPUT | PERCENT DIFF | ACTUAL DIFF |
|---|---|---|---|---|
| 1 | 0.9680E+01 | 0.9569E+01 | 1.15 | 0.1109E+00 |
| 2 | 0.4130E+01 | 0.3893E+01 | 5.73 | 0.2367E+00 |
| 3 | 0.1361E+02 | 0.1117E+02 | 17.93 | 0.2440E+01 |
| 4 | 0.2070E+01 | 0.3975E+01 | -92.05 | -0.1905E+01 |
| 5 | 0.8120E+01 | 0.7247E+01 | 10.75 | 0.8733E+00 |
| 6 | 0.1639E+02 | 0.1295E+02 | 21.02 | 0.3444E+01 |
| 7 | 0.1069E+02 | 0.9738E+01 | 8.91 | 0.9525E+00 |
| 8 | 0.1371E+02 | 0.1322E+02 | 3.59 | 0.4922E+00 |
| 9 | 0.8210E+01 | 0.8347E+01 | -1.67 | -0.1369E+00 |
| 10 | 0.4600E+01 | 0.6261E+01 | -36.11 | -0.1661E+01 |
| 11 | 0.4790E+01 | 0.5280E+01 | -10.22 | -0.4896E+00 |
| 12 | 0.1457E+02 | 0.1374E+02 | 5.70 | 0.8312E+00 |
| 13 | 0.1510E+02 | 0.1409E+02 | 6.69 | 0.1010E+01 |
| 14 | 0.5720E+01 | 0.4360E+01 | 23.78 | 0.1360E+01 |
| 15 | 0.9560E+01 | 0.9586E+01 | -0.28 | -0.2633E-01 |
| 16 | 0.1000E+01 | -0.3314E+00 | 133.14 | 0.1331E+01 |
| 17 | 0.5360E+01 | 0.8135E+01 | -51.78 | -0.2775E+01 |
| 18 | 0.1642E+02 | 0.1423E+02 | 13.32 | 0.2188E+01 |
| 19 | 0.1591E+02 | 0.1547E+02 | 2.79 | 0.4437E+00 |
| 20 | 0.9300E+01 | 0.8128E+01 | 12.61 | 0.1172E+01 |
| 21 | 0.1280E+02 | 0.1131E+02 | 11.62 | 0.1488E+01 |
| 22 | 0.1412E+02 | 0.1541E+02 | -9.16 | -0.1293E+01 |
| 23 | 0.1774E+02 | 0.1539E+02 | 13.26 | 0.2352E+01 |
| 24 | 0.1618E+02 | 0.1938E+02 | -19.78 | -0.3201E+01 |
| 25 | 0.1459E+02 | 0.1321E+02 | 9.43 | 0.1376E+01 |
| 26 | 0.7160E+01 | 0.9800E+01 | -36.87 | -0.2640E+01 |
| 27 | 0.5860E+01 | 0.7600E+01 | -29.69 | -0.1740E+01 |
| 28 | 0.6480E+01 | 0.8661E+01 | -33.66 | -0.2181E+01 |
| 29 | 0.5510E+01 | 0.7594E+01 | -37.82 | -0.2084E+01 |
| 30 | 0.6490E+01 | 0.8709E+01 | -34.19 | -0.2219E+01 |
| 31 | 0.4310E+01 | 0.5754E+01 | -33.51 | -0.1444E+01 |
| 32 | 0.3160E+01 | 0.4188E+01 | -32.53 | -0.1028E+01 |
| 33 | 0.3230E+01 | 0.1763E+01 | 45.40 | 0.1467E+01 |
| 34 | 0.1880E+01 | 0.9391E+00 | 50.05 | 0.9409E+00 |
| 35 | 0.2030E+01 | 0.9313E+00 | 54.12 | 0.1099E+01 |
| 36 | 0.2220E+01 | 0.8561E+00 | 61.44 | 0.1364E+01 |
| 37 | 0.1378E+02 | 0.1423E+02 | -3.29 | -0.4532E+00 |
| 38 | 0.1348E+02 | 0.1361E+02 | -0.98 | -0.1317E+00 |
| 39 | 0.1364E+02 | 0.1479E+02 | -8.43 | -0.1149E+01 |
| 40 | 0.6540E+01 | 0.6057E+01 | 7.39 | 0.4831E+00 |
| 41 | 0.8240E+01 | 0.6815E+01 | 17.29 | 0.1425E+01 |
| 42 | 0.1618E+02 | 0.1407E+02 | 13.06 | 0.2113E+01 |
| 43 | 0.7540E+01 | 0.8497E+01 | -12.69 | -0.9569E+00 |
| 44 | 0.9680E+01 | 0.9090E+01 | 6.10 | 0.5901E+00 |
| 45 | 0.1262E+02 | 0.1371E+02 | -8.67 | -0.1095E+01 |
| 46 | 0.9600E+00 | 0.2741E+01 | -185.48 | -0.1781E+01 |
| 47 | 0.1017E+02 | 0.1200E+02 | -17.95 | -0.1826E+01 |
| 48 | 0.1363E+02 | 0.1300E+02 | 4.64 | 0.6321E+00 |

MODEL NUMBER: 3

| | |
|---|---|
| MULTIPLE CORRELATION (R) | 0.9388E+00 |
| STD ERR OF ESTIMATE (SE) | 0.1796E+01 |
| SUM OF SQUARED ERRORS | 0.1387E+03 |
| F TEST | 0.7981E+02 |
| SUM OF RESIDUALS | -0.1031E-11 |

| WAVE-LENGTH | MODEL COEFFICIENT | STANDARD ERROR COEFF | T-VALUE |
|---|---|---|---|
| 2345.0 | 0.2057E+03 | 0.2231E+02 | 0.9222E+01 |
| 1923.0 | -0.1104E+04 | 0.1917E+03 | 0.5756E+01 |
| 1951.0 | 0.1120E+04 | 0.2385E+03 | 0.4695E+01 |
| 2191.0 | -0.2009E+03 | 0.8960E+02 | 0.2242E+01 |
| INTERCEPT | 0.1088E+02 | | |

ANALYSIS OF VARIANCE FOR THE REGRESSION

| VARIATION SOURCE | DF | SUM OF SQ | MEAN SQ | F VALUE |
|---|---|---|---|---|
| ATTRIB TO REGRESSION | 4 | 0.1030E+04 | 0.2574E+03 | 0.7981E+02 |
| DEV FROM REGRESSION | 43 | 0.1387E+03 | 0.3225E+01 | |
| TOTAL | 47 | 0.1168E+04 | | |

| EXP NUM | ACTUAL | MODEL OUTPUT | PERCENT DIFF | ACTUAL DIFF |
|---|---|---|---|---|
| 1 | 0.9680E+01 | 0.7701E+01 | 20.44 | 0.1979E+01 |
| 2 | 0.4130E+01 | 0.3982E+01 | 3.58 | 0.1478E+00 |
| 3 | 0.1361E+02 | 0.1176E+02 | 13.62 | 0.1854E+01 |
| 4 | 0.2070E+01 | 0.4309E+01 | -108.16 | -0.2239E+01 |
| 5 | 0.8120E+01 | 0.7770E+01 | 4.32 | 0.3504E+00 |
| 6 | 0.1639E+02 | 0.1217E+02 | 25.74 | 0.4219E+01 |
| 7 | 0.1069E+02 | 0.9486E+01 | 11.26 | 0.1204E+01 |
| 8 | 0.1371E+02 | 0.1303E+02 | 4.96 | 0.6801E+00 |
| 9 | 0.8210E+01 | 0.7935E+01 | 3.35 | 0.2754E+00 |
| 10 | 0.4600E+01 | 0.5884E+01 | -27.90 | -0.1284E+01 |
| 11 | 0.4790E+01 | 0.5936E+01 | -23.92 | -0.1146E+01 |
| 12 | 0.1457E+02 | 0.1335E+02 | 8.40 | 0.1223E+01 |
| 13 | 0.1510E+02 | 0.1346E+02 | 10.83 | 0.1635E+01 |
| 14 | 0.5720E+01 | 0.3381E+01 | 40.89 | 0.2339E+01 |
| 15 | 0.9560E+01 | 0.1004E+02 | -5.07 | -0.4846E+00 |
| 16 | 0.1000E+01 | 0.3324E+00 | 66.76 | 0.6676E+00 |
| 17 | 0.5360E+01 | 0.7889E+01 | -47.18 | -0.2529E+01 |
| 18 | 0.1642E+02 | 0.1444E+02 | 12.05 | 0.1978E+01 |
| 19 | 0.1591E+02 | 0.1504E+02 | 5.48 | 0.8720E+00 |
| 20 | 0.9300E+01 | 0.7976E+01 | 14.24 | 0.1324E+01 |
| 21 | 0.1280E+02 | 0.1109E+02 | 13.34 | 0.1707E+01 |
| 22 | 0.1412E+02 | 0.1542E+02 | -9.22 | -0.1302E+01 |
| 23 | 0.1774E+02 | 0.1515E+02 | 14.58 | 0.2587E+01 |
| 24 | 0.1618E+02 | 0.1943E+02 | -20.12 | -0.3255E+01 |
| 25 | 0.1459E+02 | 0.1355E+02 | 7.11 | 0.1038E+01 |
| 26 | 0.7160E+01 | 0.1021E+02 | -42.55 | -0.3046E+01 |
| 27 | 0.5860E+01 | 0.8583E+01 | -46.47 | -0.2723E+01 |
| 28 | 0.6480E+01 | 0.9094E+01 | -40.33 | -0.2614E+01 |
| 29 | 0.5510E+01 | 0.7526E+01 | -36.59 | -0.2016E+01 |
| 30 | 0.6490E+01 | 0.8866E+01 | -36.61 | -0.2376E+01 |
| 31 | 0.4310E+01 | 0.5916E+01 | -37.27 | -0.1606E+01 |
| 32 | 0.3160E+01 | 0.3809E+01 | -20.54 | -0.6492E+00 |
| 33 | 0.3230E+01 | 0.1840E+01 | 43.03 | 0.1390E+01 |
| 34 | 0.1880E+01 | 0.5354E+00 | 71.52 | 0.1345E+01 |
| 35 | 0.2030E+01 | 0.8346E+00 | 58.89 | 0.1195E+01 |
| 36 | 0.2220E+01 | 0.1431E+01 | 35.55 | 0.7893E+00 |
| 37 | 0.1378E+02 | 0.1453E+02 | -5.42 | -0.7464E+00 |
| 38 | 0.1348E+02 | 0.1456E+02 | -8.04 | -0.1083E+01 |
| 39 | 0.1364E+02 | 0.1440E+02 | -5.59 | -0.7619E+00 |
| 40 | 0.6540E+01 | 0.6785E+01 | -3.74 | -0.2449E+00 |
| 41 | 0.8240E+01 | 0.7325E+01 | 11.10 | 0.9149E+00 |
| 42 | 0.1618E+02 | 0.1443E+02 | 10.81 | 0.1749E+01 |
| 43 | 0.7540E+01 | 0.8577E+01 | -13.76 | -0.1037E+01 |
| 44 | 0.9680E+01 | 0.8852E+01 | 8.55 | 0.8279E+00 |
| 45 | 0.1262E+02 | 0.1372E+02 | -8.72 | -0.1101E+01 |
| 46 | 0.9600E+00 | 0.2616E+01 | -172.49 | -0.1656E+01 |
| 47 | 0.1017E+02 | 0.1163E+02 | -14.40 | -0.1465E+01 |
| 48 | 0.1363E+02 | 0.1256E+02 | 7.88 | 0.1074E+01 |

MODEL NUMBER: 4

| | |
|---|---|
| MULTIPLE CORRELATION (R) | 0.9309E+00 |
| STD ERR OF ESTIMATE (SE) | 0.1882E+01 |
| SUM OF SQUARED ERRORS | 0.1558E+03 |
| F TEST | 0.9531E+02 |
| SUM OF RESIDUALS | -0.1038E-11 |

| WAVE-LENGTH | MODEL COEFFICIENT | STANDARD ERROR COEFF | T-VALUE |
|---|---|---|---|
| 2347.0 | 0.1884E+03 | 0.2206E+02 | 0.8540E+01 |
| 1923.0 | -0.8600E+03 | 0.1706E+03 | 0.5040E+01 |
| 1951.0 | 0.7074E+03 | 0.1673E+03 | 0.4230E+01 |
| INTERCEPT | 0.1178E+02 | | |

ANALYSIS OF VARIANCE FOR THE REGRESSION

| VARIATION SOURCE | DF | SUM OF SQ | MEAN SQ | F VALUE |
|---|---|---|---|---|
| ATTRIB TO REGRESSION | 3 | 0.1013E+04 | 0.3375E+03 | 0.9531E+02 |
| DEV FROM REGRESSION | 44 | 0.1558E+03 | 0.3541E+01 | |
| TOTAL | 47 | 0.1168E+04 | | |

| EXP NUM | ACTUAL | MODEL OUTPUT | PERCENT DIFF | ACTUAL DIFF |
|---|---|---|---|---|
| 1 | 0.9680E+01 | 0.8724E+01 | 9.87 | 0.9556E+00 |
| 2 | 0.4130E+01 | 0.5217E+01 | -26.32 | -0.1087E+01 |
| 3 | 0.1361E+02 | 0.1219E+02 | 10.43 | 0.1420E+01 |
| 4 | 0.2070E+01 | 0.4319E+01 | -108.64 | -0.2249E+01 |
| 5 | 0.8120E+01 | 0.8643E+01 | -6.44 | -0.5229E+00 |
| 6 | 0.1639E+02 | 0.1217E+02 | 25.77 | 0.4223E+01 |
| 7 | 0.1069E+02 | 0.8786E+01 | 17.81 | 0.1904E+01 |
| 8 | 0.1371E+02 | 0.1307E+02 | 4.67 | 0.6402E+00 |
| 9 | 0.8210E+01 | 0.7590E+01 | 7.55 | 0.6201E+00 |
| 10 | 0.4600E+01 | 0.5698E+01 | -23.87 | -0.1098E+01 |
| 11 | 0.4790E+01 | 0.6728E+01 | -40.47 | -0.1938E+01 |
| 12 | 0.1457E+02 | 0.1381E+02 | 5.19 | 0.7563E+00 |
| 13 | 0.1510E+02 | 0.1304E+02 | 13.65 | 0.2061E+01 |
| 14 | 0.5720E+01 | 0.1899E+01 | 66.80 | 0.3821E+01 |
| 15 | 0.9560E+01 | 0.9609E+01 | -0.52 | -0.4940E-01 |
| 16 | 0.1000E+01 | 0.4895E+00 | 51.05 | 0.5105E+00 |
| 17 | 0.5360E+01 | 0.6986E+01 | -30.33 | -0.1626E+01 |
| 18 | 0.1642E+02 | 0.1472E+02 | 10.37 | 0.1703E+01 |
| 19 | 0.1591E+02 | 0.1514E+02 | 4.87 | 0.7743E+00 |
| 20 | 0.9300E+01 | 0.7646E+01 | 17.79 | 0.1654E+01 |
| 21 | 0.1280E+02 | 0.1063E+02 | 16.98 | 0.2174E+01 |
| 22 | 0.1412E+02 | 0.1465E+02 | -3.74 | -0.5286E+00 |
| 23 | 0.1774E+02 | 0.1495E+02 | 15.74 | 0.2793E+01 |
| 24 | 0.1618E+02 | 0.1927E+02 | -19.08 | -0.3087E+01 |
| 25 | 0.1459E+02 | 0.1355E+02 | 7.10 | 0.1036E+01 |
| 26 | 0.7160E+01 | 0.1003E+02 | -40.04 | -0.2867E+01 |
| 27 | 0.5860E+01 | 0.8844E+01 | -50.92 | -0.2984E+01 |
| 28 | 0.6480E+01 | 0.9275E+01 | -43.14 | -0.2795E+01 |
| 29 | 0.5510E+01 | 0.7964E+01 | -44.54 | -0.2454E+01 |
| 30 | 0.6490E+01 | 0.9139E+01 | -40.81 | -0.2649E+01 |
| 31 | 0.4310E+01 | 0.6162E+01 | -42.96 | -0.1852E+01 |
| 32 | 0.3160E+01 | 0.3810E+01 | -20.57 | -0.6501E+00 |
| 33 | 0.3230E+01 | 0.2454E+01 | 24.03 | 0.7760E+00 |
| 34 | 0.1880E+01 | 0.5351E+00 | 71.54 | 0.1345E+01 |
| 35 | 0.2030E+01 | 0.9405E+00 | 53.67 | 0.1090E+01 |
| 36 | 0.2220E+01 | 0.9753E+00 | 56.07 | 0.1245E+01 |
| 37 | 0.1378E+02 | 0.1496E+02 | -8.59 | -0.1184E+01 |
| 38 | 0.1348E+02 | 0.1511E+02 | -12.13 | -0.1635E+01 |
| 39 | 0.1364E+02 | 0.1425E+02 | -4.49 | -0.6126E+00 |
| 40 | 0.6540E+01 | 0.7083E+01 | -8.31 | -0.5432E+00 |
| 41 | 0.8240E+01 | 0.7103E+01 | 13.80 | 0.1137E+01 |
| 42 | 0.1618E+02 | 0.1483E+02 | 8.34 | 0.1350E+01 |
| 43 | 0.7540E+01 | 0.8699E+01 | -15.37 | -0.1159E+01 |
| 44 | 0.9680E+01 | 0.7846E+01 | 18.95 | 0.1834E+01 |
| 45 | 0.1262E+02 | 0.1269E+02 | -0.58 | -0.7308E-01 |
| 46 | 0.9600E+00 | 0.3304E+01 | -244.16 | -0.2344E+01 |
| 47 | 0.1017E+02 | 0.1112E+02 | -9.31 | -0.9464E+00 |
| 48 | 0.1363E+02 | 0.1252E+02 | 8.16 | 0.1112E+01 |

MODEL NUMBER: 5

| | |
|---|---|
| MULTIPLE CORRELATION (R) | 0.9384E+00 |
| STD ERR OF ESTIMATE (SE) | 0.1801E+01 |
| SUM OF SQUARED ERRORS | 0.1395E+03 |
| F TEST | 0.7927E+02 |
| SUM OF RESIDUALS | -0.1314E-11 |

| WAVE-LENGTH | MODEL COEFFICIENT | STANDARD ERROR COEFF | T-VALUE |
|---|---|---|---|
| 2311.0 | 0.1747E+03 | 0.2087E+02 | 0.8370E+01 |
| 1927.0 | -0.1740E+04 | 0.4008E+03 | 0.4342E+01 |
| 1951.0 | 0.2358E+04 | 0.7359E+03 | 0.3205E+01 |
| 1978.0 | -0.7652E+03 | 0.3534E+03 | 0.2165E+01 |
| INTERCEPT | 0.1140E+02 | | |

ANALYSIS OF VARIANCE FOR THE REGRESSION

| VARIATION SOURCE | DF | SUM OF SQ | MEAN SQ | F VALUE |
|---|---|---|---|---|
| ATTRIB TO REGRESSION | 4 | 0.1029E+04 | 0.2572E+03 | 0.7927E+02 |
| DEV FROM REGRESSION | 43 | 0.1395E+03 | 0.3245E+01 | |
| TOTAL | 47 | 0.1168E+04 | | |

| EXP NUM | ACTUAL | MODEL OUTPUT | PERCENT DIFF | ACTUAL DIFF |
|---|---|---|---|---|
| 1 | 0.9680E+01 | 0.8287E+01 | 14.39 | 0.1393E+01 |
| 2 | 0.4130E+01 | 0.4422E+01 | -7.07 | -0.2922E+00 |
| 3 | 0.1361E+02 | 0.1135E+02 | 16.61 | 0.2260E+01 |
| 4 | 0.2070E+01 | 0.3368E+01 | -62.73 | -0.1298E+01 |
| 5 | 0.8120E+01 | 0.7951E+01 | 2.08 | 0.1687E+00 |
| 6 | 0.1639E+02 | 0.1250E+02 | 23.74 | 0.3891E+01 |
| 7 | 0.1069E+02 | 0.8730E+01 | 18.33 | 0.1960E+01 |
| 8 | 0.1371E+02 | 0.1276E+02 | 6.95 | 0.9525E+00 |
| 9 | 0.8210E+01 | 0.7414E+01 | 9.70 | 0.7965E+00 |
| 10 | 0.4600E+01 | 0.6016E+01 | -30.79 | -0.1416E+01 |
| 11 | 0.4790E+01 | 0.6857E+01 | -43.15 | -0.2067E+01 |
| 12 | 0.1457E+02 | 0.1366E+02 | 6.25 | 0.9109E+00 |
| 13 | 0.1510E+02 | 0.1316E+02 | 12.88 | 0.1945E+01 |
| 14 | 0.5720E+01 | 0.2372E+01 | 58.53 | 0.3348E+01 |
| 15 | 0.9560E+01 | 0.9826E+01 | -2.79 | -0.2664E+00 |
| 16 | 0.1000E+01 | 0.9218E+00 | 7.82 | 0.7820E-01 |
| 17 | 0.5360E+01 | 0.7728E+01 | -44.18 | -0.2368E+01 |
| 18 | 0.1642E+02 | 0.1480E+02 | 9.88 | 0.1622E+01 |
| 19 | 0.1591E+02 | 0.1554E+02 | 2.33 | 0.3705E+00 |
| 20 | 0.9300E+01 | 0.8439E+01 | 9.26 | 0.8608E+00 |
| 21 | 0.1280E+02 | 0.1137E+02 | 11.16 | 0.1428E+01 |
| 22 | 0.1412E+02 | 0.1458E+02 | -3.29 | -0.4650E+00 |
| 23 | 0.1774E+02 | 0.1503E+02 | 15.27 | 0.2709E+01 |
| 24 | 0.1618E+02 | 0.1926E+02 | -19.07 | -0.3085E+01 |
| 25 | 0.1459E+02 | 0.1341E+02 | 8.09 | 0.1180E+01 |
| 26 | 0.7160E+01 | 0.9563E+01 | -33.56 | -0.2403E+01 |
| 27 | 0.5860E+01 | 0.7727E+01 | -31.87 | -0.1867E+01 |
| 28 | 0.6480E+01 | 0.8413E+01 | -29.82 | -0.1933E+01 |
| 29 | 0.5510E+01 | 0.7782E+01 | -41.24 | -0.2272E+01 |
| 30 | 0.6490E+01 | 0.9089E+01 | -40.04 | -0.2599E+01 |
| 31 | 0.4310E+01 | 0.6393E+01 | -48.33 | -0.2083E+01 |
| 32 | 0.3160E+01 | 0.3478E+01 | -10.06 | -0.3181E+00 |
| 33 | 0.3230E+01 | 0.1876E+01 | 41.92 | 0.1354E+01 |
| 34 | 0.1880E+01 | 0.7048E-01 | 96.25 | 0.1810E+01 |
| 35 | 0.2030E+01 | 0.7630E+00 | 62.41 | 0.1267E+01 |
| 36 | 0.2220E+01 | 0.1312E+01 | 40.91 | 0.9083E+00 |
| 37 | 0.1378E+02 | 0.1401E+02 | -1.68 | -0.2314E+00 |
| 38 | 0.1348E+02 | 0.1458E+02 | -8.17 | -0.1101E+01 |
| 39 | 0.1364E+02 | 0.1454E+02 | -6.59 | -0.8988E+00 |
| 40 | 0.6540E+01 | 0.6800E+01 | -3.98 | -0.2602E+00 |
| 41 | 0.8240E+01 | 0.7605E+01 | 7.70 | 0.6348E+00 |
| 42 | 0.1618E+02 | 0.1476E+02 | 8.81 | 0.1425E+01 |
| 43 | 0.7540E+01 | 0.9808E+01 | -30.08 | -0.2268E+01 |
| 44 | 0.9680E+01 | 0.9227E+01 | 4.68 | 0.4528E+00 |
| 45 | 0.1262E+02 | 0.1431E+02 | -13.38 | -0.1688E+01 |
| 46 | 0.9600E+00 | 0.3485E+01 | -263.03 | -0.2525E+01 |
| 47 | 0.1017E+02 | 0.1126E+02 | -10.68 | -0.1086E+01 |
| 48 | 0.1363E+02 | 0.1256E+02 | 7.83 | 0.1067E+01 |

MODEL NUMBER: 6

| | |
|---|---|
| MULTIPLE CORRELATION (R) | 0.9508E+00 |
| STD ERR OF ESTIMATE (SE) | 0.1615E+01 |
| SUM OF SQUARED ERRORS | 0.1122E+03 |
| F TEST | 0.1012E+03 |
| SUM OF RESIDUALS | -0.4170E-12 |

| WAVE-LENGTH | MODEL COEFFICIENT | STANDARD ERROR COEFF | T-VALUE |
|---|---|---|---|
| 2387.0 | 0.2517E+03 | 0.2204E+02 | 0.1142E+02 |
| 1923.0 | -0.5478E+03 | 0.6666E+02 | 0.8218E+01 |
| 2099.0 | 0.6358E+03 | 0.1002E+03 | 0.6347E+01 |
| 2223.0 | -0.3242E+03 | 0.7249E+02 | 0.4473E+01 |
| INTERCEPT | 0.1310E+02 | | |

ANALYSIS OF VARIANCE FOR THE REGRESSION

| VARIATION SOURCE | DF | SUM OF SQ | MEAN SQ | F VALUE |
|---|---|---|---|---|
| ATTRIB TO REGRESSION | 4 | 0.1056E+04 | 0.2640E+03 | 0.1012E+03 |
| DEV FROM REGRESSION | 43 | 0.1122E+03 | 0.2609E+01 | |
| TOTAL | 47 | 0.1168E+04 | | |

| EXP NUM | ACTUAL | MODEL OUTPUT | PERCENT DIFF | ACTUAL DIFF |
|---|---|---|---|---|
| 1 | 0.9680E+01 | 0.8532E+01 | 11.86 | 0.1148E+01 |
| 2 | 0.4130E+01 | 0.4689E+01 | -13.53 | -0.5588E+00 |
| 3 | 0.1361E+02 | 0.1183E+02 | 13.06 | 0.1778E+01 |
| 4 | 0.2070E+01 | 0.4322E+01 | -108.81 | -0.2252E+01 |
| 5 | 0.8120E+01 | 0.7957E+01 | 2.00 | 0.1627E+00 |
| 6 | 0.1639E+02 | 0.1371E+02 | 16.38 | 0.2685E+01 |
| 7 | 0.1069E+02 | 0.8479E+01 | 20.69 | 0.2211E+01 |
| 8 | 0.1371E+02 | 0.1244E+02 | 9.23 | 0.1265E+01 |
| 9 | 0.8210E+01 | 0.7344E+01 | 10.55 | 0.8658E+00 |
| 10 | 0.4600E+01 | 0.5228E+01 | -13.65 | -0.6279E+00 |
| 11 | 0.4790E+01 | 0.6002E+01 | -25.31 | -0.1212E+01 |
| 12 | 0.1457E+02 | 0.1398E+02 | 4.04 | 0.5883E+00 |
| 13 | 0.1510E+02 | 0.1354E+02 | 10.34 | 0.1562E+01 |
| 14 | 0.5720E+01 | 0.4891E+01 | 14.49 | 0.8286E+00 |
| 15 | 0.9560E+01 | 0.1196E+02 | -25.12 | -0.2402E+01 |
| 16 | 0.1000E+01 | 0.1302E+01 | -30.20 | -0.3020E+00 |
| 17 | 0.5360E+01 | 0.6093E+01 | -13.68 | -0.7334E+00 |
| 18 | 0.1642E+02 | 0.1473E+02 | 10.31 | 0.1693E+01 |
| 19 | 0.1591E+02 | 0.1448E+02 | 8.97 | 0.1427E+01 |
| 20 | 0.9300E+01 | 0.7195E+01 | 22.64 | 0.2105E+01 |
| 21 | 0.1280E+02 | 0.1051E+02 | 17.85 | 0.2285E+01 |
| 22 | 0.1412E+02 | 0.1579E+02 | -11.85 | -0.1673E+01 |
| 23 | 0.1774E+02 | 0.1582E+02 | 10.81 | 0.1918E+01 |
| 24 | 0.1618E+02 | 0.1857E+02 | -14.75 | -0.2386E+01 |
| 25 | 0.1459E+02 | 0.1380E+02 | 5.39 | 0.7863E+00 |
| 26 | 0.7160E+01 | 0.9455E+01 | -32.05 | -0.2295E+01 |
| 27 | 0.5860E+01 | 0.7827E+01 | -33.57 | -0.1967E+01 |
| 28 | 0.6480E+01 | 0.8810E+01 | -35.95 | -0.2330E+01 |
| 29 | 0.5510E+01 | 0.7195E+01 | -30.58 | -0.1685E+01 |
| 30 | 0.6490E+01 | 0.8008E+01 | -23.38 | -0.1518E+01 |
| 31 | 0.4310E+01 | 0.6259E+01 | -45.22 | -0.1949E+01 |
| 32 | 0.3160E+01 | 0.3418E+01 | -8.16 | -0.2580E+00 |
| 33 | 0.3230E+01 | 0.1709E+01 | 47.09 | 0.1521E+01 |
| 34 | 0.1880E+01 | 0.7081E+00 | 62.33 | 0.1172E+01 |
| 35 | 0.2030E+01 | 0.1285E+01 | 36.70 | 0.7451E+00 |
| 36 | 0.2220E+01 | 0.2531E+01 | -14.02 | -0.3112E+00 |
| 37 | 0.1378E+02 | 0.1518E+02 | -10.13 | -0.1396E+01 |
| 38 | 0.1348E+02 | 0.1432E+02 | -6.23 | -0.8397E+00 |
| 39 | 0.1364E+02 | 0.1518E+02 | -11.26 | -0.1536E+01 |
| 40 | 0.6540E+01 | 0.6956E+01 | -6.36 | -0.4161E+00 |
| 41 | 0.8240E+01 | 0.6359E+01 | 22.83 | 0.1881E+01 |
| 42 | 0.1618E+02 | 0.1496E+02 | 7.56 | 0.1223E+01 |
| 43 | 0.7540E+01 | 0.7413E+01 | 1.68 | 0.1270E+00 |
| 44 | 0.9680E+01 | 0.7477E+01 | 22.76 | 0.2203E+01 |
| 45 | 0.1262E+02 | 0.1417E+02 | -12.31 | -0.1554E+01 |
| 46 | 0.9600E+00 | 0.1565E+01 | -63.03 | -0.6051E+00 |
| 47 | 0.1017E+02 | 0.1187E+02 | -16.72 | -0.1700E+01 |
| 48 | 0.1363E+02 | 0.1330E+02 | 2.40 | 0.3267E+00 |

MODEL NUMBER: 7

| | |
|---|---|
| MULTIPLE CORRELATION (R) | 0.9515E+00 |
| STD ERR OF ESTIMATE (SE) | 0.1603E+01 |
| SUM OF SQUARED ERRORS | 0.1106E+03 |
| F TEST | 0.1029E+03 |
| SUM OF RESIDUALS | -0.1593E-11 |

| WAVE-LENGTH | MODEL COEFFICIENT | STANDARD ERROR COEFF | T-VALUE |
|---|---|---|---|
| 2399.0 | 0.2990E+03 | 0.2711E+02 | 0.1103E+02 |
| 1923.0 | -0.7588E+03 | 0.9470E+02 | 0.8013E+01 |
| 2129.0 | 0.9724E+03 | 0.1555E+03 | 0.6252E+01 |
| 2191.0 | -0.4920E+03 | 0.1115E+03 | 0.4413E+01 |
| INTERCEPT | 0.1369E+02 | | |

ANALYSIS OF VARIANCE FOR THE REGRESSION

| VARIATION SOURCE | DF | SUM OF SQ | MEAN SQ | F VALUE |
|---|---|---|---|---|
| ATTRIB TO REGRESSION | 4 | 0.1058E+04 | 0.2644E+03 | 0.1029E+03 |
| DEV FROM REGRESSION | 43 | 0.1106E+03 | 0.2571E+01 | |
| TOTAL | 47 | 0.1168E+04 | | |

| EXP NUM | ACTUAL | MODEL OUTPUT | PERCENT DIFF | ACTUAL DIFF |
|---|---|---|---|---|
| 1 | 0.9680E+01 | 0.9014E+01 | 6.89 | 0.6665E+00 |
| 2 | 0.4130E+01 | 0.5846E+01 | -41.55 | -0.1716E+01 |
| 3 | 0.1361E+02 | 0.1201E+02 | 11.73 | 0.1597E+01 |
| 4 | 0.2070E+01 | 0.4475E+01 | -116.16 | -0.2405E+01 |
| 5 | 0.8120E+01 | 0.8221E+01 | -1.24 | -0.1007E+00 |
| 6 | 0.1639E+02 | 0.1380E+02 | 15.78 | 0.2586E+01 |
| 7 | 0.1069E+02 | 0.8175E+01 | 23.53 | 0.2515E+01 |
| 8 | 0.1371E+02 | 0.1271E+02 | 7.31 | 0.1003E+01 |
| 9 | 0.8210E+01 | 0.7153E+01 | 12.87 | 0.1057E+01 |
| 10 | 0.4600E+01 | 0.5550E+01 | -20.64 | -0.9497E+00 |
| 11 | 0.4790E+01 | 0.6708E+01 | -40.04 | -0.1918E+01 |
| 12 | 0.1457E+02 | 0.1482E+02 | -1.68 | -0.2453E+00 |
| 13 | 0.1510E+02 | 0.1386E+02 | 8.21 | 0.1240E+01 |
| 14 | 0.5720E+01 | 0.5186E+01 | 9.33 | 0.5339E+00 |
| 15 | 0.9560E+01 | 0.1321E+02 | -38.16 | -0.3648E+01 |
| 16 | 0.1000E+01 | 0.3138E+01 | -213.80 | -0.2138E+01 |
| 17 | 0.5360E+01 | 0.6302E+01 | -17.57 | -0.9419E+00 |
| 18 | 0.1642E+02 | 0.1521E+02 | 7.39 | 0.1213E+01 |
| 19 | 0.1591E+02 | 0.1506E+02 | 5.33 | 0.8481E+00 |
| 20 | 0.9300E+01 | 0.8389E+01 | 9.80 | 0.9112E+00 |
| 21 | 0.1280E+02 | 0.1096E+02 | 14.34 | 0.1836E+01 |
| 22 | 0.1412E+02 | 0.1597E+02 | -13.11 | -0.1850E+01 |
| 23 | 0.1774E+02 | 0.1595E+02 | 10.07 | 0.1787E+01 |
| 24 | 0.1618E+02 | 0.1842E+02 | -13.82 | -0.2236E+01 |
| 25 | 0.1459E+02 | 0.1346E+02 | 7.73 | 0.1127E+01 |
| 26 | 0.7160E+01 | 0.8575E+01 | -19.76 | -0.1415E+01 |
| 27 | 0.5860E+01 | 0.7386E+01 | -26.04 | -0.1526E+01 |
| 28 | 0.6480E+01 | 0.8309E+01 | -28.23 | -0.1829E+01 |
| 29 | 0.5510E+01 | 0.6867E+01 | -24.62 | -0.1357E+01 |
| 30 | 0.6490E+01 | 0.7441E+01 | -14.65 | -0.9507E+00 |
| 31 | 0.4310E+01 | 0.5887E+01 | -36.60 | -0.1577E+01 |
| 32 | 0.3160E+01 | 0.3057E+01 | 3.27 | 0.1034E+00 |
| 33 | 0.3230E+01 | 0.1330E+01 | 58.82 | 0.1900E+01 |
| 34 | 0.1880E+01 | 0.5244E+00 | 72.11 | 0.1356E+01 |
| 35 | 0.2030E+01 | 0.7918E+00 | 60.99 | 0.1238E+01 |
| 36 | 0.2220E+01 | 0.1771E+01 | 20.23 | 0.4490E+00 |
| 37 | 0.1378E+02 | 0.1472E+02 | -6.85 | -0.9444E+00 |
| 38 | 0.1348E+02 | 0.1436E+02 | -6.49 | -0.8752E+00 |
| 39 | 0.1364E+02 | 0.1362E+02 | 0.18 | 0.2448E-01 |
| 40 | 0.6540E+01 | 0.6075E+01 | 7.11 | 0.4652E+00 |
| 41 | 0.8240E+01 | 0.5574E+01 | 32.36 | 0.2666E+01 |
| 42 | 0.1618E+02 | 0.1467E+02 | 9.32 | 0.1508E+01 |
| 43 | 0.7540E+01 | 0.7973E+01 | -5.75 | -0.4334E+00 |
| 44 | 0.9680E+01 | 0.7465E+01 | 22.88 | 0.2215E+01 |
| 45 | 0.1262E+02 | 0.1352E+02 | -7.13 | -0.8992E+00 |
| 46 | 0.9600E+00 | 0.1352E+01 | -40.82 | -0.3919E+00 |
| 47 | 0.1017E+02 | 0.1133E+02 | -11.37 | -0.1156E+01 |
| 48 | 0.1363E+02 | 0.1297E+02 | 4.84 | 0.6597E+00 |

MODEL NUMBER: 8

| | |
|---|---|
| MULTIPLE CORRELATION (R) | 0.9276E+00 |
| STD ERR OF ESTIMATE (SE) | 0.1904E+01 |
| SUM OF SQUARED ERRORS | 0.1631E+03 |
| F TEST | 0.1387E+03 |
| SUM OF RESIDUALS | 0.2811E-11 |

| WAVE-LENGTH | MODEL COEFFICIENT | STANDARD ERROR COEFF | T-VALUE |
|---|---|---|---|
| 1727.0 | 0.2886E+04 | 0.3609E+03 | 0.7999E+01 |
| 1705.0 | -0.2852E+04 | 0.3614E+03 | 0.7892E+01 |
| INTERCEPT | 0.1181E+02 | | |

ANALYSIS OF VARIANCE FOR THE REGRESSION

| VARIATION SOURCE | DF | SUM OF SQ | MEAN SQ | F VALUE |
|---|---|---|---|---|
| ATTRIB TO REGRESSION | 2 | 0.1005E+04 | 0.5026E+03 | 0.1387E+03 |
| DEV FROM REGRESSION | 45 | 0.1631E+03 | 0.3623E+01 | |
| TOTAL | 47 | 0.1168E+04 | | |

| EXP NUM | ACTUAL | MODEL OUTPUT | PERCENT DIFF | ACTUAL DIFF |
|---|---|---|---|---|
| 1 | 0.9680E+01 | 0.9203E+01 | 4.92 | 0.4765E+00 |
| 2 | 0.4130E+01 | 0.5678E+01 | -37.48 | -0.1548E+01 |
| 3 | 0.1361E+02 | 0.1338E+02 | 1.66 | 0.2265E+00 |
| 4 | 0.2070E+01 | 0.5659E+01 | -173.38 | -0.3589E+01 |
| 5 | 0.8120E+01 | 0.9417E+01 | -15.97 | -0.1297E+01 |
| 6 | 0.1639E+02 | 0.1368E+02 | 16.54 | 0.2710E+01 |
| 7 | 0.1069E+02 | 0.8711E+01 | 18.51 | 0.1979E+01 |
| 8 | 0.1371E+02 | 0.1408E+02 | -2.71 | -0.3713E+00 |
| 9 | 0.8210E+01 | 0.9172E+01 | -11.72 | -0.9619E+00 |
| 10 | 0.4600E+01 | 0.5987E+01 | -30.15 | -0.1387E+01 |
| 11 | 0.4790E+01 | 0.7001E+01 | -46.16 | -0.2211E+01 |
| 12 | 0.1457E+02 | 0.1533E+02 | -5.22 | -0.7611E+00 |
| 13 | 0.1510E+02 | 0.1493E+02 | 1.10 | 0.1661E+00 |
| 14 | 0.5720E+01 | 0.2705E+01 | 52.71 | 0.3015E+01 |
| 15 | 0.9560E+01 | 0.1039E+02 | -8.68 | -0.8296E+00 |
| 16 | 0.1000E+01 | 0.2448E+01 | -144.83 | -0.1448E+01 |
| 17 | 0.5360E+01 | 0.7338E+01 | -36.90 | -0.1978E+01 |
| 18 | 0.1642E+02 | 0.1433E+02 | 12.74 | 0.2093E+01 |
| 19 | 0.1591E+02 | 0.1452E+02 | 8.75 | 0.1392E+01 |
| 20 | 0.9300E+01 | 0.7136E+01 | 23.26 | 0.2164E+01 |
| 21 | 0.1280E+02 | 0.1003E+02 | 21.64 | 0.2770E+01 |
| 22 | 0.1412E+02 | 0.1402E+02 | 0.72 | 0.1016E+00 |
| 23 | 0.1774E+02 | 0.1428E+02 | 19.51 | 0.3462E+01 |
| 24 | 0.1618E+02 | 0.1858E+02 | -14.86 | -0.2404E+01 |
| 25 | 0.1459E+02 | 0.1302E+02 | 10.75 | 0.1568E+01 |
| 26 | 0.7160E+01 | 0.8974E+01 | -25.34 | -0.1814E+01 |
| 27 | 0.5860E+01 | 0.8544E+01 | -45.80 | -0.2684E+01 |
| 28 | 0.6480E+01 | 0.8112E+01 | -25.19 | -0.1632E+01 |
| 29 | 0.5510E+01 | 0.6788E+01 | -23.20 | -0.1278E+01 |
| 30 | 0.6490E+01 | 0.7702E+01 | -18.68 | -0.1212E+01 |
| 31 | 0.4310E+01 | 0.4108E+01 | 4.68 | 0.2017E+00 |
| 32 | 0.3160E+01 | 0.3124E+01 | 1.15 | 0.3618E-01 |
| 33 | 0.3230E+01 | 0.1666E+01 | 48.41 | 0.1564E+01 |
| 34 | 0.1880E+01 | 0.5941E+00 | 68.40 | 0.1286E+01 |
| 35 | 0.2030E+01 | 0.6351E+00 | 68.71 | 0.1395E+01 |
| 36 | 0.2220E+01 | 0.1692E+01 | 23.77 | 0.5277E+00 |
| 37 | 0.1378E+02 | 0.1652E+02 | -19.91 | -0.2744E+01 |
| 38 | 0.1348E+02 | 0.1593E+02 | -18.21 | -0.2455E+01 |
| 39 | 0.1364E+02 | 0.1376E+02 | -0.87 | -0.1198E+00 |
| 40 | 0.6540E+01 | 0.7265E+01 | -11.09 | -0.7254E+00 |
| 41 | 0.8240E+01 | 0.7155E+01 | 13.17 | 0.1085E+01 |
| 42 | 0.1618E+02 | 0.1342E+02 | 17.03 | 0.2755E+01 |
| 43 | 0.7540E+01 | 0.8401E+01 | -11.42 | -0.8611E+00 |
| 44 | 0.9680E+01 | 0.7529E+01 | 22.23 | 0.2151E+01 |
| 45 | 0.1262E+02 | 0.1177E+02 | 6.71 | 0.8474E+00 |
| 46 | 0.9600E+00 | 0.3218E+01 | -235.18 | -0.2258E+01 |
| 47 | 0.1017E+02 | 0.1125E+02 | -10.64 | -0.1082E+01 |
| 48 | 0.1363E+02 | 0.9952E+01 | 26.99 | 0.3678E+01 |

MODEL NUMBER: 9

| | |
|---|---|
| MULTIPLE CORRELATION (R) | 0.9410E+00 |
| STD ERR OF ESTIMATE (SE) | 0.1764E+01 |
| SUM OF SQUARED ERRORS | 0.1338E+03 |
| F TEST | 0.8311E+02 |
| SUM OF RESIDUALS | -0.1603E-12 |

| WAVE-LENGTH | MODEL COEFFICIENT | STANDARD ERROR COEFF | T-VALUE |
|---|---|---|---|
| 2300.0 | 0.2228E+03 | 0.2372E+02 | 0.9394E+01 |
| 1927.0 | -0.1195E+04 | 0.1956E+03 | 0.6111E+01 |
| 1951.0 | 0.1190E+04 | 0.2433E+03 | 0.4891E+01 |
| 2191.0 | -0.1959E+03 | 0.8874E+02 | 0.2207E+01 |
| INTERCEPT | 0.1082E+02 | | |

ANALYSIS OF VARIANCE FOR THE REGRESSION

| VARIATION SOURCE | DF | SUM OF SQ | MEAN SQ | F VALUE |
|---|---|---|---|---|
| ATTRIB TO REGRESSION | 4 | 0.1035E+04 | 0.2586E+03 | 0.8311E+02 |
| DEV FROM REGRESSION | 43 | 0.1338E+03 | 0.3112E+01 | |
| TOTAL | 47 | 0.1168E+04 | | |

| EXP NUM | ACTUAL | MODEL OUTPUT | PERCENT DIFF | ACTUAL DIFF |
|---|---|---|---|---|
| 1 | 0.9680E+01 | 0.7855E+01 | 18.86 | 0.1825E+01 |
| 2 | 0.4130E+01 | 0.3939E+01 | 4.62 | 0.1909E+00 |
| 3 | 0.1361E+02 | 0.1176E+02 | 13.61 | 0.1852E+01 |
| 4 | 0.2070E+01 | 0.3721E+01 | -79.77 | -0.1651E+01 |
| 5 | 0.8120E+01 | 0.7640E+01 | 5.91 | 0.4800E+00 |
| 6 | 0.1639E+02 | 0.1256E+02 | 23.35 | 0.3828E+01 |
| 7 | 0.1069E+02 | 0.9232E+01 | 13.64 | 0.1458E+01 |
| 8 | 0.1371E+02 | 0.1294E+02 | 5.61 | 0.7695E+00 |
| 9 | 0.8210E+01 | 0.7699E+01 | 6.22 | 0.5109E+00 |
| 10 | 0.4600E+01 | 0.5644E+01 | -22.69 | -0.1044E+01 |
| 11 | 0.4790E+01 | 0.6133E+01 | -28.04 | -0.1343E+01 |
| 12 | 0.1457E+02 | 0.1397E+02 | 4.10 | 0.5975E+00 |
| 13 | 0.1510E+02 | 0.1388E+02 | 8.06 | 0.1217E+01 |
| 14 | 0.5720E+01 | 0.3533E+01 | 38.23 | 0.2187E+01 |
| 15 | 0.9560E+01 | 0.1003E+02 | -4.92 | -0.4700E+00 |
| 16 | 0.1000E+01 | 0.4214E+00 | 57.86 | 0.5786E+00 |
| 17 | 0.5360E+01 | 0.7470E+01 | -39.36 | -0.2110E+01 |
| 18 | 0.1642E+02 | 0.1435E+02 | 12.61 | 0.2071E+01 |
| 19 | 0.1591E+02 | 0.1460E+02 | 8.25 | 0.1313E+01 |
| 20 | 0.9300E+01 | 0.7555E+01 | 18.77 | 0.1745E+01 |
| 21 | 0.1280E+02 | 0.1051E+02 | 17.90 | 0.2291E+01 |
| 22 | 0.1412E+02 | 0.1512E+02 | -7.10 | -0.1002E+01 |
| 23 | 0.1774E+02 | 0.1511E+02 | 14.84 | 0.2633E+01 |
| 24 | 0.1618E+02 | 0.1939E+02 | -19.85 | -0.3212E+01 |
| 25 | 0.1459E+02 | 0.1364E+02 | 6.49 | 0.9464E+00 |
| 26 | 0.7160E+01 | 0.9977E+01 | -39.34 | -0.2817E+01 |
| 27 | 0.5860E+01 | 0.8168E+01 | -39.39 | -0.2308E+01 |
| 28 | 0.6480E+01 | 0.9154E+01 | -41.27 | -0.2674E+01 |
| 29 | 0.5510E+01 | 0.7664E+01 | -39.10 | -0.2154E+01 |
| 30 | 0.6490E+01 | 0.9102E+01 | -40.25 | -0.2612E+01 |
| 31 | 0.4310E+01 | 0.5841E+01 | -35.52 | -0.1531E+01 |
| 32 | 0.3160E+01 | 0.3818E+01 | -20.81 | -0.6577E+00 |
| 33 | 0.3230E+01 | 0.1857E+01 | 42.51 | 0.1373E+01 |
| 34 | 0.1880E+01 | 0.5151E+00 | 72.60 | 0.1365E+01 |
| 35 | 0.2030E+01 | 0.1085E+01 | 46.54 | 0.9448E+00 |
| 36 | 0.2220E+01 | 0.1800E+01 | 18.94 | 0.4205E+00 |
| 37 | 0.1378E+02 | 0.1436E+02 | -4.19 | -0.5771E+00 |
| 38 | 0.1348E+02 | 0.1436E+02 | -6.55 | -0.8827E+00 |
| 39 | 0.1364E+02 | 0.1450E+02 | -6.32 | -0.8626E+00 |
| 40 | 0.6540E+01 | 0.6459E+01 | 1.24 | 0.8126E-01 |
| 41 | 0.8240E+01 | 0.7106E+01 | 13.76 | 0.1134E+01 |
| 42 | 0.1618E+02 | 0.1457E+02 | 9.98 | 0.1614E+01 |
| 43 | 0.7540E+01 | 0.8865E+01 | -17.58 | -0.1325E+01 |
| 44 | 0.9680E+01 | 0.9106E+01 | 5.93 | 0.5741E+00 |
| 45 | 0.1262E+02 | 0.1451E+02 | -14.95 | -0.1887E+01 |
| 46 | 0.9600E+00 | 0.2869E+01 | -198.82 | -0.1909E+01 |
| 47 | 0.1017E+02 | 0.1197E+02 | -17.70 | -0.1800E+01 |
| 48 | 0.1363E+02 | 0.1280E+02 | 6.10 | 0.8311E+00 |

MODEL NUMBER: 10

| | |
|---|---|
| MULTIPLE CORRELATION (R) | 0.9294E+00 |
| STD ERR OF ESTIMATE (SE) | 0.1881E+01 |
| SUM OF SQUARED ERRORS | 0.1592E+03 |
| F TEST | 0.1426E+03 |
| SUM OF RESIDUALS | -0.6208E-12 |

| WAVE-LENGTH | MODEL COEFFICIENT | STANDARD ERROR COEFF | T-VALUE |
|---|---|---|---|
| 1712.0 | 0.1505E+04 | 0.1811E+03 | 0.8314E+01 |
| 1691.0 | -0.1479E+04 | 0.1825E+03 | 0.8102E+01 |
| INTERCEPT | 0.1098E+02 | | |

ANALYSIS OF VARIANCE FOR THE REGRESSION

| VARIATION SOURCE | DF | SUM OF SQ | MEAN SQ | F VALUE |
|---|---|---|---|---|
| ATTRIB TO REGRESSION | 2 | 0.1009E+04 | 0.5045E+03 | 0.1426E+03 |
| DEV FROM REGRESSION | 45 | 0.1592E+03 | 0.3538E+01 | |
| TOTAL | 47 | 0.1168E+04 | | |

| EXP NUM | ACTUAL | MODEL OUTPUT | PERCENT DIFF | ACTUAL DIFF |
|---|---|---|---|---|
| 1 | 0.9680E+01 | 0.1018E+02 | -5.20 | -0.5033E+00 |
| 2 | 0.4130E+01 | 0.6212E+01 | -50.41 | -0.2082E+01 |
| 3 | 0.1361E+02 | 0.1366E+02 | -0.35 | -0.4709E-01 |
| 4 | 0.2070E+01 | 0.6324E+01 | -205.49 | -0.4254E+01 |
| 5 | 0.8120E+01 | 0.8951E+01 | -10.24 | -0.8314E+00 |
| 6 | 0.1639E+02 | 0.1204E+02 | 26.55 | 0.4352E+01 |
| 7 | 0.1069E+02 | 0.9806E+01 | 8.27 | 0.8837E+00 |
| 8 | 0.1371E+02 | 0.1435E+02 | -4.70 | -0.6447E+00 |
| 9 | 0.8210E+01 | 0.7966E+01 | 2.97 | 0.2439E+00 |
| 10 | 0.4600E+01 | 0.5065E+01 | -10.10 | -0.4645E+00 |
| 11 | 0.4790E+01 | 0.5690E+01 | -18.80 | -0.9004E+00 |
| 12 | 0.1457E+02 | 0.1403E+02 | 3.68 | 0.5364E+00 |
| 13 | 0.1510E+02 | 0.1457E+02 | 3.53 | 0.5333E+00 |
| 14 | 0.5720E+01 | 0.2231E+01 | 60.99 | 0.3489E+01 |
| 15 | 0.9560E+01 | 0.9043E+01 | 5.41 | 0.5173E+00 |
| 16 | 0.1000E+01 | 0.1795E+01 | -79.46 | -0.7946E+00 |
| 17 | 0.5360E+01 | 0.6891E+01 | -28.55 | -0.1531E+01 |
| 18 | 0.1642E+02 | 0.1510E+02 | 8.02 | 0.1317E+01 |
| 19 | 0.1591E+02 | 0.1412E+02 | 11.27 | 0.1794E+01 |
| 20 | 0.9300E+01 | 0.7742E+01 | 16.76 | 0.1558E+01 |
| 21 | 0.1280E+02 | 0.1086E+02 | 15.13 | 0.1936E+01 |
| 22 | 0.1412E+02 | 0.1438E+02 | -1.84 | -0.2598E+00 |
| 23 | 0.1774E+02 | 0.1383E+02 | 22.06 | 0.3914E+01 |
| 24 | 0.1618E+02 | 0.1895E+02 | -17.15 | -0.2775E+01 |
| 25 | 0.1459E+02 | 0.1214E+02 | 16.82 | 0.2454E+01 |
| 26 | 0.7160E+01 | 0.9206E+01 | -28.57 | -0.2046E+01 |
| 27 | 0.5860E+01 | 0.8448E+01 | -44.16 | -0.2588E+01 |
| 28 | 0.6480E+01 | 0.9228E+01 | -42.41 | -0.2748E+01 |
| 29 | 0.5510E+01 | 0.6803E+01 | -23.47 | -0.1293E+01 |
| 30 | 0.6490E+01 | 0.8219E+01 | -26.65 | -0.1729E+01 |
| 31 | 0.4310E+01 | 0.4073E+01 | 5.49 | 0.2366E+00 |
| 32 | 0.3160E+01 | 0.3083E+01 | 2.43 | 0.7678E-01 |
| 33 | 0.3230E+01 | 0.1619E+01 | 49.88 | 0.1611E+01 |
| 34 | 0.1880E+01 | 0.4634E+00 | 75.35 | 0.1417E+01 |
| 35 | 0.2030E+01 | 0.3812E+00 | 81.22 | 0.1649E+01 |
| 36 | 0.2220E+01 | 0.1933E+01 | 12.92 | 0.2867E+00 |
| 37 | 0.1378E+02 | 0.1579E+02 | -14.58 | -0.2010E+01 |
| 38 | 0.1348E+02 | 0.1403E+02 | -4.11 | -0.5544E+00 |
| 39 | 0.1364E+02 | 0.1412E+02 | -3.50 | -0.4773E+00 |
| 40 | 0.6540E+01 | 0.7524E+01 | -15.05 | -0.9844E+00 |
| 41 | 0.8240E+01 | 0.6921E+01 | 16.01 | 0.1319E+01 |
| 42 | 0.1618E+02 | 0.1530E+02 | 5.44 | 0.8805E+00 |
| 43 | 0.7540E+01 | 0.8027E+01 | -6.46 | -0.4871E+00 |
| 44 | 0.9680E+01 | 0.7879E+01 | 18.61 | 0.1801E+01 |
| 45 | 0.1262E+02 | 0.1286E+02 | -1.92 | -0.2427E+00 |
| 46 | 0.9600E+00 | 0.3931E+01 | -309.50 | -0.2971E+01 |
| 47 | 0.1017E+02 | 0.1188E+02 | -16.79 | -0.1708E+01 |
| 48 | 0.1363E+02 | 0.1151E+02 | 15.55 | 0.2120E+01 |

TRAINING SET MODELS

First Derivative of Log 1/R Diffuse Reflectance Spectra

INITIAL WAVELENGTHS FOR COMPOSITE MODELS
AND ASSOCIATED LOCAL MINIMUM SUM OF
SQUARED ERROR (SSE) VALUES:

| MODEL NUMBER | WAVELENGTH | SSE |
|---|---|---|
| 1 | 1673.0 | 0.3586E+03 |
| 2 | 2060.0 | 0.4061E+03 |
| 3 | 1685.0 | 0.4083E+03 |
| 4 | 1739.0 | 0.4602E+03 |
| 5 | 2387.0 | 0.4780E+03 |
| 6 | 1868.0 | 0.4905E+03 |
| 7 | 1633.0 | 0.4956E+03 |
| 8 | 1835.0 | 0.5213E+03 |
| 9 | 2091.0 | 0.5352E+03 |
| 10 | 2044.0 | 0.5428E+03 |

BEST MODEL FOUND WAS MODEL NUMBER: 4

MODEL NUMBER: 1

| | |
|---|---|
| MULTIPLE CORRELATION (R) | 0.9593E+00 |
| STD ERR OF ESTIMATE (SE) | 0.1472E+01 |
| SUM OF SQUARED ERRORS | 0.9320E+02 |
| F TEST | 0.1240E+03 |
| SUM OF RESIDUALS | 0.8882E-15 |

| WAVE-LENGTH | MODEL COEFFICIENT | STANDARD ERROR COEFF | T-VALUE |
|---|---|---|---|
| 2233.0 | 0.1593E+05 | 0.1225E+04 | 0.1301E+02 |
| 1870.0 | -0.3739E+05 | 0.4935E+04 | 0.7577E+01 |
| 2150.0 | 0.1478E+05 | 0.3325E+04 | 0.4444E+01 |
| 2108.0 | -0.2174E+05 | 0.5615E+04 | 0.3871E+01 |
| INTERCEPT | 0.1243E+02 | | |

ANALYSIS OF VARIANCE FOR THE REGRESSION

| VARIATION SOURCE | DF | SUM OF SQ | MEAN SQ | F VALUE |
|---|---|---|---|---|
| ATTRIB TO REGRESSION | 4 | 0.1075E+04 | 0.2688E+03 | 0.1240E+03 |
| DEV FROM REGRESSION | 43 | 0.9320E+02 | 0.2167E+01 | |
| TOTAL | 47 | 0.1168E+04 | | |

| EXP NUM | ACTUAL | MODEL OUTPUT | PERCENT DIFF | ACTUAL DIFF |
|---|---|---|---|---|
| 1 | 0.9680E+01 | 0.8540E+01 | 11.78 | 0.1140E+01 |
| 2 | 0.4130E+01 | 0.4927E+01 | -19.29 | -0.7965E+00 |
| 3 | 0.1361E+02 | 0.1284E+02 | 5.66 | 0.7699E+00 |
| 4 | 0.2070E+01 | 0.5960E+01 | -187.90 | -0.3890E+01 |
| 5 | 0.8120E+01 | 0.8055E+01 | 0.80 | 0.6534E-01 |
| 6 | 0.1639E+02 | 0.1360E+02 | 17.03 | 0.2790E+01 |
| 7 | 0.1069E+02 | 0.1087E+02 | -1.66 | -0.1777E+00 |
| 8 | 0.1371E+02 | 0.1339E+02 | 2.30 | 0.3156E+00 |
| 9 | 0.8210E+01 | 0.7304E+01 | 11.03 | 0.9058E+00 |
| 10 | 0.4600E+01 | 0.4810E+01 | -4.56 | -0.2099E+00 |
| 11 | 0.4790E+01 | 0.5721E+01 | -19.43 | -0.9309E+00 |
| 12 | 0.1457E+02 | 0.1574E+02 | -8.03 | -0.1170E+01 |
| 13 | 0.1510E+02 | 0.1469E+02 | 2.69 | 0.4060E+00 |
| 14 | 0.5720E+01 | 0.6714E+01 | -17.38 | -0.9941E+00 |
| 15 | 0.9560E+01 | 0.1105E+02 | -15.61 | -0.1493E+01 |
| 16 | 0.1000E+01 | 0.1256E-01 | 98.74 | 0.9874E+00 |
| 17 | 0.5360E+01 | 0.6487E+01 | -21.02 | -0.1127E+01 |
| 18 | 0.1642E+02 | 0.1462E+02 | 10.99 | 0.1804E+01 |
| 19 | 0.1591E+02 | 0.1515E+02 | 4.77 | 0.7591E+00 |
| 20 | 0.9300E+01 | 0.6458E+01 | 30.55 | 0.2842E+01 |
| 21 | 0.1280E+02 | 0.9815E+01 | 23.32 | 0.2985E+01 |
| 22 | 0.1412E+02 | 0.1535E+02 | -8.74 | -0.1233E+01 |
| 23 | 0.1774E+02 | 0.1634E+02 | 7.92 | 0.1404E+01 |
| 24 | 0.1618E+02 | 0.1901E+02 | -17.48 | -0.2828E+01 |
| 25 | 0.1459E+02 | 0.1272E+02 | 12.81 | 0.1869E+01 |
| 26 | 0.7160E+01 | 0.8655E+01 | -20.87 | -0.1495E+01 |
| 27 | 0.5860E+01 | 0.5932E+01 | -1.23 | -0.7211E-01 |
| 28 | 0.6480E+01 | 0.6985E+01 | -7.80 | -0.5053E+00 |
| 29 | 0.5510E+01 | 0.5574E+01 | -1.16 | -0.6415E-01 |
| 30 | 0.6490E+01 | 0.7543E+01 | -16.22 | -0.1053E+01 |
| 31 | 0.4310E+01 | 0.4942E+01 | -14.65 | -0.6315E+00 |
| 32 | 0.3160E+01 | 0.3893E+01 | -23.20 | -0.7331E+00 |
| 33 | 0.3230E+01 | 0.1707E+01 | 47.16 | 0.1523E+01 |
| 34 | 0.1880E+01 | 0.1572E+01 | 16.41 | 0.3085E+00 |
| 35 | 0.2030E+01 | 0.1587E+01 | 21.81 | 0.4427E+00 |
| 36 | 0.2220E+01 | 0.1931E+01 | 13.03 | 0.2893E+00 |
| 37 | 0.1378E+02 | 0.1400E+02 | -1.63 | -0.2241E+00 |
| 38 | 0.1348E+02 | 0.1378E+02 | -2.21 | -0.2977E+00 |
| 39 | 0.1364E+02 | 0.1472E+02 | -7.88 | -0.1075E+01 |
| 40 | 0.6540E+01 | 0.6482E+01 | 0.89 | 0.5819E-01 |
| 41 | 0.8240E+01 | 0.7110E+01 | 13.71 | 0.1130E+01 |
| 42 | 0.1618E+02 | 0.1382E+02 | 14.59 | 0.2361E+01 |
| 43 | 0.7540E+01 | 0.7118E+01 | 5.59 | 0.4217E+00 |
| 44 | 0.9680E+01 | 0.9333E+01 | 3.58 | 0.3468E+00 |
| 45 | 0.1262E+02 | 0.1381E+02 | -9.40 | -0.1186E+01 |
| 46 | 0.9600E+00 | 0.2474E+01 | -157.69 | -0.1514E+01 |
| 47 | 0.1017E+02 | 0.1207E+02 | -18.66 | -0.1898E+01 |
| 48 | 0.1363E+02 | 0.1396E+02 | -2.40 | -0.3276E+00 |

MODEL NUMBER: 2

| | |
|---|---|
| MULTIPLE CORRELATION (R) | 0.9418E+00 |
| STD ERR OF ESTIMATE (SE) | 0.1733E+01 |
| SUM OF SQUARED ERRORS | 0.1321E+03 |
| F TEST | 0.1150E+03 |
| SUM OF RESIDUALS | -0.8171E-13 |

| WAVE-LENGTH | MODEL COEFFICIENT | STANDARD ERROR COEFF | T-VALUE |
|---|---|---|---|
| 1672.0 | 0.4641E+05 | 0.5199E+04 | 0.8927E+01 |
| 2108.0 | -0.4620E+05 | 0.5281E+04 | 0.8749E+01 |
| 2325.0 | -0.1433E+05 | 0.5195E+04 | 0.2758E+01 |
| INTERCEPT | 0.1134E+02 | | |

ANALYSIS OF VARIANCE FOR THE REGRESSION

| VARIATION SOURCE | DF | SUM OF SQ | MEAN SQ | F VALUE |
|---|---|---|---|---|
| ATTRIB TO REGRESSION | 3 | 0.1036E+04 | 0.3454E+03 | 0.1150E+03 |
| DEV FROM REGRESSION | 44 | 0.1321E+03 | 0.3003E+01 | |
| TOTAL | 47 | 0.1168E+04 | | |

| EXP NUM | ACTUAL | MODEL OUTPUT | PERCENT DIFF | ACTUAL DIFF |
|---|---|---|---|---|
| 1 | 0.9680E+01 | 0.7738E+01 | 20.06 | 0.1942E+01 |
| 2 | 0.4130E+01 | 0.4134E+01 | -0.09 | -0.3675E-02 |
| 3 | 0.1361E+02 | 0.1382E+02 | -1.52 | -0.2066E+00 |
| 4 | 0.2070E+01 | 0.4202E+01 | -103.02 | -0.2132E+01 |
| 5 | 0.8120E+01 | 0.8739E+01 | -7.62 | -0.6190E+00 |
| 6 | 0.1639E+02 | 0.1321E+02 | 19.42 | 0.3182E+01 |
| 7 | 0.1069E+02 | 0.9032E+01 | 15.51 | 0.1658E+01 |
| 8 | 0.1371E+02 | 0.1506E+02 | -9.88 | -0.1355E+01 |
| 9 | 0.8210E+01 | 0.8392E+01 | -2.22 | -0.1824E+00 |
| 10 | 0.4600E+01 | 0.4844E+01 | -5.31 | -0.2441E+00 |
| 11 | 0.4790E+01 | 0.7367E+01 | -53.80 | -0.2577E+01 |
| 12 | 0.1457E+02 | 0.1558E+02 | -6.91 | -0.1007E+01 |
| 13 | 0.1510E+02 | 0.1425E+02 | 5.63 | 0.8503E+00 |
| 14 | 0.5720E+01 | 0.4710E+01 | 17.66 | 0.1010E+01 |
| 15 | 0.9560E+01 | 0.1032E+02 | -7.96 | -0.7614E+00 |
| 16 | 0.1000E+01 | 0.1038E+01 | -3.84 | -0.3836E-01 |
| 17 | 0.5360E+01 | 0.6884E+01 | -28.44 | -0.1524E+01 |
| 18 | 0.1642E+02 | 0.1395E+02 | 15.06 | 0.2473E+01 |
| 19 | 0.1591E+02 | 0.1429E+02 | 10.17 | 0.1618E+01 |
| 20 | 0.9300E+01 | 0.6402E+01 | 31.16 | 0.2898E+01 |
| 21 | 0.1280E+02 | 0.9486E+01 | 25.89 | 0.3314E+01 |
| 22 | 0.1412E+02 | 0.1493E+02 | -5.71 | -0.8065E+00 |
| 23 | 0.1774E+02 | 0.1561E+02 | 12.03 | 0.2133E+01 |
| 24 | 0.1618E+02 | 0.1941E+02 | -19.96 | -0.3230E+01 |
| 25 | 0.1459E+02 | 0.1235E+02 | 15.36 | 0.2241E+01 |
| 26 | 0.7160E+01 | 0.9666E+01 | -34.99 | -0.2506E+01 |
| 27 | 0.5860E+01 | 0.7145E+01 | -21.93 | -0.1285E+01 |
| 28 | 0.6480E+01 | 0.7691E+01 | -18.69 | -0.1211E+01 |
| 29 | 0.5510E+01 | 0.6140E+01 | -11.44 | -0.6301E+00 |
| 30 | 0.6490E+01 | 0.8643E+01 | -33.18 | -0.2153E+01 |
| 31 | 0.4310E+01 | 0.5777E+01 | -34.03 | -0.1467E+01 |
| 32 | 0.3160E+01 | 0.4035E+01 | -27.68 | -0.8746E+00 |
| 33 | 0.3230E+01 | 0.2526E+01 | 21.80 | 0.7041E+00 |
| 34 | 0.1880E+01 | 0.1394E+01 | 25.85 | 0.4859E+00 |
| 35 | 0.2030E+01 | 0.9077E+00 | 55.28 | 0.1122E+01 |
| 36 | 0.2220E+01 | 0.2277E+01 | -2.57 | -0.5710E-01 |
| 37 | 0.1378E+02 | 0.1437E+02 | -4.26 | -0.5877E+00 |
| 38 | 0.1348E+02 | 0.1459E+02 | -8.20 | -0.1106E+01 |
| 39 | 0.1364E+02 | 0.1504E+02 | -10.27 | -0.1401E+01 |
| 40 | 0.6540E+01 | 0.5636E+01 | 13.82 | 0.9037E+00 |
| 41 | 0.8240E+01 | 0.6555E+01 | 20.45 | 0.1685E+01 |
| 42 | 0.1618E+02 | 0.1470E+02 | 9.17 | 0.1483E+01 |
| 43 | 0.7540E+01 | 0.6813E+01 | 9.64 | 0.7272E+00 |
| 44 | 0.9680E+01 | 0.7657E+01 | 20.90 | 0.2023E+01 |
| 45 | 0.1262E+02 | 0.1346E+02 | -6.69 | -0.8448E+00 |
| 46 | 0.9600E+00 | 0.4262E+01 | -343.91 | -0.3302E+01 |
| 47 | 0.1017E+02 | 0.1145E+02 | -12.63 | -0.1284E+01 |
| 48 | 0.1363E+02 | 0.1269E+02 | 6.91 | 0.9421E+00 |

MODEL NUMBER: 3

| | |
|---|---|
| MULTIPLE CORRELATION (R) | 0.9487E+00 |
| STD ERR OF ESTIMATE (SE) | 0.1647E+01 |
| SUM OF SQUARED ERRORS | 0.1167E+03 |
| F TEST | 0.9688E+02 |
| SUM OF RESIDUALS | -0.2665E-13 |

| WAVE-LENGTH | MODEL COEFFICIENT | STANDARD ERROR COEFF | T-VALUE |
|---|---|---|---|
| 1735.0 | -0.3196E+05 | 0.3036E+04 | 0.1053E+02 |
| 1618.0 | 0.7453E+05 | 0.1372E+05 | 0.5431E+01 |
| 1929.0 | 0.1912E+05 | 0.5273E+04 | 0.3626E+01 |
| 1572.0 | -0.3289E+05 | 0.1203E+05 | 0.2734E+01 |
| INTERCEPT | 0.1302E+02 | | |

ANALYSIS OF VARIANCE FOR THE REGRESSION

| VARIATION SOURCE | DF | SUM OF SQ | MEAN SQ | F VALUE |
|---|---|---|---|---|
| ATTRIB TO REGRESSION | 4 | 0.1052E+04 | 0.2629E+03 | 0.9688E+02 |
| DEV FROM REGRESSION | 43 | 0.1167E+03 | 0.2714E+01 | |
| TOTAL | 47 | 0.1168E+04 | | |

| EXP NUM | ACTUAL | MODEL OUTPUT | PERCENT DIFF | ACTUAL DIFF |
|---|---|---|---|---|
| 1 | 0.9680E+01 | 0.8826E+01 | 8.83 | 0.8545E+00 |
| 2 | 0.4130E+01 | 0.4619E+01 | -11.84 | -0.4889E+00 |
| 3 | 0.1361E+02 | 0.1330E+02 | 2.31 | 0.3143E+00 |
| 4 | 0.2070E+01 | 0.6121E+01 | -195.72 | -0.4051E+01 |
| 5 | 0.8120E+01 | 0.8518E+01 | -4.90 | -0.3982E+00 |
| 6 | 0.1639E+02 | 0.1566E+02 | 4.44 | 0.7282E+00 |
| 7 | 0.1069E+02 | 0.1069E+02 | 0.02 | 0.2027E-02 |
| 8 | 0.1371E+02 | 0.1316E+02 | 4.04 | 0.5544E+00 |
| 9 | 0.8210E+01 | 0.9372E+01 | -14.15 | -0.1162E+01 |
| 10 | 0.4600E+01 | 0.4788E+01 | -4.08 | -0.1878E+00 |
| 11 | 0.4790E+01 | 0.6357E+01 | -32.71 | -0.1567E+01 |
| 12 | 0.1457E+02 | 0.1494E+02 | -2.53 | -0.3686E+00 |
| 13 | 0.1510E+02 | 0.1519E+02 | -0.59 | -0.8874E-01 |
| 14 | 0.5720E+01 | 0.3939E+01 | 31.14 | 0.1781E+01 |
| 15 | 0.9560E+01 | 0.1018E+02 | -6.45 | -0.6168E+00 |
| 16 | 0.1000E+01 | 0.3050E+01 | -205.01 | -0.2050E+01 |
| 17 | 0.5360E+01 | 0.6691E+01 | -24.84 | -0.1331E+01 |
| 18 | 0.1642E+02 | 0.1617E+02 | 1.55 | 0.2540E+00 |
| 19 | 0.1591E+02 | 0.1626E+02 | -2.21 | -0.3520E+00 |
| 20 | 0.9300E+01 | 0.7134E+01 | 23.29 | 0.2166E+01 |
| 21 | 0.1280E+02 | 0.9698E+01 | 24.24 | 0.3102E+01 |
| 22 | 0.1412E+02 | 0.1405E+02 | 0.46 | 0.6516E-01 |
| 23 | 0.1774E+02 | 0.1580E+02 | 10.95 | 0.1943E+01 |
| 24 | 0.1618E+02 | 0.1818E+02 | -12.35 | -0.1998E+01 |
| 25 | 0.1459E+02 | 0.1283E+02 | 12.08 | 0.1763E+01 |
| 26 | 0.7160E+01 | 0.9787E+01 | -36.69 | -0.2627E+01 |
| 27 | 0.5860E+01 | 0.8391E+01 | -43.19 | -0.2531E+01 |
| 28 | 0.6480E+01 | 0.8015E+01 | -23.69 | -0.1535E+01 |
| 29 | 0.5510E+01 | 0.6432E+01 | -16.73 | -0.9220E+00 |
| 30 | 0.6490E+01 | 0.7051E+01 | -8.64 | -0.5610E+00 |
| 31 | 0.4310E+01 | 0.4655E+01 | -8.00 | -0.3447E+00 |
| 32 | 0.3160E+01 | 0.4275E+01 | -35.27 | -0.1115E+01 |
| 33 | 0.3230E+01 | 0.1416E+01 | 56.16 | 0.1814E+01 |
| 34 | 0.1880E+01 | 0.6418E+00 | 65.86 | 0.1238E+01 |
| 35 | 0.2030E+01 | 0.4485E+00 | 77.91 | 0.1582E+01 |
| 36 | 0.2220E+01 | 0.2230E+01 | -0.46 | -0.1032E-01 |
| 37 | 0.1378E+02 | 0.1547E+02 | -12.29 | -0.1693E+01 |
| 38 | 0.1348E+02 | 0.1440E+02 | -6.85 | -0.9236E+00 |
| 39 | 0.1364E+02 | 0.1312E+02 | 3.81 | 0.5190E+00 |
| 40 | 0.6540E+01 | 0.6354E+01 | 2.85 | 0.1862E+00 |
| 41 | 0.8240E+01 | 0.6352E+01 | 22.91 | 0.1888E+01 |
| 42 | 0.1618E+02 | 0.1218E+02 | 24.74 | 0.4003E+01 |
| 43 | 0.7540E+01 | 0.6273E+01 | 16.81 | 0.1267E+01 |
| 44 | 0.9680E+01 | 0.8635E+01 | 10.80 | 0.1045E+01 |
| 45 | 0.1262E+02 | 0.1245E+02 | 1.37 | 0.1732E+00 |
| 46 | 0.9600E+00 | 0.1810E+01 | -88.56 | -0.8502E+00 |
| 47 | 0.1017E+02 | 0.1172E+02 | -15.25 | -0.1551E+01 |
| 48 | 0.1363E+02 | 0.1155E+02 | 15.26 | 0.2080E+01 |

MODEL NUMBER: 4

| | |
|---|---|
| MULTIPLE CORRELATION (R) | 0.9673E+00 |
| STD ERR OF ESTIMATE (SE) | 0.1323E+01 |
| SUM OF SQUARED ERRORS | 0.7526E+02 |
| F TEST | 0.1561E+03 |
| SUM OF RESIDUALS | -0.4574E-13 |

| WAVE-LENGTH | MODEL COEFFICIENT | STANDARD ERROR COEFF | T-VALUE |
|---|---|---|---|
| 1984.0 | 0.7302E+05 | 0.4605E+04 | 0.1586E+02 |
| 2234.0 | 0.1258E+05 | 0.1176E+04 | 0.1070E+02 |
| 1799.0 | -0.4685E+05 | 0.4949E+04 | 0.9466E+01 |
| 2020.0 | -0.3554E+05 | 0.5840E+04 | 0.6085E+01 |
| INTERCEPT | 0.1397E+02 | | |

ANALYSIS OF VARIANCE FOR THE REGRESSION

| VARIATION SOURCE | DF | SUM OF SQ | MEAN SQ | F VALUE |
|---|---|---|---|---|
| ATTRIB TO REGRESSION | 4 | 0.1093E+04 | 0.2733E+03 | 0.1561E+03 |
| DEV FROM REGRESSION | 43 | 0.7526E+02 | 0.1750E+01 | |
| TOTAL | 47 | 0.1168E+04 | | |

| EXP NUM | ACTUAL | MODEL OUTPUT | PERCENT DIFF | ACTUAL DIFF |
|---|---|---|---|---|
| 1 | 0.9680E+01 | 0.1004E+02 | -3.76 | -0.3642E+00 |
| 2 | 0.4130E+01 | 0.6232E+01 | -50.90 | -0.2102E+01 |
| 3 | 0.1361E+02 | 0.1136E+02 | 16.52 | 0.2248E+01 |
| 4 | 0.2070E+01 | 0.4641E+01 | -124.18 | -0.2571E+01 |
| 5 | 0.8120E+01 | 0.8326E+01 | -2.54 | -0.2061E+00 |
| 6 | 0.1639E+02 | 0.1583E+02 | 3.40 | 0.5577E+00 |
| 7 | 0.1069E+02 | 0.9181E+01 | 14.11 | 0.1509E+01 |
| 8 | 0.1371E+02 | 0.1409E+02 | -2.75 | -0.3770E+00 |
| 9 | 0.8210E+01 | 0.7618E+01 | 7.22 | 0.5925E+00 |
| 10 | 0.4600E+01 | 0.5177E+01 | -12.54 | -0.5766E+00 |
| 11 | 0.4790E+01 | 0.4893E+01 | -2.14 | -0.1027E+00 |
| 12 | 0.1457E+02 | 0.1201E+02 | 17.59 | 0.2563E+01 |
| 13 | 0.1510E+02 | 0.1378E+02 | 8.77 | 0.1324E+01 |
| 14 | 0.5720E+01 | 0.5980E+01 | -4.54 | -0.2595E+00 |
| 15 | 0.9560E+01 | 0.9396E+01 | 1.72 | 0.1641E+00 |
| 16 | 0.1000E+01 | 0.5173E+00 | 48.27 | 0.4827E+00 |
| 17 | 0.5360E+01 | 0.6231E+01 | -16.25 | -0.8709E+00 |
| 18 | 0.1642E+02 | 0.1445E+02 | 11.98 | 0.1967E+01 |
| 19 | 0.1591E+02 | 0.1603E+02 | -0.74 | -0.1183E+00 |
| 20 | 0.9300E+01 | 0.8359E+01 | 10.12 | 0.9409E+00 |
| 21 | 0.1280E+02 | 0.1235E+02 | 3.55 | 0.4548E+00 |
| 22 | 0.1412E+02 | 0.1676E+02 | -18.66 | -0.2635E+01 |
| 23 | 0.1774E+02 | 0.1613E+02 | 9.09 | 0.1613E+01 |
| 24 | 0.1618E+02 | 0.1660E+02 | -2.57 | -0.4158E+00 |
| 25 | 0.1459E+02 | 0.1414E+02 | 3.07 | 0.4477E+00 |
| 26 | 0.7160E+01 | 0.7599E+01 | -6.13 | -0.4389E+00 |
| 27 | 0.5860E+01 | 0.6034E+01 | -2.98 | -0.1745E+00 |
| 28 | 0.6480E+01 | 0.6409E+01 | 1.09 | 0.7070E-01 |
| 29 | 0.5510E+01 | 0.5208E+01 | 5.49 | 0.3023E+00 |
| 30 | 0.6490E+01 | 0.7202E+01 | -10.97 | -0.7121E+00 |
| 31 | 0.4310E+01 | 0.3059E+01 | 29.03 | 0.1251E+01 |
| 32 | 0.3160E+01 | 0.5384E+01 | -70.38 | -0.2224E+01 |
| 33 | 0.3230E+01 | 0.2119E+01 | 34.38 | 0.1111E+01 |
| 34 | 0.1880E+01 | 0.1702E+01 | 9.48 | 0.1781E+00 |
| 35 | 0.2030E+01 | 0.2025E+01 | 0.23 | 0.4662E-02 |
| 36 | 0.2220E+01 | 0.3434E+01 | -54.67 | -0.1214E+01 |
| 37 | 0.1378E+02 | 0.1627E+02 | -18.06 | -0.2489E+01 |
| 38 | 0.1348E+02 | 0.1584E+02 | -17.48 | -0.2356E+01 |
| 39 | 0.1364E+02 | 0.1441E+02 | -5.66 | -0.7722E+00 |
| 40 | 0.6540E+01 | 0.7045E+01 | -7.72 | -0.5049E+00 |
| 41 | 0.8240E+01 | 0.7669E+01 | 6.92 | 0.5706E+00 |
| 42 | 0.1618E+02 | 0.1380E+02 | 14.68 | 0.2375E+01 |
| 43 | 0.7540E+01 | 0.6962E+01 | 7.67 | 0.5785E+00 |
| 44 | 0.9680E+01 | 0.9041E+01 | 6.60 | 0.6392E+00 |
| 45 | 0.1262E+02 | 0.1269E+02 | -0.54 | -0.6765E-01 |
| 46 | 0.9600E+00 | 0.6265E-01 | 93.47 | 0.8974E+00 |
| 47 | 0.1017E+02 | 0.1117E+02 | -9.85 | -0.1002E+01 |
| 48 | 0.1363E+02 | 0.1392E+02 | -2.11 | -0.2880E+00 |

MODEL NUMBER: 5

| | |
|---|---|
| MULTIPLE CORRELATION (R) | 0.9613E+00 |
| STD ERR OF ESTIMATE (SE) | 0.1436E+01 |
| SUM OF SQUARED ERRORS | 0.8865E+02 |
| F TEST | 0.1309E+03 |
| SUM OF RESIDUALS | 0.2931E-13 |

| WAVE-LENGTH | MODEL COEFFICIENT | STANDARD ERROR COEFF | T-VALUE |
|---|---|---|---|
| 2168.0 | -0.2294E+05 | 0.2243E+04 | 0.1022E+02 |
| 1986.0 | 0.4876E+05 | 0.5527E+04 | 0.8823E+01 |
| 1796.0 | -0.4352E+05 | 0.7946E+04 | 0.5477E+01 |
| 1711.0 | 0.2989E+05 | 0.8753E+04 | 0.3415E+01 |
| INTERCEPT | 0.1221E+02 | | |

ANALYSIS OF VARIANCE FOR THE REGRESSION

| VARIATION SOURCE | DF | SUM OF SQ | MEAN SQ | F VALUE |
|---|---|---|---|---|
| ATTRIB TO REGRESSION | 4 | 0.1080E+04 | 0.2699E+03 | 0.1309E+03 |
| DEV FROM REGRESSION | 43 | 0.8865E+02 | 0.2062E+01 | |
| TOTAL | 47 | 0.1168E+04 | | |

| EXP NUM | ACTUAL | MODEL OUTPUT | PERCENT DIFF | ACTUAL DIFF |
|---|---|---|---|---|
| 1 | 0.9680E+01 | 0.9304E+01 | 3.88 | 0.3760E+00 |
| 2 | 0.4130E+01 | 0.6533E+01 | -58.18 | -0.2403E+01 |
| 3 | 0.1361E+02 | 0.1119E+02 | 17.75 | 0.2415E+01 |
| 4 | 0.2070E+01 | 0.3454E+01 | -66.87 | -0.1384E+01 |
| 5 | 0.8120E+01 | 0.8733E+01 | -7.55 | -0.6133E+00 |
| 6 | 0.1639E+02 | 0.1494E+02 | 8.83 | 0.1447E+01 |
| 7 | 0.1069E+02 | 0.8602E+01 | 19.53 | 0.2088E+01 |
| 8 | 0.1371E+02 | 0.1388E+02 | -1.25 | -0.1716E+00 |
| 9 | 0.8210E+01 | 0.7044E+01 | 14.21 | 0.1166E+01 |
| 10 | 0.4600E+01 | 0.4054E+01 | 11.87 | 0.5461E+00 |
| 11 | 0.4790E+01 | 0.5263E+01 | -9.87 | -0.4729E+00 |
| 12 | 0.1457E+02 | 0.1362E+02 | 6.55 | 0.9540E+00 |
| 13 | 0.1510E+02 | 0.1546E+02 | -2.42 | -0.3649E+00 |
| 14 | 0.5720E+01 | 0.5721E+01 | -0.02 | -0.1197E-02 |
| 15 | 0.9560E+01 | 0.1143E+02 | -19.61 | -0.1874E+01 |
| 16 | 0.1000E+01 | 0.1756E+01 | -75.60 | -0.7560E+00 |
| 17 | 0.5360E+01 | 0.5009E+01 | 6.55 | 0.3512E+00 |
| 18 | 0.1642E+02 | 0.1578E+02 | 3.91 | 0.6421E+00 |
| 19 | 0.1591E+02 | 0.1473E+02 | 7.39 | 0.1176E+01 |
| 20 | 0.9300E+01 | 0.6953E+01 | 25.23 | 0.2347E+01 |
| 21 | 0.1280E+02 | 0.1127E+02 | 11.94 | 0.1529E+01 |
| 22 | 0.1412E+02 | 0.1492E+02 | -5.66 | -0.7987E+00 |
| 23 | 0.1774E+02 | 0.1644E+02 | 7.30 | 0.1295E+01 |
| 24 | 0.1618E+02 | 0.1745E+02 | -7.87 | -0.1274E+01 |
| 25 | 0.1459E+02 | 0.1321E+02 | 9.45 | 0.1379E+01 |
| 26 | 0.7160E+01 | 0.8067E+01 | -12.67 | -0.9069E+00 |
| 27 | 0.5860E+01 | 0.6721E+01 | -14.69 | -0.8609E+00 |
| 28 | 0.6480E+01 | 0.7475E+01 | -15.35 | -0.9946E+00 |
| 29 | 0.5510E+01 | 0.5637E+01 | -2.31 | -0.1271E+00 |
| 30 | 0.6490E+01 | 0.7831E+01 | -20.66 | -0.1341E+01 |
| 31 | 0.4310E+01 | 0.4730E+01 | -9.74 | -0.4200E+00 |
| 32 | 0.3160E+01 | 0.5766E+01 | -82.48 | -0.2606E+01 |
| 33 | 0.3230E+01 | 0.2815E+01 | 12.86 | 0.4153E+00 |
| 34 | 0.1880E+01 | 0.2346E+01 | -24.79 | -0.4661E+00 |
| 35 | 0.2030E+01 | 0.2493E+01 | -22.81 | -0.4631E+00 |
| 36 | 0.2220E+01 | 0.3582E+01 | -61.33 | -0.1362E+01 |
| 37 | 0.1378E+02 | 0.1552E+02 | -12.61 | -0.1738E+01 |
| 38 | 0.1348E+02 | 0.1665E+02 | -23.51 | -0.3170E+01 |
| 39 | 0.1364E+02 | 0.1334E+02 | 2.21 | 0.3014E+00 |
| 40 | 0.6540E+01 | 0.6200E+01 | 5.21 | 0.3405E+00 |
| 41 | 0.8240E+01 | 0.6268E+01 | 23.93 | 0.1972E+01 |
| 42 | 0.1618E+02 | 0.1514E+02 | 6.43 | 0.1041E+01 |
| 43 | 0.7540E+01 | 0.5600E+01 | 25.73 | 0.1940E+01 |
| 44 | 0.9680E+01 | 0.7735E+01 | 20.09 | 0.1945E+01 |
| 45 | 0.1262E+02 | 0.1349E+02 | -6.88 | -0.8689E+00 |
| 46 | 0.9600E+00 | -0.2060E+00 | 121.45 | 0.1166E+01 |
| 47 | 0.1017E+02 | 0.1206E+02 | -18.57 | -0.1888E+01 |
| 48 | 0.1363E+02 | 0.1314E+02 | 3.61 | 0.4926E+00 |

MODEL NUMBER: 6

| | |
|---|---|
| MULTIPLE CORRELATION (R) | 0.9637E+00 |
| STD ERR OF ESTIMATE (SE) | 0.1391E+01 |
| SUM OF SQUARED ERRORS | 0.8322E+02 |
| F TEST | 0.1402E+03 |
| SUM OF RESIDUALS | 0.2442E-13 |

| WAVE-LENGTH | MODEL COEFFICIENT | STANDARD ERROR COEFF | T-VALUE |
|---|---|---|---|
| 2234.0 | 0.1174E+05 | 0.1264E+04 | 0.9286E+01 |
| 1792.0 | -0.3093E+05 | 0.5329E+04 | 0.5805E+01 |
| 1983.0 | 0.3885E+05 | 0.6923E+04 | 0.5611E+01 |
| 1868.0 | -0.1796E+05 | 0.6614E+04 | 0.2715E+01 |
| INTERCEPT | 0.1242E+02 | | |

ANALYSIS OF VARIANCE FOR THE REGRESSION

| VARIATION SOURCE | DF | SUM OF SQ | MEAN SQ | F VALUE |
|---|---|---|---|---|
| ATTRIB TO REGRESSION | 4 | 0.1085E+04 | 0.2713E+03 | 0.1402E+03 |
| DEV FROM REGRESSION | 43 | 0.8322E+02 | 0.1935E+01 | |
| TOTAL | 47 | 0.1168E+04 | | |

| EXP NUM | ACTUAL | MODEL OUTPUT | PERCENT DIFF | ACTUAL DIFF |
|---|---|---|---|---|
| 1 | 0.9680E+01 | 0.8401E+01 | 13.21 | 0.1279E+01 |
| 2 | 0.4130E+01 | 0.5366E+01 | -29.93 | -0.1236E+01 |
| 3 | 0.1361E+02 | 0.1084E+02 | 20.33 | 0.2767E+01 |
| 4 | 0.2070E+01 | 0.3861E+01 | -86.50 | -0.1791E+01 |
| 5 | 0.8120E+01 | 0.7063E+01 | 13.01 | 0.1057E+01 |
| 6 | 0.1639E+02 | 0.1431E+02 | 12.67 | 0.2077E+01 |
| 7 | 0.1069E+02 | 0.9378E+01 | 12.27 | 0.1312E+01 |
| 8 | 0.1371E+02 | 0.1284E+02 | 6.32 | 0.8667E+00 |
| 9 | 0.8210E+01 | 0.8196E+01 | 0.17 | 0.1418E-01 |
| 10 | 0.4600E+01 | 0.5466E+01 | -18.83 | -0.8660E+00 |
| 11 | 0.4790E+01 | 0.5376E+01 | -12.23 | -0.5858E+00 |
| 12 | 0.1457E+02 | 0.1475E+02 | -1.23 | -0.1796E+00 |
| 13 | 0.1510E+02 | 0.1586E+02 | -5.02 | -0.7580E+00 |
| 14 | 0.5720E+01 | 0.7410E+01 | -29.55 | -0.1690E+01 |
| 15 | 0.9560E+01 | 0.1107E+02 | -15.82 | -0.1513E+01 |
| 16 | 0.1000E+01 | 0.1419E+01 | -41.89 | -0.4189E+00 |
| 17 | 0.5360E+01 | 0.4989E+01 | 6.93 | 0.3714E+00 |
| 18 | 0.1642E+02 | 0.1521E+02 | 7.38 | 0.1212E+01 |
| 19 | 0.1591E+02 | 0.1574E+02 | 1.09 | 0.1736E+00 |
| 20 | 0.9300E+01 | 0.6466E+01 | 30.48 | 0.2834E+01 |
| 21 | 0.1280E+02 | 0.1104E+02 | 13.76 | 0.1761E+01 |
| 22 | 0.1412E+02 | 0.1528E+02 | -8.23 | -0.1161E+01 |
| 23 | 0.1774E+02 | 0.1630E+02 | 8.13 | 0.1442E+01 |
| 24 | 0.1618E+02 | 0.1886E+02 | -16.58 | -0.2683E+01 |
| 25 | 0.1459E+02 | 0.1355E+02 | 7.11 | 0.1038E+01 |
| 26 | 0.7160E+01 | 0.8269E+01 | -15.50 | -0.1109E+01 |
| 27 | 0.5860E+01 | 0.7594E+01 | -29.58 | -0.1734E+01 |
| 28 | 0.6480E+01 | 0.6388E+01 | 1.42 | 0.9216E-01 |
| 29 | 0.5510E+01 | 0.5273E+01 | 4.30 | 0.2370E+00 |
| 30 | 0.6490E+01 | 0.7565E+01 | -16.56 | -0.1075E+01 |
| 31 | 0.4310E+01 | 0.4168E+01 | 3.30 | 0.1421E+00 |
| 32 | 0.3160E+01 | 0.5140E+01 | -62.67 | -0.1980E+01 |
| 33 | 0.3230E+01 | 0.2775E+01 | 14.07 | 0.4545E+00 |
| 34 | 0.1880E+01 | 0.1757E+01 | 6.52 | 0.1226E+00 |
| 35 | 0.2030E+01 | 0.2134E+01 | -5.11 | -0.1036E+00 |
| 36 | 0.2220E+01 | 0.2433E+01 | -9.58 | -0.2127E+00 |
| 37 | 0.1378E+02 | 0.1521E+02 | -10.36 | -0.1428E+01 |
| 38 | 0.1348E+02 | 0.1468E+02 | -8.92 | -0.1203E+01 |
| 39 | 0.1364E+02 | 0.1297E+02 | 4.92 | 0.6715E+00 |
| 40 | 0.6540E+01 | 0.6092E+01 | 6.85 | 0.4481E+00 |
| 41 | 0.8240E+01 | 0.6192E+01 | 24.85 | 0.2048E+01 |
| 42 | 0.1618E+02 | 0.1427E+02 | 11.78 | 0.1905E+01 |
| 43 | 0.7540E+01 | 0.7338E+01 | 2.68 | 0.2021E+00 |
| 44 | 0.9680E+01 | 0.8434E+01 | 12.87 | 0.1246E+01 |
| 45 | 0.1262E+02 | 0.1451E+02 | -14.99 | -0.1892E+01 |
| 46 | 0.9600E+00 | 0.1115E+01 | -16.16 | -0.1552E+00 |
| 47 | 0.1017E+02 | 0.1187E+02 | -16.68 | -0.1696E+01 |
| 48 | 0.1363E+02 | 0.1393E+02 | -2.21 | -0.3010E+00 |

MODEL NUMBER: 7

| | |
|---|---|
| MULTIPLE CORRELATION (R) | 0.9446E+00 |
| STD ERR OF ESTIMATE (SE) | 0.1711E+01 |
| SUM OF SQUARED ERRORS | 0.1259E+03 |
| F TEST | 0.8902E+02 |
| SUM OF RESIDUALS | -0.7105E-13 |

| WAVE-LENGTH | MODEL COEFFICIENT | STANDARD ERROR COEFF | T-VALUE |
|---|---|---|---|
| 1735.0 | -0.3368E+05 | 0.3250E+04 | 0.1036E+02 |
| 1931.0 | 0.2876E+05 | 0.7950E+04 | 0.3618E+01 |
| 1633.0 | 0.3739E+05 | 0.1097E+05 | 0.3408E+01 |
| 2095.0 | 0.1743E+05 | 0.7461E+04 | 0.2335E+01 |
| INTERCEPT | 0.1302E+02 | | |

ANALYSIS OF VARIANCE FOR THE REGRESSION

| VARIATION SOURCE | DF | SUM OF SQ | MEAN SQ | F VALUE |
|---|---|---|---|---|
| ATTRIB TO REGRESSION | 4 | 0.1042E+04 | 0.2606E+03 | 0.8902E+02 |
| DEV FROM REGRESSION | 43 | 0.1259E+03 | 0.2928E+01 | |
| TOTAL | 47 | 0.1168E+04 | | |

| EXP NUM | ACTUAL | MODEL OUTPUT | PERCENT DIFF | ACTUAL DIFF |
|---|---|---|---|---|
| 1 | 0.9680E+01 | 0.8141E+01 | 15.90 | 0.1539E+01 |
| 2 | 0.4130E+01 | 0.5456E+01 | -32.10 | -0.1326E+01 |
| 3 | 0.1361E+02 | 0.1276E+02 | 6.21 | 0.8458E+00 |
| 4 | 0.2070E+01 | 0.5164E+01 | -149.45 | -0.3094E+01 |
| 5 | 0.8120E+01 | 0.8015E+01 | 1.29 | 0.1048E+00 |
| 6 | 0.1639E+02 | 0.1395E+02 | 14.89 | 0.2440E+01 |
| 7 | 0.1069E+02 | 0.9186E+01 | 14.07 | 0.1504E+01 |
| 8 | 0.1371E+02 | 0.1337E+02 | 2.45 | 0.3362E+00 |
| 9 | 0.8210E+01 | 0.7296E+01 | 11.13 | 0.9136E+00 |
| 10 | 0.4600E+01 | 0.4722E+01 | -2.66 | -0.1222E+00 |
| 11 | 0.4790E+01 | 0.6994E+01 | -46.02 | -0.2204E+01 |
| 12 | 0.1457E+02 | 0.1399E+02 | 3.97 | 0.5786E+00 |
| 13 | 0.1510E+02 | 0.1391E+02 | 7.86 | 0.1186E+01 |
| 14 | 0.5720E+01 | 0.3116E+01 | 45.53 | 0.2604E+01 |
| 15 | 0.9560E+01 | 0.1060E+02 | -10.92 | -0.1044E+01 |
| 16 | 0.1000E+01 | 0.3170E+01 | -216.99 | -0.2170E+01 |
| 17 | 0.5360E+01 | 0.6235E+01 | -16.32 | -0.8749E+00 |
| 18 | 0.1642E+02 | 0.1617E+02 | 1.54 | 0.2533E+00 |
| 19 | 0.1591E+02 | 0.1576E+02 | 0.97 | 0.1537E+00 |
| 20 | 0.9300E+01 | 0.8008E+01 | 13.90 | 0.1292E+01 |
| 21 | 0.1280E+02 | 0.9682E+01 | 24.36 | 0.3118E+01 |
| 22 | 0.1412E+02 | 0.1520E+02 | -7.66 | -0.1081E+01 |
| 23 | 0.1774E+02 | 0.1528E+02 | 13.86 | 0.2458E+01 |
| 24 | 0.1618E+02 | 0.1874E+02 | -15.81 | -0.2559E+01 |
| 25 | 0.1459E+02 | 0.1306E+02 | 10.49 | 0.1530E+01 |
| 26 | 0.7160E+01 | 0.1021E+02 | -42.61 | -0.3051E+01 |
| 27 | 0.5860E+01 | 0.7533E+01 | -28.55 | -0.1673E+01 |
| 28 | 0.6480E+01 | 0.8508E+01 | -31.30 | -0.2028E+01 |
| 29 | 0.5510E+01 | 0.6319E+01 | -14.68 | -0.8090E+00 |
| 30 | 0.6490E+01 | 0.7732E+01 | -19.14 | -0.1242E+01 |
| 31 | 0.4310E+01 | 0.5299E+01 | -22.94 | -0.9886E+00 |
| 32 | 0.3160E+01 | 0.3802E+01 | -20.33 | -0.6423E+00 |
| 33 | 0.3230E+01 | 0.1646E+01 | 49.04 | 0.1584E+01 |
| 34 | 0.1880E+01 | 0.2585E+00 | 86.25 | 0.1621E+01 |
| 35 | 0.2030E+01 | 0.2654E+00 | 86.93 | 0.1765E+01 |
| 36 | 0.2220E+01 | 0.1810E+01 | 18.45 | 0.4095E+00 |
| 37 | 0.1378E+02 | 0.1411E+02 | -2.37 | -0.3273E+00 |
| 38 | 0.1348E+02 | 0.1577E+02 | -17.01 | -0.2293E+01 |
| 39 | 0.1364E+02 | 0.1381E+02 | -1.24 | -0.1695E+00 |
| 40 | 0.6540E+01 | 0.6714E+01 | -2.67 | -0.1744E+00 |
| 41 | 0.8240E+01 | 0.7086E+01 | 14.01 | 0.1154E+01 |
| 42 | 0.1618E+02 | 0.1391E+02 | 14.04 | 0.2272E+01 |
| 43 | 0.7540E+01 | 0.7560E+01 | -0.26 | -0.1991E-01 |
| 44 | 0.9680E+01 | 0.8627E+01 | 10.87 | 0.1053E+01 |
| 45 | 0.1262E+02 | 0.1262E+02 | 0.03 | 0.3160E-02 |
| 46 | 0.9600E+00 | 0.2864E+01 | -198.32 | -0.1904E+01 |
| 47 | 0.1017E+02 | 0.1281E+02 | -25.91 | -0.2635E+01 |
| 48 | 0.1363E+02 | 0.1192E+02 | 12.55 | 0.1711E+01 |

MODEL NUMBER: 8

| | |
|---|---|
| MULTIPLE CORRELATION (R) | 0.9614E+00 |
| STD ERR OF ESTIMATE (SE) | 0.1433E+01 |
| SUM OF SQUARED ERRORS | 0.8836E+02 |
| F TEST | 0.1314E+03 |
| SUM OF RESIDUALS | 0.3109E-14 |

| WAVE-LENGTH | MODEL COEFFICIENT | STANDARD ERROR COEFF | T-VALUE |
|---|---|---|---|
| 1793.0 | -0.4199E+05 | 0.3937E+04 | 0.1066E+02 |
| 1986.0 | 0.3835E+05 | 0.5712E+04 | 0.6714E+01 |
| 1931.0 | 0.1857E+05 | 0.4752E+04 | 0.3907E+01 |
| 2235.0 | 0.8037E+04 | 0.2184E+04 | 0.3679E+01 |
| INTERCEPT | 0.1327E+02 | | |

ANALYSIS OF VARIANCE FOR THE REGRESSION

| VARIATION SOURCE | DF | SUM OF SQ | MEAN SQ | F VALUE |
|---|---|---|---|---|
| ATTRIB TO REGRESSION | 4 | 0.1080E+04 | 0.2700E+03 | 0.1314E+03 |
| DEV FROM REGRESSION | 43 | 0.8836E+02 | 0.2055E+01 | |
| TOTAL | 47 | 0.1168E+04 | | |

| EXP NUM | ACTUAL | MODEL OUTPUT | PERCENT DIFF | ACTUAL DIFF |
|---|---|---|---|---|
| 1 | 0.9680E+01 | 0.8850E+01 | 8.58 | 0.8305E+00 |
| 2 | 0.4130E+01 | 0.6748E+01 | -63.39 | -0.2618E+01 |
| 3 | 0.1361E+02 | 0.1238E+02 | 9.03 | 0.1229E+01 |
| 4 | 0.2070E+01 | 0.4802E+01 | -131.98 | -0.2732E+01 |
| 5 | 0.8120E+01 | 0.8407E+01 | -3.54 | -0.2871E+00 |
| 6 | 0.1639E+02 | 0.1559E+02 | 4.90 | 0.8032E+00 |
| 7 | 0.1069E+02 | 0.1080E+02 | -1.00 | -0.1066E+00 |
| 8 | 0.1371E+02 | 0.1435E+02 | -4.65 | -0.6370E+00 |
| 9 | 0.8210E+01 | 0.8171E+01 | 0.47 | 0.3855E-01 |
| 10 | 0.4600E+01 | 0.5418E+01 | -17.78 | -0.8179E+00 |
| 11 | 0.4790E+01 | 0.6566E+01 | -37.08 | -0.1776E+01 |
| 12 | 0.1457E+02 | 0.1480E+02 | -1.61 | -0.2341E+00 |
| 13 | 0.1510E+02 | 0.1436E+02 | 4.92 | 0.7426E+00 |
| 14 | 0.5720E+01 | 0.5677E+01 | 0.76 | 0.4322E-01 |
| 15 | 0.9560E+01 | 0.1083E+02 | -13.31 | -0.1272E+01 |
| 16 | 0.1000E+01 | 0.1126E+01 | -12.62 | -0.1262E+00 |
| 17 | 0.5360E+01 | 0.4757E+01 | 11.24 | 0.6027E+00 |
| 18 | 0.1642E+02 | 0.1544E+02 | 5.95 | 0.9775E+00 |
| 19 | 0.1591E+02 | 0.1530E+02 | 3.82 | 0.6079E+00 |
| 20 | 0.9300E+01 | 0.6870E+01 | 26.13 | 0.2430E+01 |
| 21 | 0.1280E+02 | 0.1031E+02 | 19.48 | 0.2493E+01 |
| 22 | 0.1412E+02 | 0.1486E+02 | -5.21 | -0.7360E+00 |
| 23 | 0.1774E+02 | 0.1592E+02 | 10.25 | 0.1819E+01 |
| 24 | 0.1618E+02 | 0.1795E+02 | -10.97 | -0.1775E+01 |
| 25 | 0.1459E+02 | 0.1407E+02 | 3.58 | 0.5222E+00 |
| 26 | 0.7160E+01 | 0.8801E+01 | -22.91 | -0.1641E+01 |
| 27 | 0.5860E+01 | 0.7437E+01 | -26.91 | -0.1577E+01 |
| 28 | 0.6480E+01 | 0.7119E+01 | -9.86 | -0.6389E+00 |
| 29 | 0.5510E+01 | 0.6266E+01 | -13.72 | -0.7558E+00 |
| 30 | 0.6490E+01 | 0.7354E+01 | -13.31 | -0.8641E+00 |
| 31 | 0.4310E+01 | 0.4607E+01 | -6.90 | -0.2974E+00 |
| 32 | 0.3160E+01 | 0.5279E+01 | -67.05 | -0.2119E+01 |
| 33 | 0.3230E+01 | 0.2144E+01 | 33.62 | 0.1086E+01 |
| 34 | 0.1880E+01 | 0.9917E+00 | 47.25 | 0.8883E+00 |
| 35 | 0.2030E+01 | 0.1711E+01 | 15.73 | 0.3193E+00 |
| 36 | 0.2220E+01 | 0.2006E+01 | 9.66 | 0.2143E+00 |
| 37 | 0.1378E+02 | 0.1442E+02 | -4.67 | -0.6432E+00 |
| 38 | 0.1348E+02 | 0.1538E+02 | -14.09 | -0.1899E+01 |
| 39 | 0.1364E+02 | 0.1236E+02 | 9.40 | 0.1282E+01 |
| 40 | 0.6540E+01 | 0.4770E+01 | 27.07 | 0.1770E+01 |
| 41 | 0.8240E+01 | 0.5365E+01 | 34.89 | 0.2875E+01 |
| 42 | 0.1618E+02 | 0.1351E+02 | 16.50 | 0.2669E+01 |
| 43 | 0.7540E+01 | 0.6603E+01 | 12.42 | 0.9366E+00 |
| 44 | 0.9680E+01 | 0.8778E+01 | 9.32 | 0.9022E+00 |
| 45 | 0.1262E+02 | 0.1375E+02 | -8.95 | -0.1130E+01 |
| 46 | 0.9600E+00 | 0.7978E+00 | 16.89 | 0.1622E+00 |
| 47 | 0.1017E+02 | 0.1183E+02 | -16.33 | -0.1660E+01 |
| 48 | 0.1363E+02 | 0.1353E+02 | 0.72 | 0.9807E-01 |

MODEL NUMBER: 9

| | |
|---|---|
| MULTIPLE CORRELATION (R) | 0.9536E+00 |
| STD ERR OF ESTIMATE (SE) | 0.1570E+01 |
| SUM OF SQUARED ERRORS | 0.1060E+03 |
| F TEST | 0.1078E+03 |
| SUM OF RESIDUALS | -0.2842E-13 |

| WAVE-LENGTH | MODEL COEFFICIENT | STANDARD ERROR COEFF | T-VALUE |
|---|---|---|---|
| 1668.0 | 0.3866E+05 | 0.6301E+04 | 0.6136E+01 |
| 2108.0 | -0.3491E+05 | 0.6392E+04 | 0.5461E+01 |
| 2327.0 | -0.1957E+05 | 0.4027E+04 | 0.4859E+01 |
| 1582.0 | 0.2970E+05 | 0.1116E+05 | 0.2662E+01 |
| INTERCEPT | 0.1222E+02 | | |

ANALYSIS OF VARIANCE FOR THE REGRESSION

| VARIATION SOURCE | DF | SUM OF SQ | MEAN SQ | F VALUE |
|---|---|---|---|---|
| ATTRIB TO REGRESSION | 4 | 0.1062E+04 | 0.2656E+03 | 0.1078E+03 |
| DEV FROM REGRESSION | 43 | 0.1060E+03 | 0.2464E+01 | |
| TOTAL | 47 | 0.1168E+04 | | |

| EXP NUM | ACTUAL | MODEL OUTPUT | PERCENT DIFF | ACTUAL DIFF |
|---|---|---|---|---|
| 1 | 0.9680E+01 | 0.8780E+01 | 9.30 | 0.8998E+00 |
| 2 | 0.4130E+01 | 0.4867E+01 | -17.84 | -0.7367E+00 |
| 3 | 0.1361E+02 | 0.1392E+02 | -2.28 | -0.3099E+00 |
| 4 | 0.2070E+01 | 0.3762E+01 | -81.73 | -0.1692E+01 |
| 5 | 0.8120E+01 | 0.7737E+01 | 4.72 | 0.3833E+00 |
| 6 | 0.1639E+02 | 0.1435E+02 | 12.46 | 0.2043E+01 |
| 7 | 0.1069E+02 | 0.9059E+01 | 15.25 | 0.1631E+01 |
| 8 | 0.1371E+02 | 0.1494E+02 | -8.95 | -0.1227E+01 |
| 9 | 0.8210E+01 | 0.8049E+01 | 1.96 | 0.1609E+00 |
| 10 | 0.4600E+01 | 0.4115E+01 | 10.54 | 0.4848E+00 |
| 11 | 0.4790E+01 | 0.6744E+01 | -40.80 | -0.1954E+01 |
| 12 | 0.1457E+02 | 0.1517E+02 | -4.13 | -0.6010E+00 |
| 13 | 0.1510E+02 | 0.1373E+02 | 9.10 | 0.1374E+01 |
| 14 | 0.5720E+01 | 0.3476E+01 | 39.23 | 0.2244E+01 |
| 15 | 0.9560E+01 | 0.1045E+02 | -9.33 | -0.8917E+00 |
| 16 | 0.1000E+01 | 0.1351E+01 | -35.11 | -0.3511E+00 |
| 17 | 0.5360E+01 | 0.6283E+01 | -17.22 | -0.9228E+00 |
| 18 | 0.1642E+02 | 0.1470E+02 | 10.49 | 0.1722E+01 |
| 19 | 0.1591E+02 | 0.1473E+02 | 7.40 | 0.1178E+01 |
| 20 | 0.9300E+01 | 0.7213E+01 | 22.44 | 0.2087E+01 |
| 21 | 0.1280E+02 | 0.1003E+02 | 21.60 | 0.2765E+01 |
| 22 | 0.1412E+02 | 0.1565E+02 | -10.81 | -0.1526E+01 |
| 23 | 0.1774E+02 | 0.1587E+02 | 10.56 | 0.1874E+01 |
| 24 | 0.1618E+02 | 0.1834E+02 | -13.34 | -0.2158E+01 |
| 25 | 0.1459E+02 | 0.1292E+02 | 11.43 | 0.1668E+01 |
| 26 | 0.7160E+01 | 0.1006E+02 | -40.41 | -0.2893E+01 |
| 27 | 0.5860E+01 | 0.7621E+01 | -30.06 | -0.1761E+01 |
| 28 | 0.6480E+01 | 0.8243E+01 | -27.21 | -0.1763E+01 |
| 29 | 0.5510E+01 | 0.6205E+01 | -12.62 | -0.6954E+00 |
| 30 | 0.6490E+01 | 0.8426E+01 | -29.83 | -0.1936E+01 |
| 31 | 0.4310E+01 | 0.5105E+01 | -18.44 | -0.7949E+00 |
| 32 | 0.3160E+01 | 0.4260E+01 | -34.80 | -0.1100E+01 |
| 33 | 0.3230E+01 | 0.2250E+01 | 30.35 | 0.9803E+00 |
| 34 | 0.1880E+01 | 0.5600E+00 | 70.21 | 0.1320E+01 |
| 35 | 0.2030E+01 | 0.3878E+00 | 80.90 | 0.1642E+01 |
| 36 | 0.2220E+01 | 0.2761E+01 | -24.36 | -0.5408E+00 |
| 37 | 0.1378E+02 | 0.1473E+02 | -6.89 | -0.9494E+00 |
| 38 | 0.1348E+02 | 0.1347E+02 | 0.06 | 0.8312E-02 |
| 39 | 0.1364E+02 | 0.1482E+02 | -8.64 | -0.1179E+01 |
| 40 | 0.6540E+01 | 0.6215E+01 | 4.97 | 0.3252E+00 |
| 41 | 0.8240E+01 | 0.6876E+01 | 16.56 | 0.1364E+01 |
| 42 | 0.1618E+02 | 0.1464E+02 | 9.52 | 0.1540E+01 |
| 43 | 0.7540E+01 | 0.7721E+01 | -2.40 | -0.1808E+00 |
| 44 | 0.9680E+01 | 0.7210E+01 | 25.52 | 0.2470E+01 |
| 45 | 0.1262E+02 | 0.1309E+02 | -3.69 | -0.4656E+00 |
| 46 | 0.9600E+00 | 0.4072E+01 | -324.22 | -0.3112E+01 |
| 47 | 0.1017E+02 | 0.1118E+02 | -9.93 | -0.1009E+01 |
| 48 | 0.1363E+02 | 0.1304E+02 | 4.30 | 0.5867E+00 |

MODEL NUMBER: 10

| | |
|---|---|
| MULTIPLE CORRELATION (R) | 0.9446E+00 |
| STD ERR OF ESTIMATE (SE) | 0.1711E+01 |
| SUM OF SQUARED ERRORS | 0.1259E+03 |
| F TEST | 0.8902E+02 |
| SUM OF RESIDUALS | -0.7105E-13 |

| WAVE-LENGTH | MODEL COEFFICIENT | STANDARD ERROR COEFF | T-VALUE |
|---|---|---|---|
| 1735.0 | -0.3368E+05 | 0.3250E+04 | 0.1036E+02 |
| 1931.0 | 0.2876E+05 | 0.7950E+04 | 0.3618E+01 |
| 1633.0 | 0.3739E+05 | 0.1097E+05 | 0.3408E+01 |
| 2095.0 | 0.1743E+05 | 0.7461E+04 | 0.2335E+01 |
| INTERCEPT | 0.1302E+02 | | |

ANALYSIS OF VARIANCE FOR THE REGRESSION

| VARIATION SOURCE | DF | SUM OF SQ | MEAN SQ | F VALUE |
|---|---|---|---|---|
| ATTRIB TO REGRESSION | 4 | 0.1042E+04 | 0.2606E+03 | 0.8902E+02 |
| DEV FROM REGRESSION | 43 | 0.1259E+03 | 0.2928E+01 | |
| TOTAL | 47 | 0.1168E+04 | | |

| EXP NUM | ACTUAL | MODEL OUTPUT | PERCENT DIFF | ACTUAL DIFF |
|---|---|---|---|---|
| 1 | 0.9680E+01 | 0.8141E+01 | 15.90 | 0.1539E+01 |
| 2 | 0.4130E+01 | 0.5456E+01 | -32.10 | -0.1326E+01 |
| 3 | 0.1361E+02 | 0.1276E+02 | 6.21 | 0.8458E+00 |
| 4 | 0.2070E+01 | 0.5164E+01 | -149.45 | -0.3094E+01 |
| 5 | 0.8120E+01 | 0.8015E+01 | 1.29 | 0.1048E+00 |
| 6 | 0.1639E+02 | 0.1395E+02 | 14.89 | 0.2440E+01 |
| 7 | 0.1069E+02 | 0.9186E+01 | 14.07 | 0.1504E+01 |
| 8 | 0.1371E+02 | 0.1337E+02 | 2.45 | 0.3362E+00 |
| 9 | 0.8210E+01 | 0.7296E+01 | 11.13 | 0.9136E+00 |
| 10 | 0.4600E+01 | 0.4722E+01 | -2.66 | -0.1222E+00 |
| 11 | 0.4790E+01 | 0.6994E+01 | -46.02 | -0.2204E+01 |
| 12 | 0.1457E+02 | 0.1399E+02 | 3.97 | 0.5786E+00 |
| 13 | 0.1510E+02 | 0.1391E+02 | 7.86 | 0.1186E+01 |
| 14 | 0.5720E+01 | 0.3116E+01 | 45.53 | 0.2604E+01 |
| 15 | 0.9560E+01 | 0.1060E+02 | -10.92 | -0.1044E+01 |
| 16 | 0.1000E+01 | 0.3170E+01 | -216.99 | -0.2170E+01 |
| 17 | 0.5360E+01 | 0.6235E+01 | -16.32 | -0.8749E+00 |
| 18 | 0.1642E+02 | 0.1617E+02 | 1.54 | 0.2533E+00 |
| 19 | 0.1591E+02 | 0.1576E+02 | 0.97 | 0.1537E+00 |
| 20 | 0.9300E+01 | 0.8008E+01 | 13.90 | 0.1292E+01 |
| 21 | 0.1280E+02 | 0.9682E+01 | 24.36 | 0.3118E+01 |
| 22 | 0.1412E+02 | 0.1520E+02 | -7.66 | -0.1081E+01 |
| 23 | 0.1774E+02 | 0.1528E+02 | 13.86 | 0.2458E+01 |
| 24 | 0.1618E+02 | 0.1874E+02 | -15.81 | -0.2559E+01 |
| 25 | 0.1459E+02 | 0.1306E+02 | 10.49 | 0.1530E+01 |
| 26 | 0.7160E+01 | 0.1021E+02 | -42.61 | -0.3051E+01 |
| 27 | 0.5860E+01 | 0.7533E+01 | -28.55 | -0.1673E+01 |
| 28 | 0.6480E+01 | 0.8508E+01 | -31.30 | -0.2028E+01 |
| 29 | 0.5510E+01 | 0.6319E+01 | -14.68 | -0.8090E+00 |
| 30 | 0.6490E+01 | 0.7732E+01 | -19.14 | -0.1242E+01 |
| 31 | 0.4310E+01 | 0.5299E+01 | -22.94 | -0.9886E+00 |
| 32 | 0.3160E+01 | 0.3802E+01 | -20.33 | -0.6423E+00 |
| 33 | 0.3230E+01 | 0.1646E+01 | 49.04 | 0.1584E+01 |
| 34 | 0.1880E+01 | 0.2585E+00 | 86.25 | 0.1621E+01 |
| 35 | 0.2030E+01 | 0.2654E+00 | 86.93 | 0.1765E+01 |
| 36 | 0.2220E+01 | 0.1810E+01 | 18.45 | 0.4095E+00 |
| 37 | 0.1378E+02 | 0.1411E+02 | -2.37 | -0.3273E+00 |
| 38 | 0.1348E+02 | 0.1577E+02 | -17.01 | -0.2293E+01 |
| 39 | 0.1364E+02 | 0.1381E+02 | -1.24 | -0.1695E+00 |
| 40 | 0.6540E+01 | 0.6714E+01 | -2.67 | -0.1744E+00 |
| 41 | 0.8240E+01 | 0.7086E+01 | 14.01 | 0.1154E+01 |
| 42 | 0.1618E+02 | 0.1391E+02 | 14.04 | 0.2272E+01 |
| 43 | 0.7540E+01 | 0.7560E+01 | -0.26 | -0.1991E-01 |
| 44 | 0.9680E+01 | 0.8627E+01 | 10.87 | 0.1053E+01 |
| 45 | 0.1262E+02 | 0.1262E+02 | 0.03 | 0.3160E-02 |
| 46 | 0.9600E+00 | 0.2864E+01 | -198.32 | -0.1904E+01 |
| 47 | 0.1017E+02 | 0.1281E+02 | -25.91 | -0.2635E+01 |
| 48 | 0.1363E+02 | 0.1192E+02 | 12.55 | 0.1711E+01 |

TRAINING SET MODELS

Second Derivative of Log 1/R Diffuse Reflectance Spectra

INITIAL WAVELENGTHS FOR COMPOSITE MODELS
AND ASSOCIATED LOCAL MINIMUM SUM OF
SQUARED ERROR (SSE) VALUES:

| MODEL NUMBER | WAVELENGTH | SSE |
|---|---|---|
| 1 | 1905.5 | 0.4373E+03 |
| 2 | 1733.5 | 0.4868E+03 |
| 3 | 2376.5 | 0.4883E+03 |
| 4 | 1715.5 | 0.5149E+03 |
| 5 | 1697.5 | 0.5977E+03 |
| 6 | 1518.5 | 0.5982E+03 |
| 7 | 2189.5 | 0.6004E+03 |
| 8 | 1792.5 | 0.6132E+03 |
| 9 | 2288.5 | 0.6135E+03 |
| 10 | 1769.5 | 0.6185E+03 |

BEST MODEL FOUND WAS MODEL NUMBER: 5

MODEL NUMBER: 1

| | |
|---|---|
| MULTIPLE CORRELATION (R) | 0.9462E+00 |
| STD ERR OF ESTIMATE (SE) | 0.1687E+01 |
| SUM OF SQUARED ERRORS | 0.1223E+03 |
| F TEST | 0.9194E+02 |
| SUM OF RESIDUALS | -0.5818E-13 |

| WAVE-LENGTH | MODEL COEFFICIENT | STANDARD ERROR COEFF | T-VALUE |
|---|---|---|---|
| 1905.5 | 0.1974E+05 | 0.2237E+04 | 0.8825E+01 |
| 1697.5 | -0.4746E+05 | 0.8134E+04 | 0.5835E+01 |
| 1991.5 | -0.2803E+05 | 0.6410E+04 | 0.4373E+01 |
| 1764.5 | -0.2630E+05 | 0.7872E+04 | 0.3341E+01 |
| INTERCEPT | 0.9442E+01 | | |

ANALYSIS OF VARIANCE FOR THE REGRESSION

| VARIATION SOURCE | DF | SUM OF SQ | MEAN SQ | F VALUE |
|---|---|---|---|---|
| ATTRIB TO REGRESSION | 4 | 0.1046E+04 | 0.2615E+03 | 0.9194E+02 |
| DEV FROM REGRESSION | 43 | 0.1223E+03 | 0.2844E+01 | |
| TOTAL | 47 | 0.1168E+04 | | |

| EXP NUM | ACTUAL | MODEL OUTPUT | PERCENT DIFF | ACTUAL DIFF |
|---|---|---|---|---|
| 1 | 0.9680E+01 | 0.9939E+01 | -2.68 | -0.2591E+00 |
| 2 | 0.4130E+01 | 0.7014E+01 | -69.84 | -0.2884E+01 |
| 3 | 0.1361E+02 | 0.1259E+02 | 7.47 | 0.1016E+01 |
| 4 | 0.2070E+01 | 0.5848E+01 | -182.49 | -0.3778E+01 |
| 5 | 0.8120E+01 | 0.7793E+01 | 4.03 | 0.3269E+00 |
| 6 | 0.1639E+02 | 0.1501E+02 | 8.40 | 0.1376E+01 |
| 7 | 0.1069E+02 | 0.1002E+02 | 6.30 | 0.6735E+00 |
| 8 | 0.1371E+02 | 0.1382E+02 | -0.78 | -0.1072E+00 |
| 9 | 0.8210E+01 | 0.9026E+01 | -9.94 | -0.8158E+00 |
| 10 | 0.4600E+01 | 0.6321E+01 | -37.41 | -0.1721E+01 |
| 11 | 0.4790E+01 | 0.6470E+01 | -35.07 | -0.1680E+01 |
| 12 | 0.1457E+02 | 0.1320E+02 | 9.43 | 0.1374E+01 |
| 13 | 0.1510E+02 | 0.1391E+02 | 7.90 | 0.1192E+01 |
| 14 | 0.5720E+01 | 0.5768E+01 | -0.84 | -0.4792E-01 |
| 15 | 0.9560E+01 | 0.9137E+01 | 4.42 | 0.4227E+00 |
| 16 | 0.1000E+01 | 0.3989E+00 | 60.11 | 0.6011E+00 |
| 17 | 0.5360E+01 | 0.5369E+01 | -0.17 | -0.9258E-02 |
| 18 | 0.1642E+02 | 0.1441E+02 | 12.24 | 0.2010E+01 |
| 19 | 0.1591E+02 | 0.1613E+02 | -1.40 | -0.2223E+00 |
| 20 | 0.9300E+01 | 0.7692E+01 | 17.29 | 0.1608E+01 |
| 21 | 0.1280E+02 | 0.1061E+02 | 17.14 | 0.2194E+01 |
| 22 | 0.1412E+02 | 0.1352E+02 | 4.23 | 0.5970E+00 |
| 23 | 0.1774E+02 | 0.1607E+02 | 9.40 | 0.1668E+01 |
| 24 | 0.1618E+02 | 0.1960E+02 | -21.17 | -0.3425E+01 |
| 25 | 0.1459E+02 | 0.1201E+02 | 17.71 | 0.2584E+01 |
| 26 | 0.7160E+01 | 0.7086E+01 | 1.04 | 0.7436E-01 |
| 27 | 0.5860E+01 | 0.5977E+01 | -2.00 | -0.1172E+00 |
| 28 | 0.6480E+01 | 0.8350E+01 | -28.86 | -0.1870E+01 |
| 29 | 0.5510E+01 | 0.7195E+01 | -30.58 | -0.1685E+01 |
| 30 | 0.6490E+01 | 0.8768E+01 | -35.09 | -0.2278E+01 |
| 31 | 0.4310E+01 | 0.3719E+01 | 13.72 | 0.5914E+00 |
| 32 | 0.3160E+01 | 0.5164E+01 | -63.42 | -0.2004E+01 |
| 33 | 0.3230E+01 | 0.1141E+01 | 64.68 | 0.2089E+01 |
| 34 | 0.1880E+01 | 0.2119E+01 | -12.70 | -0.2388E+00 |
| 35 | 0.2030E+01 | 0.1754E+01 | 13.57 | 0.2755E+00 |
| 36 | 0.2220E+01 | -0.1063E+01 | 147.87 | 0.3283E+01 |
| 37 | 0.1378E+02 | 0.1416E+02 | -2.78 | -0.3834E+00 |
| 38 | 0.1348E+02 | 0.1540E+02 | -14.22 | -0.1917E+01 |
| 39 | 0.1364E+02 | 0.1262E+02 | 7.49 | 0.1022E+01 |
| 40 | 0.6540E+01 | 0.7815E+01 | -19.49 | -0.1275E+01 |
| 41 | 0.8240E+01 | 0.6528E+01 | 20.77 | 0.1712E+01 |
| 42 | 0.1618E+02 | 0.1565E+02 | 3.25 | 0.5251E+00 |
| 43 | 0.7540E+01 | 0.7844E+01 | -4.03 | -0.3036E+00 |
| 44 | 0.9680E+01 | 0.9236E+01 | 4.59 | 0.4441E+00 |
| 45 | 0.1262E+02 | 0.1324E+02 | -4.89 | -0.6166E+00 |
| 46 | 0.9600E+00 | 0.2342E+01 | -143.96 | -0.1382E+01 |
| 47 | 0.1017E+02 | 0.1154E+02 | -13.51 | -0.1374E+01 |
| 48 | 0.1363E+02 | 0.1090E+02 | 20.05 | 0.2733E+01 |

MODEL NUMBER: 2

| | |
|---|---|
| MULTIPLE CORRELATION (R) | 0.9529E+00 |
| STD ERR OF ESTIMATE (SE) | 0.1581E+01 |
| SUM OF SQUARED ERRORS | 0.1074E+03 |
| F TEST | 0.1061E+03 |
| SUM OF RESIDUALS | -0.8571E-13 |

| WAVE-LENGTH | MODEL COEFFICIENT | STANDARD ERROR COEFF | T-VALUE |
|---|---|---|---|
| 1886.5 | -0.1642E+05 | 0.1618E+04 | 0.1015E+02 |
| 1765.5 | -0.5230E+05 | 0.5649E+04 | 0.9258E+01 |
| 2236.5 | -0.1403E+05 | 0.1625E+04 | 0.8632E+01 |
| 1976.5 | 0.2699E+05 | 0.1025E+05 | 0.2633E+01 |
| INTERCEPT | 0.1242E+02 | | |

ANALYSIS OF VARIANCE FOR THE REGRESSION

| VARIATION SOURCE | DF | SUM OF SQ | MEAN SQ | F VALUE |
|---|---|---|---|---|
| ATTRIB TO REGRESSION | 4 | 0.1061E+04 | 0.2652E+03 | 0.1061E+03 |
| DEV FROM REGRESSION | 43 | 0.1074E+03 | 0.2499E+01 | |
| TOTAL | 47 | 0.1168E+04 | | |

| EXP NUM | ACTUAL | MODEL OUTPUT | PERCENT DIFF | ACTUAL DIFF |
|---|---|---|---|---|
| 1 | 0.9680E+01 | 0.8098E+01 | 16.34 | 0.1582E+01 |
| 2 | 0.4130E+01 | 0.6260E+01 | -51.58 | -0.2130E+01 |
| 3 | 0.1361E+02 | 0.1161E+02 | 14.68 | 0.1998E+01 |
| 4 | 0.2070E+01 | 0.5261E+01 | -154.18 | -0.3191E+01 |
| 5 | 0.8120E+01 | 0.9183E+01 | -13.09 | -0.1063E+01 |
| 6 | 0.1639E+02 | 0.1710E+02 | -4.34 | -0.7106E+00 |
| 7 | 0.1069E+02 | 0.1145E+02 | -7.12 | -0.7612E+00 |
| 8 | 0.1371E+02 | 0.1286E+02 | 6.22 | 0.8534E+00 |
| 9 | 0.8210E+01 | 0.9860E+01 | -20.10 | -0.1650E+01 |
| 10 | 0.4600E+01 | 0.5511E+01 | -19.80 | -0.9107E+00 |
| 11 | 0.4790E+01 | 0.6270E+01 | -30.90 | -0.1480E+01 |
| 12 | 0.1457E+02 | 0.1343E+02 | 7.83 | 0.1141E+01 |
| 13 | 0.1510E+02 | 0.1544E+02 | -2.25 | -0.3394E+00 |
| 14 | 0.5720E+01 | 0.5911E+01 | -3.35 | -0.1914E+00 |
| 15 | 0.9560E+01 | 0.1170E+02 | -22.34 | -0.2136E+01 |
| 16 | 0.1000E+01 | 0.1673E+01 | -67.33 | -0.6733E+00 |
| 17 | 0.5360E+01 | 0.4566E+01 | 14.81 | 0.7937E+00 |
| 18 | 0.1642E+02 | 0.1663E+02 | -1.26 | -0.2066E+00 |
| 19 | 0.1591E+02 | 0.1653E+02 | -3.90 | -0.6203E+00 |
| 20 | 0.9300E+01 | 0.6921E+01 | 25.59 | 0.2379E+01 |
| 21 | 0.1280E+02 | 0.8060E+01 | 37.03 | 0.4740E+01 |
| 22 | 0.1412E+02 | 0.1494E+02 | -5.83 | -0.8236E+00 |
| 23 | 0.1774E+02 | 0.1514E+02 | 14.66 | 0.2600E+01 |
| 24 | 0.1618E+02 | 0.1655E+02 | -2.31 | -0.3742E+00 |
| 25 | 0.1459E+02 | 0.1324E+02 | 9.25 | 0.1349E+01 |
| 26 | 0.7160E+01 | 0.7979E+01 | -11.44 | -0.8193E+00 |
| 27 | 0.5860E+01 | 0.6763E+01 | -15.42 | -0.9033E+00 |
| 28 | 0.6480E+01 | 0.7159E+01 | -10.48 | -0.6790E+00 |
| 29 | 0.5510E+01 | 0.4409E+01 | 19.99 | 0.1101E+01 |
| 30 | 0.6490E+01 | 0.6889E+01 | -6.14 | -0.3988E+00 |
| 31 | 0.4310E+01 | 0.4599E+01 | -6.71 | -0.2893E+00 |
| 32 | 0.3160E+01 | 0.5028E+01 | -59.11 | -0.1868E+01 |
| 33 | 0.3230E+01 | 0.1924E+01 | 40.43 | 0.1306E+01 |
| 34 | 0.1880E+01 | 0.1667E+01 | 11.31 | 0.2127E+00 |
| 35 | 0.2030E+01 | 0.2245E+01 | -10.58 | -0.2148E+00 |
| 36 | 0.2220E+01 | 0.4619E+00 | 79.19 | 0.1758E+01 |
| 37 | 0.1378E+02 | 0.1081E+02 | 21.54 | 0.2969E+01 |
| 38 | 0.1348E+02 | 0.1425E+02 | -5.71 | -0.7697E+00 |
| 39 | 0.1364E+02 | 0.1471E+02 | -7.85 | -0.1071E+01 |
| 40 | 0.6540E+01 | 0.6870E+01 | -5.04 | -0.3299E+00 |
| 41 | 0.8240E+01 | 0.7079E+01 | 14.09 | 0.1161E+01 |
| 42 | 0.1618E+02 | 0.1560E+02 | 3.56 | 0.5761E+00 |
| 43 | 0.7540E+01 | 0.7735E+01 | -2.58 | -0.1946E+00 |
| 44 | 0.9680E+01 | 0.8315E+01 | 14.10 | 0.1365E+01 |
| 45 | 0.1262E+02 | 0.1473E+02 | -16.70 | -0.2107E+01 |
| 46 | 0.9600E+00 | 0.2317E+01 | -141.37 | -0.1357E+01 |
| 47 | 0.1017E+02 | 0.1021E+02 | -0.36 | -0.3672E-01 |
| 48 | 0.1363E+02 | 0.1321E+02 | 3.05 | 0.4156E+00 |

MODEL NUMBER: 3

| | |
|---|---|
| MULTIPLE CORRELATION (R) | 0.9444E+00 |
| STD ERR OF ESTIMATE (SE) | 0.1714E+01 |
| SUM OF SQUARED ERRORS | 0.1264E+03 |
| F TEST | 0.8864E+02 |
| SUM OF RESIDUALS | -0.9504E-13 |

| WAVE-LENGTH | MODEL COEFFICIENT | STANDARD ERROR COEFF | T-VALUE |
|---|---|---|---|
| 1713.5 | -0.7611E+05 | 0.1131E+05 | 0.6729E+01 |
| 2196.5 | -0.2962E+05 | 0.4441E+04 | 0.6670E+01 |
| 1725.5 | -0.1888E+05 | 0.4238E+04 | 0.4456E+01 |
| 1952.5 | -0.3521E+05 | 0.8844E+04 | 0.3981E+01 |
| INTERCEPT | 0.1145E+02 | | |

ANALYSIS OF VARIANCE FOR THE REGRESSION

| VARIATION SOURCE | DF | SUM OF SQ | MEAN SQ | F VALUE |
|---|---|---|---|---|
| ATTRIB TO REGRESSION | 4 | 0.1042E+04 | 0.2605E+03 | 0.8864E+02 |
| DEV FROM REGRESSION | 43 | 0.1264E+03 | 0.2939E+01 | |
| TOTAL | 47 | 0.1168E+04 | | |

| EXP NUM | ACTUAL | MODEL OUTPUT | PERCENT DIFF | ACTUAL DIFF |
|---|---|---|---|---|
| 1 | 0.9680E+01 | 0.1052E+02 | -8.69 | -0.8410E+00 |
| 2 | 0.4130E+01 | 0.4698E+01 | -13.75 | -0.5677E+00 |
| 3 | 0.1361E+02 | 0.1152E+02 | 15.37 | 0.2092E+01 |
| 4 | 0.2070E+01 | 0.5824E+01 | -181.37 | -0.3754E+01 |
| 5 | 0.8120E+01 | 0.9904E+01 | -21.97 | -0.1784E+01 |
| 6 | 0.1639E+02 | 0.1445E+02 | 11.82 | 0.1937E+01 |
| 7 | 0.1069E+02 | 0.1051E+02 | 1.66 | 0.1779E+00 |
| 8 | 0.1371E+02 | 0.1365E+02 | 0.46 | 0.6352E-01 |
| 9 | 0.8210E+01 | 0.7923E+01 | 3.49 | 0.2868E+00 |
| 10 | 0.4600E+01 | 0.5322E+01 | -15.70 | -0.7220E+00 |
| 11 | 0.4790E+01 | 0.5081E+01 | -6.08 | -0.2911E+00 |
| 12 | 0.1457E+02 | 0.1601E+02 | -9.90 | -0.1443E+01 |
| 13 | 0.1510E+02 | 0.1620E+02 | -7.27 | -0.1097E+01 |
| 14 | 0.5720E+01 | 0.5320E+01 | 6.99 | 0.3998E+00 |
| 15 | 0.9560E+01 | 0.1015E+02 | -6.13 | -0.5860E+00 |
| 16 | 0.1000E+01 | 0.1197E+01 | -19.68 | -0.1968E+00 |
| 17 | 0.5360E+01 | 0.4666E+01 | 12.95 | 0.6939E+00 |
| 18 | 0.1642E+02 | 0.1341E+02 | 18.33 | 0.3010E+01 |
| 19 | 0.1591E+02 | 0.1596E+02 | -0.30 | -0.4695E-01 |
| 20 | 0.9300E+01 | 0.5546E+01 | 40.36 | 0.3754E+01 |
| 21 | 0.1280E+02 | 0.1080E+02 | 15.61 | 0.1998E+01 |
| 22 | 0.1412E+02 | 0.1252E+02 | 11.31 | 0.1597E+01 |
| 23 | 0.1774E+02 | 0.1623E+02 | 8.51 | 0.1509E+01 |
| 24 | 0.1618E+02 | 0.1742E+02 | -7.68 | -0.1243E+01 |
| 25 | 0.1459E+02 | 0.1158E+02 | 20.60 | 0.3006E+01 |
| 26 | 0.7160E+01 | 0.7903E+01 | -10.37 | -0.7426E+00 |
| 27 | 0.5860E+01 | 0.8962E+01 | -52.94 | -0.3102E+01 |
| 28 | 0.6480E+01 | 0.6239E+01 | 3.72 | 0.2411E+00 |
| 29 | 0.5510E+01 | 0.4877E+01 | 11.49 | 0.6333E+00 |
| 30 | 0.6490E+01 | 0.8865E+01 | -36.60 | -0.2375E+01 |
| 31 | 0.4310E+01 | 0.4276E+01 | 0.79 | 0.3413E-01 |
| 32 | 0.3160E+01 | 0.4606E+01 | -45.75 | -0.1446E+01 |
| 33 | 0.3230E+01 | 0.1729E+01 | 46.47 | 0.1501E+01 |
| 34 | 0.1880E+01 | 0.3564E+00 | 81.04 | 0.1524E+01 |
| 35 | 0.2030E+01 | 0.2913E+01 | -43.50 | -0.8830E+00 |
| 36 | 0.2220E+01 | 0.1493E+01 | 32.73 | 0.7266E+00 |
| 37 | 0.1378E+02 | 0.1464E+02 | -6.28 | -0.8650E+00 |
| 38 | 0.1348E+02 | 0.1407E+02 | -4.37 | -0.5886E+00 |
| 39 | 0.1364E+02 | 0.1513E+02 | -10.95 | -0.1494E+01 |
| 40 | 0.6540E+01 | 0.6661E+01 | -1.86 | -0.1215E+00 |
| 41 | 0.8240E+01 | 0.8344E+01 | -1.26 | -0.1042E+00 |
| 42 | 0.1618E+02 | 0.1463E+02 | 9.57 | 0.1549E+01 |
| 43 | 0.7540E+01 | 0.6915E+01 | 8.29 | 0.6248E+00 |
| 44 | 0.9680E+01 | 0.8351E+01 | 13.73 | 0.1329E+01 |
| 45 | 0.1262E+02 | 0.1377E+02 | -9.08 | -0.1146E+01 |
| 46 | 0.9600E+00 | 0.3542E+01 | -268.93 | -0.2582E+01 |
| 47 | 0.1017E+02 | 0.1295E+02 | -27.33 | -0.2779E+01 |
| 48 | 0.1363E+02 | 0.1151E+02 | 15.52 | 0.2115E+01 |

MODEL NUMBER: 4

| | |
|---|---|
| MULTIPLE CORRELATION (R) | 0.9496E+00 |
| STD ERR OF ESTIMATE (SE) | 0.1633E+01 |
| SUM OF SQUARED ERRORS | 0.1147E+03 |
| F TEST | 0.9871E+02 |
| SUM OF RESIDUALS | -0.2620E-13 |

| WAVE-LENGTH | MODEL COEFFICIENT | STANDARD ERROR COEFF | T-VALUE |
|---|---|---|---|
| 1715.5 | -0.6993E+05 | 0.8243E+04 | 0.8483E+01 |
| 2017.5 | -0.4642E+05 | 0.7473E+04 | 0.6212E+01 |
| 2216.5 | 0.3854E+04 | 0.9270E+03 | 0.4158E+01 |
| 1514.5 | -0.4489E+05 | 0.1175E+05 | 0.3821E+01 |
| INTERCEPT | 0.1369E+02 | | |

ANALYSIS OF VARIANCE FOR THE REGRESSION

| VARIATION SOURCE | DF | SUM OF SQ | MEAN SQ | F VALUE |
|---|---|---|---|---|
| ATTRIB TO REGRESSION | 4 | 0.1054E+04 | 0.2634E+03 | 0.9871E+02 |
| DEV FROM REGRESSION | 43 | 0.1147E+03 | 0.2668E+01 | |
| TOTAL | 47 | 0.1168E+04 | | |

| EXP NUM | ACTUAL | MODEL OUTPUT | PERCENT DIFF | ACTUAL DIFF |
|---|---|---|---|---|
| 1 | 0.9680E+01 | 0.9381E+01 | 3.09 | 0.2987E+00 |
| 2 | 0.4130E+01 | 0.3955E+01 | 4.25 | 0.1755E+00 |
| 3 | 0.1361E+02 | 0.7821E+01 | 42.53 | 0.5789E+01 |
| 4 | 0.2070E+01 | 0.5633E+01 | -172.12 | -0.3563E+01 |
| 5 | 0.8120E+01 | 0.9365E+01 | -15.33 | -0.1245E+01 |
| 6 | 0.1639E+02 | 0.1340E+02 | 18.23 | 0.2987E+01 |
| 7 | 0.1069E+02 | 0.1034E+02 | 3.29 | 0.3519E+00 |
| 8 | 0.1371E+02 | 0.1427E+02 | -4.11 | -0.5632E+00 |
| 9 | 0.8210E+01 | 0.9134E+01 | -11.26 | -0.9241E+00 |
| 10 | 0.4600E+01 | 0.4768E+01 | -3.64 | -0.1675E+00 |
| 11 | 0.4790E+01 | 0.5714E+01 | -19.29 | -0.9238E+00 |
| 12 | 0.1457E+02 | 0.1468E+02 | -0.78 | -0.1139E+00 |
| 13 | 0.1510E+02 | 0.1335E+02 | 11.59 | 0.1750E+01 |
| 14 | 0.5720E+01 | 0.4483E+01 | 21.62 | 0.1237E+01 |
| 15 | 0.9560E+01 | 0.1141E+02 | -19.36 | -0.1851E+01 |
| 16 | 0.1000E+01 | 0.2052E+01 | -105.24 | -0.1052E+01 |
| 17 | 0.5360E+01 | 0.5623E+01 | -4.92 | -0.2635E+00 |
| 18 | 0.1642E+02 | 0.1582E+02 | 3.64 | 0.5971E+00 |
| 19 | 0.1591E+02 | 0.1541E+02 | 3.16 | 0.5034E+00 |
| 20 | 0.9300E+01 | 0.7653E+01 | 17.71 | 0.1647E+01 |
| 21 | 0.1280E+02 | 0.1153E+02 | 9.91 | 0.1269E+01 |
| 22 | 0.1412E+02 | 0.1523E+02 | -7.85 | -0.1108E+01 |
| 23 | 0.1774E+02 | 0.1778E+02 | -0.25 | -0.4440E-01 |
| 24 | 0.1618E+02 | 0.1708E+02 | -5.56 | -0.9003E+00 |
| 25 | 0.1459E+02 | 0.1330E+02 | 8.82 | 0.1287E+01 |
| 26 | 0.7160E+01 | 0.8610E+01 | -20.26 | -0.1450E+01 |
| 27 | 0.5860E+01 | 0.8040E+01 | -37.19 | -0.2180E+01 |
| 28 | 0.6480E+01 | 0.7914E+01 | -22.13 | -0.1434E+01 |
| 29 | 0.5510E+01 | 0.7430E+01 | -34.85 | -0.1920E+01 |
| 30 | 0.6490E+01 | 0.8434E+01 | -29.96 | -0.1944E+01 |
| 31 | 0.4310E+01 | 0.2890E+01 | 32.95 | 0.1420E+01 |
| 32 | 0.3160E+01 | 0.4354E+01 | -37.78 | -0.1194E+01 |
| 33 | 0.3230E+01 | 0.2459E+01 | 23.86 | 0.7706E+00 |
| 34 | 0.1880E+01 | 0.1179E+01 | 37.27 | 0.7006E+00 |
| 35 | 0.2030E+01 | 0.1794E+01 | 11.62 | 0.2360E+00 |
| 36 | 0.2220E+01 | 0.1599E+01 | 27.98 | 0.6211E+00 |
| 37 | 0.1378E+02 | 0.1283E+02 | 6.87 | 0.9462E+00 |
| 38 | 0.1348E+02 | 0.1336E+02 | 0.87 | 0.1174E+00 |
| 39 | 0.1364E+02 | 0.1326E+02 | 2.81 | 0.3834E+00 |
| 40 | 0.6540E+01 | 0.6814E+01 | -4.18 | -0.2735E+00 |
| 41 | 0.8240E+01 | 0.8892E+01 | -7.92 | -0.6523E+00 |
| 42 | 0.1618E+02 | 0.1626E+02 | -0.52 | -0.8385E-01 |
| 43 | 0.7540E+01 | 0.6039E+01 | 19.91 | 0.1501E+01 |
| 44 | 0.9680E+01 | 0.7349E+01 | 24.08 | 0.2331E+01 |
| 45 | 0.1262E+02 | 0.1456E+02 | -15.39 | -0.1942E+01 |
| 46 | 0.9600E+00 | 0.1396E+01 | -45.45 | -0.4363E+00 |
| 47 | 0.1017E+02 | 0.1177E+02 | -15.70 | -0.1597E+01 |
| 48 | 0.1363E+02 | 0.1272E+02 | 6.65 | 0.9069E+00 |

MODEL NUMBER: 5

| | |
|---|---|
| MULTIPLE CORRELATION (R) | 0.9611E+00 |
| STD ERR OF ESTIMATE (SE) | 0.1440E+01 |
| SUM OF SQUARED ERRORS | 0.8922E+02 |
| F TEST | 0.1300E+03 |
| SUM OF RESIDUALS | -0.1332E-13 |

| WAVE-LENGTH | MODEL COEFFICIENT | STANDARD ERROR COEFF | T-VALUE |
|---|---|---|---|
| 1906.5 | 0.2675E+05 | 0.1866E+04 | 0.1434E+02 |
| 1714.5 | -0.6785E+05 | 0.7977E+04 | 0.8505E+01 |
| 1874.5 | 0.2527E+05 | 0.3309E+04 | 0.7638E+01 |
| 2023.5 | 0.2312E+05 | 0.6896E+04 | 0.3353E+01 |
| INTERCEPT | 0.1432E+02 | | |

ANALYSIS OF VARIANCE FOR THE REGRESSION

| VARIATION SOURCE | DF | SUM OF SQ | MEAN SQ | F VALUE |
|---|---|---|---|---|
| ATTRIB TO REGRESSION | 4 | 0.1079E+04 | 0.2698E+03 | 0.1300E+03 |
| DEV FROM REGRESSION | 43 | 0.8922E+02 | 0.2075E+01 | |
| TOTAL | 47 | 0.1168E+04 | | |

| EXP NUM | ACTUAL | MODEL OUTPUT | PERCENT DIFF | ACTUAL DIFF |
|---|---|---|---|---|
| 1 | 0.9680E+01 | 0.9445E+01 | 2.42 | 0.2347E+00 |
| 2 | 0.4130E+01 | 0.4245E+01 | -2.78 | -0.1148E+00 |
| 3 | 0.1361E+02 | 0.1229E+02 | 9.71 | 0.1322E+01 |
| 4 | 0.2070E+01 | 0.4845E+01 | -134.04 | -0.2775E+01 |
| 5 | 0.8120E+01 | 0.9194E+01 | -13.22 | -0.1074E+01 |
| 6 | 0.1639E+02 | 0.1691E+02 | -3.17 | -0.5191E+00 |
| 7 | 0.1069E+02 | 0.1080E+02 | -1.02 | -0.1090E+00 |
| 8 | 0.1371E+02 | 0.1331E+02 | 2.93 | 0.4015E+00 |
| 9 | 0.8210E+01 | 0.9113E+01 | -11.00 | -0.9032E+00 |
| 10 | 0.4600E+01 | 0.5429E+01 | -18.02 | -0.8288E+00 |
| 11 | 0.4790E+01 | 0.5949E+01 | -24.20 | -0.1159E+01 |
| 12 | 0.1457E+02 | 0.1442E+02 | 1.00 | 0.1451E+00 |
| 13 | 0.1510E+02 | 0.1424E+02 | 5.69 | 0.8588E+00 |
| 14 | 0.5720E+01 | 0.5109E+01 | 10.67 | 0.6105E+00 |
| 15 | 0.9560E+01 | 0.1024E+02 | -7.09 | -0.6778E+00 |
| 16 | 0.1000E+01 | 0.7846E-01 | 92.15 | 0.9215E+00 |
| 17 | 0.5360E+01 | 0.7489E+01 | -39.73 | -0.2129E+01 |
| 18 | 0.1642E+02 | 0.1577E+02 | 3.96 | 0.6499E+00 |
| 19 | 0.1591E+02 | 0.1589E+02 | 0.14 | 0.2246E-01 |
| 20 | 0.9300E+01 | 0.9226E+01 | 0.80 | 0.7417E-01 |
| 21 | 0.1280E+02 | 0.1113E+02 | 13.04 | 0.1670E+01 |
| 22 | 0.1412E+02 | 0.1585E+02 | -12.24 | -0.1728E+01 |
| 23 | 0.1774E+02 | 0.1577E+02 | 11.09 | 0.1967E+01 |
| 24 | 0.1618E+02 | 0.1801E+02 | -11.30 | -0.1829E+01 |
| 25 | 0.1459E+02 | 0.1064E+02 | 27.07 | 0.3950E+01 |
| 26 | 0.7160E+01 | 0.9027E+01 | -26.07 | -0.1867E+01 |
| 27 | 0.5860E+01 | 0.8279E+01 | -41.28 | -0.2419E+01 |
| 28 | 0.6480E+01 | 0.7199E+01 | -11.10 | -0.7192E+00 |
| 29 | 0.5510E+01 | 0.6815E+01 | -23.69 | -0.1305E+01 |
| 30 | 0.6490E+01 | 0.7738E+01 | -19.24 | -0.1248E+01 |
| 31 | 0.4310E+01 | 0.3592E+01 | 16.65 | 0.7175E+00 |
| 32 | 0.3160E+01 | 0.2757E+01 | 12.77 | 0.4035E+00 |
| 33 | 0.3230E+01 | 0.1499E+01 | 53.60 | 0.1731E+01 |
| 34 | 0.1880E+01 | 0.1135E+01 | 39.63 | 0.7450E+00 |
| 35 | 0.2030E+01 | 0.1499E+01 | 26.16 | 0.5311E+00 |
| 36 | 0.2220E+01 | 0.4494E+00 | 79.76 | 0.1771E+01 |
| 37 | 0.1378E+02 | 0.1235E+02 | 10.41 | 0.1434E+01 |
| 38 | 0.1348E+02 | 0.1348E+02 | 0.01 | 0.2002E-02 |
| 39 | 0.1364E+02 | 0.1249E+02 | 8.44 | 0.1151E+01 |
| 40 | 0.6540E+01 | 0.7239E+01 | -10.68 | -0.6985E+00 |
| 41 | 0.8240E+01 | 0.7626E+01 | 7.45 | 0.6142E+00 |
| 42 | 0.1618E+02 | 0.1454E+02 | 10.15 | 0.1642E+01 |
| 43 | 0.7540E+01 | 0.6163E+01 | 18.27 | 0.1377E+01 |
| 44 | 0.9680E+01 | 0.8247E+01 | 14.80 | 0.1433E+01 |
| 45 | 0.1262E+02 | 0.1273E+02 | -0.85 | -0.1076E+00 |
| 46 | 0.9600E+00 | 0.3243E+01 | -237.77 | -0.2283E+01 |
| 47 | 0.1017E+02 | 0.1167E+02 | -14.74 | -0.1499E+01 |
| 48 | 0.1363E+02 | 0.1402E+02 | -2.84 | -0.3870E+00 |

MODEL NUMBER: 6

| | |
|---|---|
| MULTIPLE CORRELATION (R) | 0.9611E+00 |
| STD ERR OF ESTIMATE (SE) | 0.1441E+01 |
| SUM OF SQUARED ERRORS | 0.8923E+02 |
| F TEST | 0.1300E+03 |
| SUM OF RESIDUALS | -0.8882E-15 |

| WAVE-LENGTH | MODEL COEFFICIENT | STANDARD ERROR COEFF | T-VALUE |
|---|---|---|---|
| 2239.5 | -0.2165E+05 | 0.1967E+04 | 0.1101E+02 |
| 1724.5 | -0.3334E+05 | 0.3094E+04 | 0.1077E+02 |
| 1977.5 | 0.5074E+05 | 0.8191E+04 | 0.6194E+01 |
| 1911.5 | 0.9225E+04 | 0.1634E+04 | 0.5645E+01 |
| INTERCEPT | 0.1329E+02 | | |

ANALYSIS OF VARIANCE FOR THE REGRESSION

| VARIATION SOURCE | DF | SUM OF SQ | MEAN SQ | F VALUE |
|---|---|---|---|---|
| ATTRIB TO REGRESSION | 4 | 0.1079E+04 | 0.2698E+03 | 0.1300E+03 |
| DEV FROM REGRESSION | 43 | 0.8923E+02 | 0.2075E+01 | |
| TOTAL | 47 | 0.1168E+04 | | |

| EXP NUM | ACTUAL | MODEL OUTPUT | PERCENT DIFF | ACTUAL DIFF |
|---|---|---|---|---|
| 1 | 0.9680E+01 | 0.7313E+01 | 24.45 | 0.2367E+01 |
| 2 | 0.4130E+01 | 0.6067E+01 | -46.91 | -0.1937E+01 |
| 3 | 0.1361E+02 | 0.1190E+02 | 12.54 | 0.1707E+01 |
| 4 | 0.2070E+01 | 0.5155E+01 | -149.03 | -0.3085E+01 |
| 5 | 0.8120E+01 | 0.9504E+01 | -17.04 | -0.1384E+01 |
| 6 | 0.1639E+02 | 0.1584E+02 | 3.35 | 0.5492E+00 |
| 7 | 0.1069E+02 | 0.9974E+01 | 6.70 | 0.7160E+00 |
| 8 | 0.1371E+02 | 0.1454E+02 | -6.03 | -0.8262E+00 |
| 9 | 0.8210E+01 | 0.9877E+01 | -20.31 | -0.1667E+01 |
| 10 | 0.4600E+01 | 0.3368E+01 | 26.77 | 0.1232E+01 |
| 11 | 0.4790E+01 | 0.4752E+01 | 0.79 | 0.3807E-01 |
| 12 | 0.1457E+02 | 0.1285E+02 | 11.79 | 0.1717E+01 |
| 13 | 0.1510E+02 | 0.1504E+02 | 0.39 | 0.5922E-01 |
| 14 | 0.5720E+01 | 0.5130E+01 | 10.32 | 0.5901E+00 |
| 15 | 0.9560E+01 | 0.1185E+02 | -23.94 | -0.2289E+01 |
| 16 | 0.1000E+01 | 0.1460E+00 | 85.40 | 0.8540E+00 |
| 17 | 0.5360E+01 | 0.5485E+01 | -2.33 | -0.1248E+00 |
| 18 | 0.1642E+02 | 0.1536E+02 | 6.48 | 0.1064E+01 |
| 19 | 0.1591E+02 | 0.1406E+02 | 11.63 | 0.1850E+01 |
| 20 | 0.9300E+01 | 0.8253E+01 | 11.26 | 0.1047E+01 |
| 21 | 0.1280E+02 | 0.1052E+02 | 17.82 | 0.2281E+01 |
| 22 | 0.1412E+02 | 0.1593E+02 | -12.78 | -0.1805E+01 |
| 23 | 0.1774E+02 | 0.1560E+02 | 12.04 | 0.2136E+01 |
| 24 | 0.1618E+02 | 0.1778E+02 | -9.90 | -0.1601E+01 |
| 25 | 0.1459E+02 | 0.1407E+02 | 3.56 | 0.5189E+00 |
| 26 | 0.7160E+01 | 0.8403E+01 | -17.37 | -0.1243E+01 |
| 27 | 0.5860E+01 | 0.7358E+01 | -25.56 | -0.1498E+01 |
| 28 | 0.6480E+01 | 0.7191E+01 | -10.98 | -0.7114E+00 |
| 29 | 0.5510E+01 | 0.3506E+01 | 36.38 | 0.2004E+01 |
| 30 | 0.6490E+01 | 0.7016E+01 | -8.11 | -0.5262E+00 |
| 31 | 0.4310E+01 | 0.5271E+01 | -22.30 | -0.9612E+00 |
| 32 | 0.3160E+01 | 0.5603E+01 | -77.32 | -0.2443E+01 |
| 33 | 0.3230E+01 | 0.2400E+01 | 25.70 | 0.8302E+00 |
| 34 | 0.1880E+01 | 0.1920E+01 | -2.12 | -0.3982E-01 |
| 35 | 0.2030E+01 | 0.1980E+01 | 2.46 | 0.4984E-01 |
| 36 | 0.2220E+01 | 0.1796E+01 | 19.11 | 0.4243E+00 |
| 37 | 0.1378E+02 | 0.1435E+02 | -4.15 | -0.5717E+00 |
| 38 | 0.1348E+02 | 0.1448E+02 | -7.44 | -0.1003E+01 |
| 39 | 0.1364E+02 | 0.1520E+02 | -11.45 | -0.1562E+01 |
| 40 | 0.6540E+01 | 0.6955E+01 | -6.34 | -0.4149E+00 |
| 41 | 0.8240E+01 | 0.6962E+01 | 15.51 | 0.1278E+01 |
| 42 | 0.1618E+02 | 0.1459E+02 | 9.83 | 0.1591E+01 |
| 43 | 0.7540E+01 | 0.8117E+01 | -7.65 | -0.5767E+00 |
| 44 | 0.9680E+01 | 0.9216E+01 | 4.79 | 0.4637E+00 |
| 45 | 0.1262E+02 | 0.1346E+02 | -6.66 | -0.8411E+00 |
| 46 | 0.9600E+00 | 0.1221E+01 | -27.14 | -0.2605E+00 |
| 47 | 0.1017E+02 | 0.9921E+01 | 2.45 | 0.2495E+00 |
| 48 | 0.1363E+02 | 0.1187E+02 | 12.89 | 0.1757E+01 |

MODEL NUMBER: 7

| | |
|---|---|
| MULTIPLE CORRELATION (R) | 0.9421E+00 |
| STD ERR OF ESTIMATE (SE) | 0.1748E+01 |
| SUM OF SQUARED ERRORS | 0.1314E+03 |
| F TEST | 0.8485E+02 |
| SUM OF RESIDUALS | 0.1155E-13 |

| WAVE-LENGTH | MODEL COEFFICIENT | STANDARD ERROR COEFF | T-VALUE |
|---|---|---|---|
| 2226.5 | 0.2517E+05 | 0.3877E+04 | 0.6491E+01 |
| 1882.5 | -0.1555E+05 | 0.2522E+04 | 0.6167E+01 |
| 1733.5 | -0.4237E+05 | 0.9668E+04 | 0.4383E+01 |
| 2189.5 | -0.1095E+05 | 0.4144E+04 | 0.2643E+01 |
| INTERCEPT | 0.1133E+02 | | |

ANALYSIS OF VARIANCE FOR THE REGRESSION

| VARIATION SOURCE | DF | SUM OF SQ | MEAN SQ | F VALUE |
|---|---|---|---|---|
| ATTRIB TO REGRESSION | 4 | 0.1037E+04 | 0.2592E+03 | 0.8485E+02 |
| DEV FROM REGRESSION | 43 | 0.1314E+03 | 0.3055E+01 | |
| TOTAL | 47 | 0.1168E+04 | | |

| EXP NUM | ACTUAL | MODEL OUTPUT | PERCENT DIFF | ACTUAL DIFF |
|---|---|---|---|---|
| 1 | 0.9680E+01 | 0.8724E+01 | 9.87 | 0.9557E+00 |
| 2 | 0.4130E+01 | 0.1897E+01 | 54.07 | 0.2233E+01 |
| 3 | 0.1361E+02 | 0.1115E+02 | 18.06 | 0.2458E+01 |
| 4 | 0.2070E+01 | 0.4567E+01 | -120.61 | -0.2497E+01 |
| 5 | 0.8120E+01 | 0.7743E+01 | 4.65 | 0.3773E+00 |
| 6 | 0.1639E+02 | 0.1523E+02 | 7.08 | 0.1161E+01 |
| 7 | 0.1069E+02 | 0.8659E+01 | 19.00 | 0.2031E+01 |
| 8 | 0.1371E+02 | 0.1256E+02 | 8.41 | 0.1153E+01 |
| 9 | 0.8210E+01 | 0.7952E+01 | 3.15 | 0.2582E+00 |
| 10 | 0.4600E+01 | 0.6825E+01 | -48.37 | -0.2225E+01 |
| 11 | 0.4790E+01 | 0.5759E+01 | -20.23 | -0.9691E+00 |
| 12 | 0.1457E+02 | 0.1629E+02 | -11.81 | -0.1720E+01 |
| 13 | 0.1510E+02 | 0.1417E+02 | 6.13 | 0.9264E+00 |
| 14 | 0.5720E+01 | 0.7058E+01 | -23.40 | -0.1338E+01 |
| 15 | 0.9560E+01 | 0.1174E+02 | -22.82 | -0.2181E+01 |
| 16 | 0.1000E+01 | 0.1030E+01 | -2.99 | -0.2987E-01 |
| 17 | 0.5360E+01 | 0.7121E+01 | -32.85 | -0.1761E+01 |
| 18 | 0.1642E+02 | 0.1622E+02 | 1.23 | 0.2019E+00 |
| 19 | 0.1591E+02 | 0.1654E+02 | -3.94 | -0.6262E+00 |
| 20 | 0.9300E+01 | 0.6908E+01 | 25.72 | 0.2392E+01 |
| 21 | 0.1280E+02 | 0.1045E+02 | 18.37 | 0.2351E+01 |
| 22 | 0.1412E+02 | 0.1603E+02 | -13.55 | -0.1914E+01 |
| 23 | 0.1774E+02 | 0.1665E+02 | 6.15 | 0.1091E+01 |
| 24 | 0.1618E+02 | 0.1849E+02 | -14.27 | -0.2308E+01 |
| 25 | 0.1459E+02 | 0.1339E+02 | 8.23 | 0.1200E+01 |
| 26 | 0.7160E+01 | 0.8422E+01 | -17.62 | -0.1262E+01 |
| 27 | 0.5860E+01 | 0.6556E+01 | -11.88 | -0.6962E+00 |
| 28 | 0.6480E+01 | 0.7615E+01 | -17.51 | -0.1135E+01 |
| 29 | 0.5510E+01 | 0.7323E+01 | -32.90 | -0.1813E+01 |
| 30 | 0.6490E+01 | 0.8103E+01 | -24.85 | -0.1613E+01 |
| 31 | 0.4310E+01 | 0.5577E+01 | -29.39 | -0.1267E+01 |
| 32 | 0.3160E+01 | 0.5241E+01 | -65.84 | -0.2081E+01 |
| 33 | 0.3230E+01 | 0.3085E+01 | 4.49 | 0.1449E+00 |
| 34 | 0.1880E+01 | 0.1599E+01 | 14.93 | 0.2806E+00 |
| 35 | 0.2030E+01 | 0.3240E+01 | -59.59 | -0.1210E+01 |
| 36 | 0.2220E+01 | 0.1727E+01 | 22.19 | 0.4926E+00 |
| 37 | 0.1378E+02 | 0.1337E+02 | 2.94 | 0.4056E+00 |
| 38 | 0.1348E+02 | 0.1207E+02 | 10.44 | 0.1408E+01 |
| 39 | 0.1364E+02 | 0.1589E+02 | -16.48 | -0.2249E+01 |
| 40 | 0.6540E+01 | 0.7144E+01 | -9.24 | -0.6042E+00 |
| 41 | 0.8240E+01 | 0.6675E+01 | 18.99 | 0.1565E+01 |
| 42 | 0.1618E+02 | 0.1329E+02 | 17.88 | 0.2892E+01 |
| 43 | 0.7540E+01 | 0.7906E+01 | -4.86 | -0.3663E+00 |
| 44 | 0.9680E+01 | 0.6092E+01 | 37.06 | 0.3588E+01 |
| 45 | 0.1262E+02 | 0.1358E+02 | -7.60 | -0.9593E+00 |
| 46 | 0.9600E+00 | 0.1671E+01 | -74.04 | -0.7108E+00 |
| 47 | 0.1017E+02 | 0.9896E+01 | 2.69 | 0.2736E+00 |
| 48 | 0.1363E+02 | 0.9936E+01 | 27.11 | 0.3694E+01 |

MODEL NUMBER: 8

| | |
|---|---|
| MULTIPLE CORRELATION (R) | 0.9540E+00 |
| STD ERR OF ESTIMATE (SE) | 0.1562E+01 |
| SUM OF SQUARED ERRORS | 0.1050E+03 |
| F TEST | 0.1089E+03 |
| SUM OF RESIDUALS | -0.5285E-13 |

| WAVE-LENGTH | MODEL COEFFICIENT | STANDARD ERROR COEFF | T-VALUE |
|---|---|---|---|
| 1908.5 | 0.2069E+05 | 0.1604E+04 | 0.1290E+02 |
| 2224.5 | 0.1060E+05 | 0.1374E+04 | 0.7711E+01 |
| 2256.5 | 0.1560E+05 | 0.2385E+04 | 0.6542E+01 |
| 1976.5 | 0.3195E+05 | 0.9855E+04 | 0.3242E+01 |
| INTERCEPT | 0.1231E+02 | | |

ANALYSIS OF VARIANCE FOR THE REGRESSION

| VARIATION SOURCE | DF | SUM OF SQ | MEAN SQ | F VALUE |
|---|---|---|---|---|
| ATTRIB TO REGRESSION | 4 | 0.1063E+04 | 0.2658E+03 | 0.1089E+03 |
| DEV FROM REGRESSION | 43 | 0.1050E+03 | 0.2441E+01 | |
| TOTAL | 47 | 0.1168E+04 | | |

| EXP NUM | ACTUAL | MODEL OUTPUT | PERCENT DIFF | ACTUAL DIFF |
|---|---|---|---|---|
| 1 | 0.9680E+01 | 0.6353E+01 | 34.37 | 0.3327E+01 |
| 2 | 0.4130E+01 | 0.4234E+01 | -2.52 | -0.1042E+00 |
| 3 | 0.1361E+02 | 0.1064E+02 | 21.80 | 0.2967E+01 |
| 4 | 0.2070E+01 | 0.5194E+01 | -150.91 | -0.3124E+01 |
| 5 | 0.8120E+01 | 0.8762E+01 | -7.91 | -0.6421E+00 |
| 6 | 0.1639E+02 | 0.1498E+02 | 8.61 | 0.1411E+01 |
| 7 | 0.1069E+02 | 0.1015E+02 | 5.09 | 0.5439E+00 |
| 8 | 0.1371E+02 | 0.1207E+02 | 11.96 | 0.1640E+01 |
| 9 | 0.8210E+01 | 0.9337E+01 | -13.72 | -0.1127E+01 |
| 10 | 0.4600E+01 | 0.5414E+01 | -17.70 | -0.8143E+00 |
| 11 | 0.4790E+01 | 0.5471E+01 | -14.22 | -0.6812E+00 |
| 12 | 0.1457E+02 | 0.1336E+02 | 8.31 | 0.1211E+01 |
| 13 | 0.1510E+02 | 0.1524E+02 | -0.92 | -0.1385E+00 |
| 14 | 0.5720E+01 | 0.6273E+01 | -9.67 | -0.5534E+00 |
| 15 | 0.9560E+01 | 0.1102E+02 | -15.25 | -0.1458E+01 |
| 16 | 0.1000E+01 | 0.7202E+00 | 27.98 | 0.2798E+00 |
| 17 | 0.5360E+01 | 0.6612E+01 | -23.36 | -0.1252E+01 |
| 18 | 0.1642E+02 | 0.1636E+02 | 0.36 | 0.5981E-01 |
| 19 | 0.1591E+02 | 0.1474E+02 | 7.38 | 0.1174E+01 |
| 20 | 0.9300E+01 | 0.8264E+01 | 11.14 | 0.1036E+01 |
| 21 | 0.1280E+02 | 0.1150E+02 | 10.14 | 0.1298E+01 |
| 22 | 0.1412E+02 | 0.1603E+02 | -13.50 | -0.1906E+01 |
| 23 | 0.1774E+02 | 0.1712E+02 | 3.50 | 0.6205E+00 |
| 24 | 0.1618E+02 | 0.1902E+02 | -17.53 | -0.2836E+01 |
| 25 | 0.1459E+02 | 0.1495E+02 | -2.44 | -0.3553E+00 |
| 26 | 0.7160E+01 | 0.8934E+01 | -24.78 | -0.1774E+01 |
| 27 | 0.5860E+01 | 0.7417E+01 | -26.57 | -0.1557E+01 |
| 28 | 0.6480E+01 | 0.7899E+01 | -21.90 | -0.1419E+01 |
| 29 | 0.5510E+01 | 0.5942E+01 | -7.85 | -0.4323E+00 |
| 30 | 0.6490E+01 | 0.7934E+01 | -22.24 | -0.1444E+01 |
| 31 | 0.4310E+01 | 0.6375E+01 | -47.91 | -0.2065E+01 |
| 32 | 0.3160E+01 | 0.5533E+01 | -75.09 | -0.2373E+01 |
| 33 | 0.3230E+01 | 0.2842E+01 | 12.01 | 0.3878E+00 |
| 34 | 0.1880E+01 | 0.2540E+01 | -35.13 | -0.6604E+00 |
| 35 | 0.2030E+01 | 0.2103E+01 | -3.58 | -0.7263E-01 |
| 36 | 0.2220E+01 | 0.1744E+01 | 21.43 | 0.4758E+00 |
| 37 | 0.1378E+02 | 0.1295E+02 | 5.99 | 0.8260E+00 |
| 38 | 0.1348E+02 | 0.1358E+02 | -0.75 | -0.1012E+00 |
| 39 | 0.1364E+02 | 0.1534E+02 | -12.48 | -0.1702E+01 |
| 40 | 0.6540E+01 | 0.6014E+01 | 8.04 | 0.5256E+00 |
| 41 | 0.8240E+01 | 0.6627E+01 | 19.57 | 0.1613E+01 |
| 42 | 0.1618E+02 | 0.1512E+02 | 6.57 | 0.1063E+01 |
| 43 | 0.7540E+01 | 0.5607E+01 | 25.63 | 0.1933E+01 |
| 44 | 0.9680E+01 | 0.6729E+01 | 30.49 | 0.2951E+01 |
| 45 | 0.1262E+02 | 0.1295E+02 | -2.60 | -0.3283E+00 |
| 46 | 0.9600E+00 | 0.4271E+00 | 55.51 | 0.5329E+00 |
| 47 | 0.1017E+02 | 0.8691E+01 | 14.55 | 0.1479E+01 |
| 48 | 0.1363E+02 | 0.1207E+02 | 11.47 | 0.1564E+01 |

MODEL NUMBER: 9

| | |
|---|---|
| MULTIPLE CORRELATION (R) | 0.9360E+00 |
| STD ERR OF ESTIMATE (SE) | 0.1835E+01 |
| SUM OF SQUARED ERRORS | 0.1447E+03 |
| F TEST | 0.7603E+02 |
| SUM OF RESIDUALS | -0.3109E-13 |

| WAVE-LENGTH | MODEL COEFFICIENT | STANDARD ERROR COEFF | T-VALUE |
|---|---|---|---|
| 1514.5 | -0.6915E+05 | 0.9952E+04 | 0.6948E+01 |
| 1713.5 | -0.7159E+05 | 0.1154E+05 | 0.6203E+01 |
| 1989.5 | -0.2894E+05 | 0.7699E+04 | 0.3759E+01 |
| 2288.5 | -0.7191E+04 | 0.2137E+04 | 0.3365E+01 |
| INTERCEPT | 0.1239E+02 | | |

ANALYSIS OF VARIANCE FOR THE REGRESSION

| VARIATION SOURCE | DF | SUM OF SQ | MEAN SQ | F VALUE |
|---|---|---|---|---|
| ATTRIB TO REGRESSION | 4 | 0.1024E+04 | 0.2559E+03 | 0.7603E+02 |
| DEV FROM REGRESSION | 43 | 0.1447E+03 | 0.3366E+01 | |
| TOTAL | 47 | 0.1168E+04 | | |

| EXP NUM | ACTUAL | MODEL OUTPUT | PERCENT DIFF | ACTUAL DIFF |
|---|---|---|---|---|
| 1 | 0.9680E+01 | 0.1066E+02 | -10.08 | -0.9755E+00 |
| 2 | 0.4130E+01 | 0.3726E+01 | 9.78 | 0.4041E+00 |
| 3 | 0.1361E+02 | 0.9146E+01 | 32.80 | 0.4464E+01 |
| 4 | 0.2070E+01 | 0.5895E+01 | -184.76 | -0.3825E+01 |
| 5 | 0.8120E+01 | 0.9548E+01 | -17.58 | -0.1428E+01 |
| 6 | 0.1639E+02 | 0.1174E+02 | 28.35 | 0.4646E+01 |
| 7 | 0.1069E+02 | 0.9390E+01 | 12.16 | 0.1300E+01 |
| 8 | 0.1371E+02 | 0.1515E+02 | -10.50 | -0.1440E+01 |
| 9 | 0.8210E+01 | 0.1049E+02 | -27.79 | -0.2281E+01 |
| 10 | 0.4600E+01 | 0.6644E+01 | -44.44 | -0.2044E+01 |
| 11 | 0.4790E+01 | 0.7391E+01 | -54.30 | -0.2601E+01 |
| 12 | 0.1457E+02 | 0.1413E+02 | 3.01 | 0.4384E+00 |
| 13 | 0.1510E+02 | 0.1460E+02 | 3.28 | 0.4960E+00 |
| 14 | 0.5720E+01 | 0.5523E+01 | 3.45 | 0.1971E+00 |
| 15 | 0.9560E+01 | 0.9905E+01 | -3.61 | -0.3453E+00 |
| 16 | 0.1000E+01 | 0.2042E+01 | -104.23 | -0.1042E+01 |
| 17 | 0.5360E+01 | 0.4639E+01 | 13.45 | 0.7207E+00 |
| 18 | 0.1642E+02 | 0.1575E+02 | 4.09 | 0.6722E+00 |
| 19 | 0.1591E+02 | 0.1539E+02 | 3.28 | 0.5220E+00 |
| 20 | 0.9300E+01 | 0.8486E+01 | 8.75 | 0.8138E+00 |
| 21 | 0.1280E+02 | 0.1269E+02 | 0.83 | 0.1066E+00 |
| 22 | 0.1412E+02 | 0.1211E+02 | 14.21 | 0.2007E+01 |
| 23 | 0.1774E+02 | 0.1506E+02 | 15.12 | 0.2683E+01 |
| 24 | 0.1618E+02 | 0.1759E+02 | -8.69 | -0.1406E+01 |
| 25 | 0.1459E+02 | 0.1255E+02 | 13.96 | 0.2037E+01 |
| 26 | 0.7160E+01 | 0.7500E+01 | -4.74 | -0.3396E+00 |
| 27 | 0.5860E+01 | 0.7951E+01 | -35.69 | -0.2091E+01 |
| 28 | 0.6480E+01 | 0.6538E+01 | -0.90 | -0.5846E-01 |
| 29 | 0.5510E+01 | 0.6191E+01 | -12.36 | -0.6811E+00 |
| 30 | 0.6490E+01 | 0.8860E+01 | -36.52 | -0.2370E+01 |
| 31 | 0.4310E+01 | 0.2930E+01 | 32.02 | 0.1380E+01 |
| 32 | 0.3160E+01 | 0.3970E+01 | -25.64 | -0.8101E+00 |
| 33 | 0.3230E+01 | 0.2560E+01 | 20.75 | 0.6703E+00 |
| 34 | 0.1880E+01 | 0.2904E+00 | 84.56 | 0.1590E+01 |
| 35 | 0.2030E+01 | 0.1138E+01 | 43.92 | 0.8916E+00 |
| 36 | 0.2220E+01 | 0.3614E-01 | 98.37 | 0.2184E+01 |
| 37 | 0.1378E+02 | 0.1410E+02 | -2.35 | -0.3243E+00 |
| 38 | 0.1348E+02 | 0.1492E+02 | -10.72 | -0.1444E+01 |
| 39 | 0.1364E+02 | 0.1243E+02 | 8.86 | 0.1208E+01 |
| 40 | 0.6540E+01 | 0.7707E+01 | -17.85 | -0.1167E+01 |
| 41 | 0.8240E+01 | 0.7684E+01 | 6.75 | 0.5564E+00 |
| 42 | 0.1618E+02 | 0.1461E+02 | 9.71 | 0.1572E+01 |
| 43 | 0.7540E+01 | 0.8541E+01 | -13.28 | -0.1001E+01 |
| 44 | 0.9680E+01 | 0.7586E+01 | 21.63 | 0.2094E+01 |
| 45 | 0.1262E+02 | 0.1343E+02 | -6.42 | -0.8099E+00 |
| 46 | 0.9600E+00 | 0.2775E+01 | -189.02 | -0.1815E+01 |
| 47 | 0.1017E+02 | 0.1158E+02 | -13.82 | -0.1406E+01 |
| 48 | 0.1363E+02 | 0.1558E+02 | -14.28 | -0.1947E+01 |

MODEL NUMBER: 10

| | |
|---|---|
| MULTIPLE CORRELATION (R) | 0.9588E+00 |
| STD ERR OF ESTIMATE (SE) | 0.1481E+01 |
| SUM OF SQUARED ERRORS | 0.9429E+02 |
| F TEST | 0.1224E+03 |
| SUM OF RESIDUALS | 0.1865E-13 |

| WAVE-LENGTH | MODEL COEFFICIENT | STANDARD ERROR COEFF | T-VALUE |
|---|---|---|---|
| 1905.5 | 0.2455E+05 | 0.2141E+04 | 0.1147E+02 |
| 1872.5 | 0.2846E+05 | 0.3308E+04 | 0.8602E+01 |
| 1715.5 | -0.6491E+05 | 0.8127E+04 | 0.7987E+01 |
| 1978.5 | 0.3206E+05 | 0.8026E+04 | 0.3994E+01 |
| INTERCEPT | 0.1322E+02 | | |

ANALYSIS OF VARIANCE FOR THE REGRESSION

| VARIATION SOURCE | DF | SUM OF SQ | MEAN SQ | F VALUE |
|---|---|---|---|---|
| ATTRIB TO REGRESSION | 4 | 0.1074E+04 | 0.2685E+03 | 0.1224E+03 |
| DEV FROM REGRESSION | 43 | 0.9429E+02 | 0.2193E+01 | |
| TOTAL | 47 | 0.1168E+04 | | |

| EXP NUM | ACTUAL | MODEL OUTPUT | PERCENT DIFF | ACTUAL DIFF |
|---|---|---|---|---|
| 1 | 0.9680E+01 | 0.8495E+01 | 12.24 | 0.1185E+01 |
| 2 | 0.4130E+01 | 0.4305E+01 | -4.24 | -0.1752E+00 |
| 3 | 0.1361E+02 | 0.1012E+02 | 25.62 | 0.3486E+01 |
| 4 | 0.2070E+01 | 0.4582E+01 | -121.38 | -0.2512E+01 |
| 5 | 0.8120E+01 | 0.9337E+01 | -14.99 | -0.1217E+01 |
| 6 | 0.1639E+02 | 0.1511E+02 | 7.79 | 0.1278E+01 |
| 7 | 0.1069E+02 | 0.9464E+01 | 11.46 | 0.1226E+01 |
| 8 | 0.1371E+02 | 0.1368E+02 | 0.22 | 0.3055E-01 |
| 9 | 0.8210E+01 | 0.1011E+02 | -23.09 | -0.1895E+01 |
| 10 | 0.4600E+01 | 0.5564E+01 | -20.96 | -0.9640E+00 |
| 11 | 0.4790E+01 | 0.5478E+01 | -14.36 | -0.6879E+00 |
| 12 | 0.1457E+02 | 0.1372E+02 | 5.82 | 0.8480E+00 |
| 13 | 0.1510E+02 | 0.1657E+02 | -9.74 | -0.1471E+01 |
| 14 | 0.5720E+01 | 0.5552E+01 | 2.94 | 0.1683E+00 |
| 15 | 0.9560E+01 | 0.1092E+02 | -14.20 | -0.1357E+01 |
| 16 | 0.1000E+01 | 0.4627E+00 | 53.73 | 0.5373E+00 |
| 17 | 0.5360E+01 | 0.7542E+01 | -40.72 | -0.2182E+01 |
| 18 | 0.1642E+02 | 0.1460E+02 | 11.07 | 0.1818E+01 |
| 19 | 0.1591E+02 | 0.1469E+02 | 7.64 | 0.1216E+01 |
| 20 | 0.9300E+01 | 0.9714E+01 | -4.45 | -0.4137E+00 |
| 21 | 0.1280E+02 | 0.1145E+02 | 10.56 | 0.1352E+01 |
| 22 | 0.1412E+02 | 0.1385E+02 | 1.91 | 0.2692E+00 |
| 23 | 0.1774E+02 | 0.1604E+02 | 9.61 | 0.1704E+01 |
| 24 | 0.1618E+02 | 0.1766E+02 | -9.16 | -0.1482E+01 |
| 25 | 0.1459E+02 | 0.1145E+02 | 21.52 | 0.3139E+01 |
| 26 | 0.7160E+01 | 0.8674E+01 | -21.15 | -0.1514E+01 |
| 27 | 0.5860E+01 | 0.8209E+01 | -40.09 | -0.2349E+01 |
| 28 | 0.6480E+01 | 0.6574E+01 | -1.45 | -0.9405E-01 |
| 29 | 0.5510E+01 | 0.5411E+01 | 1.79 | 0.9866E-01 |
| 30 | 0.6490E+01 | 0.7581E+01 | -16.82 | -0.1091E+01 |
| 31 | 0.4310E+01 | 0.3965E+01 | 8.01 | 0.3451E+00 |
| 32 | 0.3160E+01 | 0.3470E+01 | -9.81 | -0.3099E+00 |
| 33 | 0.3230E+01 | 0.1432E+01 | 55.67 | 0.1798E+01 |
| 34 | 0.1880E+01 | 0.1742E+01 | 7.35 | 0.1382E+00 |
| 35 | 0.2030E+01 | 0.1692E+01 | 16.66 | 0.3383E+00 |
| 36 | 0.2220E+01 | -0.5707E+00 | 125.71 | 0.2791E+01 |
| 37 | 0.1378E+02 | 0.1470E+02 | -6.65 | -0.9169E+00 |
| 38 | 0.1348E+02 | 0.1340E+02 | 0.56 | 0.7577E-01 |
| 39 | 0.1364E+02 | 0.1331E+02 | 2.45 | 0.3339E+00 |
| 40 | 0.6540E+01 | 0.7607E+01 | -16.32 | -0.1067E+01 |
| 41 | 0.8240E+01 | 0.7830E+01 | 4.98 | 0.4101E+00 |
| 42 | 0.1618E+02 | 0.1711E+02 | -5.73 | -0.9267E+00 |
| 43 | 0.7540E+01 | 0.6828E+01 | 9.44 | 0.7119E+00 |
| 44 | 0.9680E+01 | 0.8458E+01 | 12.62 | 0.1222E+01 |
| 45 | 0.1262E+02 | 0.1354E+02 | -7.27 | -0.9178E+00 |
| 46 | 0.9600E+00 | 0.3310E+01 | -244.76 | -0.2350E+01 |
| 47 | 0.1017E+02 | 0.1122E+02 | -10.32 | -0.1050E+01 |
| 48 | 0.1363E+02 | 0.1320E+02 | 3.13 | 0.4271E+00 |

# APPENDIX B

## POINT GRADE ESTIMATES FOR THE BITUMEN CONTENT OF CORE

## BASED ON SAMPLES OF VARYING INCREMENT SIZE

Point Grade Estimates for the Bitumen Content of the Test Core Section Obtained at 1 cm Sampling Intervals.

| DEPTH (m) | BITUMEN CONTENT WT % | DEPTH (m) | BITUMEN CONTENT WT % | DEPTH (m) | BITUMEN CONTENT WT % | DEPTH (m) | BITUMEN CONTENT WT % |
|---|---|---|---|---|---|---|---|
| 84.100 | 14.08 | 84.650 | 4.88 | 85.200 | 5.75 | 85.750 | 16.60 |
| 84.110 | 13.06 | 84.660 | 4.18 | 85.210 | 8.02 | 85.760 | 14.07 |
| 84.120 | 10.79 | 84.670 | 3.76 | 85.220 | 10.50 | 85.770 | 16.29 |
| 84.130 | 13.51 | 84.680 | 4.61 | 85.230 | 7.39 | 85.780 | 16.02 |
| 84.140 | 15.44 | 84.690 | 4.76 | 85.240 | 8.11 | 85.790 | 13.91 |
| 84.150 | 14.67 | 84.700 | 9.58 | 85.250 | 8.18 | 85.800 | 14.53 |
| 84.160 | 14.13 | 84.710 | 9.81 | 85.260 | 8.20 | 85.810 | 16.77 |
| 84.170 | 13.27 | 84.720 | 9.39 | 85.270 | 9.68 | 85.820 | 15.49 |
| 84.180 | 11.96 | 84.730 | 5.88 | 85.280 | 8.61 | 85.830 | 14.79 |
| 84.190 | 12.74 | 84.740 | 10.98 | 85.290 | 7.48 | 85.840 | 13.60 |
| 84.200 | 11.84 | 84.750 | 6.93 | 85.300 | 11.75 | 85.850 | 13.17 |
| 84.210 | 9.18 | 84.760 | 5.98 | 85.310 | 13.98 | 85.860 | 12.27 |
| 84.220 | 13.19 | 84.770 | 6.11 | 85.320 | 11.99 | 85.870 | 15.81 |
| 84.230 | 11.58 | 84.780 | 7.25 | 85.330 | 13.51 | 85.880 | 12.01 |
| 84.240 | 15.01 | 84.790 | 12.22 | 85.340 | 17.13 | 85.890 | 4.38 |
| 84.250 | 15.83 | 84.800 | 11.05 | 85.350 | 16.89 | 85.900 | 15.21 |
| 84.260 | 16.20 | 84.810 | 13.81 | 85.360 | 17.48 | 85.910 | 16.04 |
| 84.270 | 11.99 | 84.820 | 13.77 | 85.370 | 19.62 | 85.920 | 18.18 |
| 84.280 | 14.15 | 84.830 | 10.32 | 85.380 | 16.59 | 85.930 | 15.69 |
| 84.290 | 11.97 | 84.840 | 13.30 | 85.390 | 16.17 | 85.940 | 16.78 |
| 84.300 | 12.39 | 84.850 | 11.01 | 85.400 | 15.62 | 85.950 | 16.93 |
| 84.310 | 8.32 | 84.860 | 8.30 | 85.410 | 17.35 | 85.960 | 15.44 |
| 84.320 | 8.27 | 84.870 | 14.26 | 85.420 | 16.60 | 85.970 | 14.19 |
| 84.330 | 12.54 | 84.880 | 15.37 | 85.430 | 16.79 | 85.980 | 13.48 |
| 84.340 | 8.95 | 84.890 | 13.23 | 85.440 | 17.00 | 85.990 | 14.45 |
| 84.350 | 4.64 | 84.900 | 12.70 | 85.450 | 19.31 | 86.000 | 16.48 |
| 84.360 | 13.18 | 84.910 | 11.73 | 85.460 | 15.59 | 86.010 | 15.55 |
| 84.370 | 16.95 | 84.920 | 10.62 | 85.470 | 14.29 | 86.020 | 12.74 |
| 84.380 | 14.82 | 84.930 | 11.33 | 85.480 | 18.50 | 86.030 | 15.93 |
| 84.390 | 15.47 | 84.940 | 12.00 | 85.490 | 17.94 | 86.040 | 14.58 |
| 84.400 | 11.08 | 84.950 | 11.18 | 85.500 | 16.12 | 86.050 | 6.05 |
| 84.410 | 13.72 | 84.960 | 9.78 | 85.510 | 17.01 | 86.060 | 6.23 |
| 84.420 | 15.65 | 84.970 | 14.52 | 85.520 | 16.23 | 86.070 | 11.64 |
| 84.430 | 11.36 | 84.980 | 12.99 | 85.530 | 16.03 | 86.080 | 12.69 |
| 84.440 | 8.97 | 84.990 | 15.08 | 85.540 | 16.82 | 86.090 | 12.34 |
| 84.450 | 9.54 | 85.000 | 11.27 | 85.550 | 18.38 | 86.100 | 10.39 |
| 84.460 | 12.04 | 85.010 | 4.89 | 85.560 | 14.59 | 86.110 | 10.42 |
| 84.470 | 12.06 | 85.020 | 5.48 | 85.570 | 18.31 | 86.120 | 10.35 |
| 84.480 | 12.37 | 85.030 | 5.17 | 85.580 | 16.75 | 86.130 | 3.18 |
| 84.490 | 11.27 | 85.040 | 6.27 | 85.590 | 16.37 | 86.140 | 8.40 |
| 84.500 | 16.79 | 85.050 | 4.87 | 85.600 | 14.63 | 86.150 | 3.43 |
| 84.510 | 13.08 | 85.060 | 7.61 | 85.610 | 15.62 | 86.160 | 8.97 |
| 84.520 | 9.64 | 85.070 | 8.60 | 85.620 | 12.34 | 86.170 | 6.02 |
| 84.530 | 6.23 | 85.080 | 5.89 | 85.630 | 17.07 | 86.180 | 6.85 |
| 84.540 | 14.11 | 85.090 | 9.59 | 85.640 | 13.85 | 86.190 | 0.17 |
| 84.550 | 15.11 | 85.100 | 11.33 | 85.650 | 12.25 | 86.200 | 8.25 |
| 84.560 | 10.04 | 85.110 | 11.15 | 85.660 | 15.10 | 86.210 | 7.49 |
| 84.570 | 11.87 | 85.120 | 11.68 | 85.670 | 13.44 | 86.220 | 3.04 |
| 84.580 | 9.03 | 85.130 | 7.93 | 85.680 | 12.99 | 86.230 | 1.68 |
| 84.590 | 0.51 | 85.140 | 5.92 | 85.690 | 13.70 | 86.240 | 11.04 |
| 84.600 | 5.67 | 85.150 | 3.24 | 85.700 | 12.24 | 86.250 | 5.44 |
| 84.610 | 12.09 | 85.160 | 9.32 | 85.710 | 8.35 | 86.260 | 12.68 |
| 84.620 | 8.81 | 85.170 | 14.30 | 85.720 | 11.61 | 86.270 | 8.11 |
| 84.630 | 10.27 | 85.180 | 14.71 | 85.730 | 16.99 | 86.280 | 7.88 |
| 84.640 | 3.48 | 85.190 | 11.04 | 85.740 | 16.95 | 86.290 | 2.12 |

Point Grade Estimates for the Bitumen Content of the Test Core Section Obtained at 1 cm Sampling Intervals (Cont'd).

| DEPTH (m) | BITUMEN CONTENT WT % | DEPTH (m) | BITUMEN CONTENT WT % | DEPTH (m) | BITUMEN CONTENT WT % | DEPTH (m) | BITUMEN CONTENT WT % |
|---|---|---|---|---|---|---|---|
| 86.300 | 2.60 | 86.850 | 6.50 | 87.400 | 11.78 | 87.950 | 0.08 |
| 86.310 | 5.68 | 86.860 | 10.00 | 87.410 | 16.61 | 87.960 | 4.25 |
| 86.320 | 3.85 | 86.870 | 13.41 | 87.420 | 17.03 | 87.970 | 8.73 |
| 86.330 | 0.00 | 86.880 | 13.80 | 87.430 | 11.88 | 87.980 | 10.31 |
| 86.340 | 0.80 | 86.890 | 11.48 | 87.440 | 12.90 | 87.990 | 11.68 |
| 86.350 | 3.90 | 86.900 | 13.40 | 87.450 | 12.69 | 88.000 | 12.04 |
| 86.360 | 2.02 | 86.910 | 7.01 | 87.460 | 13.11 | 88.010 | 4.74 |
| 86.370 | 2.30 | 86.920 | 7.66 | 87.470 | 12.65 | 88.020 | 2.16 |
| 86.380 | 1.70 | 86.930 | 4.83 | 87.480 | 16.26 | 88.030 | 10.00 |
| 86.390 | 1.41 | 86.940 | 4.13 | 87.490 | 14.63 | 88.040 | 17.14 |
| 86.400 | 2.90 | 86.950 | 4.08 | 87.500 | 16.90 | 88.050 | 12.68 |
| 86.410 | 2.12 | 86.960 | 3.52 | 87.510 | 13.19 | 88.060 | 12.47 |
| 86.420 | 4.23 | 86.970 | 5.63 | 87.520 | 12.51 | 88.070 | 13.52 |
| 86.430 | 3.21 | 86.980 | 8.24 | 87.530 | 11.32 | 88.080 | 13.40 |
| 86.440 | 3.64 | 86.990 | 8.85 | 87.540 | 14.06 | 88.090 | 9.04 |
| 86.450 | 3.14 | 87.000 | 8.34 | 87.550 | 14.92 | 88.100 | 13.27 |
| 86.460 | 5.38 | 87.010 | 6.50 | 87.560 | 12.81 | 88.110 | 15.55 |
| 86.470 | 4.72 | 87.020 | 4.15 | 87.570 | 12.38 | 88.120 | 15.91 |
| 86.480 | 6.07 | 87.030 | 3.61 | 87.580 | 12.21 | 88.130 | 14.70 |
| 86.490 | 3.98 | 87.040 | 3.79 | 87.590 | 12.43 | 88.140 | 13.45 |
| 86.500 | 3.85 | 87.050 | 3.67 | 87.600 | 15.63 | 88.150 | 14.79 |
| 86.510 | 6.68 | 87.060 | 3.56 | 87.610 | 15.76 | 88.160 | 8.75 |
| 86.520 | 3.78 | 87.070 | 4.01 | 87.620 | 13.85 | 88.170 | 7.66 |
| 86.530 | 3.33 | 87.080 | 2.66 | 87.630 | 14.22 | 88.180 | 11.35 |
| 86.540 | 5.66 | 87.090 | 1.75 | 87.640 | 8.65 | 88.190 | 10.72 |
| 86.550 | 4.53 | 87.100 | 3.12 | 87.650 | 13.31 | 88.200 | 14.01 |
| 86.560 | 6.54 | 87.110 | 6.85 | 87.660 | 12.03 | 88.210 | 14.61 |
| 86.570 | 3.55 | 87.120 | 5.06 | 87.670 | 13.91 | 88.220 | 15.07 |
| 86.580 | 3.06 | 87.130 | 3.05 | 87.680 | 12.34 | 88.230 | 12.39 |
| 86.590 | 4.27 | 87.140 | 7.04 | 87.690 | 13.25 | 88.240 | 12.27 |
| 86.600 | 6.27 | 87.150 | 7.30 | 87.700 | 9.11 | 88.250 | 11.26 |
| 86.610 | 5.07 | 87.160 | 11.33 | 87.710 | 14.35 | 88.260 | 6.93 |
| 86.620 | 7.20 | 87.170 | 7.26 | 87.720 | 12.55 | 88.270 | 6.96 |
| 86.630 | 7.22 | 87.180 | 9.43 | 87.730 | 9.54 | 88.280 | 2.54 |
| 86.640 | 6.95 | 87.190 | 10.46 | 87.740 | 13.62 | 88.290 | 9.45 |
| 86.650 | 7.75 | 87.200 | 9.06 | 87.750 | 12.34 | 88.300 | 17.58 |
| 86.660 | 5.20 | 87.210 | 14.34 | 87.760 | 11.98 | 88.310 | 10.21 |
| 86.670 | 3.62 | 87.220 | 11.94 | 87.770 | 14.64 | 88.320 | 12.23 |
| 86.680 | 7.20 | 87.230 | 9.23 | 87.780 | 15.58 | 88.330 | 12.38 |
| 86.690 | 6.41 | 87.240 | 11.50 | 87.790 | 12.65 | 88.340 | 14.78 |
| 86.700 | 7.20 | 87.250 | 10.13 | 87.800 | 11.82 | 88.350 | 11.98 |
| 86.710 | 4.59 | 87.260 | 14.84 | 87.810 | 13.89 | 88.360 | 12.33 |
| 86.720 | 4.38 | 87.270 | 13.40 | 87.820 | 11.81 | | |
| 86.730 | 6.03 | 87.280 | 16.26 | 87.830 | 11.61 | | |
| 86.740 | 3.53 | 87.290 | 14.41 | 87.840 | 9.57 | | |
| 86.750 | 7.59 | 87.300 | 15.88 | 87.850 | 11.07 | | |
| 86.760 | 8.93 | 87.310 | 13.65 | 87.860 | 10.92 | | |
| 86.770 | 9.67 | 87.320 | 12.38 | 87.870 | 9.70 | | |
| 86.780 | 6.97 | 87.330 | 12.78 | 87.880 | 11.17 | | |
| 86.790 | 9.00 | 87.340 | 14.34 | 87.890 | 9.48 | | |
| 86.800 | 14.14 | 87.350 | 14.06 | 87.900 | 7.22 | | |
| 86.810 | 10.20 | 87.360 | 12.83 | 87.910 | 8.44 | | |
| 86.820 | 9.63 | 87.370 | 14.94 | 87.920 | 6.97 | | |
| 86.830 | 13.24 | 87.380 | 15.83 | 87.930 | 5.44 | | |
| 86.840 | 9.90 | 87.390 | 13.55 | 87.940 | 3.04 | | |

Point Grade Estimates for the Bitumen Content of the Test Core Section Obtained at 2 cm Sampling Intervals.

| DEPTH (m) | BITUMEN CONTENT WT % | DEPTH (m) | BITUMEN CONTENT WT % | DEPTH (m) | BITUMEN CONTENT WT % | DEPTH (m) | BITUMEN CONTENT WT % |
|---|---|---|---|---|---|---|---|
| 84.105 | 13.57 | 85.205 | 6.89 | 86.305 | 4.14 | 87.405 | 14.20 |
| 84.125 | 12.15 | 85.225 | 8.95 | 86.325 | 1.93 | 87.425 | 14.46 |
| 84.145 | 15.06 | 85.245 | 8.14 | 86.345 | 2.35 | 87.445 | 12.79 |
| 84.165 | 13.70 | 85.265 | 8.94 | 86.365 | 2.16 | 87.465 | 12.88 |
| 84.185 | 12.35 | 85.285 | 8.05 | 86.385 | 1.55 | 87.485 | 15.45 |
| 84.205 | 10.51 | 85.305 | 12.87 | 86.405 | 2.51 | 87.505 | 15.04 |
| 84.225 | 12.37 | 85.325 | 12.75 | 86.425 | 3.72 | 87.525 | 11.91 |
| 84.245 | 15.42 | 85.345 | 17.01 | 86.445 | 3.39 | 87.545 | 14.49 |
| 84.265 | 14.10 | 85.365 | 16.55 | 86.465 | 5.05 | 87.565 | 12.59 |
| 84.285 | 13.06 | 85.385 | 16.38 | 86.485 | 5.01 | 87.585 | 12.32 |
| 84.305 | 10.35 | 85.405 | 16.49 | 86.505 | 5.26 | 87.605 | 15.69 |
| 84.325 | 10.40 | 85.425 | 16.70 | 86.525 | 3.55 | 87.625 | 14.03 |
| 84.345 | 6.79 | 85.445 | 18.16 | 86.545 | 5.09 | 87.645 | 10.98 |
| 84.365 | 15.07 | 85.465 | 14.94 | 86.565 | 5.05 | 87.665 | 12.97 |
| 84.385 | 15.15 | 85.485 | 18.22 | 86.585 | 3.66 | 87.685 | 12.79 |
| 84.405 | 12.40 | 85.505 | 16.57 | 86.605 | 5.67 | 87.705 | 11.73 |
| 84.425 | 13.51 | 85.525 | 16.13 | 86.625 | 7.21 | 87.725 | 11.05 |
| 84.445 | 9.25 | 85.545 | 17.60 | 86.645 | 7.35 | 87.745 | 12.98 |
| 84.465 | 12.05 | 85.565 | 16.45 | 86.665 | 4.41 | 87.765 | 13.31 |
| 84.485 | 11.82 | 85.585 | 16.56 | 86.685 | 6.80 | 87.785 | 14.11 |
| 84.505 | 14.94 | 85.605 | 15.13 | 86.705 | 5.89 | 87.805 | 12.86 |
| 84.525 | 7.93 | 85.625 | 14.71 | 86.725 | 5.20 | 87.825 | 11.71 |
| 84.545 | 14.61 | 85.645 | 12.95 | 86.745 | 5.56 | 87.845 | 10.32 |
| 84.565 | 10.96 | 85.665 | 14.27 | 86.765 | 9.30 | 87.865 | 10.31 |
| 84.585 | 4.77 | 85.685 | 13.34 | 86.785 | 7.99 | 87.885 | 10.32 |
| 84.605 | 8.88 | 85.705 | 10.30 | 86.805 | 12.17 | 87.905 | 7.83 |
| 84.625 | 9.54 | 85.725 | 14.30 | 86.825 | 11.43 | 87.925 | 6.20 |
| 84.645 | 4.17 | 85.745 | 16.77 | 86.845 | 8.20 | 87.945 | 1.55 |
| 84.665 | 3.97 | 85.765 | 15.18 | 86.865 | 11.71 | 87.965 | 6.49 |
| 84.685 | 4.68 | 85.785 | 14.97 | 86.885 | 12.64 | 87.985 | 10.99 |
| 84.705 | 9.70 | 85.805 | 15.65 | 86.905 | 10.20 | 88.005 | 8.39 |
| 84.725 | 7.64 | 85.825 | 15.14 | 86.925 | 8.25 | 88.025 | 6.08 |
| 84.745 | 8.96 | 85.845 | 13.39 | 86.945 | 4.11 | 88.045 | 14.91 |
| 84.765 | 6.05 | 85.865 | 14.04 | 86.965 | 4.57 | 88.065 | 12.99 |
| 84.785 | 9.74 | 85.885 | 8.19 | 86.985 | 8.55 | 88.085 | 11.22 |
| 84.805 | 12.43 | 85.905 | 15.62 | 87.005 | 7.42 | 88.105 | 14.56 |
| 84.825 | 12.05 | 85.925 | 16.94 | 87.025 | 3.88 | 88.125 | 15.30 |
| 84.845 | 12.15 | 85.945 | 16.85 | 87.045 | 3.73 | 88.145 | 14.12 |
| 84.865 | 11.28 | 85.965 | 14.81 | 87.065 | 3.79 | 88.165 | 8.20 |
| 84.885 | 14.30 | 85.985 | 13.96 | 87.085 | 2.20 | 88.185 | 11.04 |
| 84.905 | 12.22 | 86.005 | 16.01 | 87.105 | 4.99 | 88.205 | 14.31 |
| 84.925 | 10.98 | 86.025 | 14.33 | 87.125 | 4.05 | 88.225 | 13.73 |
| 84.945 | 11.59 | 86.045 | 10.30 | 87.145 | 7.17 | 88.245 | 11.77 |
| 84.965 | 12.15 | 86.065 | 8.93 | 87.165 | 9.29 | 88.265 | 6.94 |
| 84.985 | 14.03 | 86.085 | 12.52 | 87.185 | 9.94 | 88.285 | 5.99 |
| 85.005 | 8.08 | 86.105 | 10.40 | 87.205 | 11.70 | 88.305 | 13.89 |
| 85.025 | 5.33 | 86.125 | 6.76 | 87.225 | 10.59 | 88.325 | 12.31 |
| 85.045 | 5.57 | 86.145 | 5.91 | 87.245 | 10.81 | 88.345 | 13.37 |
| 85.065 | 8.11 | 86.165 | 7.50 | 87.265 | 14.12 | | |
| 85.085 | 7.74 | 86.185 | 3.51 | 87.285 | 15.34 | | |
| 85.105 | 11.24 | 86.205 | 7.87 | 87.305 | 14.76 | | |
| 85.125 | 9.81 | 86.225 | 2.36 | 87.325 | 12.58 | | |
| 85.145 | 4.58 | 86.245 | 8.24 | 87.345 | 14.20 | | |
| 85.165 | 11.81 | 86.265 | 10.40 | 87.365 | 13.88 | | |
| 85.185 | 12.87 | 86.285 | 4.99 | 87.385 | 14.69 | | |

Point Grade Estimates for the Bitumen Content of the Test Core Section Obtained at 5 cm Sampling Intervals.

| DEPTH (m) | BITUMEN CONTENT WT % | DEPTH (m) | BITUMEN CONTENT WT % | DEPTH (m) | BITUMEN CONTENT WT % | DEPTH (m) | BITUMEN CONTENT WT % |
|---|---|---|---|---|---|---|---|
| 84.120 | 13.38 | 85.370 | 17.35 | 86.620 | 6.54 | 87.870 | 10.47 |
| 84.170 | 13.35 | 85.420 | 16.67 | 86.670 | 6.04 | 87.920 | 6.22 |
| 84.220 | 12.15 | 85.470 | 17.12 | 86.720 | 5.14 | 87.970 | 7.01 |
| 84.270 | 14.03 | 85.520 | 16.44 | 86.770 | 8.44 | 88.020 | 9.22 |
| 84.320 | 10.09 | 85.570 | 16.88 | 86.820 | 11.42 | 88.070 | 12.22 |
| 84.370 | 13.01 | 85.620 | 14.66 | 86.870 | 11.04 | 88.120 | 14.63 |
| 84.420 | 12.16 | 85.670 | 13.50 | 86.920 | 7.41 | 88.170 | 10.66 |
| 84.470 | 11.45 | 85.720 | 13.23 | 86.970 | 6.07 | 88.220 | 13.67 |
| 84.520 | 11.97 | 85.770 | 15.38 | 87.020 | 5.28 | 88.270 | 7.43 |
| 84.570 | 9.31 | 85.820 | 15.04 | 87.070 | 3.13 | 88.320 | 13.43 |
| 84.620 | 8.06 | 85.870 | 11.53 | 87.120 | 5.02 | | |
| 84.670 | 4.44 | 85.920 | 16.38 | 87.170 | 9.15 | | |
| 84.720 | 9.13 | 85.970 | 14.90 | 87.220 | 11.22 | | |
| 84.770 | 7.70 | 86.020 | 15.05 | 87.270 | 13.81 | | |
| 84.820 | 12.45 | 86.070 | 9.79 | 87.320 | 13.81 | | |
| 84.870 | 12.43 | 86.120 | 8.55 | 87.370 | 14.24 | | |
| 84.920 | 11.68 | 86.170 | 5.09 | 87.420 | 14.04 | | |
| 84.970 | 12.71 | 86.220 | 6.30 | 87.470 | 13.87 | | |
| 85.020 | 6.62 | 86.270 | 7.24 | 87.520 | 13.59 | | |
| 85.070 | 7.31 | 86.320 | 2.59 | 87.570 | 12.95 | | |
| 85.120 | 9.60 | 86.370 | 2.27 | 87.620 | 13.62 | | |
| 85.170 | 10.52 | 86.420 | 3.22 | 87.670 | 12.97 | | |
| 85.220 | 7.96 | 86.470 | 4.65 | 87.720 | 11.83 | | |
| 85.270 | 8.43 | 86.520 | 4.66 | 87.770 | 13.43 | | |
| 85.320 | 13.67 | 86.570 | 4.39 | 87.820 | 11.74 | | |

Point Grade Estimates for the Bitumen Content of the Test Core Section Obtained at 10 cm Sampling Intervals.

| DEPTH (m) | BITUMEN CONTENT WT % | DEPTH (m) | BITUMEN CONTENT WT % | DEPTH (m) | BITUMEN CONTENT WT % | DEPTH (m) | BITUMEN CONTENT WT % |
|---|---|---|---|---|---|---|---|
| 84.145 | 13.37 | 85.345 | 15.51 | 86.545 | 4.52 | 87.745 | 12.63 |
| 84.245 | 13.09 | 85.445 | 16.90 | 86.645 | 6.29 | 87.845 | 11.10 |
| 84.345 | 11.55 | 85.545 | 16.66 | 86.745 | 6.79 | 87.945 | 6.61 |
| 84.445 | 11.81 | 85.645 | 14.08 | 86.845 | 11.23 | 88.045 | 10.72 |
| 84.545 | 10.64 | 85.745 | 14.30 | 86.945 | 8.74 | 88.145 | 12.84 |
| 84.645 | 6.25 | 85.845 | 13.28 | 87.045 | 4.20 | 88.245 | 10.55 |
| 84.745 | 8.41 | 85.945 | 15.64 | 87.145 | 7.09 | | |
| 84.845 | 12.44 | 86.045 | 12.42 | 87.245 | 12.51 | | |
| 84.945 | 12.19 | 86.145 | 8.82 | 87.345 | 14.02 | | |
| 85.045 | 6.97 | 86.245 | 6.77 | 87.445 | 13.95 | | |
| 85.145 | 10.06 | 86.345 | 2.43 | 87.545 | 13.27 | | |
| 85.245 | 8.19 | 86.445 | 3.93 | 87.645 | 13.29 | | |

Point Grade Estimates for the Bitumen Content of the Test Core Section Obtained at 20 cm Sampling Intervals.

| DEPTH (m) | BITUMEN CONTENT WT % | DEPTH (m) | BITUMEN CONTENT WT % | DEPTH (m) | BITUMEN CONTENT WT % | DEPTH (m) | BITUMEN CONTENT WT % |
|---|---|---|---|---|---|---|---|
| 84.195 | 13.23 | 85.395 | 16.20 | 86.595 | 5.41 | 87.795 | 11.87 |
| 84.395 | 11.68 | 85.595 | 15.37 | 86.795 | 9.01 | 87.995 | 8.67 |
| 84.595 | 8.44 | 85.795 | 13.79 | 86.995 | 5.47 | 88.195 | 11.80 |
| 84.795 | 10.43 | 85.995 | 14.03 | 87.195 | 9.80 | | |
| 84.995 | 9.58 | 86.195 | 6.80 | 87.395 | 13.99 | | |
| 85.195 | 9.13 | 86.395 | 3.18 | 87.595 | 13.28 | | |

Point Grade Estimates for the Bitumen Content of Core 22–38–60–0–0–0 Obtained at 2 m Sampling Intervals. Results Obtained by Reconstitution of Original Data Series.

| DEPTH (m) | BITUMEN CONTENT WT % | DEPTH (m) | BITUMEN CONTENT WT % | DEPTH (m) | BITUMEN CONTENT WT % | DEPTH (m) | BITUMEN CONTENT WT % |
|---|---|---|---|---|---|---|---|
| 50.000 | 2.56 | 66.000 | 13.26 | 82.000 | 12.01 | 98.000 | 11.14 |
| 52.000 | 5.84 | 68.000 | 11.30 | 84.000 | 12.45 | 100.000 | 9.55 |
| 54.000 | 11.98 | 70.000 | 10.70 | 86.000 | 9.60 | 102.000 | 15.04 |
| 56.000 | 8.30 | 72.000 | 11.41 | 88.000 | 5.58 | 104.000 | 13.90 |
| 58.000 | 6.59 | 74.000 | 12.00 | 90.000 | 10.64 | 106.000 | 12.55 |
| 60.000 | 4.10 | 76.000 | 10.22 | 92.000 | 14.77 | | |
| 62.000 | 2.64 | 78.000 | 13.47 | 94.000 | 14.90 | | |
| 64.000 | 7.36 | 80.000 | 12.48 | 96.000 | 14.31 | | |

# APPENDIX C

## EXPERIMENTAL SEMI-VARIOGRAMS AND AUTOCORRELATION FUNCTIONS FOR CORE SAMPLES OF VARYING INCREMENT SIZE

Point Grade Estimates for the Bitumen Content of the Test Core Section Obtained at 1 cm Sampling Intervals.

MEAN GRADE = 10.58 % Bitumen

VARIANCE = 19.596

N = 427 Samples

| DISTANCE BETWEEN SAMPLES (cm) | AUTOCORRELATION COEFFICIENT (r) | EXPERIMENTAL SEMI-VARIOGRAM γ(h) |
|---|---|---|
| 0 | 1.000 | 0.000 |
| 1 | 0.776 | 4.387 |
| 2 | 0.662 | 6.629 |
| 3 | 0.626 | 7.354 |
| 4 | 0.609 | 7.682 |
| 5 | 0.589 | 8.462 |
| 6 | 0.572 | 8.431 |
| 7 | 0.568 | 8.496 |
| 8 | 0.556 | 8.753 |
| 9 | 0.525 | 9.357 |
| 10 | 0.500 | 9.864 |
| 11 | 0.467 | 10.521 |
| 12 | 0.445 | 10.982 |
| 13 | 0.408 | 11.736 |
| 14 | 0.384 | 12.246 |
| 15 | 0.345 | 13.007 |
| 16 | 0.328 | 13.340 |
| 17 | 0.340 | 13.099 |
| 18 | 0.323 | 13.470 |
| 19 | 0.290 | 14.157 |
| 20 | 0.264 | 14.701 |
| 21 | 0.234 | 15.320 |
| 22 | 0.226 | 15.501 |
| 23 | 0.215 | 15.753 |
| 24 | 0.242 | 15.216 |
| 25 | 0.205 | 15.980 |
| 26 | 0.202 | 16.015 |
| 27 | 0.182 | 16.445 |
| 28 | 0.152 | 17.036 |
| 29 | 0.137 | 17.354 |
| 30 | 0.143 | 17.238 |
| 31 | 0.118 | 17.775 |
| 32 | 0.128 | 17.606 |
| 33 | 0.127 | 17.388 |
| 34 | 0.119 | 17.793 |
| 35 | 0.097 | 18.210 |
| 36 | 0.119 | 17.782 |
| 37 | 0.120 | 17.787 |
| 38 | 0.104 | 18.150 |
| 39 | 0.090 | 18.473 |
| 40 | 0.065 | 19.229 |

Point Grade Estimates for the Bitumen Content of the Test Core Section Obtained at 1 cm Sampling Intervals (Cont'd).

| DISTANCE BETWEEN SAMPLES (cm) | AUTOCORRELATION COEFFICIENT (r) | EXPERIMENTAL SEMI-VARIOGRAM V(h) |
|---|---|---|
| 41 | 0.081 | 19.071 |
| 42 | 0.085 | 18.904 |
| 43 | 0.089 | 18.810 |
| 44 | 0.089 | 18.809 |
| 45 | 0.043 | 19.345 |
| 46 | 0.034 | 19.547 |
| 47 | 0.025 | 19.768 |
| 48 | 0.024 | 19.841 |
| 49 | 0.016 | 20.044 |
| 50 | 0.004 | 20.223 |
| 51 | 0.011 | 20.087 |
| 52 | -0.017 | 20.712 |
| 53 | -0.041 | 21.262 |
| 54 | -0.049 | 21.483 |
| 55 | -0.018 | 20.774 |
| 56 | -0.008 | 20.620 |
| 57 | -0.041 | 21.279 |
| 58 | -0.067 | 21.799 |
| 59 | -0.075 | 21.945 |
| 60 | -0.072 | 21.872 |
| 61 | -0.065 | 21.770 |
| 62 | -0.074 | 22.022 |
| 63 | -0.087 | 22.535 |
| 64 | -0.139 | 23.420 |
| 65 | -0.168 | 24.081 |
| 66 | -0.174 | 24.228 |
| 67 | -0.190 | 24.577 |
| 68 | -0.203 | 24.869 |
| 69 | -0.182 | 24.496 |
| 70 | -0.195 | 24.795 |
| 71 | -0.227 | 25.530 |
| 72 | -0.234 | 25.730 |
| 73 | -0.217 | 25.414 |
| 74 | -0.238 | 25.904 |
| 75 | -0.268 | 26.517 |
| 76 | -0.269 | 26.609 |
| 77 | -0.291 | 27.094 |
| 78 | -0.292 | 27.170 |
| 79 | -0.273 | 26.782 |
| 80 | -0.259 | 26.557 |
| 81 | -0.270 | 26.844 |
| 82 | -0.276 | 27.000 |
| 83 | -0.288 | 26.893 |
| 84 | -0.287 | 26.941 |
| 85 | -0.260 | 26.855 |
| 86 | -0.276 | 27.254 |
| 87 | -0.282 | 27.402 |
| 88 | -0.284 | 27.450 |
| 89 | -0.298 | 27.759 |
| 90 | -0.292 | 27.661 |

Point Grade Estimates for the Bitumen Content of the Test Core Section Obtained at 1 cm Sampling Intervals (Cont'd).

| DISTANCE BETWEEN SAMPLES (cm) | AUTOCORRELATION COEFFICIENT (r) | EXPERIMENTAL SEMI-VARIOGRAM Y(h) |
|---|---|---|
| 91 | -0.303 | 27.954 |
| 92 | -0.301 | 27.918 |
| 93 | -0.292 | 27.760 |
| 94 | -0.298 | 27.925 |
| 95 | -0.323 | 28.414 |
| 96 | -0.333 | 28.598 |
| 97 | -0.343 | 28.863 |
| 98 | -0.346 | 29.001 |
| 99 | -0.354 | 29.161 |
| 100 | -0.350 | 29.119 |
| 101 | -0.378 | 29.791 |
| 102 | -0.355 | 29.360 |
| 103 | -0.342 | 29.128 |
| 104 | -0.347 | 29.316 |
| 105 | -0.363 | 29.704 |
| 106 | -0.349 | 29.373 |
| 107 | -0.347 | 29.355 |
| 108 | -0.344 | 29.313 |
| 109 | -0.344 | 29.297 |
| 110 | -0.346 | 29.409 |
| 111 | -0.335 | 29.166 |
| 112 | -0.320 | 28.922 |
| 113 | -0.318 | 28.975 |
| 114 | -0.309 | 28.858 |
| 115 | -0.315 | 29.067 |
| 116 | -0.301 | 28.817 |
| 117 | -0.278 | 28.373 |
| 118 | -0.267 | 28.219 |
| 119 | -0.257 | 28.102 |
| 120 | -0.209 | 27.082 |
| 121 | -0.204 | 27.052 |
| 122 | -0.212 | 27.271 |
| 123 | -0.184 | 26.700 |
| 124 | -0.163 | 26.961 |
| 125 | -0.170 | 26.277 |
| 126 | -0.173 | 26.311 |
| 127 | -0.162 | 25.736 |
| 128 | -0.157 | 25.619 |
| 129 | -0.123 | 24.754 |
| 130 | -0.105 | 24.288 |
| 131 | -0.107 | 24.280 |
| 132 | -0.105 | 24.133 |
| 133 | -0.096 | 23.871 |
| 134 | -0.082 | 23.480 |
| 135 | -0.070 | 23.145 |
| 136 | -0.067 | 22.987 |
| 137 | -0.052 | 22.672 |
| 138 | -0.049 | 22.685 |
| 139 | -0.058 | 22.813 |
| 140 | -0.048 | 22.534 |

Point Grade Estimates for the Bitumen Content of the Test Core Section Obtained at 1 cm Sampling Intervals (Cont'd).

| DISTANCE BETWEEN SAMPLES (cm) | AUTOCORRELATION COEFFICIENT (r) | EXPERIMENTAL SEMI-VARIOGRAM γ(h) |
|---|---|---|
| 141 | -0.033 | 22.128 |
| 142 | -0.010 | 21.575 |
| 143 | 0.000 | 21.328 |
| 144 | 0.008 | 21.112 |
| 145 | 0.017 | 20.920 |
| 146 | 0.034 | 20.512 |
| 147 | 0.029 | 20.628 |
| 148 | -0.002 | 21.254 |
| 149 | 0.019 | 20.781 |
| 150 | 0.030 | 20.543 |
| 151 | 0.039 | 20.402 |
| 152 | 0.035 | 20.500 |
| 153 | 0.085 | 19.515 |
| 154 | 0.087 | 19.435 |
| 155 | 0.049 | 20.306 |
| 156 | 0.042 | 20.527 |
| 157 | 0.062 | 20.110 |
| 158 | 0.044 | 20.547 |
| 159 | 0.033 | 20.844 |
| 160 | 0.033 | 20.904 |
| 161 | 0.044 | 20.735 |
| 162 | 0.055 | 20.559 |
| 163 | 0.063 | 20.396 |
| 164 | 0.071 | 20.193 |
| 165 | 0.075 | 20.066 |
| 166 | 0.080 | 19.714 |
| 167 | 0.086 | 19.851 |
| 168 | 0.085 | 19.863 |
| 169 | 0.101 | 19.558 |
| 170 | 0.148 | 18.582 |
| 171 | 0.145 | 18.639 |
| 172 | 0.122 | 19.134 |
| 173 | 0.138 | 18.869 |
| 174 | 0.138 | 18.870 |
| 175 | 0.128 | 19.125 |
| 176 | 0.152 | 18.665 |
| 177 | 0.165 | 18.451 |
| 178 | 0.180 | 18.130 |
| 179 | 0.191 | 17.905 |
| 180 | 0.217 | 17.299 |
| 181 | 0.218 | 17.324 |
| 182 | 0.211 | 17.475 |
| 183 | 0.216 | 17.351 |
| 184 | 0.239 | 16.869 |
| 185 | 0.209 | 17.483 |
| 186 | 0.212 | 17.448 |
| 187 | 0.238 | 16.919 |
| 188 | 0.250 | 16.719 |
| 189 | 0.227 | 17.255 |
| 190 | 0.228 | 17.265 |

Point Grade Estimates for the Bitumen Content of the Test Core Section Obtained at 1 cm Sampling Intervals (Cont'd).

| DISTANCE BETWEEN SAMPLES (cm) | AUTOCORRELATION COEFFICIENT (r) | EXPERIMENTAL SEMI-VARIOGRAM Y(h) |
|---|---|---|
| 191 | 0.176 | 18.347 |
| 192 | 0.164 | 18.590 |
| 193 | 0.188 | 18.190 |
| 194 | 0.202 | 17.881 |
| 195 | 0.166 | 18.637 |
| 196 | 0.175 | 18.402 |
| 197 | 0.156 | 18.763 |
| 198 | 0.171 | 18.468 |
| 199 | 0.169 | 18.503 |
| 200 | 0.154 | 18.811 |

Point Grade Estimates for the Bitumen Content of the Test Core Section Obtained at 2 cm Sampling Intervals.

MEAN GRADE = 10.56 % Bitumen

VARIANCE = 17.934

N = 213

| DISTANCE BETWEEN SAMPLES (cm) | AUTOCORRELATION COEFFICIENT (r) | EXPERIMENTAL SEMI-VARIOGRAM γ(h) |
|---|---|---|
| 0 | 1.000 | 0.000 |
| 2 | 0.777 | 3.881 |
| 4 | 0.670 | 5.769 |
| 6 | 0.650 | 6.128 |
| 8 | 0.618 | 6.693 |
| 10 | 0.580 | 7.721 |
| 12 | 0.496 | 8.883 |
| 14 | 0.427 | 10.121 |
| 16 | 0.365 | 11.223 |
| 18 | 0.367 | 11.226 |
| 20 | 0.297 | 12.498 |
| 22 | 0.249 | 13.392 |
| 24 | 0.256 | 13.301 |
| 26 | 0.224 | 13.880 |
| 28 | 0.173 | 14.816 |
| 30 | 0.148 | 15.265 |
| 32 | 0.141 | 15.425 |
| 34 | 0.140 | 15.464 |
| 36 | 0.128 | 15.755 |
| 38 | 0.117 | 16.018 |
| 40 | 0.068 | 16.955 |
| 42 | 0.076 | 16.672 |
| 44 | 0.071 | 16.797 |
| 46 | 0.041 | 17.369 |
| 48 | 0.021 | 17.813 |
| 50 | 0.014 | 17.957 |
| 52 | -0.019 | 18.655 |
| 54 | -0.048 | 19.263 |
| 56 | -0.009 | 18.522 |
| 58 | -0.078 | 19.740 |
| 60 | -0.073 | 19.633 |
| 62 | -0.087 | 19.972 |
| 64 | -0.150 | 21.223 |
| 66 | -0.208 | 22.403 |
| 68 | -0.211 | 22.499 |
| 70 | -0.225 | 22.860 |
| 72 | -0.253 | 23.510 |
| 74 | -0.263 | 23.774 |
| 76 | -0.314 | 24.767 |
| 78 | -0.324 | 25.083 |
| 80 | -0.287 | 24.452 |

Point Grade Estimates for the Bitumen Content of the Test Core Section Obtained at 2 cm Sampling Intervals (Cont'd).

| DISTANCE BETWEEN SAMPLES (cm) | AUTOCORRELATION COEFFICIENT (r) | EXPERIMENTAL SEMI-VARIOGRAM Y(h) |
|---|---|---|
| 82 | -0.303 | 24.819 |
| 84 | -0.297 | 24.842 |
| 86 | -0.303 | 25.005 |
| 88 | -0.324 | 25.461 |
| 90 | -0.325 | 25.538 |
| 92 | -0.338 | 25.906 |
| 94 | -0.333 | 25.791 |
| 96 | -0.375 | 26.620 |
| 98 | -0.381 | 26.802 |
| 100 | -0.403 | 27.315 |
| 102 | -0.397 | 27.312 |
| 104 | -0.392 | 27.348 |
| 106 | -0.387 | 27.201 |
| 108 | -0.380 | 27.130 |
| 110 | -0.387 | 27.338 |
| 112 | -0.356 | 26.854 |
| 114 | -0.351 | 26.916 |
| 116 | -0.332 | 26.703 |
| 118 | -0.294 | 26.109 |
| 120 | -0.242 | 25.203 |
| 122 | -0.225 | 24.940 |
| 124 | -0.183 | 24.068 |
| 126 | -0.185 | 23.954 |
| 128 | -0.165 | 23.188 |
| 130 | -0.125 | 22.228 |
| 132 | -0.107 | 21.713 |
| 134 | -0.096 | 21.320 |
| 136 | -0.061 | 20.523 |
| 138 | -0.064 | 20.630 |
| 140 | -0.048 | 20.131 |
| 142 | -0.015 | 19.368 |
| 144 | 0.018 | 18.704 |
| 146 | 0.023 | 18.551 |
| 148 | 0.014 | 18.718 |
| 150 | 0.038 | 18.248 |
| 152 | 0.055 | 17.983 |
| 154 | 0.086 | 17.453 |
| 156 | 0.052 | 18.183 |
| 158 | 0.057 | 18.180 |
| 160 | 0.034 | 18.724 |
| 162 | 0.056 | 18.364 |
| 164 | 0.088 | 17.781 |
| 166 | 0.094 | 17.624 |
| 168 | 0.090 | 17.725 |
| 170 | 0.159 | 16.415 |
| 172 | 0.153 | 16.574 |
| 174 | 0.146 | 16.765 |
| 176 | 0.177 | 16.265 |
| 178 | 0.200 | 15.820 |
| 180 | 0.247 | 14.993 |

Point Grade Estimates for the Bitumen Content of the Test Core Section Obtained at 2 cm Sampling Intervals.

| DISTANCE BETWEEN SAMPLES (cm) | AUTOCORRELATION COEFFICIENT (r) | EXPERIMENTAL SEMI-VARIOGRAM Y(h) |
|---|---|---|
| 182 | 0.242 | 15.119 |
| 184 | 0.270 | 14.861 |
| 186 | 0.246 | 15.012 |
| 188 | 0.288 | 14.326 |
| 190 | 0.233 | 15.399 |
| 192 | 0.210 | 15.808 |
| 194 | 0.226 | 15.584 |
| 196 | 0.195 | 16.152 |
| 198 | 0.193 | 16.145 |
| 200 | 0.189 | 16.247 |

Point Grade Estimates for the Bitumen Content of the Test Core Section Obtained at 5 cm Sampling Intervals.

MEAN GRADE = 10.56 % Bitumen

VARIANCE = 15.048

N = 85

| DISTANCE BETWEEN SAMPLES | AUTOCORRELATION COEFFICIENT (r) | EXPERIMENTAL SEMI-VARIOGRAM Y(h) |
|---|---|---|
| 0 | 1.000 | 0.000 |
| 5 | 0.786 | 3.194 |
| 10 | 0.658 | 5.174 |
| 15 | 0.467 | 8.069 |
| 20 | 0.365 | 9.684 |
| 25 | 0.272 | 11.150 |
| 30 | 0.164 | 12.927 |
| 35 | 0.160 | 13.119 |
| 40 | 0.091 | 14.308 |
| 45 | 0.078 | 14.595 |
| 50 | -0.003 | 16.076 |
| 55 | -0.035 | 16.763 |
| 60 | -0.083 | 17.438 |
| 65 | -0.187 | 19.345 |
| 70 | -0.272 | 20.896 |
| 75 | -0.340 | 22.191 |
| 80 | -0.346 | 22.518 |
| 85 | -0.332 | 22.495 |
| 90 | -0.379 | 23.447 |
| 95 | -0.403 | 23.940 |
| 100 | -0.454 | 24.927 |
| 105 | -0.440 | 24.943 |
| 110 | -0.425 | 24.940 |
| 115 | -0.382 | 24.511 |
| 120 | -0.279 | 23.025 |
| 125 | -0.216 | 21.834 |
| 130 | -0.138 | 19.782 |
| 135 | -0.105 | 18.900 |
| 140 | -0.035 | 17.441 |
| 145 | 0.011 | 16.573 |
| 150 | 0.048 | 15.892 |
| 155 | 0.054 | 15.901 |
| 160 | 0.041 | 16.325 |
| 165 | 0.115 | 15.139 |
| 170 | 0.158 | 14.473 |
| 175 | 0.205 | 13.762 |
| 180 | 0.259 | 13.001 |
| 185 | 0.335 | 11.783 |
| 190 | 0.286 | 12.687 |
| 195 | 0.252 | 13.267 |
| 200 | 0.225 | 13.680 |

Point Grade Estimates for the Bitumen Content of the Test Core Section Obtained at 10 cm Sampling Intervals.

MEAN GRADE = 10.52 % Bitumen

VARIANCE = 13.937

N = 42

| DISTANCE BETWEEN SAMPLES (cm) | AUTOCORRELATION COEFFICIENT (r) | EXPERIMENTAL SEMI-VARIOGRAM Y(h) |
|---|---|---|
| 0 | 1.000 | 0.000 |
| 10 | 0.688 | 4.326 |
| 20 | 0.396 | 8.475 |
| 30 | 0.194 | 11.598 |
| 40 | 0.118 | 12.849 |
| 50 | 0.000 | 14.937 |
| 60 | -0.083 | 16.285 |
| 70 | -0.285 | 19.648 |
| 80 | -0.380 | 21.488 |
| 90 | -0.423 | 23.454 |
| 100 | -0.498 | 23.800 |
| 110 | -0.442 | 23.551 |
| 120 | -0.298 | 21.593 |
| 130 | -0.145 | 18.403 |
| 140 | -0.047 | 16.403 |
| 150 | 0.043 | 14.836 |
| 160 | 0.070 | 14.609 |
| 170 | 0.214 | 12.582 |
| 180 | 0.338 | 10.964 |
| 190 | 0.406 | 10.187 |
| 200 | 0.350 | 11.308 |

Point Grade Estimates for the Bitumen Content of the Test Core Section Obtained at 20 cm Sampling Intervals.

MEAN GRADE = 10.82 % Bitumen

VARIANCE = 12.148

N = 21

| DISTANCE BETWEEN SAMPLES (cm) | AUTOCORRELATION COEFFICIENT (r) | EXPERIMENTAL SEMI-VARIOGRAM Y(h) |
|---|---|---|
| 0 | 1.000 | 0.000 |
| 20 | 0.530 | 5.614 |
| 40 | 0.087 | 11.361 |
| 60 | -0.109 | 14.372 |
| 80 | -0.450 | 19.540 |
| 100 | -0.567 | 21.762 |
| 120 | -0.319 | 19.487 |
| 140 | -0.062 | 14.601 |
| 160 | 0.117 | 12.289 |
| 180 | 0.399 | 8.887 |
| 200 | 0.416 | 9.408 |

Point Grade Estimates for the Bitumen Content of Core 22-38-60-0-0-0 Obtained at 2 m Sampling Intervals. Results Obtained by Reconstitution of Original Data Series.

MEAN GRADE = 10.37 % Bitumen

VARIANCE = 13.007

N = 29

| DISTANCE BETWEEN SAMPLES (METRES) | AUTOCORRELATION COEFFICIENT (r) | EXPERIMENTAL SEMI-VARIOGRAM γ(h) |
|---|---|---|
| 0 | 1.000 | 0.000 |
| 2 | 0.309 | 4.706 |
| 4 | 0.139 | 10.164 |
| 6 | 0.109 | 10.574 |
| 8 | 0.178 | 10.105 |
| 10 | 0.391 | 7.684 |
| 12 | 0.572 | 6.074 |
| 14 | 0.193 | 9.843 |
| 16 | -0.151 | 12.939 |
| 18 | 0.033 | 11.892 |
| 20 | -0.001 | 11.809 |
| 22 | -0.056 | 12.901 |
| 24 | 0.420 | 9.691 |
| 26 | 0.630 | 8.520 |
| 28 | 0.407 | 11.653 |

Fortran Source Code Listing for Program SEMIVAR, an Algorithm for Calculating the Semi-Variogram and Autocorrelation Function for a Sequential Data Series.

```
C************************ SEMIVAR ******************************
C
C    ROUTINE TO COMPUTE SEMI-VARIOGRAM AND AUTOCORRELATION
C    FUNCTION OF A DATA SEQUENCE FROM ZERO LAG TO LAG=N/2.
C
C    INPUT SEQUENCE IS XIN AND CONTAINS N POINTS.
C
C    SEMI-VARIOGRAM AND AUTOCORRELATION COEFFICIENTS ARE
C    RETURNED IN XOUT WHICH IS LAG POINTS LONG.
C
C***************************************************************
REAL XIN(500),XOUT(250),LOUT(250),SEMIVAR(250)
INTEGER*2 DESCR(20)
BYTE TDESCR(40),DES(30)
character*20 file ! name of output file
EQUIVALENCE (TDESCR(1),DESCR(1))
C DATA FILE/'A','U','T','O','C','R','.','D','M','P',0/
file = 'semivar.dmp'
OPEN(UNIT=1,NAME='TI:',TYPE='OLD')
C===============================================================
C OBTAIN NAME OF DATA ARRAY
C===============================================================
  2 WRITE(1,1000) ! ARRAY DESCRIPTOR
1000 FORMAT(/,T5,$,'ENTER NAME OF DATA FILE     ')
READ(1,1010,ERR=2) IDF,(DES(J),J=1,IDF)
1010 FORMAT(Q,30A1)
DES(IDF+1)=0
OPEN(UNIT=2,NAME=DES,TYPE='OLD')
READ(2,2000) N
2000 FORMAT(I4)
READ(2,2005)  IT,(TDESCR(I),I=1,IT)
2005 FORMAT(Q,40A1)
DO 4 I=1,N
READ(2,2010) XIN(I)
2010 FORMAT(F6.0)
  4 CONTINUE
CLOSE(UNIT=2)
```

Fortran Source Code Listing for Program SEMIVAR, an Algorithm for Calculating the Semi-Variogram and Autocorrelation Function for a Sequential Data Series (Cont'd).

```
C=================================================================
C CALCULATE CORRELATION FOR EACH LAG(0 TO N/4)
C=================================================================
LAG=N/2+1
DO 10 I=1,LAG
LOUT(I)=FLOAT(I-1)
SX1=0.0
SX2=0.0
        SDX=0.0
SX1X1=0.0
SX2X2=0.0
SX1X2=0.0
L=N-I+1
DO 12 J=1,L
K=J+I-1
        SDX=SDX+(XIN(J)-XIN(K))**2
SX1=SX1+XIN(J)
SX2=SX2+XIN(K)
SX1X1=SX1X1+XIN(J)**2
SX2X2=SX2X2+XIN(K)**2
SX1X2=SX1X2+XIN(J)*XIN(K)
  12 CONTINUE
AL=L
        SEMIVAR(I)=0.5*SDX/L
R=(SX1X2-SX1*SX2/AL)/
     1   SQRT((SX1X1-SX1*SX1/AL)*(SX2X2-SX2*SX2/AL))
XOUT(I)=R
  10 CONTINUE
OPEN(UNIT=2,NAME=FILE,TYPE='NEW')
WRITE(2,3000) DESCR
3000 FORMAT(1H1,T10'DESCRIPTOR : ',20A2,//,T5'LAG',
     1 T15'CORRELATION',T32'SEMIVARIOGRAM'/)
DO 24 I=1,LAG
WRITE(2,3010) (I-1),XOUT(I),SEMIVAR(I)
3010 FORMAT(I7,F17.3,F17.3)
  24 CONTINUE
CLOSE(UNIT=2)
STOP
END
```